PALEOBIOLOGY AND ORGANIC GEOCHEMISTRY OF THE SEMRI GROUP SEDIMENTS MACHAR AREA, SATNA DISTRICT, MP

UDAY BHAN

12 JULY 2012

COLLEGE OF ENGINEERING

UNIVERSITY OF PETROLEUM AND ENERGY STUDIES

12 JULY 2012

Acknowledgement

I offer my deepest regards and sincere thanks to Dr. S.J. Chopra, Chancellor, Dr. Parag Diwan, Vice- Chancellor, Dr. Deepa Verma, Director HR, Dr. Shrihari Dean, Collage of Engineering, and Prof. K.S. Mishra of University of Petroleum and Energy Studies, Dehradun, for providing me facilities, valuable suggestions and constant motivation during my research work. With deep sense of regards, I acknowledge the help and facilities provided to me by Dr. N.C. Mehrotra, Director, Birbal Sahni Institute of Palaeobotany (BSIP), Lucknow during my research work and long stay at the institute.

Besides, I consider myself fortunate to be associated with my supervisor, Dr. Mukund Sharma of the Birbal Sahni Institute of Palaeobotany, Lucknow. I express my heartfelt gratitude to him for his constant encouragement, thoughtful guidance, supervision and introducing the fascinating world of the Precambrian palaeobiology. He also helped me to select the problem for investigation, joined the field-work and continuously discussed the progress of my research work. He has also provided me an opportunity to do the geochemical analysis in Petroleum Geochemistry Department of National Geophysical Research Laboratory (NGRI), Hyderabad. He helped me in all possible ways during research work. I also express my gratitude to my Co-Supervisor, Dr. Pradeep Joshi, Head, Department of Petroleum Engineering and Earth Science, University of Petroleum and Energy Studies, Dehradun, for providing the necessary facilities for his inspirational suggestions and encouragement during the present work.

I sincerely acknowledge the support of some special individuals. Words fail me to express gratitude to Dr. Santosh K. Pandey, Research Associate, BSIP, for support and generous care. I am very grateful to Dr. K.J. Singh Mr. Veeru Kant Singh, Dr. Yogmaya Shukla and Dr. Arjun Singh Rathore, all from BSIP for their help from time to time, during my research work. I also wish to acknowledge the technical support of Mr. Syed Rashid Ali, in computer related works. I am very thankful to Mr. Keshav Ram and Mr. Chandra Bali, BSIP, Lucknow, who have helped me in laboratory works and thin section preparation.

Dr. Mukund Sharma helped me to access the facilities NGRI in various analyses. I would also like to offer my sincere thanks to Dr. A. M. Dayal, Emeritus Scientist, Mr. D.J. Patil, Dr. Devleena Mani, and Dr. T. Madawi of NGRI, Hyderabad, for Geochemical Analysis. I would also like to thank some people from my early days of research work, Dr. S. K. Rai, and Mr. Koushick Sen of Wadia Institute of Himalayan Geology, Dehradun, who w provided me some important reference material. I express my thanks to Mr. Deepak Singh who was not only my classmate in M. Tech but also my colleague at UPES, together we shared a precious company during our stay in BSIP. I am highly indebted of Mr. S. K. Jain, Geologist, Bistara Mine, Mr. P. K. Jain, Senior Geologist, Maihar Cement Factory, Maihar, M.P. for providing me core samples and permitting me to detailed study in Mining sections.

My deepest gratitude goes to my family members, Mr. S. A. Pandey, Mr. B. B. Pandey and Ms. Sangeeta Devi, for their unflagging love, dedication and support during my studies that provided the foundation for this work. My beloved wife Priyanka deserves special words of appreciation for her understanding and outstanding supports during my absence from home. While I am away from home, my son Pratyush joined us as a new family member on 2nd June 2012. I am eagerly waiting to meet him. His presence in my life will always boasts me to achieve new heights in my career.

(Uday Bhan)

CONTENTS

Chapter 1

INTRODUCTION

The Middle to Late Proterozoic Period witnessed the development of intracratonic basins on the continental shields all over the world (Windley, 1977; Condie, 1989). The Precambrian rock record represents about 85% of Earth history and is essential for investigating long term changes in the lithosphere, biosphere and atmosphere. The Vindhyan Basin is one of the several "Purana" (ancient) sedimentary basins of the Indian subcontinent (Fig.1.1). It is a sickle-shaped basin, outcropping between the Archaean Aravalli-Bundelkhand province to the north and east and the Cretaceous Deccan Traps to the south and by the Great Boundary Fault to the west (Mazumdar et al., 2000). The Vindhyan Basin is one of the largest Proterozoic intracratonic sedimentary basins of the world and comprises a ~5000 m thick sequence of sandstone, shale, limestone, dolomite with minor conglomerate and volcaniclastic rocks.

The lithological successions in basin are unmetamorphosed, tectonically little disturbed in most of the areas. It is one of the best-preserved and spread over a large area extending in central Indian states of Bihar, Uttar Pradesh, Madhya Pradesh and Rajasthan, occupying an area of 2, 00,000 sq. km. Out of this 80,000 sq. km. is covered by the Decan Trap and possibly 10,000 sq. km. lies hidden under the Gangetic alluvium (Mathur, 1965; Jokhan Ram et al., 1996). These sedimentary successions are known as the Vindhyan Supergroup (VSG). It is drained by the two major rivers, the Son and the Chambal. After these two rivers, the entire succession of the Vindhyan Supergroup is divided into the Son Valley and the Chambal Valley successions.

The earliest descriptions of the Vindhyan succession were given by Oldham (1856) and Mallet (1869). Auden (1933) provided the basic data for all the subsequent studies. Since then many workers have pursued the Vindhyan Basin from varied perspectives as sedimentary geology and tectonics evolved through time (Ahmad, 1958; Banerjee, 1964, 1974; Singh, 1973, 1980, 1985; Chanda and Bhattacharyya, 1982; Soni et al., 1987; Chakraborty and Bose, 1990, 1992; Prasad and Verma, 1991; Bhattacharyya and Morad, 1993; Chakraborty, 1993, 1995, 1996, 2001; Akhtar, 1996; Bhattacharyya, 1996; Sarkar et al., 1996, 2001, 2002, 2005a, b; Bose et al., 1997, 1998, 2001; Ram et al., 1996; Ram, 2005). The

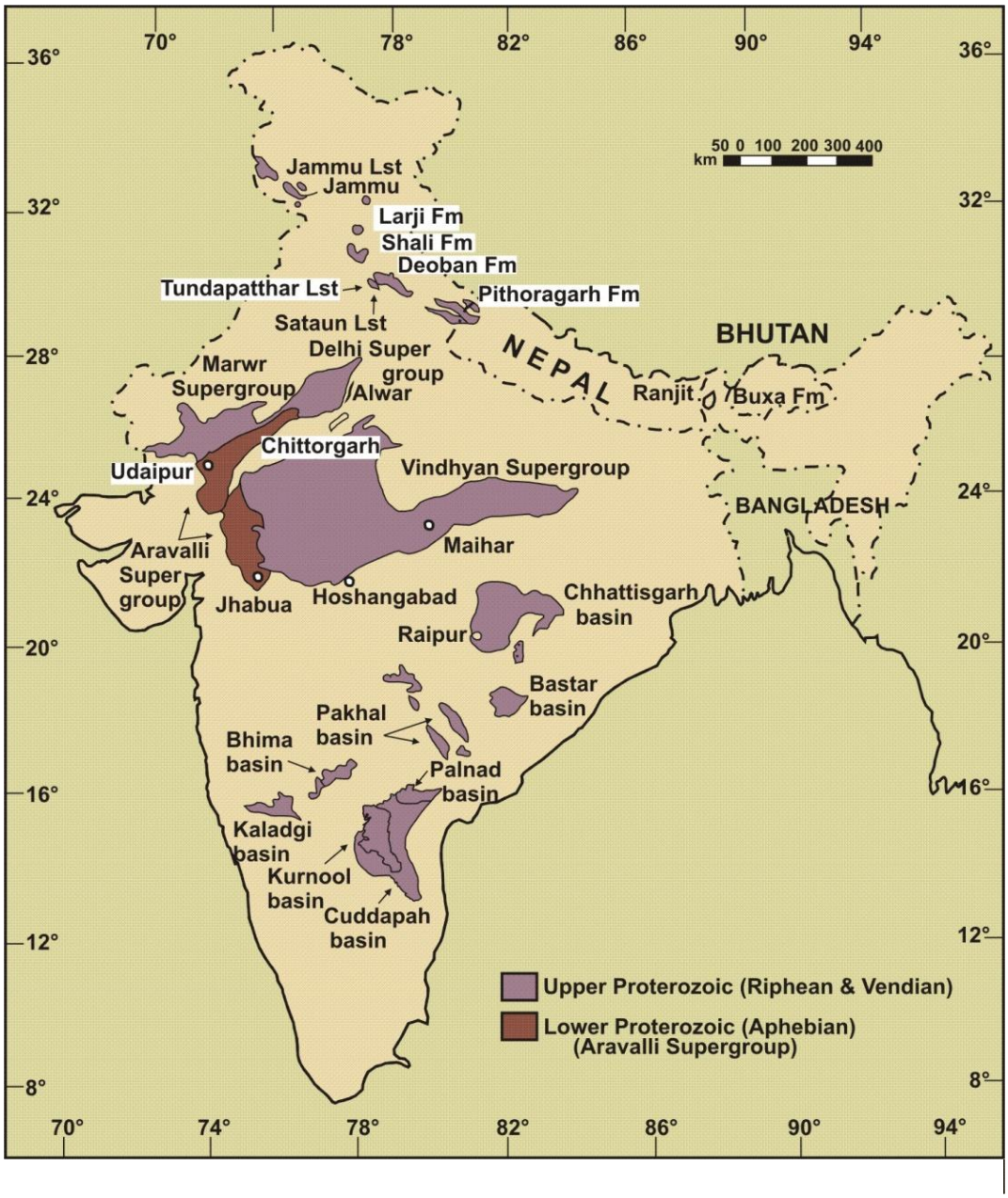

Fig. 1.1- Position map of different Proterozoic basin of India (modified after Raha and Sastry, 1982).

Vindhyan Supergroup is divided into four groups, viz. the Semri, the Kaimur, the Rewa and the Bhander, in ascending order.

The importance of the Vindhyan sequence lies in the notion that because of its vastness in time and space they contain important information on the evolution of the Earth's lithosphere, atmosphere and biosphere. However, even after decades of scrutiny we have not fully understood all the records that were uncovered from these rocks. The biggest challenge has been the difficulty in establishing links between the records found with global phenomenon, because we have not yet determined with certainty the timings of the local events. The Vindhyan

Supergroup was the focus of numerous interesting fossil discoveries for decades. It has revealed the presence of carbonaceous megafossils from different horizons (Jones 1909; Misra and Bhatnagar, 1950; Maithy and Shukla, 1984; Kumar, 1995, 2001; Kumar and Srivastava, 1997, 2003; Rai et al., 1997; Srivastava, 2004, 2005, Sharma, 2003, 2006a, b, Sharma and Shukla, 2009a, b). The recent discoveries of non-Ediacaran trace fossils (Seilacher et al., 1998) and animal body fossils (Azmi 1998) from the lower part of the supergroup have generated renewed interest in these rocks.

Geochemical and isotopic investigations on the Vindhyan rocks (e.g. Kumar et al., 2002; Ray et al., 2003) have also shown that there exist a host of valuable information of global importance that could change our views on the Proterozoic environment.

There is ongoing debate on its age of deposition. Age control on Vindhyan sedimentation is still the subject of considerable controversy as the ages of the other Purana basins (Gregory et al., 2006; Deb et al., 2007; Azmi et al., 2008; Basu et al., 2008; Malone et al., 2008). Geochronologically constrained dates suggest a very long span of deposition from Late Palaeoproterozoic to Terminal Neoproterozoic, i.e. ~1800 to 542 Ma of Vindhyan Basin. In general, the age of sedimentation for the Lower Vindhyan is far better constrained than that of the Upper Vindhyan. The Semri sediments unconformably overlie basement rock of the 1854 ± 7 Ma Hindoli Group (Deb et al., 2002) or the 2492 ± 10 Ma Bundelkhand Granites (Mondal et al., 2002). Ages from the Semri Group include a Pb–Pb isochron from the lower Kajrahat Limestone of 1721 ± 90 Ma (Sarangi et al., 2004); U–Pb zircon shale ranging from 1630.7 ± 4 to 1599 ± 8 Ma. The Rohtas Limestone in the upper part of the Lower Vindhyan has Pb–Pb ages of 1599 and 1601 Ma (Rasmussen et al., 2002; Ray et al., 2003; Sarangi et al., 2004) ages from the Porcellanites and Rampur Formation. Most authors agree with a Mesoproterozoic age for Lower Vindhyan sedimentation (~1750–1500 Ma). Recently, Bengtson et al. (2009) has proposed the age of Tirohan Limestone equivalent to the Rohtasgarh Limestone by Pb isotope analyses of the phosphorite intraclasts containing the fossils. The resulting Pb/Pb regression yields an age of 1,650 ± 89 Ma.

Since 1998, the age of the Vindhyan Supergroup (VSG) has been in focus on the basis of the latest palaeontological and geochronological findings.

At present, following views on the age of the VSG exist:

- The traditional view of Mesoproterozoic (~1400-550 Ma) or earliest Cambrian age mainly based on stromatolites and pre-1998 geochronology.
- Late Palaeoproterozoic to Late Neoproterozoic age (~1800-600 Ma) based on the latest geochronology and chemostratigraphy.

Present study on Vindhyan is not only restricted to palaeobiological interpretation but also aimed at deciphering hydrocarbon prospect of the Vindhyan basin evolution. The main interest of the present doctoral thesis is whether the Vindhyan basin be a potential source of hydrocarbon rocks covering an important time period of geological evolution.

1.1 Objectives

The objectives of the present research work are as follows:

- Palaeobiological study of the constituent formations of the Semri Group exposed around Maihar area, M.P.
- Documentation of Biomat features within carbonate rock of the Semri Group and microbial mat influence on carbonate depositional system.
- Geochemical analysis and Hydrocarbon maturation level of the Semri Group sediments exposed around Maihar area.

Chapter 2

GENERAL GEOLOGY OF THE VINDHYAN BASIN

2.1 Basement Rock

The Vindhyan basin is a sickle-shaped basin on the Bundelkhand-Aravalli Province which stabilized prior to 2.5 Ga (Eriksson et al., 1999). The Vindhyan Supergroup overlies a variety of Precambrian basement rocks including Bundelkhand Granite, Mahakoshal Group, Bijawar Group, Gwalior Group, Banded Gneissic Complex (BGC) and Chhotanagpur Gneissic Complex (CGC). The Bundelkhand Granite Complex separates the Vindhyan exposures of the Son Valley area from Chambal Valley area. The Bundelkhand Granite Complex is dominated by K-rich granite emplacement within Tonalite-Trondjhemite-Granodiorite complex (Rogers, 1986; Soni et al., 1987; Bandyopadhyay et al., 1995; Eriksson et al., 1999; Mazumder et al., 2000). The Mahakoshal Group (2.1-1.6 Ga) occurs on the southern and eastern margin of the Son Valley (Das et al., 1990; Roy and Bandyopadhyay, 1990). The Bijawar Group (2.1 Ga) remains confined on the northern and northeastern margin of Son Valley (Das et al., 1990;

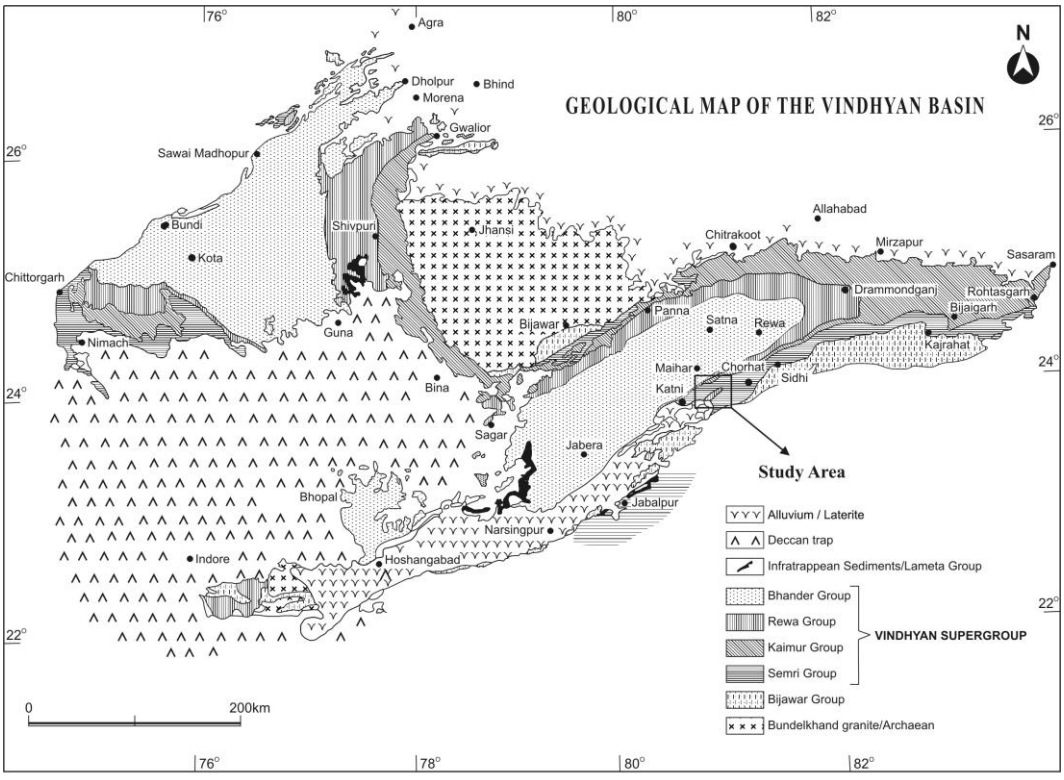

Fig. 2.1- Geological map of the Vindhyan Basin simplified after Soni et al. (1987).

Roy and Bandyopadhyay, 1990). Banded Gneissic Complex (BGC) and Gwalior Group form the basement of Vindhyan Supergroup in the Rajasthan sector (Heron, 1953). The Chhotanagpur Gneissic Complex (CGC) consisting of gneisses, granites and granodiorites with enclaves of tonalitic gneisses and ultramafic rocks forms the basement of the Vindhyan basin in most parts of eastern Son Valley area (Singh et al., 2001).

2.2 Lithostratigraphy of Vindhyan Basin

In the 19th & early 20th century, the stratigraphy of the Vindhyan Supergroup was studied by several workers (Mallet, 1869; Oldham et al., 1901; Heron, 1922, 1936; Coulson, 1927; Auden, 1933). Subsequently inter basinal correlation of spatially distributed stratigraphic units has only been established on the basis of lithological similarity (Prasad, 1984; Sastry and Moitra, 1984; Soni et al., 1987; Bhattacharyya, 1996). These workers refined the Vindhyan stratigraphy. Auden (1933) proposed the stratigraphic framework of the Vindhyan Basin in the Son Valley and divided the Vindhyan succession into four stratigraphic units. Later workers added and improved upon Auden's (1933) stratigraphy of the Vindhyan

Table 2.1- Stratigraphic succession of the Semri Group proposed by various workers.

Auden (1933)/ Prakash and Dalela(1982)	**Bhattacharyya (1996)**	**Bose et al. (2001)**
Rohtas Stage — Limestone and Shale	**Rohtas Subgroup** — Bhagwar Shale; Rohtasgarh Limestone	**Rohtas Formation** — Rohtas Limestone; Rampur Shale
Kheinjua Stage — Glauconitic Sandstone; Fawn Limestone; Olive Shale	**Kheinjua Subgroup** — Rampur Formation; Salkhan Limestone; Koldaha Shale	**Kheinjua Formation** — Chorhat Sandstone; Koldaha Shale
Porcellanite Stage — Porcellanite	**Mirzapur Subgroup** — Deonar Formation	**Porcellanite Formation**
Basal Stage — Kajrahat Limestone; Basal Conglomerate	**Mirzapur Subgroup** — Kajrahat Limestone; Arangi Shale; Deoland Formation	**Kajrahat Formation** — Kajrahat Limestone; Arangi Shale **Deoland Formation**

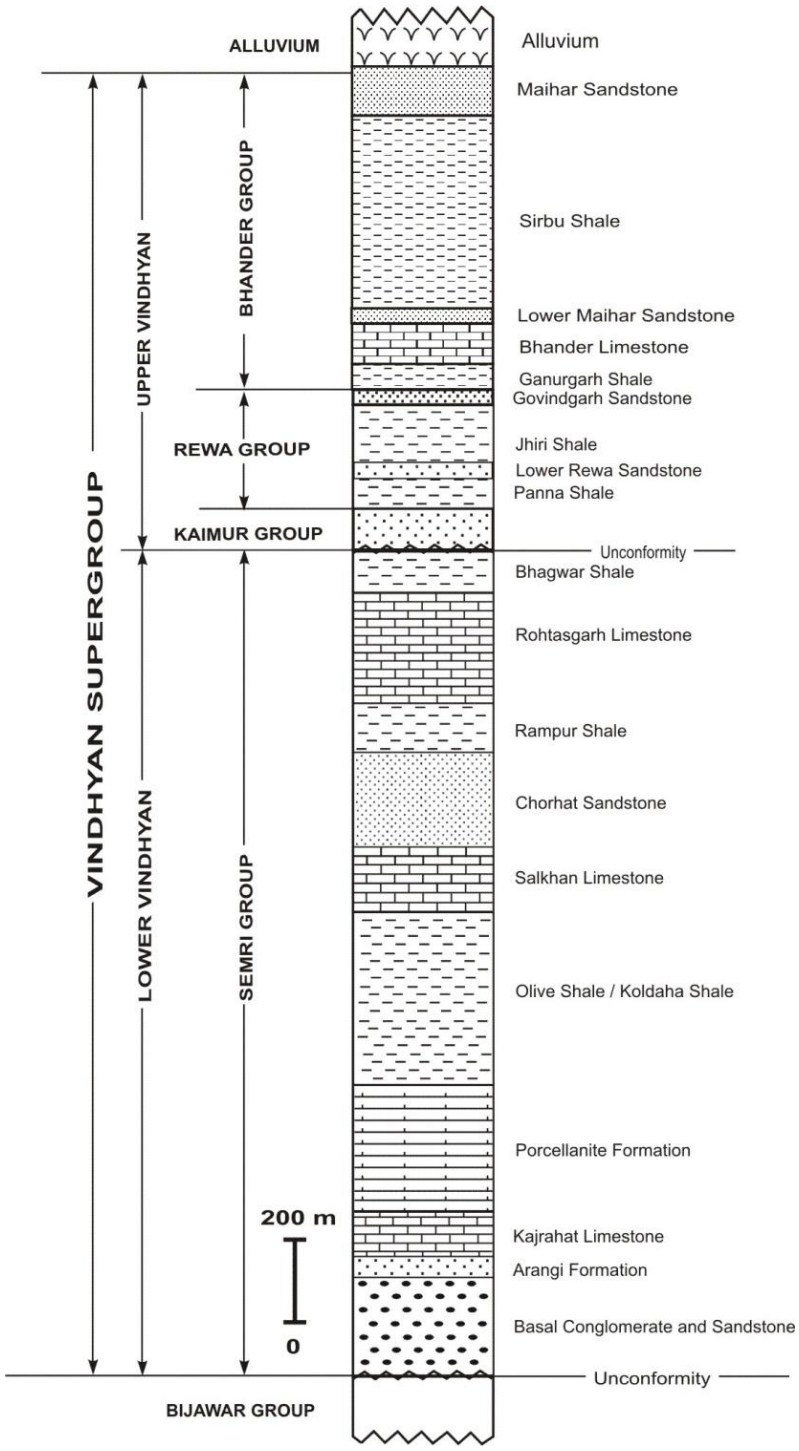

Fig. 2.2- Generalized Lithocolumn of the Vindhyan Supergroup exposed in Maihar area, M.P. (modified after Kumar and Pandey, 2008).

(Rao and Neelakantam, 1978; Chanda and Bhattacharyya, 1982; Soni et al., 1987; Bhattacharyya and Morad, 1993; Singh and Sinha, 2001; Bose et al., 2001) (Table 2.1; Fig. 2.1) and tried to correlate the Vindhyan sedimentary succession of the Son Valley with the Chambal Valley (Prasad, 1975, 1984; Kumar et al., 2005).

Sedimentary units in the Vindhyan Basin are primarily represented by shallow marine facies along with distal shelf to deep-water sediments. The maximum thickness of the entire Vindhyan Supergroup is estimated to be around 5 km, comprising mainly sandstone, shale and limestone (Bhattacharyya, 1996) and is divisible in the following stratigraphic order:

	Bhander Group
Upper Vindhyan	Rewa Group
	Kaimur Group
Lower Vindhyan	Semri Group

The Semri Group is the oldest group of the Vindhyan Supergroup. In the Maihar area, the Semri (Lower Vindhyan), Kaimur, Rewa and Bhander (Upper Vindhyan) are part of the Son Valley. The Semri Group is well exposed in the area and used for the present study. The Lower Vindhyan and Upper Vindhyan units are separated by multiple unconformities of undetermined duration (Bose et al., 2001). There is also evidence of an unconformity at, or near, the top of the Kaimur Group. The Semri Group in the Son Valley overlies the Bijawar Series of sediments and lavas, which contains volcanic rocks that Mathur (1981) correlates to the 1815 Ma Gwalior Volcanics. Prasad and Rao (2006) suggest that the Gwalior and Bijawar Series form an extensive part of the basement, as well as offering geophysical data suggest that the Hindoli Group extends beneath the Rajasthan section of the Vindhyan Basin. According to Bose et al. (2001), the Semri Group consists of five formations and is constituted of typically alternating shale, carbonate, sandstone and volcaniclastic units (Fig. 2.2). However, in the present thesis, the classification proposed by Bhattacharyya (1996) has been followed. The detailed lithostratigraphy of the Semri Group is provided below:

MIRJAPUR SUBGROUP

Deoland Formation

The Deoland Formation is dominated by conglomerate and sandstone (Prakash and Dalela, 1982; Chakraborty and Bhattacharyya, 1996a; Singh and Sihna, 2001; Bose et al., 2001). It is the lowermost unit of the Semri Group. Thickness varies from 200 m to 500 m. Auden (1933) named it as the Basal Conglomerate but Sastry and Moitra (1984) has named it as Deoland Formation. It

shows angular unconformity with the underlying Bijawar Phyllites. It is represented by sandstone, conglomerate, breccia and lenticular bands of calcareous grit, dolostone with occasional stromatolites. The pebbles are well rounded to subangular and reach up to the size of 20 cm. It has red jasper, quartzite vein, quartz, chalcedony, black shale and slate etc. Conglomerates grade horizontally into sandstone. Sandy horizons show cross bedding and parallel bedding.

Arangi Formation

The Arangi Shale consists mainly of grey shale with thin sandstone interbeds, but its exposures are very limited and confined in the Son Valley. It overlies Deoland Formation comprising mainly shales, considered at par with Basal Shale described by Rao and Neelkantam (1978).

Kajrahat Limestone

The Kajrahat Limestone consists of limestone, dolomite and shales with widespread development of stromatolites at the upper portion of this horizon (Kumar, 1982; Prakash and Dalela 1982; Banerjee, 1997; Singh et al., 2001). Rao et al. (1979) described the Kajrahat Limestone as 'Kuteshwar Limestone Formation' from the Kuteshwar area (Maihar, M.P.). It has been divided into three members as the lower flat bedded limestone, the middle biohermal limestone and the upper flat bedded limestone. Mishra et al., (1990) have given the thickness of the Kajrahat Limestone in this area as ~300 m.

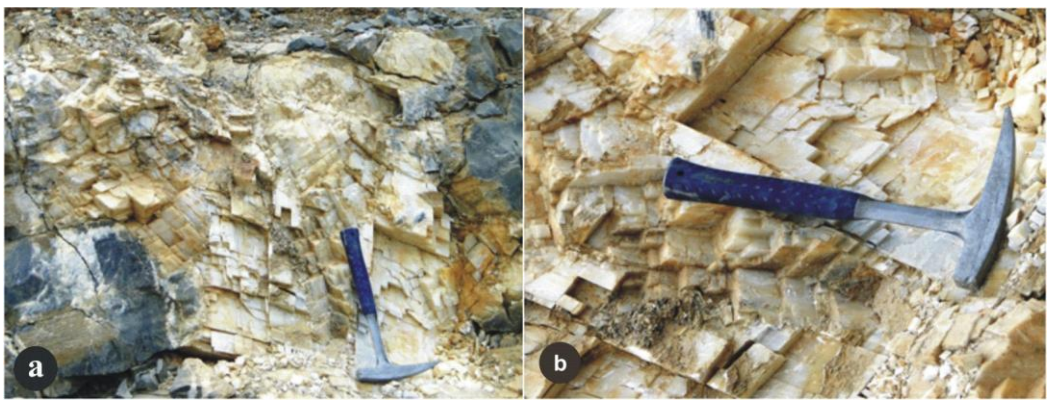

Fig. 2.3 (a, b) - Calcite veins in the Kajrahat Limestone, Kuteswar Mine, M.P.

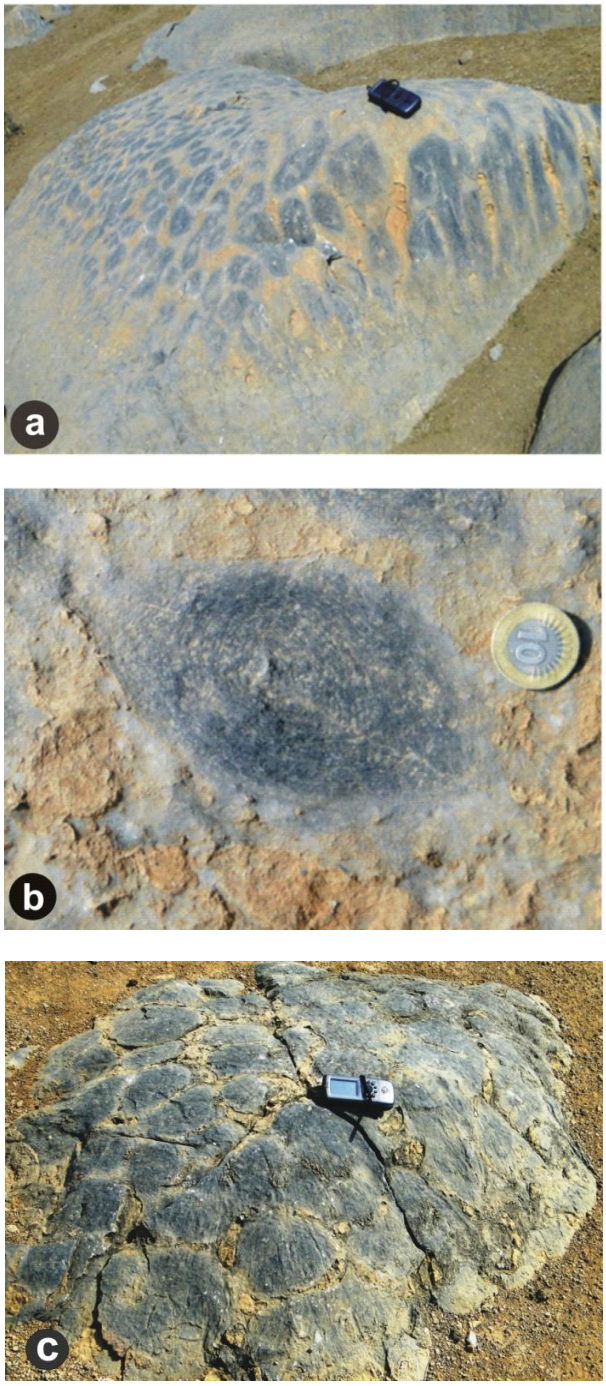

Fig. 2.4 (a, b & c) - Stromatolites in the Kajrahat Limestone, Chhoti Mahanadi River section, Kuteshwar, M.P. a- Longitudinal and plan view of the stromatolites in Chhoti Mahanadi sections; b-Plan view showing oblong section of the stromatolite column; c-Plan view of the stromatolites showing circular to oval cross sections.

In present field studies, Kajrahat Limestone is seen in two locality, Kuteswar Mine (N 23º58'29.9", E 80º48'32") and on the right bank of Chhoti Mahanadi River (N 23º58'39.9", E 80º49'48.5").

In Kuteshwar Mine, hard, compact and thick bed of dark grey colour limestone is seen, which changes into light grey to pinkish colour. Thick vein (~2m) of well crystallized calcite within the limestones is recorded (Fig. 2.3 a, b).

The Kajrahat Limestone in this place is noticed with pyrite. The precipitated 'fan fabric' structures are recorded in limestone beds which are very well exposed and radiating in upwards direction. These fan- fabrics are varied in length (1cm-10 cm).

Good exposures of the middle part of the Kajrahat Limestone are exposed on the right bank of the Chhoti Mahanadi, beneath the newly constructed bridge. There are repeated cycles of *Conophyton* in the middle part of the Kajarahat Limestone. Many forms of C*onophyton* along with *Colonnela*, *Calypso* (Fig. 2.4 a, b, c) and *Thyassagates* have been reported from this place (Kumar, 1999a). There are multimember and mono member of colonies stromatolites. Their conical laminae are laterally linked with each other. In the longitudinal view, they are linked to each other with prominent concavity and a axial zone. In the transverse section the columns are oval to elliptical in shape with outer laminae encircling other colums. At the base, the columns are about 50 cm in height and 10-25 cm in diameter.

The precipitated 'fan-fabric' structures are also very well exposed in banded and compact limestone, which has thickness up to 3 m (Fig. 2.5) in this place. The size of these structures varied from 1 cm-8 cm in length.

Figure 2.5- Fan-fabric structures exposed in the Kajarahat Limestone, Kuteshwar area, Satna District, M.P.

Deonar Formation

The sedimentary succession consisting of silicified shales, pyroclastics and volcanic tuffs, named as Porcellanite Formation (Auden, 1933; Pascoe, 1975; Singh et al., 2001; Srivastava et al., 2003), overlies the Kajrahat Formation. The term Porcellanite was first used by Mallet (1869). These rocks have been described as a stage (Auden, 1933). It attains a thickness of ~ 300 m. It has been accorded the rank of a formation and is included in the Mirzapur Subgroup by Sastry and Moitra (1984). The porcellanites are banded, hard, fine grained, varying in colour from black to pale green and show concoidal fracture. Presence of abundant pumice, euhedral quartz grains, euhedral zoned zircon crystals and volcanic bombs indicate volcanic origin of these deposites (Roy and Banerjee, 2001).

KHEINJUA SUBGROUP

The Kheinjua Stage of Auden (1933) was later termed as the Khenjua Subgroup. It has three formations stratigraphically, the Koldaha Shale (Olive Shale), the Salkhan Limestone (Kheinjua Limestone) and the Rampur Formation (Glauconitic Sandstone).

Koldaha Shale (Olive Shale)

The Porcellanites are overlain by a thick unit of the Olive coloured Shale and Siltstone with minor sandstone. The thickness varies from 70 to 120 m. This horizon has been given the name as the Koldaha Shale by Sastry and Moitra (1984). These shales are showing very thin lamination with textural and colour banding. Parallel bedding with low angle is discordances in lenticular beddings and graded bedding are noted. The Koldaha Shale is recorded near the Bansagar Lake. The thickness of this shale unit is ~10 m, with alteration of shale and siltstone (Fig. 2.6). This shale is friable and shows pencil cleaved fractures. The thick bed of sandstone is recorded at the top of this shale unit.

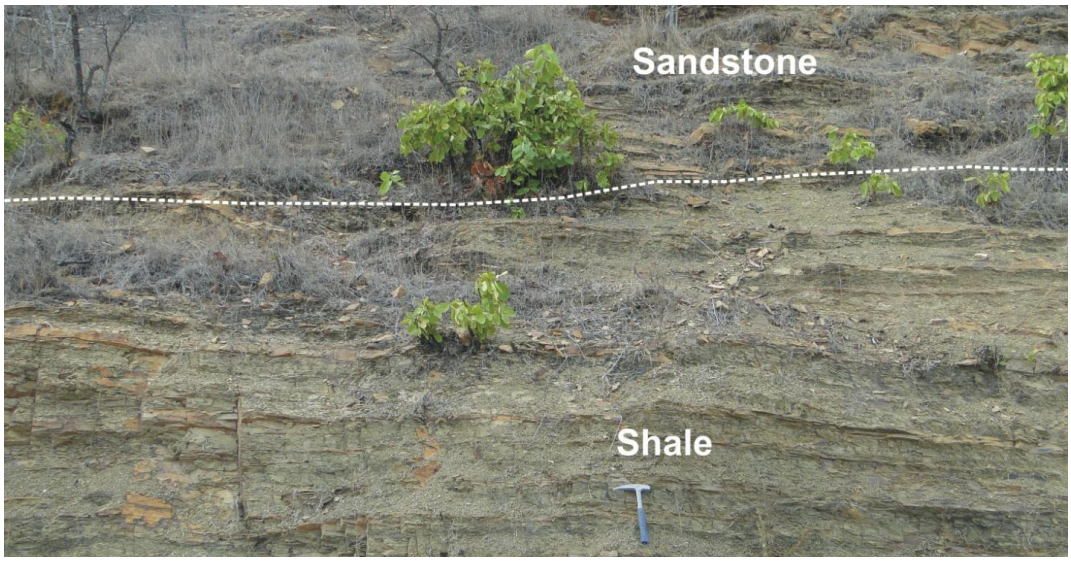

Fig. 2.6- Koldaha Shale with alteration of shale-silt–sandstone, coarsening upward sequence near Bansagar Lake, Maihar, M.P.

Salkhan Limestone

It has also been referred to as the Bargwan Limestone (Prakash and Dalela, 1982). Fawn limestone is redesignated as the Salkhan Limestone by Sastry and Moitra (1984). Its maximum thickness is ~90 m. It is made up of fawn weathering, siliceous and cherty limestone and dolostone with minor shale. The Salkhan Limestone, overlying the Koldaha Shale (earlier reported as Nauhatta Limestone Formation by Venkatachala et al., 1990) is well developed, it is extremely fine grained and cherty in nature. On the way to Bansagar Lake via Amarpatan, 5 km before Lake (N-24^{o}08'. 042", E- 81^{o}00'.647"), chertified Salkhan Limestone is recorded (Fig. 2.7). This chert is dense, black in colour and waxy lusture on freshely broken concoidal faces. Edgewise conglomerate bed is horizontally exposed between limestone beds on this place (Fig. 2.8). Megaripples and mud cracks are also exposed on bedding suface of the Salkhan Limestone (Fig. 2.9).

Rampur Formation

The 85-m thick Rampur Shale belongs to the lower part of the Rohtas Formation (Sarkar et al., 2002). This formation is glauconite bearing sandstone horizon which is redesignated as the Rampur Formation by Rao and Neelkantam (1978). Thickness of this formation varies between 100-800 m (Sastry and Moitra 1984).

The shales show ripple marks, small scale cross bedding and mud cracks. The Rampur Formation is exposed near Kudri Village, located at N-24° 9.28', E-80° 59.05'. Shales are mostly hetrollithic, well sorted siltstones/fine grain sandstones filled with gutters marks and wrinkle marks with local spill over. Different kind of sole features are noted. The gutter fills are planer, cheveron, wavy and hummocky laminated (Fig. 2.10). In these shales, well preserved carbonaceous megafossils and Microbial Induced Sedimentary Structures (MISS) are recorded.

ROHTAS SUBGROUP

Rohtasgarh Limestone

Fig. 2.7- Chertified Salkhan Limestone near Bansagar Lake, Maihar area, M.P.

Fig. 2.8- Edgewise conglomerate, exposed in the Salkhan Limestone exposed in Maihar area, M.P.

Fig. 2.9- Patterns of megaripples on the Salkhan Limestone, near Bansagar Lake, Maihar area, M.P.

Fig. 2.10 Distribution of Rampur shale near Rampur village, Maihar area, M.P.

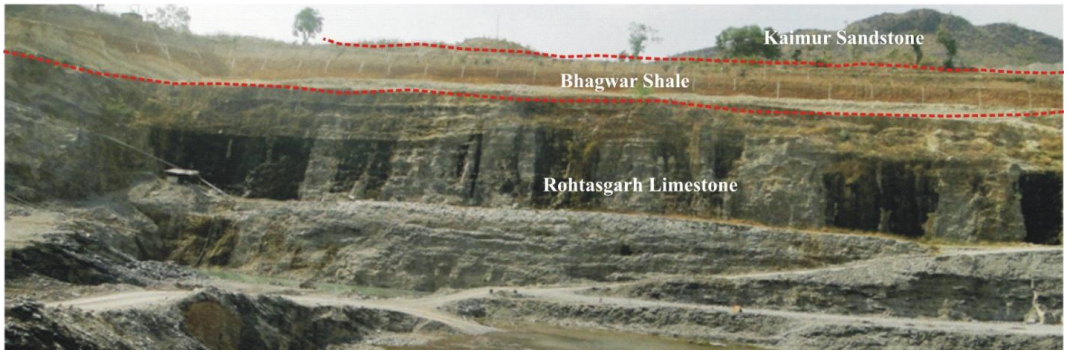

Fig. 2.11- Contacts of the Rohtasgarh Limestone, the Bhagwar Shale and the Kaimur Sandstone in Bistara Mine, Katni District, M.P.

It is the basal unit of the Rohtas Subgroup comprising greyish to greyish black limestone and shales. Its thickness varies ~200 in east to 500 m in the west in Rewa District. At places, it shows development of nodules within the shales. Mostly it shows parallel lamination. In present study, the general geology of Rohtasgarh Limestone is observed at different localities such as, Badanpur Mine (N-24° 10.37', E-80° 51.37') of Maihar Cement Factory, Bistara Mine (N-23° 58'.372", E- 80° 27'.107") and Amehta Mine (N-24° 01'.111', E- 80° 32.848'). In these areas, limestone is present in the subsurface. The upper horizon of the Rohtasgarh Limestone is represented by the grey shales, calcareous shales and silicified shales (Fig. 2.11).

Amehta and Bistara Mines have yielded very well preserved megascopic carbonaceous forms. This area is tectonically little disturbed. The folded beds are dipping at high angle in Amehta and Bistara mines. Calcite veins, microbial mat structures and slicken-side like calcite sheets are very common in these areas. Dark black shales alteration within limestones is recorded (Fig. 2.12 a, b).

The black shale units are ~1 cm to 15 cm thick bed between limestone beds.

Fig. 2.12 (a, b) - Rohtasgarh Limestone with the alteration of black shale exposed in Amehta Mine, M.P.

Fig. 2.13-Pyrite bearing Noduler Limestone is exposed in Badwar Village, Maihar area, M.P.

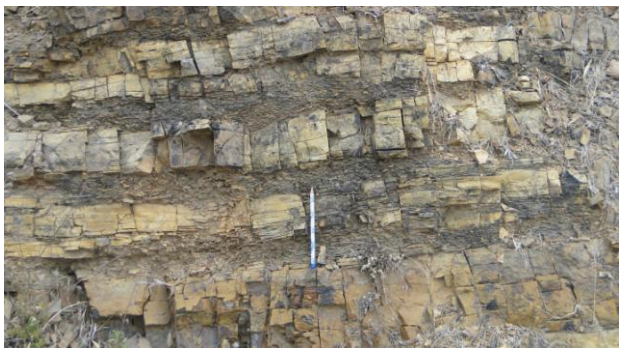

Fig. 2.14- Bhagwar Shale with Porcellanite bands exposed in Maihar area, M.P.

Nodules are recorded from the Rohtasgarh Limestone in a dug-bore-well. These nodules are pyrite bearing, which are exposed horizontally along the interbeded limestone and grey shales near Badwar Village (Fig. 2.13). This intercalation of black shale and limestone gradually passes into the Bhagwar Shale which is exposed at higher reaches of the section and on the road section to Kymore. The Bhagwar Shale is capped by Kaimur Sandstone.

Bhagwar Shale

It is the uppermost lithounit of the Rohtas Formation and also the youngest lithounit of the Semri Group in the Son Valley area. Its thickness varies from 20-125 m. It is represented by silicified shale, sandstone and carbonaceous shale. The contact of Rohtasgarh Limestone and Bhagwar Shale is seen near Bistara Mine, exposed between Rohtasgarh Limestone and Kaimur Group. A small patches the Bhagwar Shale and Porcellanite is exposed at N-24° 14’ 395”, E- 81° 01’ 829” near Maihar (Fig. 2.14). There is ~ 2 m thick section with small lateral extent exposed.

KAIMUR GROUP

The Kaimur Group derives its name from Kymore range in Central India. The name was first suggested by Oldham (1856) for the lowest Series of Vindhyan System. The Kaimur Group is an assemblage of sandstone, shale, flagstone and porcellanites and rest upon the Semri Group. The lower limit is generally marked by a conglomerate of ferruginous lateritic bed throughout a large part of its margin. The Kaimur Group is exposed almost all over the Vindhyan basin and

overlaps the Semri Group. The maximum thickness is 400 m. In the Son Valley area this group has been devided into 7 lithounits by Auden (1933) (Table 2.2).

Table 2.2- Lithostratigraphic succession of the Kaimur Group.

	After Auden (1933)	**After Sastry and Moitra (1984)**
Upper Kaimur Stage	Dhandraul Quartzite Scarp Sandstone	Dhandraul Sandstone Mangesar Formation
Lower Kaimur Stage	Bijaigarh Shale Upper Quartzite Susnai Conglomeratic Breccia Silicified Shale Lower Quartzite	Bijaigarh Shale Ghaghar Sandstone Susnai Breccia Sasaram Formation

REWA GROUP

The Rewa Group was mapped first time by Medlicott (1860) in Banda and Lalitpur district of U.P. Krishnan (1968) and Vredenburg (1906) considered the Rewa Group of rocks as separate from the underlying Kaimur by a diamondiferous conglomerate. The rocks of the Rewa Group are best developed in Panna and Satna Districts (M.P.) (Rao et al., 1979). The thickness of this group varies in Son Valley from 182-296 m (Soni et al., 1987). The generalized stratigraphic succession of the Rewa Group is given bellow (Table 2.3) after Krishnan (1968) and Shastry and Moitra (1984) in the Son Valley.

Table 2.3- Lithostratigraphic succession of the Rewa Group in the Son Valley.

	After Krishnan (1968)	**After Sastry and Moitra (1984)**
Rewa Group	Upper Rewa Sandstone Jhiri Shale Lower Rewa Sandstone Panna Shale	Govindgarh Sandstone Jhiri Shale Asan Sandstone Panna Shale

BHANDER GROUP

The Bhander Group constitutes the youngest group of the Vindhyan Basin. The original classification proposed by Krishnan (1968) was modified by Shastry and Moitra (1984), (Table 2.4). The Bhander Group contains the only major carbonate unit in the upper Vindhyans, a unit containing stromatolites, ooids, and micritic layers known as the Bhander or Lakheri Limestone (Bose et al., 2001). The overlying Lower Bhander Sandstone marks a transition into shallow marine,

sometimes fluvial, sandstone typical of the Bhander Group (Bose et al., 2001). The Sirbu Shale overlies the Lower Bhander Sandstone, and is in turn overlain by the Upper Bhander Sandstone. Bose et al. (2001) observed that the upper Bhander Sandstone is primarily a unit of coarse, red sandstones, and may represent former barrier islands, sand bars, beaches and fluvial systems (Akhtar, 1996).

Table 2.4- Lithostratigraphic succession of the Bhander Group in the Son Valley.

	After Rao in Awasthi (1964)	**After Sastry and Moitra (1984)**
Bhander Group	Maihar Sandstone	Shikoda Sandstone
	Sirbu Shale	Sirbu Shale
		Bundi Hill Sandstone
	Bhander Limestone	Lakheri Limestone
	Ganurgarh Shale	Ganurgarh Shale

2.3 Palaeogeography of the Vindhyan basin

There have been several attempts to describe the depositional setting and palaeogeography of the Vindhyan basin. Most of the workers considered the Vindhyan succession as nearshore marine deposits with intermittent subaerial exposure (Auden, 1933; Valdiya et al., 1982; Chanda and Bhattacharyya, 1982). In other cases, tidal, barrier bar, beach and lagoonal facies were considered to be dominating in the Vindhyan succession (Banerjee, 1964, 1974; Misra, 1969; Singh, 1973, 1985; Rao and Neelkantam, 1978; Chanda and Bhattacharyya, 1982; Prakash and Dalela, 1982; Prasad and Verma, 1991; Akhtar, 1996; Chakraborty, 2001; Anbarasu, 2001). Banerjee (1974) considered its deposition in shallow marine beach and barrier island and lagoon complex settings. Chanda and Battacharyya (1982) considered it as shallow marine, tidal flat lagoon- sand wave complex. Singh (1973, 1980,1985) considered it as shallow littoral sea, shoal bar complex and lagoon. Basumallick et al. (1996) made some important observations of tidal cyclicity within the predominantly lagoon-tidal flat originated Lower Bhander Sandstone. However, the palaeogeographic interpretations were seldom substantiated by process related facies analysis. Palaeogeographic interpretations of the Vindhyan Supegroup were based mainly on the studies of younger formations of the Vindhyan Supegroup in the Son Valley. The workers extrapolated the palaeogeographic interpretations of the Upper Vindhyan to the Semri Group. Going beyond the shallow marine interpretation for the Vindhyan Supergroup Bhattacharyya and Morad (1993) proposed fluvial origin of the

sandstones of the Kaimur Formation. Chakraborty (1993, 1996) recognized eolian longitudinal dunes from the Kaimur Formation and Bose and Chakraborty (1994) identified fluvial and eolian deposits in the Rewa Formation. Bose et al. (1999) took a process related approach to recognize longitudinal eolian dunes from the Bhander Formation. In a significant departure to the earlier interpretations Bhattacharyya (1996) considered the Kaimur Formation as fluvio-lacustrine. Facies analysis and its palaeogeographic interpretation in the Vindhyan basin have mostly been carried out in last two decades (Bose and Chaudhuri, 1990; Chakraborty and Bose, 1990, 1992; Chakraborty, 1995; Sarkar et al., 1996, 2002; Bose et al., 1997a; Chakraborty et al., 1998; Banerjee, 2000; Chakraborty, 2004; Banerjee et al., 2005; Banerjee and Jeevankumar, 2003, 2005a, b). Bose et al. (2001) presented most comprehensive palaeogeographic synthesis of the Vindhyan Supegroup in the Son Valley. According to them Vindhyan sedimentation took place dominantly in shelf setting and the Vindhyan succession encompasses several cycles of progradation and retrogradation. Prasad (1984) considered shallow marine intertidal to supratidal flat for most part of the Vindhyan. Chaudhuri and Bose (1982) recognized eolian signature in the Rewa Formation. Based on detailed facies analysis, Bose et al. (1988) considered the Kaimur Formation as storm-dominated shelf product. Casshyap et al. (2001) and Raza et al. (2002) identified barrier inlet, lagoon to tidal flat environment of deposition for the Semri Group.

2.3.1 Palaeogeography of the Semri Group

The present state of the knowledge about the palaeogeography of the Semri Group is discussed below:

Earlier workers considered the basal conglomerate at the base of the Deoland Formation as of glacial origin (Dubey and Chaudhary, 1952; Chaudhary, 1953; Ahmad 1955, 1971, 1981; Mathur, 1954, 1960, 1981, 1989). Ghosh (1971a), Banerjee (1974) and Lakshmanan (1968), considered beach origin for the sandstone and conglomerate near the base of the Vindhyan. Prakesh and Dalela (1982) and Rao and Neelakantam (1978) considered Deoland Formation as shallow marine product. The sandstone and conglomerate were also interpreted as fluvial deposits (Singh, 1973; Sharma, 1980) and fan delta deposits (Chakraborty

and Bhattacharyya, 1996a). Williams and Schmidt (1996) considered the basal conglomerate on the northern flank of the Vindhyan Basin in the Son Valley as mass-flow deposits and ruled out glacial origin because of lack of characteristic features. Bose et al. (2001) considered Deoland Formation as shallow shelf deposits.

The Arangi Shale has very scanty exposure in most parts of the Son Valley area. Nevertheless, the Arangi Shale was interpreted as lagoonal deposits (Singh, 1973; Banerjee, 1974; Gupta et al., 2003). Coaly matters reported from the Arangi Shale were considered as biogenic on the basis of stable isotopic studies (Mathur, 1964; Krishnamurthy et al., 1986).

The Kajrahat Limestone, with profuse development of stromatolites, was considered as tidal flat deposits (Singh, 1973; Banerjee 1974; Chanda and Bhattacharyya, 1982; Prakash and Dalela, 1982). Banerjee (1997) and Bose et al. (2001), however, considered that depositional setting fluctuated between subtidal to supratidal.

The Porcellanite Formation was considered as of pyroclastic origin (Auden, 1933; Ghosh, 1977; Srivastava, 1977; Rao and Neelakandam, 1978; Mehrotra et al., 1985; Srivastava et al., 2003). Differences in opinion, however, existed regarding the depositional setting of the Porcellanite Formation. Srivastava (1977) considered it subaerial volcanic ash fall deposit. Ghosh (1971b) and Chakraborty et al. (1996) considered it as deep marine product. Singh (1973) considered it as lagoonal in origin. Bose et al. (2001) recorded several shallow subaqueous to subaerial transitions within the thick volcaniclastics and considered it as dominantly ash fall type of deposits. Srivastava et al. (2003), considered it as fissure and vent type of submarine volcanism in a tidal flat setting.

The Kheinjua Formation was considered exclusively as lagoon-tidal flat by Singh (1973), Banerjee (1974) and Akhtar (1996). Sarkar et al. (2002), Banerjee (1997, 2000), Bose et al. (1997a, 2001) and Banerjee and Jeevankumar (2003, 2005a) recorded offshore to shoreface transition within the Koldaha Shale. Based on seismic studies Ram et al. (1996) considered that the Semri Group to have attained the maximum bathymetry during the Koldaha Shale deposition.

The Fawn Limestone is generally considered as intertidal to supratidal deposit (Rao and Neelakantam, 1978; Prakash and Dalela, 1982; Chakraborty et al., 1996; Sharma, 1996; Sharma and Sergeev, 2004). The Rampur Formation

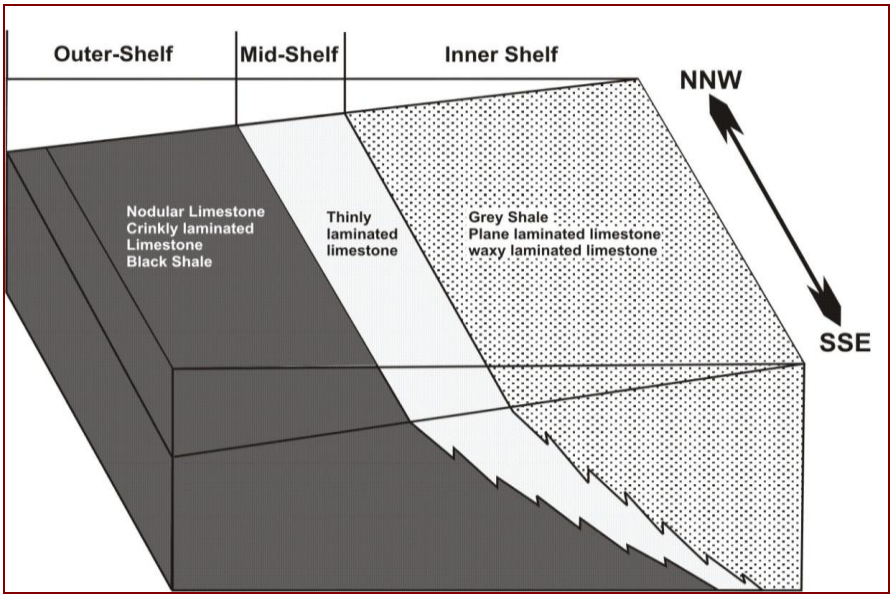

Fig. 2.15- Conceptual three-dimensional reconstruction of palaeogeographic distribution of the facies comprising the Rohtas Limestone. Palaeoshoreline alignment indicated (after Banerjee & Jeevankumar, 2007)

developed under temperate storm- dominated shelves (Sarkar et al., 2002, Fig. 2.15).

The Chorhat Sandstone was generally considered as shallow marine origin by all the workers (Singh, 1973; Banerjee, 1974; Rao and Neelakantam, 1978; Srivastava, 1978; Chanda and Bhattacharyya, 1982; Akhtar, 1996; Sarkar et al., 1996; Banerjee, 1997; Bose et al., 2001; Sarkar et al., 2005a, b).

A tidal-flat environment of deposition was suggested for the Rohtas Formation by the early workers (Singh, 1973; Banerjee, 1974; Prakash and Dalela, 1982; Chanda and Bhattacharyya, 1982). Chakraborty et al. (1996b) reported mass-flow conglomerate and possible turbidite sequences from the Rohtas

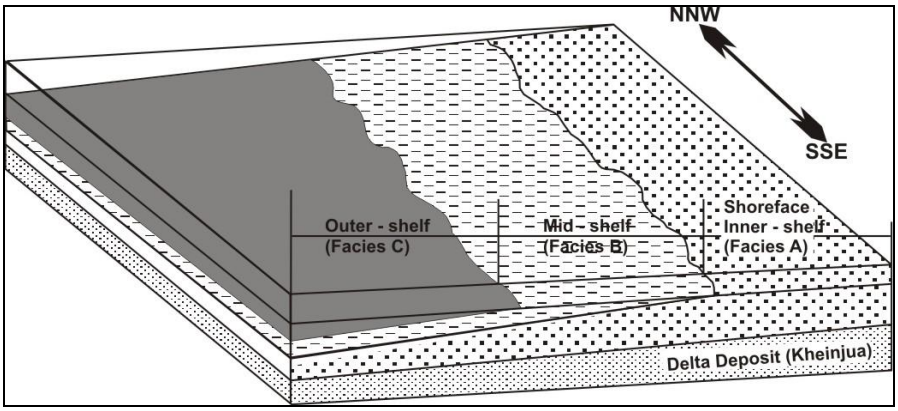

Fig. 2.16- Three-dimensional reconstruction of palaeogeographic variation between the facies, and their superposition as a result of continuing transgression on the Kheinjua deltaic system. Palaeoshoreline alignment is indicating (after Sarkar et al., 2000).

Limestone and considered it as slope deposit. On the contrary, Chatterjee and Sen (1988) and Banerjee (1997) considered the succession as open shelf originated. Chatterjee and Sen (1988) conducted spectral analysis of limestone-shale thickness variations and indicated a long ranging rhythmic depositional process in response to eustatic sea level fluctuations. Bose et al. (2001) and Banerjee et al. (2007) recorded overall shoaling upward trend in the predominantly shelf originated Rohtas Limestone (Fig. 2.16).

The different views of Singh (1973), Banerjee (1974) and Bose et al. (2001) are summarized in Table 2.5.

Table 2.5- Depositional environment of the Vindhyan Supergroup exposed in the Son Valley area..

	Fm.	**Member**	**Depositional Environment**		
			After Singh (1973)	**After Banerjee (1974)**	**After Bose et al. (2001)**
UPPER VINDHYAN	Bhander	Upper Bhander Sandstone	Tidal flat shoal complex	Tidal flat	Fluvio- eolian and marginally marine
		Sirbu Shale	Lagoon	Tidal flat (superatidal)	Lagoon to shelf
		Lower Bhander Sandstone		Tidal flat	Coastal playa
		Bhander Limestone	Carbonate tidal flat	Carbonate tidal flat	Shallow marine
		Ganurgarh Shale		Lagoon and tidal flat	
	Rewa	Rewa Sandstone	Shoal beach complex	Barrier beach dune	Tidal to fluvio-eolian
		Rewa Shale	Lagoon	Lagoon	Shelf
	Kaimur	Upper Kaimur	Shoal complex	Barrier beach	Shelf to fluvio eolian
		Lower Kaimur	Tidal flat	Barrier bar to tidal flat	Intertidal to shelf
LOWER VINDHYAN	Rohtas	Rohtas Limestone	Carbonate tidal flat (subtidal to intertidal)	Lagoon	Shelf
		Rampur Shale	Tidal flat (intertidal)	Carbonate tidal flat	Shelf
	Kheinjua	Chorhat Sandstone			Shallow marine
		Koldaha Shale	Lagoon	Lagoon to tidal flat	Dominantly shelf deltaic fluvial
	Porcellanite		Lagoon	Lagoon	Shallow marine
	Kajrahat	Kajrahat Limestone	Carbonate tidal flat (subtidal to intertidal)	Lagoon (tidal flat toward top)	Subtidal to peritidal
		Arangi Shale	Lagoon	Shallow marginal lagoon	Shelf
	Deoland		High gradient coastal rivers	Marine and beach	Shallow shelf

2.4 Tectono-sedimentation model of the Vindhyan basin

Accumulation of a huge thickness of shallow water sediments in intracratonic basins indicates synsedimentary subsidence. Like palaeogeographic interpretations there exists conflicting views regarding the origin and evolution of the Vindhyan Basin (Table 2.6). A broad consensus is that the Vindhyan sediments were deposited in an E-W elongated intracratonic rift basin opening towards west (Bose et al., 1997a, 2001). Based on seismic investigations Kaila et al. (1989) indicated rifting in the basement with boundary faults trending E-W. Ram et al. (1996) and Ram (2005) recognized several NW-SE trending extensional faults and considered that rifting was active during the deposition of the Semri Group. They suggested that the Vindhyan Basin was originated as an intracratonic half-graben basin with well defined pre-, syn- and post- rift phases of development. Bose et al. (1997a) supported the rift basin origin of the Vindhyan basin based on sedimentary attributes including palaeoseismic features, palaeodrainage pattern, palaeocurrent data and petrology of sandstones. Bose et al. (1997a, 2001) considered the Vindhyan Basin in Son valley as a EW elongated half-graben which was divided into a series of sub-basins by NW-SE trending cross-faults that resulted because of dextral shear component. Furthermore, Bose et al. (2001) recorded evolution of the basin from intracratonic-rift of lower Vindhyan to intracratonic sag of upper Vindhyan. Other opinions for the affinity of the Vindhyan Basin include foreland basin, intracratonic basin, strike-slip basin and syneclise (Table 2.6).

Table 2.6- Tectonic model of Vindhyan Supergroup exposed in the Son Valley area.

Tectonic models	Reference
Foreland basin	Auden 1933
Foreland basin	Chakraborty and Bhattacharyya, 1996a,b
Foreland basin	Raza and Casshyap, 1996
Foreland basin	Chakraborti et al. 2004
Strike slip basin	Crawford, 1978
Syncline	Chanda and Bhattacharyya, 1982
Syncline	Chaudhuri and Chanda, 1991
Syncline	Prakash and Dalela, 1982
Rift basin	Choubey, 1971
Rift basin	Naqvi and Rogers, 1987
Rift basin	Kaila et al., 1989
Rift basin	Verma and Banerjee, 1992
Rift basin	Ram et al., 1996
Intracontinental basin	Valdia, 1982
Rift to Sag Transition	Bose et al., 2001

2.5 Age of the Lower Vindhyan Basin

For many years, the age of the Vindhyan Supergroup has been a matter of discussion because of the scarcity of datable materials in the Vindhyan sedimentary successions. Venkatachala et al. (1996) proposed 1400 to 550 Ma age bracket for the Vindhyan based on a detailed review of existing radiometric and microfossil dates. The Bundelkhand Granite basement provided an age of 2505 Ma (Crawford and Compston, 1970). The Arangi Shale was dated as 1243.1±218.3 Ma (Srivastava and Rajagopalan, 1988). Glauconitic Sandstones of the Vindhyan Supegroup were dated by Vinogradov et al. (1964). The dates were recalculated by Kreuzer et al. (1977) who provided radiometric dates of 1080 ± 40 Ma for the Kheinjua Subgroup and 890 ± 40 Ma for the Kaimur Group.

The younger age limit of the Vindhyan has been provided as 550 Ma (Crawford and Compston, 1970). Most reliable of the age dating are those derived from the Kimberlite intrusion in the Kaimur Formation (Paul et al., 1975; Kumar et al., 1993). The Kimberlite pipes fixed a strict younger limit of the Semri Group as 1100 Ma. Kumar et al. (1993) reported kimberlite intrusions around 1100 Ma from several places in India and proposed that Proterozoic Kimberlite/lamproite activities in India were contemporaneous, although widely separated in space. Discovery of metazoan trace fossil from presumably 1200 Ma old Kheinjua Subgroup by Sarkar et al. (1996) and Seilacher et al. (1998) created tremendous interest in Vindhyan geology among the geochronologists, palaeontologists and sedimentologists world over. Sensational discovery of small shelly fossils by Azmi (1998) and Ediacaran fossil remains by Kathal et al. (2000) from the Semri Group created further confusion for the already existing age controversy in Vindhyan. Azmi's claim that major portion of the Vindhyan Supergoup belongs to Phanerozoic was supported by Banerjee and Frank (1999). These workers proposed a 617 ± 4 Ma age for a single sample of the Porcellanite Formation based on Ar-Ar plateau. The true age of Vindhyan was an open question during that time. All these conflicting reports, however, renewed interest in Vindhyan chronology.

Table-2.7- Revised ages of the Semri Group based on recent radiometric dates.

Formation	Geographical Position	Method	Age	References
Tirohan Limestone	Chitrakoot, M.P.	Pb-Pb, Isochron	1650 ± 89 Ma	Bengtson et al. 2009
Rohtas Limestone	Tikaria, Katni, M.P.	Pb-Pb, Isochron	1599 ± 48 Ma	Sarangi et al. 2004
Rohtas Limestone	Various localities in Son Valley, M.P. & Rajashtan	Pb-Pb, Isochron	1601 ± 130 Ma	Ray et al. 2003
Rampur Shale	Sidhi District M.P.	SHRIMP, U-Pb Zircon	1599 ± 8 Ma	Rasmussen et al. 2002
Rampur Shale (Tuff Bands)	Sidhi District M.P.	SHRIMP, U-Pb Zircon	1602 ± 10 Ma 1628 ± 12 Ma	Rasmussen et al. 2002
Deonar Formation (Two Rhyolitic volcanic horizons)	Sidhi District M.P.	U-Pb, Zircon, $^{86}Sr/^{86}Sr$ Isotope	1631 ± 1 Ma 1631 ± 5 Ma	Ray et al. 2002
Deonar Formation (Porcellanite Formation)	Sidhi District M.P.	SHRIMP, U-Pb Zircon	1628 ± 8 Ma	Rasmussen et al. 2002
Base of the Semri Group	Chitrakut area, U.P.	Rb-Sr Model ages	1409 ± 14 Ma 1531±15 Ma	Kumar et al. 2001
Basement rocks	Bundelkhand Granite	Pb-Pb Zircon (SIMS)	2492 ± 10 Ma	Mondal et al. 2002

The age of Vindhyan Supegroup is revised based on consistent radiometric dates obtained in past few years. The age of Kheinjua Subgroup is revised to 1600 Ma from the earlier estimation of 1200 Ma (Table-2.7; Kumar et al., 2001; Rasmussen et al., 2002b; Ray et al., 2002). Kumar et al. (2001) provide a 1600 ± 50 Ma age for the lower Vindhyan sediments of the northern flank of the Vindhyan basin in the Chitrakut area based on Rb/Sr dating of glauconites. However, in the Chitrakut area the Semri Group has become considerably thinner (up to 20 m) consisting mainly of stromatolitic dolostone, pellet dolostone and glauconitic sandstone and represents condensed deposits (Singh and Kumar, 1978). Ray et al. (2003) proposed roughly 1700 Ma age for the Kajrahat Limestone based on U/Pb dating of the carbonates. Rasmussen et al. (2002) and Ray et al. (2002) provided 1628 ± 8 Ma (Rasmussen et al., 2002) and 1631 ± 5 Ma (Ray et al., 2002) age for the overlying Porcellanite Formation. The SHRIMP U-Pb zircon dating of volcanic ash bed occurring within the Rampur Shale provided

1599 ± 8 Ma (Rasmussen et al., 2002). Sarangi et al. (2004) dated the Rohtas Limestone as 1599 ± 48 Ma by Pb-Pb isochron technique. Ray et al. (2003) proposed 1601 ± 130 Ma for the Rohtas Limestone by Pb-Pb isochron technique on the carbonate samples. Bengtson et al. (2009) carried out Pb isotope analyses of the phosphorite intraclasts that yielded an age of 1650 ± 89 Ma age of the fossils yielding stromatolitic unit of Chitrakoot. This unit is equivalent to the Rohtasgarh Limestone.

All the recent radiometric dates provide a much better age constraint for the Semri Group compared to the Upper Vindhyan Group. The data also suggest an age range representing Palaeoproterozoic to Mesoproterozoic transition for the Semri Group. Rathore et al. (1999) dated the glauconites of the Sirbu Shale by K-Ar methods and gave 741 ± 9 Ma as mean depositional age of the Sirbu Shale of Bhander Group. The upper age limit of the Vindhyan Supergroup can be constrained by the 650-750 Ma age data for the Bhander Limestone (Ray et al., 2003).

Chapter 3

MATERIALS AND METHODS

Detailed field observations, samples collection and their laboratory studies are the mainstay of the present work. In field work most extensive and essential geological equipments like hammer, chisel, brunton, measuring tape, and camera were used etc. Survey of India Toposheets (64A/13, and 63D/16) were consulted for the present study. The study area and sampling localites for the Lower Vindhyan exposures are mainly around Maihar area, Satna District, M.P. This chapter provides a detailed description of the methodologies adopted for work.

3.1 Field Studies

The Semri Group is well exposed around Maihar area, Satna District M.P. (Fig. 3.1). For palaeobiological investigations and geochemical studies, the samples are collected from different stratigraphic units of the Semri Group, exposed around this area. The Kajrahat Limestone, the Salkhan Limestone, the Olive Shale, the Rampur Formation and the Rohtasgah Limestone, are studied in the field.

3.2 Laboratory Methods

3.2.1 Thin Sections Preparation

Thin sections of fossiliferrous chert and carbonate rock were prepared in the section preparation lab of the Birbal Sahni Institute of Palaeobotany, Lucknow. The samples were broken into small pieces. Samples were then polished over a piece of glass by using 400, 800 and finally 1000 mesh carborundum powder. The polished smooth surface was then mounted on a glass slide using cold-setting epoxy resin (R.I.>1.54). The other side of the sample was polished in the same way. The final thickness of the sections was reduced close to 50-30 µm.

3.2.2 Microscopic Measurement

Entire microscopic observations were undertaken in BSIP, Precambrian palaeobiology laboratory. Mainly two microscopes were used for macro and microfossils studies.

Fig. 3.1- Google earth map showing field work studies and samples collection localities around Maihar area, M.P.

The Stereo-microscopy: In the present study, Stereomicroscope Leica MZ12 was used to observe, morphological features and digital photography was done to collect megafossils images on hand specimens. It uses two separate optical paths with one objective and two eyepieces to provide three-dimensional visualization of the sample under examination. The Light microscopy: Nikon Eclipse 80*i*, was used for microfossils observation and photodocumentation of palynological slides under transmitted light. Mainly chert and carbonate thin sections were observed for microfossils study.

3.2.3 Maceration

Maceration or acid digestion of rocks is a technique to extract insoluble organic microfossils from a rock matrix as carbonates, siliciclastic rocks, carbonaceous siltstone and shales. The following steps were used to extract acritarchs from the rocks: Cleaning, disaggregations, removal of carbonates, removal of silicates, and removal of fluorides, oxidation, filtration, and slide preparation. These are shown in a flow-chart (Fig. 3.2).

Cleaning and disaggregation- Samples were cleaned externally by scrub with a stiff brush to remove mud. In such cases, the elimination of possible surface contamination was censured by careful washing of the samples. They were placed in the container to be used for acid digestion, and washed with hot, running tap water until the decanted water ran clear. The sample was then washed two or three times using distilled water. Avoid violent crushing methods otherwise large size (> 500 µm) specimens of acritarch may be fragmented. Both Burzin (1990) and Butterfield et al., (1994) pointed out that bedding-parallel thin sections revealed concentrations of fossils and concluded that much of the fragmentation resulted from extraction methods.

Disaggregation is least destructive method of sample catching. Fissile shales were split along bedding surfaces using fingernails or a knife blade. Samples that required additional fragmentation were soaked in hot water to promote expansion along the partings. Alternate wetting and drying could break-up even well-consolidated samples. If above techniques fail to disaggregate then the sample were crushed either in a mortar and pestle or by using a hammer and a metal plate,

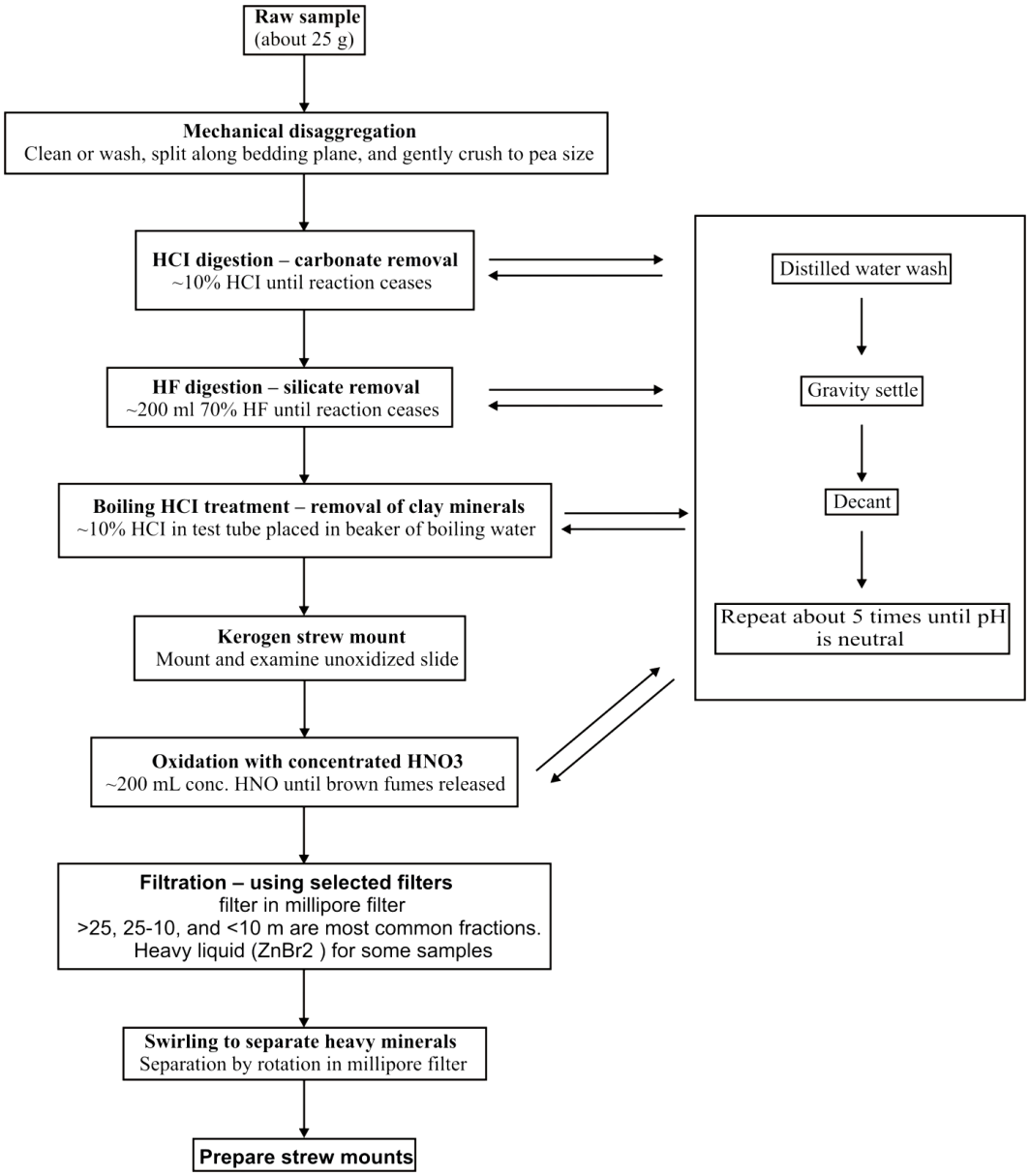

Fig. 3.2- Flow chart showing steps for extracting palynomorphs from Proterozoic samples (after K. Grey, 1999).

the samples were placed between two clean aluminum pie dishes (Phipps and Playford, 1984).

The diameter of crushed samples was 5 mm approximately. This size of sample was kept somewhat larger than that normally used for palynological preparation, but it reduced the risk of damaging larger acritarchs. Fragmented samples were then washed several times with distilled water.

Carbonate removal- Carbonate was removed by hydrochloric acid (HCl) treatment to prevent the formation of insoluble calcium and magnesium fluorides during the HF procedure. HCl treatment was carried out in the same plastic screw-topped container later used for HF acid digestion. A few milliliters (ml) of dilute

(about 10% of the stock solution) HCl were added to the sample to test the strength of the reaction. Samples that showed little or no reaction were treated directly with about 100 ml of 32% HCl. Any samples that showed a reaction were treated with gradually increasing quantities and strength of HCl until the reaction ceased. Samples were left in dilute acid for about 24 hours, and then tested again with fresh acid to check whether the reaction had ceased. The acid treatment was repeated until no further reaction was observed. The sample was then washed to near neutrality with distilled H_2O by settling and decanting after each wash (at least four washes were usually required). The solution was left slightly acidic so that any possible carbonates, precipitated when HF dissolved the silicates, would be dissolved by the residual HCl, reducing the formation of fluorides.

Fluoride removal- Gentle boiling with HCl was used to remove any precipitates that had formed during the HF processing. The decanted sample was transferred to a 500 ml, 25 mm-diameter, plastic screw-top test tube with a conical bottom. About 250 ml of 32% hydrochloric acid was added to the sample, and the contents were raised to boiling point as gently as possible by placing the tube in a beaker of water on a hotplate. Boiling was continued until the greyish, gel-like fluorides had dissolved. The sample was allowed to cool, and was then decanted, washed, and allowed to settle. The process was repeated until the pH was neutral.

Kerogen mount- A kerogen mount of the organic fraction was made at this stage as a record of the unoxidized sample and to determine thermal maturation. It was also used to estimate how much oxidation might be required.

Oxidation- About 200 ml of concentrated HNO_3 was added to the decanted sample to oxidize dark-coloured organic matter, and in some cases to remove pyrite framboids or surface encrustations. The amount of oxidation required was pre-determined from the kerogen mount or by microscopic examination of a few drops of macerate. Most samples required about 10 minutes of oxidation, but some required longer or shorter periods. Oxidation was stopped by the addition of distilled water, as soon as brown fumes were given off and the residue had changed colour from black to a honey brown. Some samples were difficult to oxidize because they contained abundant small pyritic framboids embedded in the organic matter. These pyritic particles increased the specific gravity of the organic material, causing it to settle to the bottom of the tube along with free mineral particles, and appeared to be one of the reasons why heavy-liquid separation was

generally unsuccessful. The framboids also obscure detail of the vesicle surface, although they could usually be dissolved as part of the oxidation process, provided the reaction was a gentle one. In some cases, specimens were held together by pyritic encrustation and complete removal of the framboids would fragment the specimen, so oxidation was not allowed to proceed for too long. For samples with abundant pyrite framboids, the reaction sometimes had to be stopped when only partially complete, and the residue spot-checked by microscopic examination to monitor the effectiveness of the procedure. The sample was then either thoroughly washed with distilled water by the usual decantation method until neutral, or subjected to further oxidation.

Separation of heavy minerals- Techniques involving the use of heavy-liquid fractionation (using $ZnBr_2$ or $ZnCl_2$ at specific gravities of between 2.0 and 2.2) and centrifugation to separate the organic residue from undissolved mineral particles were described in detail by Phipps and Playford (1984) and Traverse (1988). The technique was used only for a few large process-bearing acritarch preparations that had an abundance of heavy minerals that could not be separated by swirling. In the few samples for which heavy-liquid separation was attempted, the samples were still allowed to settle by gravity. Experiments to substitute non-toxic, non-corrosive sodium polytungstate ($3Na_2WO_4.9WO_3.H_2O$) for $ZnBr_2$ (Gregory and Johnston, 1987; Savage, 1988) proved unsuccessful because clean separations were not obtained, a factor probably related to the high viscosity of the liquid at the required specific gravity. Separation of organic residue and heavy-mineral grains were usually accomplished quickly and easily by a swirling method carried out in the filter funnel. At the end of the filtration process, the filter funnel was tilted to about 45° and the material trapped on the filter was washed off the cloth into the body of the funnel using about 5 ml of distilled water from a squeeze bottle. Within a few seconds, the heavy-mineral fraction began to settle out into the angle in the funnel wall. Organic material remained in suspension for a few seconds longer, and could be separated from the heavy minerals by rotating the funnel a few degrees clockwise. With a little practice, the two fractions could be cleanly separated, and the organic suspension transferred to a 5 mm-diameter, conical-based glass tube using a pipette.

Slide preparation- As for most palynological preparations, residues were mounted on microscope slides using a transparent medium. A variety of

substances are available (Traverse, 1988), but to prepare slide of macerated material the polyvinyl alcohol (Refractive index 1.4) was used as transparent medium to prevent the organic material from the fungal contamination. To make the slide of organic residue, a cover slip was placed on a hot plate at a temperature of about 100 ^{o}C. Two drops of a dispersing agent, 3% polyvinyl alcohol, were placed on the cover slip with a pipette. A few drops of residue were added to the PVA and the mixture was gently spread over the cover slip with pipette. One drop of distilled water was added to obtains the required dispersions and residue was dried out was slowly at 50 degree centigrade. After than a drop of Canada balsam was placed on microscopic slide and the slide was warmed up gently to drive off any bubble in the resin. The cover slip was then inverted and put on the microscopic slide, allowing the resin to spread by capillary action.

A little extra distilled water was added to obtain the required dispersion and the residue was dried out slowly (at about 100°C). Excess resin and air bubbles were squeezed out from below the cover slip by gently pressing on the covers slip, and the prepared slide was placed on a hotplate at a temperature of 135°C for 10–15 minutes to cure the resin. The cured slide was cleaned using a razor blade and ethanol.

Contamination issues- A further advantage of the modified techniques was a reduction of the risk of contamination, which poses a problem in Proterozoic successions where specimens can be sparse and their taxonomy is poorly known. An indication of the extent of this problem was given by Schopf (1992), it can be accessed from the comprehensive tables of micro- nanofossils and micro-dubiofossils reported from the Proterozoic (Mendelson and Schopf, 1992). Although modern pollen and most Phanerozoic fossils can be recognized if they occur as contaminants, a variety of biogenic structures and other artifacts may be introduced during preparation procedures, and can be mistaken for bonafide fossils. Contamination risks from airborne particles of organic matter and cross-contamination of samples are considerably reduced by using a minimum number of containers for each sample. Potential contaminants can be monitored if blanks (such as granite or other plutonic rocks) are processed at the same time as regular samples. Airborne particles can be collected by exposing cover slips with smears of mounting medium in the preparation area. Tap water and the various chemical reagents should be microscopically examined from time to time for potential

contaminants. Results obtained from such studies indicate that great care is needed to ensure that only organisms of undoubted Proterozoic origin are included in systematic descriptions.

3.2.4 Staining

The procedure for staining described below was adapted from Dickson (1965). For the identification of calcite and ferroan calcite, dolomite and ferroan dolomite Alizarin Red S and Potassium Ferricyanide were used. For this purpose thin sections of the rock samples were prepared without covering with the cover slip. It was cleaned for any grease or dirt adhered to the surface. The uncovered slide was then immersed for 45-50 seconds in the mixture of two solutions A and B were prepared in the following manner.

Carbonate		Staining Response		
		ARS	PF	ARS+PF
Hexagonal	Calcite	Pink Orange	None	Pink Orange
	Ferron Calcite	Pink Orange	Blue	Mauve Purple
	Dolomite	None	None	None
	Ferron Dolomite	Pale mauve	Blue Torquoice	Torquoice Green
	Siderite	None	None	None
	Magnesite	None	None	None
	Rhodochrosite	None	Pale Brown	Pale Brown
Orthorhombic	Aragonite	Pink Orange	None	Pink Orange
	Whiterite	Red	None	Red
	Cerussite	Mouve	None	Mouve

Fig. 3.3- Identification chart of stained carbonates rocks (after Dickson, 1965).

Solution A-Alizarin Red S concentration of 0.2g/100ml of 1.5% HCL (15 ml pure acid made up of 1 liter of water).

Solution B- Potassium Ferricyanide: concentration of 2g/100 ml of 1.5 % HCL.

The thin section was washed in running water for few seconds and allowed it to dry for sometimes. The thin section was studied under the petrological microscope. The identification was based on the following basis (Fig. 3.3).

3.2.5 Measurement of Total Organic Carbon (TOC)

TOC (total organic carbon) measurements of black shale and carbonate samples were carried out at Petroleum Geochemistry Department of National Geophysical Research Institute, Hyderabad. For this purpose the inorganic carbon fraction was removed first by treating the sample with about 50 mg of homogenized 63 micron powdered samples with 3-4 drops of 50% HCl to remove its inorganic carbon content and kept in the oven overnight at 105°C. The dried, HCl treated samples were taken in the Quartz boat and loaded into the furnace of the TOC analyzer for total organic carbon measurements. The model of TOC analyzer used is Soild Module 1000°C from Elementar Analysensysteme GmbH. Procedural blank and the soil standards (Boden Soil Standard, 4.1% TOC) were also analyzed in the similar way. The TOC released due to the chemical oxidation of the organic carbon is measured by the IR detector and expressed in wt %. The % RSD is ≤ 1%. Table-3.1, gives the operating conditions of the Solid Module.

Table 3.1- Technical specifications of TOC

Carrier Gas	Zero Air
Carrier gas Flow	200 ml/min
Pressure	0.9 bar
External Standard	Boden Soil Standard
Max. Temperature	900°C
Run Time	18 mins

Principle & instrumentation of TOC analyzer- The total organic carbon content analysis is based on the oxidative combustion of carbonate rocks and black shales samples in presence of platinum catalyst to form carbon dioxide and its

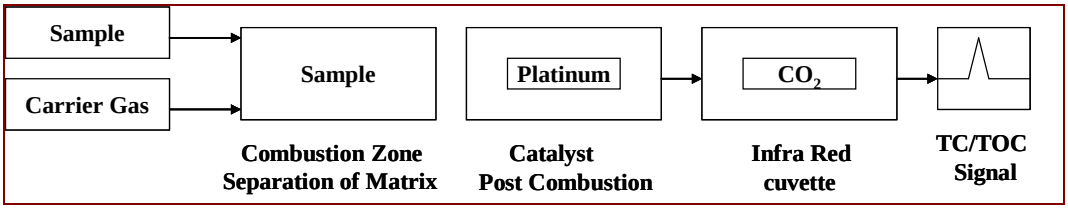

Fig. 3.4- Schematic diagram of Total Organic Carbon Analyzer (after Mani, 2008).

subsequent determination with an Infrared Detector. The total carbon determinations are carried out from the original sample while for TOC determination the sample is externally acidified and then dried before the analysis. (Fig. 3.4) shows the schematic diagram of Total Carbon Analyzer. The sample is combusted in a heated combustion reactor consisting of a pre and post combustion furnace. At lower temperature of 70°C, the purgable and inorganic carbon is removed with the carrier gas (zero air comprising of nitrogen and oxygen) and at higher temperature of 900°C, the non-purgable or the organic carbon is combusted in presence of oxygen and catalyst.

The carbon containing combustion gases are oxidized to CO_2 in presence of post combustion catalyst (platinum on ceramic carrier). The reaction gas flows through a drying unit and a halogen absorption tube where unwanted compounds are withheld. The CO_2 obtained is measured in the Infrared Detector. The liquid TOC software converts the integral of the measuring signal into a respective concentration value with the help of a stored linear calibration (Elementar Soild Module 1000°C operating manual). The lower detection limit for approximately 2 μg C absolute is ~5 ppm C with 400 mg sample weight and the linear working range is up to 1.2 mg C absolute or 100%. The precision /standard deviation is ± 0.7 μg absolute or ≤ 1%, relative for the homogeneous test substances or standards.

3.2.6 Rock- Eval Pyrolysis

The Rock Eval (RE) Pyrolysis method consists of a programmed temperature heating (in a pyrolysis oven) in an inert atmosphere (helium) of a small sample (~100 mg) to quantitatively and selectively determine (1) the free hydrocarbons contained in the sample and (2) the hydrocarbon- and oxygen-

containing compounds (CO_2) that are volatilized during the cracking of the unextractable organic matter in the sample (kerogen)

A Rock-Eval method is defined by:

- A temperature program
- Ranks of integration for surfaces recorded by the FID and the IR cells
- Parameters calculated after surfaces and peak temperatures.

Rock Eval Pyrolysis consists in estimating petroleum potential of rock samples by pyrolysis according to a programmed temperature pattern. Released hydrocarbons are monitored by a FID, forming the so-called peaks S1 (thermo-vaporized free hydrocarbons) and S2 (hydrocarbons from cracking of organic matter) (Fig 3.5 & 3.6). The CO and CO_2 released during pyrolysis can be monitored in real time by an IR cell. This complementary stage allows determination of Total Organic Carbon and Mineral Carbon content of samples. In this the the bulk rock powder is taken ~60 mg in bolt and put on Rock Eval-6 Turbo Complete Analysis-Parallel Processes (Fig. 3.7 and 3.8).

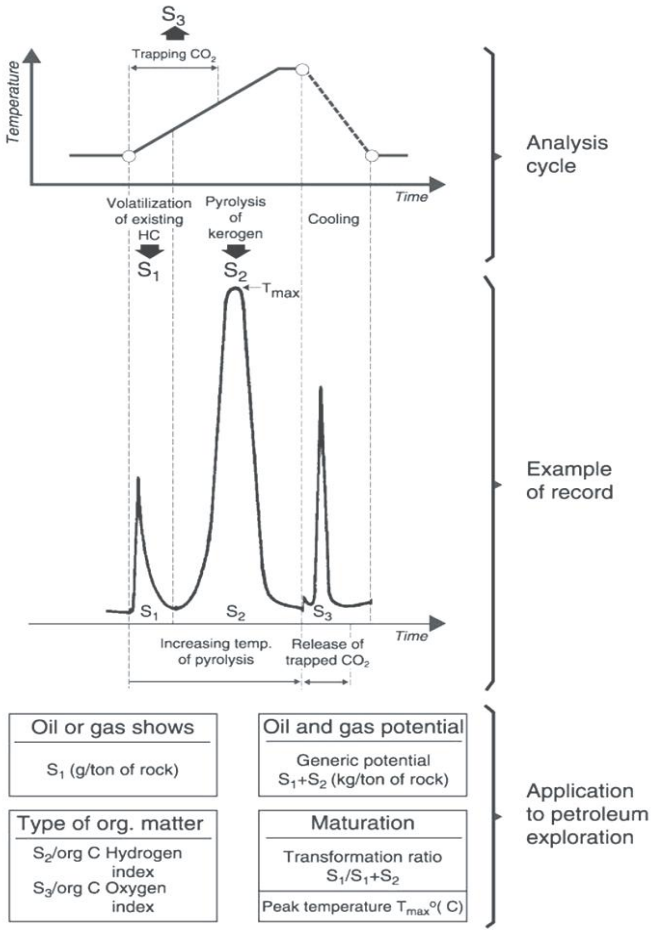

Fig. 3.5- General diagram showing the different fractions of the total organic matter of rocks analyzed the corresponding parameters and their recordings (after Mars, 2010).

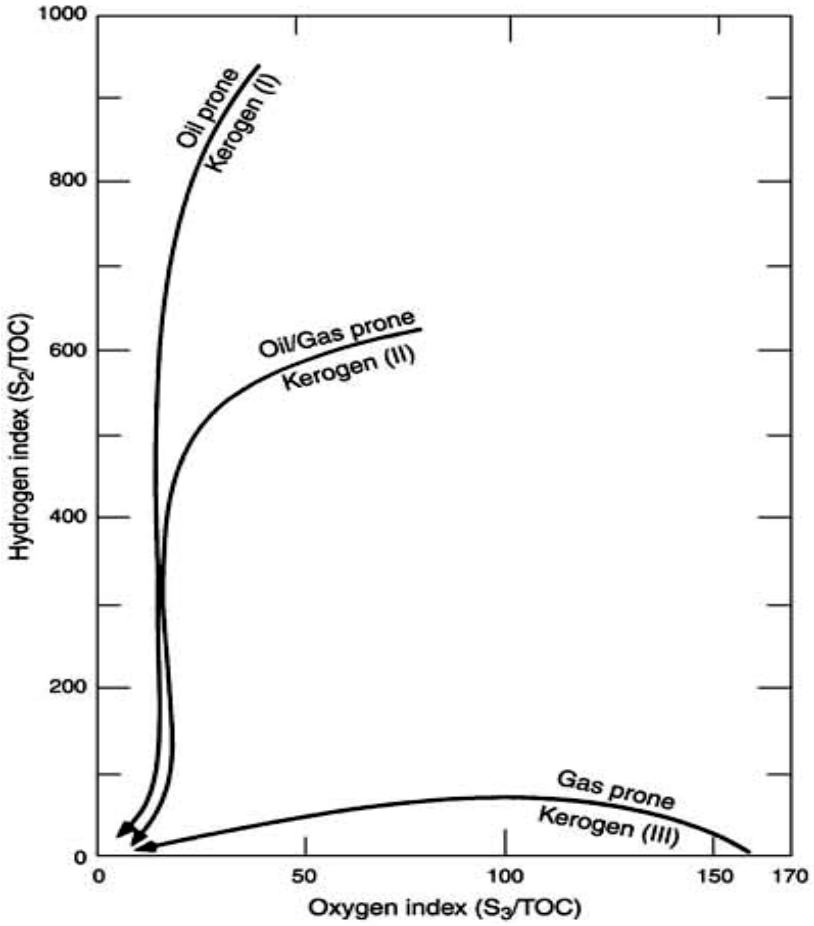

Fig. 3.6- Types of kerogen measurement graph (after Mars, 2010).

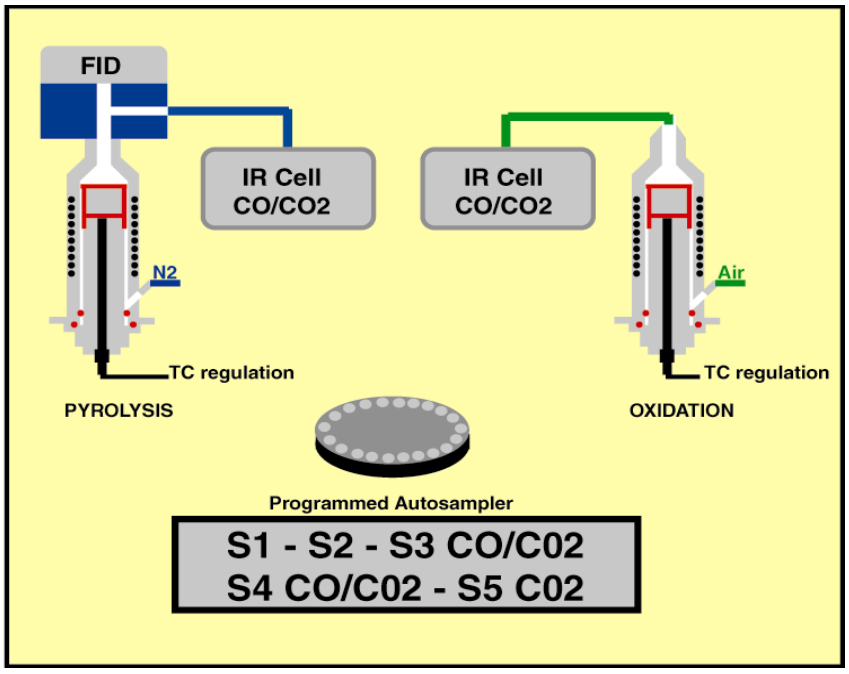

Fig. 3.7- Shows Rock Eval -6 Turbo Complete Analyses- Parallel Processes (after Mars, 2010).

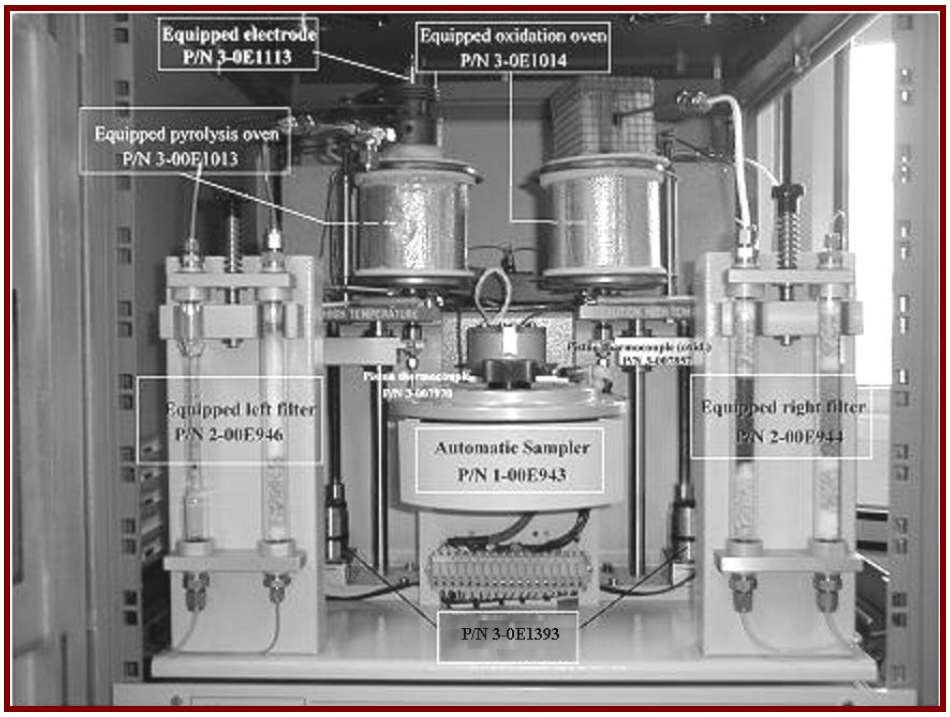

Fig. 3.8- Shows Rock Eval -6 Turbo Complete Analyses- Parallel Processes (after Mars, 2010).

Analytical Methodology- The Rock Eval Pyrolysis instrument used in the present study is RE6 (Turbo version), make of the Vinci Technologies. After obtaining a stable signal of all the detectors, the instrument was calibrated in standard mode using the IFP standard, (Tmax = 416°C; S2= 12.43). The samples were powdered homogenously and depending upon the organic matter content (about 50-70 mg of the shale and 10-20 mg of the coal), the samples were weighed in pre-oxidized crucibles. The shale/coal samples were run under analysis mode using the bulk rock method and basic cycle of RE 6**.** It is the bulk rock method used for screening of all types of samples and allows determination of the full set of available Rock-Eval parameters.

Temperature Program- It is the bulk rock method used for screening of all types of samples and allows determination of the full set of available Rock-Eval parameters (Table 3.2).

Table 3.2- Temprature programe of Rock-Eval pyrolysis.

	Initial Temperature °C	Final Temperature °C	Rate /min	Initial Step min	Final Step min	Extra Acquisition min
Pyrolysis	300	650	25	3	0	3
Oxidation	300	850	20	1	5	5

Acquisition Parameters of RE-6- Acquisition parameters during Rock-Eval Pyrolysis are described in Table-3.3.

Table 3.3- Aquisition parameters during Rock Eval Pyrolysis.

Parameter	Unit	Detector/ Oven	Name
S1	mgHC/g rock	FID / Pyrolysis	Free Hydrocarbons
S2	mgHC/g rock	FID / Pyrolysis	Oil Potential
TpS2	°C	Pyrolysis TC	Temperature for maximum of surface S2
S3	mg CO_2/g rock	IR / Pyrolysis	CO_2 from organic source
S3'	mg CO_2/g rock CO_2	IR / Pyrolysis	from mineral source
S3CO	mgCO/g rock	IR / Pyrolysis	CO_2 from organic source
S3'CO	mgCO/g rock	IR / Pyrolysis	CO from organic and mineral sources
Tmax	°C	TpS2-ΔTmax	Tmax
PI		S1/(S1+S2)	Production Index
PC	% weight	{[(S1+S2)x0.83]+[S3x12/44]+[(S3CO+S3'CO/2)x12/28]}/10	Pyrolysable Carbon org.
RC	% weight	RC CO+ RC CO_2	Residual Carbon org.
TOC	% weight	PC+RC	Total Organic Carbon
HI	Mg HC/g T OC	S2x100/TOC	Hydrogen Index
OI	mg CO_2/g TOC	S3x100/TOC	Oxygen Index
OI CO	Mg CO/g TOC	S3COx100/TOC	Oxygen Index CO
Pyro Min C	% weight	{[S3'x12/44]+[(S3'CO/2) x12/28]}/10	Pyrolysis Mineral Carbon
Oxi Min C	% weight	[S5x12/44]/10	Oxidation Mineral Carbon
Min C	% weight	Pyro MinC + Oxi MinC	Mineral Carbon

Conditions for Integration of Surfaces for RE 6- The conditions for integration of surface for Rock-Eval Pyrolysis are summarized in Figure -3.9.

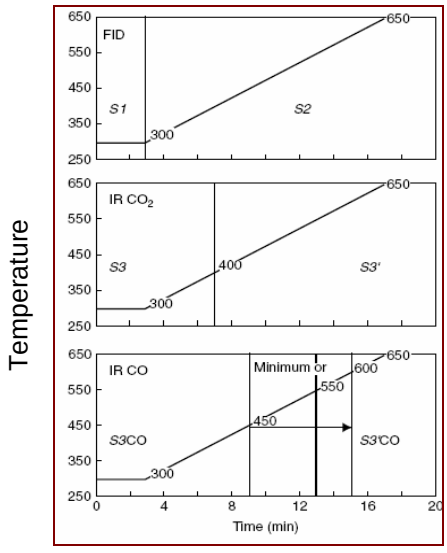

Fig. 3.9- Basic methods of Rock - Eval Pyrolisys (after Mars, 2010).

3.2.7 GC-C- IRMS

Analytical Procedure- The $\delta^{13}C$ analyses of desorbed hydrocarbons is carried out using Gas Chromatograph-Combustion-Isotope Ratio Mass Spectrometer (GC-C-IRMS) which comprises of Agilent 6890 Gas Chromatograph coupled to a Finnigan-Delta Plus^{XP} Isotope Ratio Mass Spectrometer via a GC combustion III interface. One ml of the adsorbed soil gas is injected into the Agilent 6890 GC injection port equipped with "Pora Plot Q" capillary column of length 25 cm and diameter 0.32 mm in splitless mode with Helium as carrier gas at fixed oven temperature of 28°C. The chromatographically separated hydrocarbon gases after eliminating from GC column enter a pre-oxidized Cu-Ni-Pt combustion reactor maintained at 960^{o}C where they get converted into carbon dioxide and water. The water is removed using Nafion membrane tube prior to their entry into the mass spectrometer. The purified CO_2 after combustion goes into the mass spectrometer for $^{13}C/^{12}C$ ratio measurement of the respective hydrocarbon. The GC-C-IRMS is calibrated with Natural Gas Standard (NGS-1) mixture using the ISODAT software. The $\delta^{13}C_1$ value in the sample is calculated with respect to the standard and reported relative to Pee Dee Belemnite (PDB). The precision of the isotope analysis is ±0.5%

Principle and Instrumentation of GC-C-IRMS- Stable isotope mass spectrometers are widely used to determine the ratio of ^{13}C to ^{12}C in geological samples. The basic mass spectrometer comprises of the i) ion source for fragmentation of sample molecule into ions and ii) mass analyzer for separating the ion beam according to the mass of the respective ions. The sample and reference gases are carried into the ion source of the mass spectrometer through a stream of helium as carrier gas. With the advancement of hyphenated techniques, the separation power of gas chromatograph has been coupled to the mass spectrometer along with introduction of sample combustion interface into the gas chromatograph-isotope ratio mass spectrometer (Fig. 3.10). The separated products of the sample mixture in the stream of helium at the output of the gas chromatograph are passed through an oxidation/reduction reactor and then introduced into the mass spectrometer for precise concentration determination. The open split-coupling device ensures that only a part of the sample/reference gas containing carrier gas is fed into the ion source of the MS. In this way, pulse

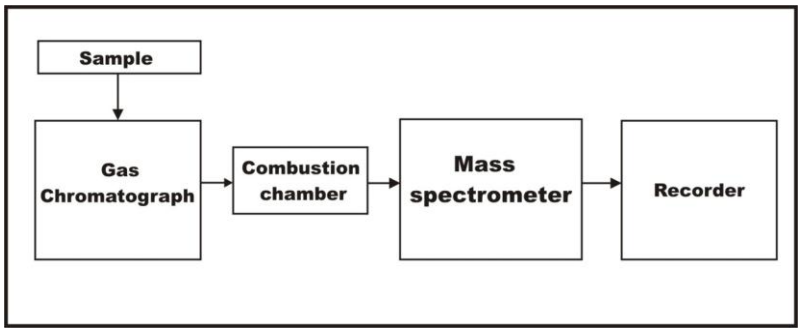

Fig. 3.10- Schematic of GC-C-IRMS (after Mani, 2008).

injection of sample gas can be analyzed, reducing the volume constraints and sample size. Figure 3.10 shows the schematic of GC-C-IRMS.

The Gas Chromatograph-Combustion (GC-C) device comprises of Agilent 6980 Gas Chromatograph fitted with Poraplot Q capillary column, oxidation and reduction reactor along with water separator. The oxidation reactor is a non porous alumina tube in which three wires of copper, nickel and platinum of 240 mm identical length and 0.125 mm internal diameter are braided and centered end to end within the tube. The reactor is inserted into the Al_2O_3 furnace operated at 940°C. The reduction reactor is placed between the double T-piece and water separator and is identical with oxidation furnace except for the reactor filling which is pure copper with three copper wires of 240 mm identical length and 0.125 mm internal diameter. The reduction temperature is maintained at 640°C. The Delta Plus XP CF-IRMS used in the isotope ratio determination comprises of i) electron impact ion source; ii) magnetic analyzer with effective magnetic deflection of radius of 180 mm and iii) self-aligning Faraday collectors. The ISODAT software is used for the data acquisition (Thermo Finnigan Delta XP Manual).

The compound specific analysis of hydrocarbon mixture for $^{13}C/^{12}C$ ratio measurement has been carried out by injecting the sample mixture consisting of C1-C5 hydrocarbons into the gas chromatograph. The individual components after chromatographic separation are converted into CO_2 and H_2O in the combustion reactor. The CO_2 gas in the analyte stream is transported into the IRMS via an open split assembly. To minimize inaccuracies in measuring the absolute amounts of ^{12}C and ^{13}C, the ratio of the two in a sample is compared with that in a standard analyzed. Table 3.1 provides the reference standards for different stable isotopes.

By definition, the standard $\delta^{m}E$ value of a standard is $0^{0}/_{00}$, so negative values of a sample indicate depletion in the heavier isotope compared with the standard and the positive values indicate enrichment in the heavier isotope (for PDB $^{13}C/^{12}C$ = 0.011237).

3.2.8 Absorbed Gas Analysis

One gram of 63 µm wet, sieved black shale sample was used to extract light gaseous hydrocarbons after acid treatment in glass degasification apparatus and was subsequently analyzed on Gas Chromatograph (GC) and Gas Chromatograph–Combustion–Isotope Ratio Mass Spectrometer (GC–C–IRMS).

During acid treatment, the dominant gas released was CO_2, which was trapped in KOH solution. The light gaseous hydrocarbons were collected by water displacement in a graduated tube fitted with rubber septa. The volume of desorbed gas was recorded and 500 µl of desorbed gas sample was injected into Varian CP 3380 GC fitted with Porapak Q column, equipped with flame ionization detector. GC was calibrated using external standards with known concentrations of

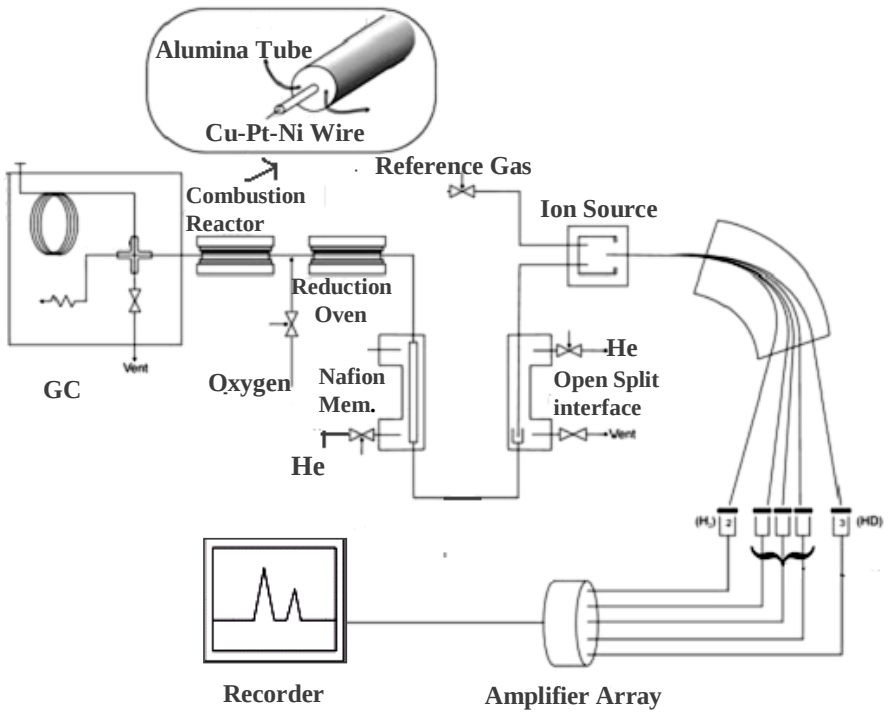

Fig. 3.11- Schematic of GC-C-IRMS (after Gavin et al., 2007).

methane, ethane, propane, *i*-butane and *n*-butane. Quantitative estimation of light gaseous hydrocarbon constituents in each sample was made using peak area measurements and correction for moisture content on wet basis was also applied. The hydrocarbon concentration values of individual hydrocarbons from methane through pentane were expressed in parts per billion (ppb) on dry-weight basis. The accuracy of measurement of C1–C4 components was < 1 mg/g. Carbon isotopic composition of light hydrocarbons from rock samples was determined using GC–C–IRMS, which comprises of Agilent 6890 GC coupled to a Finnigan- Delta PlusXP IRMS via GC combustion III interface (Fig. 3.11). Next, 1 ml of desorbed gas was injected to GC in splitless mode with helium as the carrier gas at fixed oven temperature of 28°C. The light hydrocarbon gases eluting from the GC column entered the combustion reactor maintained at 960°C, where they were converted to CO_2 and water. Nafion membrane tube was used to remove water, prior to the entry of CO_2 into the mass spectrometer. Reference standards were intermixed with samples to monitor instrumental performance. The carbon isotope ratio in the sample was determined by comparing isotope ratios with those of standards, NIST RM 8560 (IAEA NGS2) using ISODAT software. The $\delta^{13}C$ was calculated using the following equation:

$$\delta^{13}C = [(^{13}C/^{12}C)_{Sample}-(^{13}C/^{12}C)_{PDB}]/[(^{13}C/^{12}C)_{PDB} \times 1000]$$

The carbon isotopic composition was reported in per mile (‰) relative to the Pee Dee Belemnite (PDB). The precision of the isotopic analysis was ± 0.5‰. In the present study, the magnitude of each of the five organic constituents (C1, C2, C3, *i*C4 and *n*C4, iC5, nC5) in black shale sample was measured and expressed in ppb. The compositional characteristics of these hydrocarbon gases desorbed from black shale samples indicate the presence of methane (C_1), ethane (C_2), propane (C_3), *i*-butane (iC_4), *n*-butane (nC_4), i-pentane (iC5) and (nC5).

Chapter 4

PALAEOBIOLOGY

The Vindhyan Basin has been searched for evidence of life, since the beginning of twentieth century. Slightly or unmetamorphosed rocks of the Vindhyan Supergroup have wide variety of palaeobiological records. This includes microfossils, macrofossils, and organo-sedimentary structures. Many of these fossils are important clue in constraining the age of the Vindhyan Supergroup. At the same time, many of the fossil reports provide conflicting ages. Apart from biostratigraphic significance, the fossil reports illuminate the evolution of microbial and metazoan life in earth's history. Different types of microfossils were reported from both the argillaceous rocks and carbonates of the Vindhyan Supergroup by various workers (Venkatachala et al., 1996; Kumar and Srivastva, 1995; Sharma, 2006a,b,c, 2009a,b). They have interpreted that most of recorded microfossils belonged to cyanobacteria and only a few of them belong to the eukaryotic acritarchs. Sharma and Sergeev (2004) reported typical Mesoproterozoic microbiotas from the Kheinjua Formation. These microfossils record suggested Mesoproterozoic age for the Semri Group. Varied kinds of carbonaceous fossils were also reported from the Vindhyan Supegroup. Transitional organization from unicellular to multicellular in Proterozoic microorganisms was a turning point in the earth's earliest biosphere (Schopf and Klein, 1992). Prokaryotes to eukaryote (metaphytes and metazoans) diversification is considered as a key evolutionary step in the history life (Schopf et al., 1973; Woese et al., 1990; Knoll, 1992; Knoll et al., 2006; Narbonne, 2005). The large numbers of Precambrian- Cambrian sphaeromorphic, carbonaceous and branched macro-algal fossils have been studied throughout the world since 1889. In the last five decades, macroalgal (*Chuaria-Tawuia* assemblage) and multicellular meta-phytic fossils have been accumulated as a testimony to establish the evolutionary history from Late Palaeoproterozoic to Late Neoproterozoic time interval (~1100 Ma). The Proterozoic metaphytes fossils have a wide Geographical distribution in USA, Spitsbergen, Canada, Yakutia, Siberia, Australia, China, Kazakhstan, Spain, Iran, Africa, Namibia, Argentina, Antarctica, Sweden, Ukraine and Ural including India. On the basis of these records, most of the publications appearing in last few years have included varied kinds of carbonaceous fossils and palaeobiological

remains from the Proterozoic Vindhyan Supergroup. The reports of the microfossils (Kumar and Srivastava, 1992a, b, 1995; Anbarasu 2001; Sharma, 2006), carbonaceous megaremains (Kumar 1995, 2001; Rai and Guatam 1998; Azmi 1998; Sharma 2006c) and trace fossils (Sarkar et al., 1996; Seilacher et al., 1998; Chakraborty 2001) reflected the renewed attempts to understand the palaeobiology of the basin. The interest and importance lie in tracing the antiquity of the life forms and the age of the fossil bearing Vindhyan sediments that have long been an enigma (Venkatachala et al., 1996; Sharma, 2003). Apart from biostratigraphic significance, the fossil reports illuminate the evolution of microbial and metazoan life in earth's history. Different types of microfossils were reported from both the argillaceous rocks and carbonates of the Vindhyan Supergroup (Venkatachala et al., 1996; Kumar and srivastva, 1995; Sharma 2006a, b, c). On the basis of previous study and the microfossil record suggested Mesoproterozoic age for the Semri Group and Neoproterozoic age for the Upper Vindhyan Group. In the present study diverse Mesoproterozoic macrofossils, microfossils and MISS assemblage have been recorded from the different formation of the Semri Group exposed in the Maihar area, Satna District, M.P. Biostratigraphic interpretation of the assemblage and significance of the microfossils are studied.

4.1 Carbonaceous Megafossils

Macroscopic "carbonaceous" fossils such as *Grypania* (Walcott, 1899; Walter et al., 1976; Walter et al., 1990; Horodyski et al., 1993; Sharma and Shukla, 2009a, b), Katnia (Kumar, 1995; Sharma and Shukla, 2009a), *Chuaria* (Walcott, 1899; Hofmann, 1977; Amard, 1992; Vidal et al., 1993; Kumar, 1995; Talyzina, 2000; Dutta et al., 2006; Sharma et al., 2009), and *Tawuia* (Kumar, 2001; Vidal et al., 1993; Sharma et al., 2009) play a critical role in our understanding of biological evolution in the Precambrian and their environmental implications. These megascopic carbonaceous fossils known from Late Palaeoproterozoic and Early Mesoproterozoic sedimentary rocks have drawn attention of many Precambrian palaeobiologists for their affinity, taxonomic position (both debatable) and possible natural experimentation in response to advent of oxygen in the palaeoenvironment. Multicellularity, colonialism,

macroscopic size and molecular composition have implications for biologic evolution, the chemistry of the marine biosphere (O_2, CO_2, nutrients), and patterns of sedimentation (Butterfield, 2000). Unfortunately, understanding of these fossils remains limited by their relative morphological simplicity (Kumar, 2001), mode of preservation (Lamb et al., 2007), broad taphonomic variability (Samuelsson and Butterfield, 2001), and the current paucity of biochemical information (Arouri et al., 1999; Dutta et al., 2006; Sharma et al., 2009).

Global discovery of large populations of *Grypania*, millimeteric coiled macroscopic compression recorded from the Negaunee Iron Formation (Han and Runnegar, 1998; Schneider et al., 2002), microscopic carbonaceous fossils from the Changzhaugou Formation (~1848 Ma,) China (Yan, 1995; Zhang, 1997; Zhu et al., 2000), carbonaceous megafossils from Chuanglinggou Formation (1800 Ma) near Jixian, China (Hofmann and Jinbiao, 1981), macroscopic algae from 1700 Ma Tuanshanzi Formation, China (Yan, 1995; Yan and Liu, 1997), have renewed the interest in the search of antiquity of eukaryotes in Palaeoproterozoic rocks. Earlier, elliptical and circular carbonaceous forms were reported from USA and Canada (Tyler et al., 1957; Stinchcomb et al., 1965). Besides, Late Palaeoproterozoic carbonaceous remains, similar megascopic fossils were widely recorded from Mesoproterozic sediments (Kumar, 1995; Javaux et al., 2001; Walter et al., 1976; Walter et al., 1990). Similarly, *Chuaria* and *Tawuia* have been interpreted as compressed prokaryotic colonies (Sun, 1987), algae (Zhang and Walter, 1992; Vidal et al., 1993), algal reproductive stages (Vidal et al., 1993), and multicellular plant material (Kumar, 2001). The Vindhyan Supergroup has also revealed the presence of carbonaceous megafossils from different horizons (Jones 1909; Misra and Bhatnagar, 1950; Maithy and Shukla, 1984; Kumar, 1995, 2001; Kumar and Srivastava, 1997, 2003; Rai et al., 1997; Srivastava, 2004, 2005; Sharma, 2003, 2006). The present study attempts to add some new records in the palaeobiological studies of the Vindhyan Basin. Sharma and Shukla (2009a) reported the *Grypania spiralis* and *Katnia singhii* from Rohtasgarh Limestone of Lower Vindhyan and also described their taphonomy affinity and implication in age and life evolution. Here, the carbonaceous macroscopic fossil films are also reported from the Rampur Shale, exposed in Rampur Village and helically coiled megascopic carbonaceous fossils from the Rohtasgarh limestones, exposed in

Bistara and Amehta mines of the Semri Group, Satna and Katni Districts, M.P. Their Systematic paleontology is provided below:

Table 4.1- Details of collected microfossils from Lower Vindhyan, Maihar area, M.P.

Mega fossils/Species	Locality	Stratigraphic Position	Remarks
Grypania spiralis	Bistara & Amehta Mines, Katni District, M.P.	Rohtasgarh Limestone	Plate 4.1(a, d & f-k)
Katnia singhii	Bistara & Amehta Mines, Katni District, M.P.	Rohtasgarh Limestone	Plate 4.1(b, c & e)
Chuaria circularis	Rampur Village, Maihar area,Satna, Madhya Pradesh	Rampur Shale	Plate 4.2 (a-f, j, k,) Plate 4.3 (a, b, c, j-n)
Tawuia dalensis	Rampur Village, Maihar area,Satna, Madhya Pradesh	Rampur Shale	Plate 4.3, d
Tuanshanzia platyphylla	Rampur Village, Maihar area,Satna, Madhya Pradesh	Rampur Shale	Plate 4.2, (g, h, i) Plate 4.3(e-i)
Tuanshanzia lanceolata	Rampur Village, Maihar area,Satna, Madhya Pradesh	Rampur Shale	Plate 4.2, l-p

SYSTEMATIC PALAEONTOLOGY

Division- Chlorophyta:Xanthophyta

Class- Chlorophyceae:Xanthophyceae

Order- Ulotrichales:Vaucheriales

Family- Ulotrichaceae:Vaucheriaceae

Genus- *Chuaria* (Walcott, 1899; Vidal and Ford, 1985

Type species- *Chuaria circularis* (Walcott, 1899; Vidal and Ford, 1985)

(Plate 4.2 a-f, j, k, Plate 4.3 a, b, c, j-n)

Synonymy

Chuaria circularis Walcott (1899) pp. 234-235, pl. 27, figs. 12, 13.

Fermoria minima Chapman (1935), p. 115-116, pl. 1, figs. 1, 3.

Fermoria granulose Chapman (1935), p. 116, pl. 1, figs. 2, 4; pl. 2, fig.5.

Fermoria capsella Chapman (1935), p. 117, pl. 2, figs. 3-4.

Protobolella jonesi Chapman (1935), p. 117-118, pl. 1, figs. 5-6; pl. 2, fig. 1.

Fermoria minima Chapman, Sahni (1936), p. 465-466, pl. 43, figs 1-4.

Kildinella magna Timofeev (1970), pl. 1, figs. A, B.

Chuaria circularis Walcott, Ford & Breed (1973), p. 539, pl. 61, figs. 1-7; pl. 62, figs. 1- 6; pl. 63, figs. 1, 2, 4.

Chuaria circularis Walcott; Ford & Breed (1977), p. 171-173. pl. 1, figs. 1-6.

Chuaria circularis Walcott, Hofmann (1977), p. 3, fig 2.

Fermoria disc-like remains type 1-6, Maithy & Shukla (1977), p. 183, pl. 5, figs. 35-40.

Tasmanites vindhyanensis Maithy & Shukla (1977), p. 182-183, pl. 4, figs. 32-33.

Nucellosphaeridium spp. Hofmann (in Hofmann & Aitken) (1979), p. 156, figs. 12A-C.

Chuaria circularis Walcott, Hofmann (in Hofmann & Aitken) (1979), p. 157, figs. 13 K-M.

Morania? antique Fenton & Fenton, Hofmann (in Hofmann & Aitken) (1979), p. 160, figs. 13 J, 17 A (partim).

Chuaria circularis Walcott, Duan Chenghua (1982), p. 59-61, figs. 3A-J, 5A-J, O, P.

Chuaria circularis Walcott, Knoll (1982), pl. 2, fig. 1; pl. 4, figs. 7, 13.

Chuaria circularis Walcott, Mathur (1983), p. 363-364, fig. 1A.

Chuaria fermorei Mathur (1983), p. 363-364, fig. 1B.

Chuaria circularis Walcott, Suresh & Sundara Raju (1983), p. 81-82, fig. 2, 1-5.

Chuaria circularis Walcott, Hofmann (1985b), p. 342, pl. 35, figs. 2, 4; pl. 37, fig 1 (partim); pl. 38, fig. 4 (partim); pl. 39, fig. 2 (partim); text-fig. 4 (partim).

Chuaria circularis Walcott emend. Vidal & Ford (1985), p. 355-359, pl. 3, fig. A

Chuaria circularis Walcott, Sun (1987), p. 115, pl. 1, figs. 1-8; pl. 4, figs. 1-2.

Chuaria circularis Vidal & Ford (1985), Vidal, Moczydłowska & Rudavskaya (1993), p. 390-393, figs. 3A-D; fig. 4B, D.

Leiosphaeridia wimanii Brotzen (1941), Butterfield, n. comb.; Butterfield, Knoll & Swett (1994), p. 42-43, fig. 13D-F.

Chuaria circularis Walcott 1899, Butterfield, Knoll & Swett (1994), p. 32-34, figs. 8G-H, 13G-I.

Chuaria circularis Walcott, Yin & Sun (1994), p. 99-100, pl. 4 (b).

Chuaria circularis Walcott, Steiner (1994), p. 95-101, pl. 1, figs.4-17; pl. 3, figs. 1-7; pl. 4, figs. 1-4; pl. 8, fig. 2; pl. 9, figs. 1-2; pl. 11, figs. 8-10; pl. 12, figs. 4-11.

Chuaria circularis Walcott, Vidal & Ford (1985), Hofmann & Rainbird (1994), 1994, p. 724-725, pl. 1, figs. 1-6.

Chuaria circularis Walcott, Maithy & Babu (1996), p. 2, pl. 1, figs. 1, 10, 11.

Chuaria pendjariensis, Amard (1997), p. 478, fig. 3a, b.

Chuaria circularis Walcott, Rai, Shukla et al. (1997), p. 784-786, figs. 3 c-f, h-j, l-n, p-r, t-v, x-z.

Chuaria circularis Walcott, Haines (1998), p. 5, figs. 5A-D.

Chuaria circularis Walcott emend. Vidal & Ford (1985), Kumar (2001), p. 193, figs. 6a-f, h-j; figs. 14f-h.

Chuaria vindhyanensis, Kumar (2001), p. 196, figs. 14f-h.

Suketea rampuraensis, Kumar (2001), p. 203, figs. 9g, h.

Chuaria circularis Walcott emend. Vidal & Ford (1985), Kumar & Srivastava (2003), p. 146-147, pl. I, figs. a-g.

Chuaria circularis Walcott emend. Vidal & Ford (1985), Kumar & Srivastava (2003), p. 147-148, pl. I, figs. h, i, j & k. Form A, Kumar & Srivastava (2003), p. 150, pl. II, fig. a.

Bhanderia maiharensis, Kumar & Srivastava (2003), p. 149, pl. II, fig. i; pl. III, figs. b-c.

Chuaria circularis Walcott, Srivastava (2004), p. 644-646, figs. 2a-c, e, o-q.

Chuaria circularis Walcott, Srivastava & Bali (2006), p. 875, fig. 3 (1-4, 8, 10, 11, 13, 15-17).

Chuaria sp. Sharma and Shukla (2009), p.117, fig 7(J-L),

Type Material- Algonkian, Chuar terrane, Kwagunt valley, within the Grand Canyon of the Colorado, in Arizona. No type specimen was designated by Walcatt (1899). Lectotype was designated by Ford & Breed (1973), catalogued under U.S. National Museum USNM 33800.

Locality- Rampur Village, Maihar area, Satna District, Madhya Pradesh.

Stratigraphic Position- Rampur Formation, Semri Group, Vindhyan Supergroup, Early Mesoproterozoic.

Description- Circular to mostly elliptical carbonaceous compressions or impressions on the bedding surface of yellow/gray shale is preserved. Discs are smooth. Total 16 (Plate 4.2, a-f, j, k, and Plate 4.3 a-c, j-n) specimens are photographed, most of the specimens are ranging in size between from 1.03- 2.95 mm in width, and 1.16- 3.4 mm in length. These are opaque and dense black, coloured. Their outer margins are clear and distinctly preserved with the shales. No circular annulations or folds observed. Specimens occur isolated and rarely in contact with each other.

Remarks- *Chuaria* Walcott has been reviewed by a number of workers (Ford and Breed, 1973; Hofmann, 1977, 1985a, b, 1992a, b; Sun, 1987; Kumar, 1995; Sharma 2006). Walcott (1899) described *Chuaria* as circular disc like bodies, 2–5 mm in diameter which is concentrically wrinkled and usually a thin layer of dark bituminous matter covers the surface. Ford and Breed (1973) also observed the presence of irregular wrinkles in the diagnosis of *Chuaria*. However, Hofmann (1977) has described *Chuaria* without the presence of wrinkles from the Uinta Group. Kumar (1995) has also compared carbonaceous discs with *Chuaria* which are without wrinkles from the Rohtas Formation, Katni area, Madhya Pradesh. Vidal and Ford (1985) added a new dimension by suggesting that *Chuaria* should be identified only in the palynological preparations. Sun (1987), Hofmann (1992a), Kumar (1995), however, have disagreed with this suggestion and given their opinion that *Chuaria* should be identified only megascopically. Also original diagnosis by Walcott (1899) should be emended to include carbonaceous specimens with or without irregular and concentric wrinkles on the bedding surface including all such impressions whose carbonaceous matter is lost. Here only carbonaceous films as compressions or impressions are preserved. Also no special morphological features, like wrinkles and folding are observed.

Age and distribution- Commonly occurring, Mesoproterozoic to Neoproterozoic, in global distribution.

Genus – *Grypania* Walter et al. (1976)

Type species – *Grypania spiralis* (Walcott) emend.Walter et al. (1976)

(Plate 4.1, a, d and f-k)

Synonymy

Helminthoidichnites spiralis Walcott (1899), p. 236, pl. 24, Figs. 5 and 6.

*Helminthoidichnites meeki*Walcott (1899), p. 236, pl. 24, Fig. 7.

*Grypania spiralis*Walter et al. (1976), p. 877, pl. 2, Figs. 4–10.

Trace fossils Du and Tian (1985), pl. I, Fig. 28.

Grypania spiralis Hofmann (1985), p. 349, pl. 39, Fig. 4.

Grypania spiralis Walter et al. (1990), pp.140–143, p. 141, Fig. 4a, c–i, k–l.

Grypania spiralis Han and Runnegar (1992), pp. 232–234, p. 233, 234, Figs. 1, 3A–D.

Grypania spiralis Kumar (1995), pp. 178–180, p. 179, 181, Figs. 6a–d, f, I, j, 7g.

Possibly compressed ring of *G. spiralis* Kumar (1995), p. 179, Fig. 6g and h.

Grypania sp. Rai and Gautam (1998), pp. 21–22, pl. 1, Fig. e

Grypania spiralis Sharma and Shukla (2009), pp. 111-113, Figs. 4A and B, 5A, C, D, F–H, 7D, E, G, H, 8D–G, 9A and B

Locality –Bistara, Amehta Mines, Katni District, M.P.

Stratigraphic Position – Rohtas Formation, Semri Group, Vindhyan Supergroup, Early Mesoproterozoic.

Description- Flat, helically, unbranched carbonaceous bodies preserved on bedding planes, impressions, or compressions, generally helically to spirally coil and sinuously folded specimens also occur. Single to multiple coils which have closed coil (Plate 4.1, a, h) and loose coils (Plate 4.1, d, f, g, i, j) are preserved. It (Plate 4.1, d) is measuring, approximately 3.3 x 2.2 mm maximum coil diameter of the ribbons ranges between 2.2.cm (Plate 4.1, a) and 3.3 cm (Plate 4.1, d). The widths of coil in ranging between 2.7 mm and 7.6 mm. Coils are attached to each other (Plate 4.1, d). Terminations rare and no segmentations observed. Total 8 specimens, measured in our collection, presented as impressions. Impression specimens are distinct in colour from the adjacent matrix, mostly in shades of grey. All these specimens are unbranched and show no septations. These preservations are mineralized by calcite layer.

Remarks- Comparable specimens reported from Gaoyuzhuang Formation (China), Negaunee Iron Formation (USA) and the Rohtasgarh Limestone of Vindhyan Supergroup (India) showing faint or no segmentation. This type of faint segmentation has also been observed in *G. spiralis* reported from the Katni area (Kumar, 1995; Rai and Gautam, 1998, Sharma and Shukla, 2009a). Preservation of segmentation is attributed to the durability of filament during life and/or preservation conditions. It has not been established whether such segmentations were primary or secondary. Regarding segmentation, similar views were expressed for both the Belt Supergroup and the Gaoyuzhuong speciemens (Walter et al., 1990). Sharma and Shukla (2009b) reported *G. spiralis* from upper part of Rohtasgarh Limestone and suggested, such segmentation may be part and parcel of the trichome. Also observed, trichomes and filaments neither occurred together nor were found entwined and indicating that the two entities were identical. Because of this, they had separated specimens with segmentation as *K. singhii* and those without segmentation or sheath as *G. spiralis.* Most of the specimens in our collection are impressions; only a few compressions are present and separated specimens with segmentation as *K. singhii* and those without segmentation or sheath as *G. spiralis*.

Distribution- Palaeoproterozoic-Negaunee Iron Formation, USA; Mesoproterzoic- Greyson Shale, Montana, USA; Rohtas Formation, Semri Group, India; Gaoyuzhuang Formation, China.

Division: Incertae sedis.

Genus: *Katnia* Tandon and Kumar (1977b).

Type species: *Katnia singhii* Tandon and Kumar (1977b) emend. Sharma and Shukla (2009 a).

(Plate 4.1, b, c, and e)

Synonymy

Katnia singhii Tandon and Kumar (1977b) emend. Sharma and Shukla.

Annelid remain Tandon and Kumar (1977a), p. 563, Fig. 2.

Katnia singhii Tandon and Kumar (1977b), pp.126–127, p. 127,Fig. 1.

*Grypania spiralis*Walter, Du and Horodyski (1990), pp. 140–143, p. 141, Figs. 4b and j.

Grypania spiralis Kumar (1995), pp. 178–179, p. 181, Figs. 6e and 7a–e.

Grypania spiralis Rai and Gautam (1998), p. 21–22, pl. 1, Fig. f.

Grypania spiralis Shaowu (1998), pl. I, Fig. 1.

Grypania shangshuanensis Shaowu (1998), pl. I, Figs. 2–12.

Grypania linearis Shaowu (1998), pl. II, Figs. 1–7.

Grypania buccinata Shaowu (1998), pl. II, Figs. 8–12.

Locality- Bistara and Amehta Mines, Katni District, Madhya Pradesh.

Stratigraphic Position- Rohtas Formation, Semri Group, Vindhyan Supergroup, Early Mesoproterozoic.

Description- These specimens are preserved as spiral forms with maximum coil diameter 4.26 cm, coil width 0.82 cm (Plate 4.1, b & c).Width ranging between 2.4 mm and 8.2 mm. All these specimens are unbranched and showing septations. Distinctly septate, 5–12 septa per 1 cm length of coil (Plate 4.1, c and e). Three specimens are described which have double coil and upto 6 coil. These are loose coils. Impression specimens are distinct in colour from the adjacent matrix, mostly in shades of grey. These preservations are mineralized by calcite layer. Coils are separate to each other, can be identified easily.

Remarks- *K. singhii* is tightly to loosely woven spirals on the bedding surfaces are characteristic. Tandon and Kumar (1977a, b) assigned this form to the Annelida. However, after study a few specimens of *K. singhii*, Glaessner (1984) suggested cyanobacterial affinity to this form. Subsequently, Kumar (1995) reassigned *K. singhii* to *G. spiralis.* Rai and Gautam (1998) also reported *G. spiralis* from the Bistara Mine. Runnegar (1991) placed *K. singhii* and another specimen earlier described by Beer (1919) under *G. spiralis*. Mathur (1983) interpreted the lone three dimensionally preserved specimen reported by Beer as a trace fossil, and named it *Spiroichnus beerii*. The specimen described by Beer (1919) appears to have been a mould. Kumar (1995) assigned Beer's specimen to *G. spiralis*. The presence of septa is characteristic of the *K. singhii*. On this basis, it is distinguished from smooth and nonseptate forms. Sharma and Shukla (2009b) described this form from the Rohtasgarh Limestone and consider these specimens to a distinct genus. Here, the same features are also found in these fossils which have distinct morphological characteristics to *G. spiralis.* Sharma and Shukla (2009) suggested the occurrence of *K. singhii* within finely laminated strata, a very low energy lagoonal environment.

Distribution- Mesoproterzoic-Greyson Shale, Montana, USA; Rohtas Formation, Semri Group, India and Gaoyuzhuang Formation, China.

Genus- *Tawuia* Hofmann, 1979

Type species- *Tawuia dalensis* Hofmann, 1979

(Plate 4.3 d)

Synonymy

Tawuia dalensis Hofmann, Hofmann & Aitken (1979), p. 158, figs. 13A-I.

Tawuia dalensis Hofmann, Duan (1982), p. 63, figs. 5K-N.

Tawuia sinensis Duan (1982), p. 63, figs. 3 K-Q, fig. 5p (partim).

Tawuia dalensis Hofmann, Knoll (1982), pl. 3, figs. 12-14.

Tawuia suketensis Mathur (1983), p. 364, figs. 1D.

Tawuia rampuraensis Mathur (1983), p. 364, fig 1E.

Tawuia dalensis Hofmann (1985b), pl. 35, figs. 1-3; pl. 36, figs. 1-5, 7-11; pl. 37, figs. 1, 2, 4-7; pl. 38, figs. 1-3; text-figs. 3, 4 (partim).

Tawuia dalensis Hofmann, Sun (1987), p. 123, pl. 4.

Tawuia dalensis Hofmann, Vidal, Moczydłowska & Rudavskaya (1993), p. 393, figs. 4A-C.

Tawuia dalensis Hofmann, Butterfield, Knoll & Swett (1994), p. 25-26, figs. 8B-E, 23H.

Tawuia dalensis Hofmann, Steiner (1994), p. 107-111, pl. 2, figs. 1-14; pl. 5, figs. 1-2; pl. 11, fig. 7; pl. 12, figs. 5, 6.

Tawuia dalensis Hofmann, Maithy & Babu (1996), p. 2, pl. 1, figs. 1, 3.

Tawuia dalensis Hofmann (in Hofmann & Aitken), Rai, Shukla & Gautam (1997), p. 786, figs. 3 g, k, o, s, w.

Tawuia dalensis Hofmann, Kumar (2001), p. 198, figs. 9a, c, d; figs. 14 j, k.

Tilsoia khoripensis Hofmann, Kumar (2001), p. 201, fig. 9b.

Tawuia dalensis Hofmann, Kumar & Srivastava (2003), p. 148, pl. II, figs. d & g.

Tawuia dalensis Hofmann, Srivastava (2004), p. 644-646, fig. 2d.

Tawuia dalensis Hofmann, Srivastava & Bali (2006), p. 875, fig. 3 (5, 12, 23).

Type Material- Specimen collected by Aitken from the basinal sequence of Little Dal Group, Mackenzie Mountains, northwestern Canada, Holotype number GSC 57893.

Locality- Rampur Village, Maihar area, Satna District, Madhya Pradesh.

Stratigraphic position- Rampur Formation, Semri Group, Vindhyan Supergroup, Early Mesoproterozoic.

Description- Black to brown rod or ribbon-like compression, short to slender bodies, margins smooth, both ends semicircular and without terminal opening or ovate structures; generally straight gently curved but no twisting or overlapping present (Plate 4.3 d). One specimen is measured and showing these characters. Which, is 5.8 mm long and 3.0 mm broad.

Remarks -Hofmann and Aitken (1979) have defined *Tawuia* as rod and ribbon like compressions of millimetric width and centimetric length with smooth and even outline, sides parallel to slightly tapering, ends approximately semicircular. Sun (1987) has included the presence of circular bodies within *Tawuia* and absence of annulations on its surface. Present collection is showing the characters which have been identified earlier.

Age and distribution- Neoproterozoic, commonly occurring between 900 Ma to 700 Ma in Canada, China, Svalbard, India.

Genus- *Tuanshanzia* (Yan, 1995).

Type species- *Tuanshanzia platyphylla* Yan, 1995.

(Plate 4.2, g, h, i, Plate 4.3, e-i)

Synonymy

Tuanshanzia platyphylla Yan, 1995, p. 124, pl. II,figs. 9-12;
Tuanshanzia platyphylla Yan, 1997 in Yan and Liu, 1997, p. 38-39, pl. IV, figs. 11-17, 20, 21.
Tuanshanzia platyphylla Yan, Sharma, 2006, p- 32-33, Pl. I, figs. 7, 10, 13, 15, 16.
Tuanshanzia platyphylla Yan, 1995, Babu and Singh, 2011, p. 54-56, pl. 2e.

Type materials- From the Changcheng system ranging 1700-1400 Ma (Yan, 1995; Yan and Liu, 1997, 1998) belonging to Tuanshanzi Formation and Yanshan basin in Jinxian, Hubei of China, and from the Shuket Shale (Sharma, 2006c), India.

Locality- Rampur Village, Maihar area, Satna District, Madhya Pradesh.

Stratigraphic position- Rampur Formation, Semri Group, Vindhyan Supergroup, Early Mesoproterozoic.

Description Thalli oval, with rounded to rotundate apex and pointed base, pointed base appears as a stalk-like projection. Total 8 specimens are photographed (Plate 4.2, g, h, i and Plate 4.3, e-i) and measured their size. They are millimetric in size 1.1 mm to 7 mm in length and 0.2 mm to 4.5 mm in width.

Their outer margins are sharp and irregular. They have dense black colour and opaque characteristics, with no clear characteristics, preserved as carbonaceous films. They have platyphyllous blades and leaf like thallus morphology.

Remarks- The present species can be differentiated from *T. lanceolata* by their morphological features i.e. platyphyllous blades and in length to width ratio also. The small thalli of *T. platyphylla* may be a variant of *T. lanceolata* in the life cycle of algal population. Stalk-like projection is akin to parastem suggesting the specimen to be sessile thallus. These characteristics are also similar to *T. platyphylla* described by the Sharma (2006c) from the Olive Shale (Koldaha Shale) of the Semri Group, Vindhyan Supergroup.

Age and distribution- Neoproterozoic, commonly occurring between 1700-1400 Ma in Canada, China, Svalbard, India.

Type Genus*:* *Tuanshanzia* (Yan, 1995).

Type species *Tuanshanzia lanceolata* Yan, 1995

(Plate 4.2, l-p)

Synonymy

Tuanshanzia lanceolata Yan, 1995, p. 123-124, pl. II, figs. 4-8,
Tuanshanzia lanceolata Yan and Liu, 1997, p. 38, pl. IV, figs. 1-10.
Tuanshanzia lanceolata Yan, Sharma, 2006, p- 32-33, Pl. I, figs. 1, 2, 8, 9
Tuanshanzia lanceolata Yan, 1995, Babu and Singh, 2011, p. 54-56, pl.1 b, i.

Type materials- From the Changcheng system ranging 1700-1400 Ma (Yan, 1995; Yan and Liu, 1997, 1998) belonging to Tuanshanzi Formation and Yanshan basin in Jinxian, Hubei of China and from the Suket Shale (Sharma, 2006c) of Lower Vindhyan, India.

Locality- Rampur Village, Maihar area, Satna District, Madhya Pradesh.

Stratigraphic Position- Rampur Formation, Semri Group, Vindhyan Supergroup, Early Mesoproterozoic.

Description- Broad sheet-like thalli, lanceolate, widest in the middle, no folding and other features are present. Thick, narrowing and tapering towards both the ends parastem absent and with rhizoidal protuberances. Their size varies in ranges between 2.7 to 3.8 mm in length and 1.3 to 1.9 mm in width. Here total 5 specimens are measured and described (Plate 4.2, l-p).

Remarks- Flat sheet-like compression resembles the tubular thalli of some of the Phaeophyta or Chlorophyta. These are distinguished from *T. platyphylla* by larger size and length width ratio. They can be differentiated from *Lanceoforma striata* Walter et al. by sheet-like thalli and occasional lanceolate shape. No striations are observed. Size is smaller in comparison to the *Changchengia stipitata* and *Lanceoforma striata.* Present specimens are similar to *T. lanceolata* described by the Sharma (2006c) from the Olive Shale (Koldaha Shale) of the Semri Group, Vindhyan Supergroup.

Age and distribution- Commonly occurring between 1700-1400 Ma in Canada, China, Svalbard, India.

4.2 Microfossils

Several Precambrian deposits are known to contain mixed assemblages of prokaryotic and eukaryotic microorganisms from the black permineralized cherts that existed as microbial mat components or isolated (single to multicellular) organisms (Knoll et al., 2006). These microfossils have been recovered in maceration or examined in petrographic thin section and a combination of both techniques can be used to demonstrate their syngenicity and biogenicity. They were surviving in varied environment and palaeoecological condition accordingly (Sergeev, 2006). A number of publications have appeared in past years on the palaeobiological remains of the Proterozoic Vindhyan Supergroup, viz., the microfossils (Kumar and Srivastava, 1992a, b, 1995; Sharma 2006b) reflecting the renewed attempts to understand the palaeobiology of the basin. Chert is very common in Vindhyan sediments; consequently microfossils are found. Only the Salkhan Limestone Formation (Semri Group) contains a rich assemblage of various microfossils (McMenamin et al., 1983; Kumar and Srivastava, 1992a, b, 1995; Sharma, 2006) in bedded chert. Chert is a chemically precipitated and store house of well preserved fossils the world over. In the present study photosynthetic microorganisms, consisting of filaments and coccoids cyanobacterias are recorded, associated with bedded chert of the Salkhan Limestone, exposed in Maihar area, M.P. Their systematic palaeontology is provided below:

SYSTEMATIC PALAEONTOLOGY

Order- Chroococales, Wettstein 1924, emend. Rippka et al. 1979

Family- Chroococcaceae, Nageli 1849

Genus- *Coniunctiophycus,* Zhang 1981

Type species- *Coniunctiophycus gaonglobatum,* Zhang, 1981

(Plate 4.7, d, h, i, l)

Stratum typicum- Gaoyuzhuang Formation,China.

Locality- Near Bansagar Lake, Salkhan Limestone, Maihar area, M.P.

Stratigraphic position- Salkhan Limestone, Semri Group, Vindhyan Supergroup, Early Mesoproterozoic.

Description- Mostly sphaeroidal to elongated organic walled cells, occasionally polygonal, walls thin, finely granular and arranged in packets of 50–90 cells, in colony. Unit cells of pluricellular colonies range in size 2.7–3.6 μm (average 3.4 μm, wall 0.2 μm, 4 specimens measured), no external mucilage is apparent. Generally clumped in more or less globular, colonies are composed of more than 50 cells. Larger packets of cells form distinct lobes, generally accentuated due to post preservation changes. Colonies are circular to elongate and are parallel to bedding. No differentiation of cells within colonies. Surface is smooth. Cells not individually covered but colonies are encompassed by organic mucilaginous sheath. Cells randomly and compactly arranged in the colonies. Reproduction is by fission in three mutually perpendicular planes. Compactness of the colonies is probably due to daughter cells remaining aggregated. New colonies are probably formed by the fragmentation of the pre-existing colonies. Two different colonies are joined together. Length and width of colonies are in ranges between 23-30 μm and 18-23 μm respectively.

Remarks- *Coniunctiophycus gaonglobatum* colonies occur in bedded cherts. The present reported *Coniunctiophycus gaonglobatum* species is similar to described by Sharma (2006c) from Salkhan Formation of Bihar State. Their colonial habit may be compared closely with certain pleurocapsalean cyanobacteria like *Myxosarcina* and *Chroococcidiopsis* (Waterbury and Stainer 1978). Also other cyanobacteria such as *Entophysalis* sp. and other Eubacteria and certain protists, like *Chlorosarcina* may be assume such shape. Zhang (1981) described the genus *Coniunctiophycus* as complex aggregated colonies of a

number of spheroidal cells. He compared this habit to the living planktonic chroococcoid cyanobacteria *Microcystis*, *Coelosphaeridium* and *Aphanotheca*. The Salkhan assemblage of *Coniunctiophycus* conforms in all salient features to Zhang's (1981) generic diagnosis. Zhang (1981) assigned the *Coniunctiophycus gaonglobatum* to the family Chroococcaceae, close similarity of the present specimens with *Coniunctiophycus* and in absence of any reproductive body no firm systematic assignment is possible. Although Knoll et al. (1991) placed *Coniunctiophycus* under incertae sedis but considering Zhang's (1981) proposition it has been grouped in Chroococcaceae.

Distribution- Mesoproterozoic: the Gaoyuzhuang Formation, China; the Kotuikan and Yusmastakh Formations, Anabar Uplift, northern Siberia; the Salkhan Limestone, Semri Group, Vindhyan Supergroup.

Class- *Coccogoneae* Thuret, 1875

Genus- *Eoentophysalis* Hofmann, 1976, emend. Mendelson and Schopf, 1982.

Type species- *Eoentophysalis dismallakesensis* Horodyski and Donaldson, 1980, emend. Sergeev, 2006.

(Plate 4.4, l; plate 4.5, a-o)

Description- Spheroidal, ellipsoidal or polyhedral cells are enclosed by multilamellated envelopes and occurring in dyads, tetrads, octets or in larger colonies of a few tens of individuals. Colony form varies from loose clusters of gloeocapsoid cells to more regular cuboidal aggregations; colonies are typically enclosed within a translucent envelope. Cells diameters range from 4.4-9 µm. A single opaque inclusion is commonly present within cells.

Remarks- Identified *Eoentophysalis belcherensis* from Salkhan chert are identical to *Eoentophysalis belcherensis* from the Palaeoproterozoic Belcher Group of Canada (Hofmann, 1976) but measured less diameter of the cells comparatively. It is morphologically, developmentally, and environmentally essentially indistinguishable from modern *Entophysalis major* (Golubic and Hofmann, 1976). A particularly commonly occurring taxon in Palaeo-Mesoproterozoic microbial assemblages, *Eoentophysalis* is morphologically highly variable, having a complex life cycle the several stages of which can be subject to varying degrees of diagenetic post-mortem alteration (Hofmann, 1976; Golubic and Hofmann, 1976; Hofmann and Schopf, 1983; Knoll et al. 1991;

Sergeev et al. 1995; Sergeev, 2006). Although in the Salkhan cherts, colonies of *E. belcherensis,* typically similar to palmelloid colonies of the Chichkan populations of *E. dismallakesensis*. Earlier, similar form of *E. dismallakesensis* are described from the Khenjua Formation (Kumar and Srivastava, 1995) and from Salkhan Limestone (Sharma, 2006b)

Distribution- Mesoproterozoic: Dismal Lakes Group, Canada; Debengda Formation, Olenek Uplift, Siberia. Meso- Neoproterozoic: Sukhaya Tunguska Formation, Turukhansk Uplift, Siberia. Neoproterozoic: Chichkan Formation, South Kazakhstan; Yudoma Group, Siberia.

Family- Eoentophysalidaceae Geitler 1932.

Genus- *Eoentophysalis* Hofmann 1976 emend. Mendelson and Schopf 1982.

Type species- *Eoentophysalis belcherensis* Hofmann 1976 emend. Mendelson and Schopf 1982.

(Plate 4.6, a, b, c, e, g, h, j, k; Plate 4.9, b, e, i, j; Plate 4.10, c, d, e, j, Plate 4.11, g, j; Plate 4.12, c, d)

Stratum typicum- Kasegalik Formation, Canada.

Locality- Near Bansagar Lake, Salkhan Limestone, Maihar area, M.P.

Stratigraphic Position- Salkhan Limestone, Semri Group, Vindhyan Supergroup, Early Mesoproterozoic.

Description-Cells polygonal, sphaeroidal, ellipsoidal, occur in solitary or in pairs, planar tetrads, irregular clusters and colonies, occasionally distorted due to mutual compression. The size of cells varies from 2–8 μm across (with the average of 4.5 μm, 20 specimens measured). Pleuricellular aggregate of cells forming the thick sheet. Maximum length of sheet noticed is 98 μm and breadth 56 μm. Sometimes form pustulose laminae or palmelloid colonies. Dark-brown in colour. Sometimes dark black micron sized inclusions are present. Cells are enveloped by thin walls, which are sometimes weakly or darkly pigmented. Some of the enveloped double or paired ellipsoids contain spheroids (dark bleb of less than a micron size) as inclusion.

Remarks- *Eoentophysalis belcherensis* is noted in abundance in beded chert. It occurs along the dark dense black chert. These specimens are similar to the specimen described from the Kasegalik Formation of Canada both in generic and specific diagnosis. Yakschin (1990, 1991) described similar fossils from the

Mesoproterozoic Kutungda Formation of Olenek Uplift as the new genera *Eoxenococcus* Yakschin and *Corynophycus* Yakschin. Sergeev in Sergeev et al. (1995) interpreted the Kutungda population as *E. belcherensis*.

Distribution- Widely distributed in Palaeoproterozoic- and Mesoproterozoic chert; much less abundant in Neoproterozoic assemblage.

Genus- *Eosynechococcus* Hofmann 1976 emend Golovenok and Belova 1984.

Type species- *Eosynechococcus moorei* Hofmann 1976.

(Plate 4.11, k)

Stratum typicum- Kasegalik Formation, Belcher Supergroup, Canada.

Locality- Near Bansagar lake, Salkhan Limestone, Maihar area, M.P.

Stratigraphic position- Salkhan Limestone, Semri Group, Vindhyan Supergroup, Early Mesoproterozoic.

Description- Cells oblong, ellipsoidal to long rod shaped, sometimes curved to slightly constricted on one side. No covering envelope observed. Occurring solitary and loosely or closely aggregated forming irregular clumps or bowl shaped. Constriction probably representing transverse cell division can be seen. Centrally or eccentrically positioned, no dark object noticed. Dimension of cells 8 μm long and 4 μm broad (1 specimen measured).

Remarks- Population of *Eosynechococcus moorei* in the Salkhan assemblage has been found in beded chert. These are loosely preserved over the dark laminae. Salkhan population of *Eosynechococcus* confirm in all salient features with the diagnosis provided by Hofmann (1976). These are similar in size and shape described by Sharma (2006c).

Distribution- Mesoproterozoic: the Uluksan Group, Bylot Supergroup, Canada; the Kheinjua Formation, Semri Group, Vindhyan Supergroup, India; Neoproterozoic: the Bitter Springs Formation, Australia.

Genus: *Eoaphanocapsa*

Type Species- *Eoaphanocapsa oparinii* Nyberg and Schopf, 1984

(Plate 4.6, d, f, i, l; Plate 4.8, b, d, k, l, m; Plate 4.10, f)

Description- Single-walled or multilamellated spheroidal and ellipsoidal vesicles present. Diameter of cells in ranges 3.3–7 µm with envelopes , inclusions, commonly attached to the interior of the innermost wall layer, 0.5 µm. Individual

vesicle lamellae 0.2 µm thick; vesicles in loose clusters of a few to many tens of individuals commonly embedded in a diffuse organic matrix.

Remarks- *Eoaphanocapsa oparinii* colonies are relatively uncommon but distinctive element of the assemblage. These are similar in morphology and diagnosis of *Eoaphanocapsa oparinii* (Nyberg and Schopf, 1984). But measured less cells diameter of *E. oparinii* recorded from Salkhan chert, comparatively.

Distribution- Meso-Neoproterozoic, Sukhaya Tunguska Formation, Turukhansk Uplift, Siberia; Neoproterozoic, Min'yar Formation, southern Ural Mountains.

Genus- *Glenobotrydion* Schopf, 1968, emend. Nyberg and Schopf, 1984

Type species- *Glenobotrydion majorinum* Schopf, 1968, emend. Nyberg and Schopf, 1984.

(Plate 4.4, d, g, m, n, o, r)

Locality- Near Bansagar Lake, Salkhan Limestone, Maihar area, M.P.

Stratigraphic position- Salkhan Limestone, Semri Group, Vindhyan Supergroup, Early Mesoproterozoic.

Description- Single-layered spheroidal to ellipsoidal cells, defined by fine-grained thin walls that commonly contain a prominent dark spheroidal inclusion and occur in loose colonial clusters aggregates. Cells short axis range from 7 to 27.5 µm and long axis ranges 17.5-30 µm with that of the inclusions of 1.5 µm. Cells are almost globular with smooth surface with sharp margin in outer wall.

Remarks- The *Glenobotrydion majorinum* are widely reported by Sergeev and Schopf (2010), from Neoproterozoic sediments of Chichkan Formation, South Kazakhstan and Bitter Springs Formation, Australia (Schopf and Blacic, 1971), McLeary Formation, Belcher Supergroup, Australia (Hofmann, 1976). On the basis of their morphological characters they have been described as Chlorococcacean algae (Schopf and Blacic, 1971). Occurrence of *G. majorinum* in Salkhan Limestone is rare. In this study, cells are measured which have larger in size comparatively to original diagnosis.

Distribution- Neoproterozoic sediments of Chichkan Formation, South Kazakhstan (Sergeev and Schopf, 2010) and Bitter Springs Formation, Australia (Schopf and Blacic, 1971), Mc Leary Formation, Belcher Supergroup, Australia.

Class- Coccogoneae, Thuret 1875

Genus- *Huroniospora* Barghoorn, 1965

Type species- *Huroniospora microreticulata*, Barghoorn, 1965.

(Plate. 4.4, a, b, c, e, f, h-k, p, q; Plate. 4.10, a;Plate 4.11, c, d)

Stratum typicum- Gunflint Iron Formation, Canada.

Locality- Near Bansagar Lake, Salkhan Limestone, Maihar area, M.P.

Stratigraphic position- Salkhan Limestone, Semri Group, Vindhyan Supergroup, Early Mesoproterozoic.

Description- Cells are spheroidal to ellipsoidal unbranched, unicellular unattached bodies. No envelope or mucilage covering noticed. A minute aperture at the more constricted at upper end (plate 4.4, a, f, h). Spheroidal sometimes sporelike body exhibiting a thick wall of 1.2-3.5 μm with sculpture pattern regularly murate. The external wall structure is smooth. Cell diameter ranges between 7 and 26 μm (average 17.7 μm, 10 specimens, measured). The long axis ranges between 11.25-26.7 μm (average 21.7, 4 specimens, measured) and short axis ranges between 8.1-22.5 μm (average 11.1 μm, 4 specimens, measured). Reproduction is by fission. Daughter cells do not remain attached to the parent cell.

Remarks- These cells are found in bedded chert of the Salkhan Limestone. They are often set in a matrix of amorphous organic matter, which may represent uncrushed remains of mucilage. Intracellular dense mass is absent. The Salkhan population confirms in all the salient features with the specimens described by Barghoorn and Tyler (1965).

Age Distribution- Palaeoproterozoic: Kasegalik and McLeary Formations Belcher Supergroup, Canada; Franceville Group, Gabon; Mesoproterozoic: Amelia Dolomite Formation, Australia; Balbirini Dolomite, McArthur Group, Australia; Dismal Lakes Group, Canada; Kheinjua Formation, Salkhan Limestone, Semri Group, Vindhyan Supergroup, India; Sukhaya Tunguska Formation, Siberia; Neoproterozoic: Draken Conglomerate, Spitsbergen; Bitter Springs Formation, Australia.

Order- Nostocales or Oscillatoriales

Genus:- *Siphonophycus*, Schopf 1968 emend. Knoll and Golubic 1979, emend. Knoll et al. 1991.

Type species- *Siphonophycus robustum* (Schopf 1968) comb. nov. Knoll et al 1991, emend. Butterfield et al. 1994.

(Plate 4.13, a, b, j; Plate 4.14, d; Plate 4.15, a, b)

Stratum typicum- Bitter Springs Formation, Australia.

Locality- Near Bansagar Lake, Salkhan Limestone, Maihar area, M.P.

Stratigraphic position- Salkhan Limestone, Semri Group, Vindhyan Supergroup, Early Mesoproterozoic.

Description- Unbranched nonseptate tubes, curved, cylindrical to slightly compressed, they contain degraded trichome-like fragments. Surface is smooth, tube walls range from psilate to finely granulate. Specimens are rarely solitary, typically occurring entangled in masses of many individuals aligned parallel, subparallel or, less commonly, perpendicular to the bedding lamination to finely granular due to diagenetic effect, occur solitary or interwoven, forming mat (Plate 4.13, a, b). They have 1.4 to 4.0 μm widths (average 2.3 μm, 6 specimens measured), 85-88.9 μm long (incomplete). Dense masses of filaments align parallel or perpendicular to bedding lamination.

Remarks- *Siphonophycus* has been identified as the predominantly mat forming microbe in many Proterozoic benthic assemblages and sometimes found solitarily. This species is common in beded chert of Salkhan Limestone. Tubes of *Siphonophycus robustum* are considered as empty cyanobacterial (oscillatoriacean or nostocacean) sheaths (Knoll and Golubic 1979; Mendelson and Schopf 1982; Knoll et al., 1991; Sharma 2006c). Knoll et al. (1991) discussed the genus *Siphonophycus* described from Bitter Springs Formation, Australia and after the study of three form genera viz. *Siphonophycus kestron, Eomycetopsis robusta* and *Tenuofilum septatum* placed them in synonymy as *S. kestron, S. robustum, S. septatum*. Earlier Pjatiletov (1988) synonymized *Leiothrichoides* Herman (1974) with *Eomycetopsis* that was later included under the *Siphonophycus* by Knoll et al. (1991). They further argued that the larger populations of the *Siphonophycus* are presumably cyanobacterial, but *S. septatum* and *S. robustum* could be flexi-bacterial in origin (Aizenshtat et al., 1984). Many cyanobacterial species could have similar morphology and some may assume this morphology taphonomically. Zhang et al. (1998) therefore proposed that the taxonomy of the microbial sheath is form taxonomy.

Distribution- Widely distributed in Proterozoic cherts, and Phanerozoic deposits and organic walled assemblages.

Genus- *Sphaerophycus* Schopf, 1968.

Type species- *Sphaerophycus parvum* Schopf, 1968.

(Plate 4.7, a, b, c, e, f, g, n; Plate 4.8, a; Plate 4.12, a)

Stratum typicum- Bitter Springs Formation, Australia.

Locality- Near Bansagar Lake, Salkhan Limestone, Maihar area, M.P.

Stratigraphic position- Salkhan Limestone, Semri Group, Vindhyan Supergroup, Early Mesoproterozoic.

Description- Cells, small spheroids to ellipsoidal, solitary and in pair also. Sometimes loosely associated, some specimens angulated, surface texture psilate. Cell diameter ranges between 2.2 and 5 μm (average 3.6; 11 specimens, measured). Sheath encompassing cells present, typically hyaline. Daughter cells do not remain attached to the parent cell. Cells attached in a colony, size ranges, 13 X 94 μm.

Remarks- The size of *Sphaerophycus parvum* recorded from Salkhan chert is similar with the type species in the Bitter Springs Formation. On the basis of their characteristic features like small size, shape their solitary/paired occurrence they are differentiated from some other type species such as *Huroniospora* psilata, *Eosynechococcus isolatus*, etc. Knoll (1982b) described *S. wilsonii* from Draken Conglomerate, Spitsbergen but subsequently on the suggestion of Hofmann put into *S. parvum* (Knoll et al., 1991).

Age Distribution- Palaeoproterozoic: Kasegalik and McLeary Formations Belcher Supergroup, Canada; Franceville Group, Gabon; Mesoproterozoic: Amelia Dolomite Formation, Australia; Balbirini Dolomite, McArthur Group, Australia; Dismal Lakes Group, Canada; Kheinjua Formation, Salkhan Limestone, Semri Group, Vindhyan Supergroup, India; Sukhaya Tunguska Formation, Siberia; Neoproterozoic: Draken Conglomerate, Spitsbergen; Bitter Springs Formation, Australia.

Type species- *Sphaerophycus medium* Horodyski and Donaldson 1980.

(Plate 4.7, j, k, m; Plate 4.9, a, c, d, f, g; Plate 4.10, g, h, i; Plate 4.11 b)

Stratum typicum- Dismal Lakes Group.

Locality- Near Bansagar Lake, Salkhan Limestone, Maihar area, M.P.

Stratigraphic position- Salkhan Limestone, Semri Group, Vindhyan Supergroup, Early Mesoproterozoic.

Description- Cells sphaeroidal, 3–7 μm in diameter (average 4.6 μm, 12 specimens measured). Wall granular to smooth and are occuring in diad, tetrad or in linear clusters, rare unicells. Cell division by binary fission, daughter cells is not attached with the parent cell. Cells are attached in colony, size ranges 18 × 95.

Remarks- *Sphaerophycus medium* is abundant in the Salkhan population. These are randomly distributed in the amorphous organic matter. There are no solitary specimens, always found as diad and tetrad. Also Sharma (2006c), reported these type specimens as no solitary specimens, only found diad and tetrad, from stromatolitic cherts and cherty stromatolites from the Salkhan Formation, Bihar state. *Sphaerophycus medium* differentiates from the *S. parvum* by their occurrence in diad, tetrad and linear clusters. These are also distinguished by the slightly larger size. The diameter of both the species overlap somewhat as they in Akademikerbreen Group of Svalbard (Horodyski and Donaldson 1983).

Distribution- Mesoproterozoic: the Dismal Lakes Group, Canada; Kotuikan and especially, Yusmastakh Formations, Northern Siberia; Kheinjua Formation, Semri Group, India; Neoproterozoic: the Draken Conglomerate Formation, Spitsbergen and the Limestone–Dolomite "Series", East Greenland.

Genus- *Siphonophycus* Schopf, 1968, emend. Knoll & Golubic, 1979, emend. Knoll, Swett & Mark, 1991.

Type Species- *Siphonophycus kestron* Schopf, 1968.

(Plate 4.14, e, f, g)

Locality- Near Bansagar Lake, Salkhan Limestone, Maihar area, M.P.

Stratigraphic position- Salkhan Limestone, Semri Group, Vindhyan Supergroup, Early Mesoproterozoic.

Description- These are unbranched slightly curved, cylindrical to compresed. Three specimens are measured. Filaments width ranges between 3.5 μm, 6.2 μm and 6.4 μm and 35.7 μm, 36.8 μm, 68.8 μm in length (complete). They are rarely containing degraded evidently septate trichome like fragments.

Remarks- Sharma (1993) described *Archaeotrichion contortum* from the Salkhan Limestone. Morphological features are similar to the *Archaeotrichion*, *Eomycetopsis* and *Siphonophycus*. As discussed above, Knoll et al. (1991) merged *Eomycetopsis* into *Siphonophycus*. Subsequently, Butterfield (Butterfield et al; 1994) put the *Archaeotrichion contortum* as junior synonymy of *Siphonophycus septatum*. Therefore the *Archaeotrichion contortum* described by Sharma (1993) has been placed as *Siphonophycus kestron*. The smaller size diameter and non-septate nature suggest their bacterial affinity.

Distribution- Widely distributed both in chert-permineralized and compression-preserved Proterozoic assemblages.

Type Species- *Siphonophycus solidum* Golubic, 1979, emend. Butterfield, 1994.

(Plate 4.13, c-i, Plate 4.14, a.b,c)

Locality- Near Bansagar Lake, Salkhan Limestone, Maihar area, M.P.

Stratigraphic Position- Salkhan Limestone, Semri Group, Vindhyan Supergroup, Early Mesoproterozoic.

Description- Unbranched solitary nonseptate tubes, cylindrical to slightly compressed and curved with 3.2 to 10 µm broad. They rarely contain degraded trichomic fragments composed of disc-shaped cells; tube walls range from smooth to fine- or medium-grained. Length of filaments in ranges 47-109 µm (10 specimens measured).

Distribution- Widespread in peritidal mat assemblages of Proterozoic age.

Class- *Coccogoneae* (Thuret) Nageli, 1849.

Order- *Pleurocapsales* Geitler, 1925.

Genus- *Scissilisphaera* Knoll & Calder, 1983.

Type species- *Scissilisphaera regularis* Knoll & Calder, 1983.

(Plate 4.8, c, e-j)

Description- Colonies composed of four to several single to double-layered spheroidal to cuboidal envelope-enclosed cell packets, all situated on a single plane or stacked in two parallel planes, with each packets enclosing 40-100 tightly ad pressed cells. Cell diameters range from 3.1 to 5.3 µm. Their colonies are spherical, subspherical or cuboidal, ranging from 7 µm to 31 µm in size. The colour is dark brown.

Distribution- Neoproterozoic: Chichkan Formation, South Kazakhstan, Mesoproterozoic India.

Genus- *Myxococcoides* Schopf 1968.

Type species: *Myxococcoides minor* Schopf 1968.

(Plate 4.12, e, f,)

Stratum typicum- Bitter Springs Formation, Australia.

Locality- Near Bansagar Lake, Salkhan Limestone, Maihar area, M.P.

Stratigraphic Position- Salkhan Limestone, Semri Group, Vindhyan Supergroup, Early Mesoproterozoic.

Description- Cells commonly sub-spherical to ellipsoidal somewhat flattened by compression against the adjacent cells, clubbed into globular colonies. Surface structure smooth to finely granular. Cells dimension 7 μm, 7.3 μm, two specimens measured. Cells are enveloped in a granular to non-lamellated organic matrix; number of cells in colony up to 10–60. Cells randomly oriented in the colony. Occasionally distorted, may be due to mutual compression.

Remarks- Cells of this species are common in the beded cherts. These are similar as described by Schopf (1968) to the form *Myxococcoides minor* Schopf, in morphology. They are also comparable to *M. minor* described by McMenamin et al. (1983).

Distribution- Mesoproterozoic: the Uluksan Group, Bylot Supergroup, Canada; the Kheinjua Formation, Semri Group, Vindhyan Supergroup, India; Neoproterozoic: the Bitter Springs Formation, Australia.

Type species- *Myxococcoides inornata* Schopf, 1968

(Plate 4.10, b, k; Plate 4.11, f, h, l; Plate 4.12, b, g)

Stratum typicum- Bitter Springs Formation, Australia.

Locality- Near Bansagar Lake, Salkhan Limestone, Maihar area, M.P.

Stratigraphic Position- Salkhan Limestone, Semri Group, Vindhyan Supergroup, Early Mesoproterozoic.

Description- Single-layered spheroidal cells, solitary or occurring in colonies composed of few to tens of individuals embedded in a diffuse commonly well-defined organic matrix. Cell diameter ranges from 3.0 to 15.0 µm whereas the size of the colonies varies from 20.0 to 50 µm. Cell walls are 1.0 µm thick.

Some cells contain an opaque spheroidal inclusion 1.0 to 2.0 mm in diameter or, more rarely, an irregularly shaped dark body attached to their inner cell wall.

Remarks- These spheroidal microfossils here found, referred to the similar Genus *Myxococcoides* which has been defined by Schopf (1968) on the basis of their size and shape, their prokaryotic appearance, their conical habit, and their incorporation in an encompassing, amorphous, organic matrix. These may be similar to members of genus *Anacystis* Meneghini. But differ, however, from extant members of this genus in their somewhat larger cell diameters and their finely reticulate surface texture such as *M. minor* and *M. reticulata.*

Distribution- Widely distributed in Proterozoic cherts.

Order- *Pleurocapsales* Geitler, 1925.

Family- *Pleurocapsaceae* Geitler, 1925.

Genus- *Palaeopleurocapsa* Knoll, Barghoorn and Golubic, 1975.

Type species- *Palaeopleurocapsa fusiforma* Ogurtsova and Sergeev, 1987.

(Plate 4.14, h, Plate 4.15, c, d)

Description- Spheroidal, ellipsoidal, polyhedral, envelope enclosed cells tightly packed in two parallel rows, the cell packets of which are typically enclosed within spheroidal envelopes, forming spindle-shaped pseudofilamentous colonies. The diameter of the cells, 3.8-6.3 µm and length up to 68 µm, envelope-enclosed cell packets are 35 to 40. Individual cells commonly contain an opaque inclusion.

Remarks- The present records of *Palaeopleurocapsa fusiforma* are uncommon in the Salkhan chert. They are showing identical morphology of type species *Palaeopleurocapsa fusiforma* (Ogurtsova and Sergeev, 1987). *Palaeopleurocapsa fusiforma* is distinguished in the filament-like arrangement of its spheroidal vesicles produced by cell division in one plane; the pseudoparenchymatous packing of its component cells; and the occurrence of multiple sheath-like envelopes (e.g., Knoll et al. 1975). *Palaeopleurocapsa fusiforma* is distinguished from the other Chichkan species recognized from Salkhan chert by its spindle-shaped colonies and the characteristic sizes of its cells and cell packets.

Distribution: Neoproterozoic, Chichkan Formation, South Kazakhstan and Mesoproterozoic, Khenjua Formation, India.

4.3 Acritarchs

The black shales of the Rohtasgarh Limestone are investigated for acritarchs and recorded well preserved achritachs. These achritachs are separated from black shales through acid maceration technique. Detailed systematic description is provided below:

SYSTEMATIC DESCRIPTION

Group- Acritarcha Evitt, 1963.

Subgroup- Sphaeromorphite Dowinie et al., 1963.

Genus-*Dictyosphaera*

Type species- *Dictyosphaera delicate* Hu and Fu, 1982.

(Plate 4.16, j, k)

Locality- Badanpur Mine, Rohtasgarh Limestone, Maihar area, M.P.

Stratigraphic Position- Rohtasgarh Limestone, Semri Group, Vindhyan Supergroup, Mesoproterozoic.

Description- Spheroids clusters of cells. Spherical to subspherical small cells are joined in clusters. The clusters are consisting of consisting of interlocked numerous, closely packed cells of polygonal to subpolygonal units of 13-15 µm in diameter. The clusters diameters are 171 and 173 µm. Two specimens are measured.

Age Distribution- Mesoproterozoic (~1400 Ma) Ruyang Group, Shanxi Province China and Roper Group of Australia.

Genus- *Leiosphaeridia* Eisenack, 1958, emend. Downie and Sarjeant, 1963.

Type species- *Leiosphaeridia exsculpta* Timofeev, 1969 emend. Mikhailova in Yankauskas et al. 1989.

(Plate 4.16, f-i)

Locality- Badanpur Mine, Rohtasgarh Limestone, Maihar area, M.P.

Stratigraphic Position- Rohtasgarh Limestone, Semri Group, Vindhyan Supergroup, Mesoproterozoic.

Description- Flattened, spheroids, diameter ranges from 64-110 µm (4 specimens measured). The surface is covered with a fine network of wrinkles or

ridges. These are in size ranges between 8 and 11 µm in width. The wall thickness is 10 µm, distinctly preserved.

Age Distribution- Widely distributed in compression-preserved and chert-permineralized, Meso- and Neoproterozoic microfossil assemblages.

Genus- *Leiosphaeridia* Eisenack, 1958, emend. Downie and Sarjeant, 1963.

Type species- *Leiosphaeridia* sp.

(Plate 4.16, l)

Locality- Badanpur Mine, Rohtasgarh Limestone, Maihar area, M.P.

Stratigraphic Position- Rohtasgarh Limestone, Semri Group, Vindhyan Supergroup, Mesoproterozoic.

Description- Flattened, spheroids, are perforated by numerous holes and thick walled is observed. One specimen is measured in size 100 µm in diameter. The wall thickness is 10 µm. at the upper end one notch is present in length 30 µm.

Age Distribution- Mesoproterozoic, Rohtasgarh Limestone of Semri Group, Vindhyan Basin, India.

Genus- *Satka* Jankauskas 1979.

Type species- *Satka favosa* Jankauskas, 1979.

(Plate 4.16, d)

Locality- Badanpur Mine, Rohtasgarh Limestone, Maihar area, M.P.

Stratigraphic Position- Rohtasgarh Limestone, Semri Group, Vindhyan Supergroup, Mesoproterozoic.

Description- Spherical to subspherical small cells are joined in clusters. The clusters are consisting of numerous, closely packed cells of polygonal to subpolygonal units of 7.5µm in diameter. The cluster diameter is 125 µm. One specimen is measured.

Age Distribution- Early Mesoproterozoic sediments of Roper Group, central Australia and Lower belt Supergroup Montana, Mesoproterozoic Rohtasgarh Limestone Vindhyan Basin.

Genus-*Siphonophycus* Schopf, 1968.

Type species- *Siphonophycus costatus* Jankauskas, 1979.

(Plate 4.16, b)

Locality- Badanpur Mine, Rohtasgarh Limestone, Maihar area, M.P.

Stratigraphic Position- Rohtasgarh Limestone, Semri Group, Vindhyan Supergroup, Mesoproterozoic.

Description- Spirally coiled carbonaceous filament, both end of filament is prominent. Coil thickness vary in size between 2 and 6.2 µm. Coiling size is 25 µm. One specimen is measured.

Age Distribution- Widely distributed both in chert-permineralized and compression-preserved Proterozoic assemblages.

Genus-*Siphonophycus* Schopf, 1968.

Type species- *Siphonophycus* sp.

(Plate 4.16, a)

Locality- Badanpur Mine, Rohtasgarh Limestone, Maihar area, M.P.

Stratigraphic Position- Rohtasgarh Limestone, Semri Group, Vindhyan Supergroup, Mesoproterozoic.

Description- Coiled of flat carbonaceous film. Coil width is uniform in size i.e. 23.3 µm. Coiling size is 25 µm. One specimen is measured.

Genus- Genus *Trachyhystrichosphaera* Hermann, 1976 (in Timofeev, Hermann, and Mikhailova, 1976), emend. Hermann and Yankauskas, 1989 (in Yankauskas, 1989), emend. Butterfield, 1994 (in Butterfield et al., 1994).

Type species- *Trachyhystrichosphaera parva* Jankauskas, 1989.

(Plate 4.16, e)

Locality- Badanpur Mine, Rohtasgarh Limestone, Maihar area, M.P.

Stratigraphic Position- Rohtasgarh Limestone, Semri Group, Vindhyan Supergroup, Mesoproterozoic.

Description- Spheroidal with diameter 130 µm, one specimen, measured. The surface is covered with a network of wrinkles, ridges with folding. Size of these folding ridges is measured 10 µm.

Age Distribution- Early Neoproterozoic (1000-900 Ma) Lakhanda Formation of eastern Siberia Late Neoproterozoic and Terminal Proterozoic

sediments of Siberia. Mesoproterozoic, Rampur Formation and Rohtasgarh Limestone India.

Age Distribution- Mesoproterozoic, Rohtasgarh Limestone, Lower Vindhyan Basin.

4.4 Microbial mat structures

Proterozoic biosphere was dominated by microorganisms and the published record of their fossil remains were strongly dominated by stromatolites, finely laminated organosedimentary structures, due to the sediment binding and carbonate precipitating activities of microbial communities (Schopf and Klein, 1992). Whereas, Garrett (1970) suggested, microbial mats, their modern analog, today only figure prominently in restricted settings that reduces or eliminates competition and grazing by other organisms. Carbonate microbial mat deposits, where early diagenetic cementation may preserve domal morphology, lamina textures, and even filament structures (Horodyski et al., 1977). Microbiota appeared on Earth before 3.8 Ga, and perhaps flourished during the Proterozoic time (Schopf, 1999; Eriksson et al., 2000). In Precambrian setting microbial mats understandably colonized most surfaces where predatory and/or competing organisms were absent (Walter and Heys, 1985) as evidenced by the common occurrence of stromatolites and microbial laminites within Precambrian carbonate successions. However, it was suggested, microbial activity was comparatively reduced during the Phanerozoic and confined to stressful environments (Schieber, 1999; Hagadorn and Bottjer, 1999). After that, a wide variety of Mat-Induced Sedimentary Structures i.e. MISS (Noffke et al., 2001; Schieber, 2004) are reported. At times they were bizarre in nature and may be misinterpreted as trace fossils (Seilacher, 1999). Abundance of mat related structures in Proterozoic rock formations impart a distinct dimension to Proterozoic biosedimentology.

The sedimentary structures formed by interplay between microbial and physical process and their characteristics are based on the following parameters:

- Intrinsic biofactors;
- Biological response to physical disturbances of the growth base;
- Trapping/binding effects;
- Secondary physical deformation of biogenic build-ups;

- Post-burial processes;
- Bioturbation and grazing.

Pettijohn and Potter (1964) divided the sedimentary structures into four major groups:

I. Bedding external form
II. Bedding internal organization and structures
III. Bedding plane features
IV. Bedding disturbed and deformed

Microbially induced sedimentary structures (MISS) classified as a fifth category in Pettijohn and Potter's (1964) classification of primary sedimentary structures by Noffke et al. (2001). They had divided MISS in to two class: A) structures atop bedding planes and B) internal bedding structures formed due to five main biological activities (1) leveling, (2) biostabilization, (3) imprinting (4) microbial grain separation, and (5) baffling, trapping, and binding.

Class A: On bedding planes

1. leveled depositional surface, wrinkle structures
2. microbial mat chips
3. erosional remnants and pockets
4. multidirectional /palimpsest ripples
5. mat curls, shrinkage cracks

Class B: Within beds

1. sponge pore fabrics, gas domes, fenestrae structures;
2. sinoidal laminae;
3. oriented grains, benthic ooids;
4. biolaminites, mat-layer-bound grain sizes.

Schieber (2004) analyzed the influence of mat on the depositional fabrics of sedimentary rocks across a broad spectrum of physical, biological and chemical processes, and provided the information regarding the features that preserved in

sandstone, carbonate as well as in shales. Microbial mat features in sandstone shale and carbonate incorporate:

- ❋ Mat growth
- ❋ Metabolic effect
- ❋ Physical mat destruction
- ❋ Mat decay and diagenetic effect

Later, Schieber (2007) provided a detailed and more formal description which is based on the previously proposed classification scheme of Schieber (2004). They divided microbial growth features broadly into two groups. A third category viz. 'complex structures' has been incorporated to include complementing the range of features.

Complex Structures

These classifications scheme of mat related structures are genetic and based on the formation of these structures. Sarkar et al. (2008), provided a classification scheme which was based on the genesis of mat induced sedimentary structure in relation to their palaeoenvironment.

(1) ML (Mat-layer) structures

(i) mid (mat-layer discoidal) structures

(ii) mlc (mat-layer crumpled) structures

(iii) mlw (mat-layer wrinkled) structures

(2) MI (mat-induced) structures

(i) misc (mat-induced surface cracks)

(ii) micr (mat-induced cracks along ripple crests)

(iii) misr (mat-induced surface ridges)

(iv) mib (mat-induced bulges)

(3) MP (mat-protected) structures

(i) mpsf (mat-protected) setulf

(ii) mppr (mat-protected patchy ripples)

(iii) mpr (mat-protected ripples)

4.4.1 Microbial Mat Structures in Lower Vindhyan

Microbial mats are different from stromatolite due to their specific microbial-physical mode of formation, their appearance and, therefore, they have been classified as a separate category within primary sedimentary structures. The classification is based on the ability of the cyanobacteria to interact with physical processes and sedimentary dynamics. Carbonate (chemical) sediments are formed by the precipitation of minerals in marine areas. Microbial mats are typically formed by filamentous, entangled organisms that produce a macroscopic "matlike" structure. Stal (2000) found the reason, why cyanobacteria are the most successful organisms at mat building results from a combination of characteristics unique to this group. Cyanobacteria are the only known oxygenic phototropic prokaryotes. They display a great resilience to changes and fluctuations of environmental conditions. As their predominant metabolism is oxygenic photosynthesis, cyanobacteria use light as an energy source, water as an electron donor and CO_2 as a carbon source. Where these requirements are met, abundant microbial mats will form. Cyanobacteria interfere with erosion, deposition, and deformation caused by wave action or currents. The bacterial activities comprise 'microbial leveling', 'biostabilization', baffling, trapping, and binding', 'microbial grain separation', and 'imprinting' (Noffke et al., 2001b). The microbes induce both surface structures, as well as intrasedimentary structures (Noffke et al., 2001b; Gerdes et al., 2000). Microbial buildups in the lower Vindhyan carbonates have been rarely studied in the past. Only, stromatolits are described from the Kajrahat and Fawn Limestone in the Semri Group. Even, these are not recorded from the Rohtasgarh Limestone.

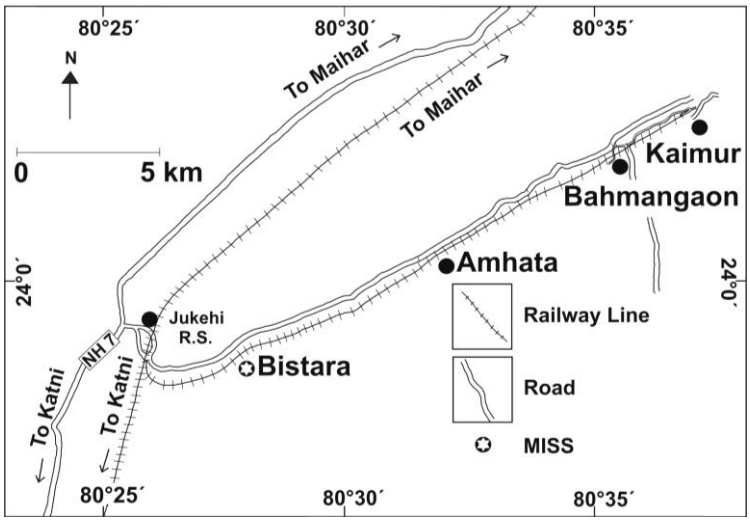

Fig. 4.1a- Location map of MISS localities, Bistara Mine, Maihar area, Katni District, Madhya Pradesh (after Sharma and Shukla, 2009).

In present study, microbial features are documented from the Rohtasgarh Limestone of the Lower Vindhyan, exposed in Maihar area, M.P. (Fig. 4.1 a, b) and Murlipahar, Bihar (Fig. 4.2, a, b), which is of Paleoproterozoic–Mesoproterozoic age.

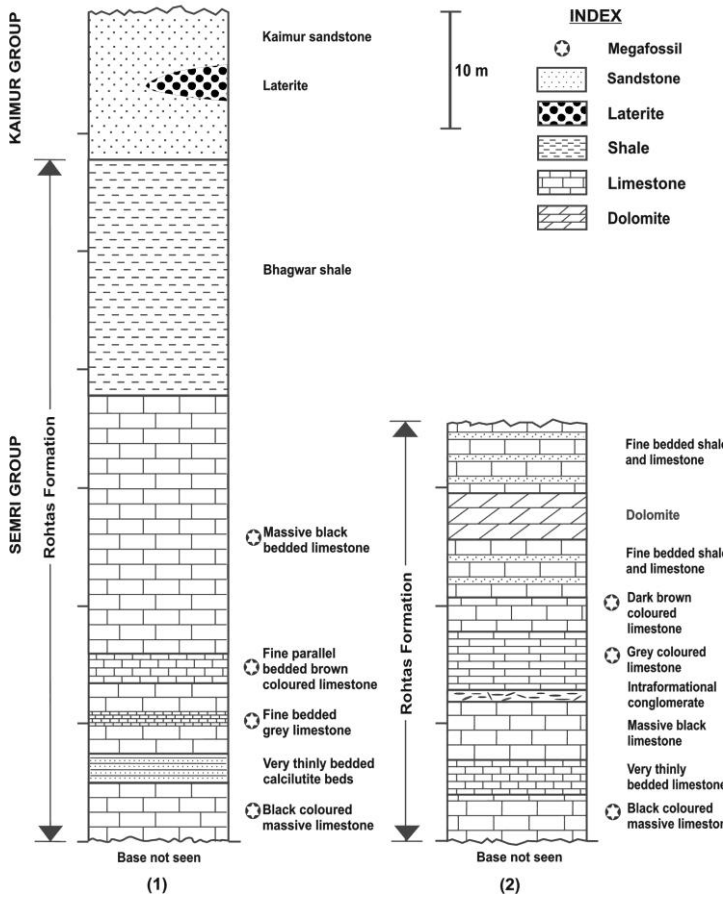

Fig. 4.1 b. Lithostratigraphic succession of the Bistara and Bahmangaon mines. Asterisks indicate the frequency of the occurrence of MISS. (1) Lithocolumn of Bistara mine and (2) lithocolumn of Bahmangaon mine (after Sharma and Shukla, 2009).

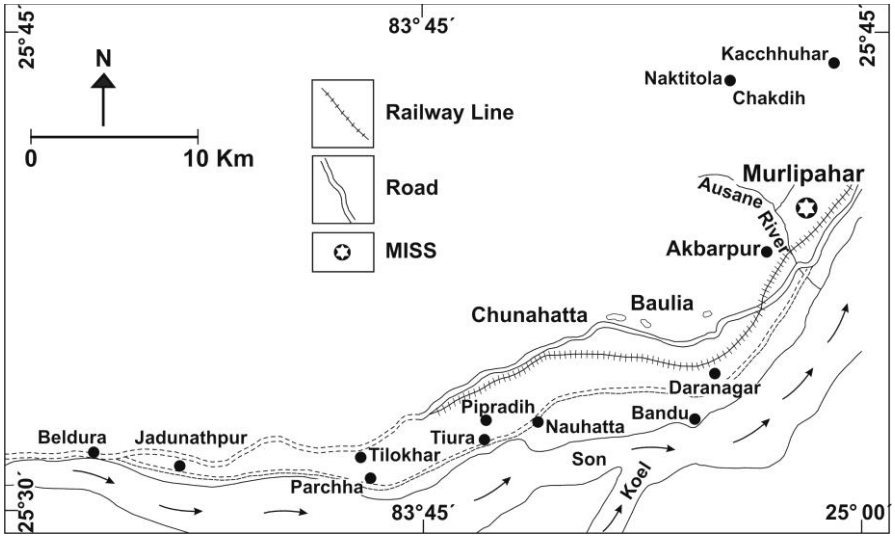

Fig. 4.2a- Location map of MISS localities, Muralipahar, Rohtas District, Bihar (after Sharma, 1993).

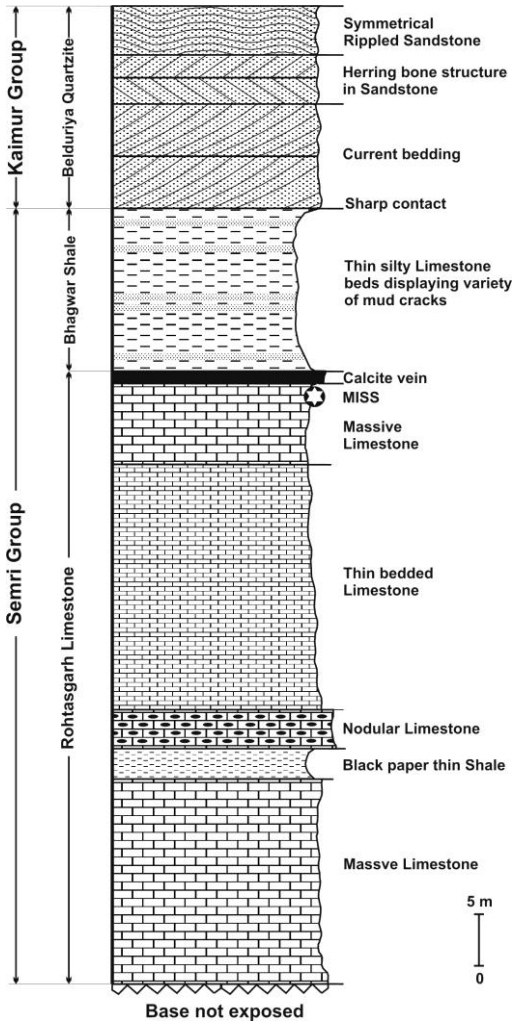

Fig. 4.2 b. Lithostratigraphic succession of the Muralipahar area, Rohtas District, Bihar (after Sharma, 1993).

A variety of structures of potential microbial mat origin occurs on bed surfaces or on bed interfaces of the Rohtasgarh Limestone as described below. These are recognized by surface morphology and described below.

4.4.2 Wrinkle structures

The minute ridges generally have a crinkled appearance, showing a pattern, parallel to each other and form a network. In networks they have cross-cut each other or may share the same crests at their meeting points (Plate, 4.17, a, b). These are sinuous to curved irregular, round to sharp crested bulges. These wrinkled structures have millimeter to centimeter sized irregular, round bulges or reticulate pattern of wrinkles (Plate, 4.18, a, b), these structures are also defined as mat growth (Eriksson et al., 2007). According to them, in modern intertidal settings wrinkle marks on mats are common in occurrence at the sediment–water interface. Gas build-up because of decay at mat bottom can generate wrinkle structures commonly with steep slopes of their troughs generated similar structures under gas pressure in experimental setting (Gerdes et al., 2000 and Pfluger, 1999). Gentle wave or current shear may also form the wrinkle structure on mat (Hagadorn and Bottjer 1997; Porada et al., 2008; Banerjee and Jeevankumar 2005). Wrinkle structures with unidirectional asymmetry in profile that is common in the Rohtasgarh Limestone might have developed under shear of gentle wave or current on a microbially mediated cohesive carbonate surface. In contrast to siliciclastic environments, in evaporitic carbonatic depositional regimes, early diagenetic mineral precipitation cements and the preservation potential of these macrostructures is much higher.

4.4.3 Mat growth structures

Mat growth-related structures are created by the changes in microbial activity, growth direction, and growth rate, in response to the environmental factors (Gerdes, 2007), and by the interplay between microbes and sedimentation (Eriksson et al., 2007). In modern mats metabolic procecess like photosynthesis have been observed to shift carbonate solubility enough to cause precipitation of carbonate minerals between and along filaments within the growing mat (Chafetz, 1992). These mineral precipitation effect can be preserved within the rock record

as irregular ooids, desciminated carbonate grains, micritic cements between terrigenous, and highly lamina specific carbonate cementation within laminated sandstone. They often show as minute pustules, tufts, and pinnacles, as well as polygonal growth ridges, on the bed surface. Mat-protected ripples (Plate 19, a, b) are common in mat structures of the Rohtasgarh Limestone exposed in Muralipahar, Rohtas District, Bihar. Due to the protection of mat layers, previously formed ripple marks are protected from wave erosion and are superimposed with subsequent ripple marks, forming irregular network patterns (Plate 20 a, b.). The microbial mats are preserved on the surface with macroreticulate features. The ripples associated with binding of microorganism and sediments are parallel to each other (Plate 20a, b). These structures are commonly considered as a type of mat growth structures (Eriksson et al., 2007).

4.4.4 Mat destruction structures

Physical destruction of mats creates a broad range of structures that may occur in situ or may be found as redeposited materials (Eriksson et al., 2007). The *Manchuriophycus* like structure are recognized in the Rohtasgarh Limestone (Plate 4.21a, b). A *Manchuriophycus*-style structure had been interpreted as resulting from thicker mats developed within the troughs, between ripples (Eriksson et al., 2007). This kind of structure is characterized by sinuous ridges waving in ripple valleys, but rarely on ripple ridges. Along the growth ridges, tiny pinnacles or pustules are preserved. The height of ripples ridges is ~2mm and width of consequent ripples is ~15mm. the microbial mats are preserved as in cuspate pattern which are uniformly distributed and aligned in same direction. The microbial impressions are preserved within these cuspate as macroreticulate features. These structures are measured, with ridges ~1 mm, width ~15 mm and length ~20 mm. Due to the protection of mat layer, previously formed ripples marks are protected from wave erosion, and are superimposed with subsequent ripple marks, forming a network patterns.

4.4.5 Mat decay structures

This type of microbial features are abundant in the Rohtasgarh Limestone which have millimetric to centimetric sizes, rounded and unattached to each other.

The size ranges, ~0.5 mm in height and ~6 mm in diameter (Plate, 4.19, c, d, e, f). These refer to the structures formed on the sediment surface or within sediments by gas and fluid escapes (Dornbos et al., 2007; Noffke et al., 2001; Gerdes et al., 2000). Gases may be derived from the decay of buried microbial mats or directly from microbial photosynthesis. Due to the sealing of impermeable mats on the sediment surface, the escaping gas will push the mat upward to form various domes or blisters. If the mat is thin or the upward-rising gas pressure is high enough, the sealing mat will break, resulting in "mud-volcano" structure or partially ruptured '*Astropolithon*' structure (Sarkar et al., 2008; Eriksson et al., 2007; Pfluger, 1999). After compaction, they may express as biscuit-like and donut-shaped structures on the bedding plane. It has been reported that in modern tidal flats and swamps, microbes can grow on gas bubbles, so that the bubbles are coated with and protected by leathery biomats (Eriksson et al., 2007; Gerdes, 2007). These microbially coated bubbles can be filled later with sediments and therefore have the potential of preservation in sediments. Resulting, the oncolite like concretions are developed (Plate, 4.19, d, f).

***Longfengshania* Structures-** Sharma et al. (1992) described the non fossils structures *Longfengshania,* from the Rohtasgarh Limestone. Our recorded structures (Plate 4.22 a, a1, b, b1, c) from the Rohtasgarh Limestone exposed in Muralipahar, Rohtas, Disctrict, Bihar, are similar to the structures were described from the same formation. These structures are non fossils structure and exhibit pear shaped microbial mat structures. These pear shaped structures are measured in size 13 mm (Plate 4.22 a1) to 23 mm (Plate 4.22 b1), the lamina are 1 to 3 mm in thickness. It was described by Du and Tian (1985). They have suggested that external mould on the limestone surface, as foliated structure with a stalk like parastem and occasional rhizome at the base. The presence of parastem is a diagnostic feature. It not only supports the foliate structure and connects it with rhizome, but also exposes it towards sunlight for photosynthesis in water. The size of both the parastem and foliate structures depend on the ecological realm. Many form exhibit surface ornamentation such as marginal rings of variable width, ring veins, and inner ring veins. Some of them appear to exhibit organic differentiation similar to that of higher plants. Maithy and Babu (1988) also reported this type of structures from the Rohtasgarh Limestone of the Semri Group and given name as *Longfengshania (Longfengshania) chopanensis*.

4.5 Precipitated Fan-Fabric structures

Studies of numerous Proterozoic and Archean radial-fibrous and laminated textures carried out during past two decades have brought the diversity and complexity of the pre-Neoproterozoic sedimentary precipitates into sharper focus. The well preserved silicified fossil assemblages are, in almost all cases, closely related to these sedimentary textures (Knoll et al., 1993; Knoll and Sergeev, 1995; Sergeev et al., 1994, 1995; Seong-Joo and Golubic, 1999, 2000; Bartley et al., 2000). Therefore, investigation of the Mesoproterozoic silicified carbonate precipitates and associated microbiotas are very important, both to understand the carbonate precipitation patterns and the role of evolving ancient microorganisms in biostratigraphy. Calcium carbonate seafloor fans are unusual features of the geologic record, and the conditions that fostered their formation are still poorly understood. Carbonate fans are common features of Archean and Palaeoproterozoic carbonate platforms (Kah and Knoll, 1996; Sumner and Grotzinger, 1996), occur mostly in intertidal settings of the Mesoproterozoic (Bartley et al., 2000), and are conspicuous features of carbonates that cap low latitude glacial deposits of the Neoproterozoic (Kennedy, 1996; Hoffman et al., 1998; Hoffman and Schrag, 2002). In present study, seafloor-precipitated carbonate fans are reported from the Kajrahat Limestone of Lower Vindhyan exposed around Maihar area, M.P. The fans occur in cm-sized beds. The precipitates apparently grew both as radiating crystals (fans) and as “beds” of upward-oriented crystals that are typically one centimeter in height (Sumner and Grotzinger, 2000). The recorded fan- fabric crystal units (originally bundles of aragonite crystals) occur both in clusters and evenly spaced across a bedding plane (Plate 4.23). Growth forms of the crystals vary from dense patches to sparsely spaced units across bedding planes. This may be evidence for the precipitates growing as fans in some beds, but as individual crystals on the seafloor in others. In vertical cross-section, the crystal size is variable. The crystals range in length from about 0.1 to 3.0 cm. The crystals display square terminations; these structures are preserved along the surface these can be also observed in thin section as mini fan fabric structures (Plate 4.24, 4.25).

4.5.1 Geological Distribution of carbonate fan-fabric

Carbonate fans are common features in early Precambrian successions but become increasingly environmentally restricted through the Mesoproterozoic and Neoproterozic sedimentary record. Seafloor-precipitated carbonates formed commonly in Archean and Palaeoproterozoic marine basins, implying that the nature of carbonate sedimentation and ocean carbonate chemistry must have been fundamentally different from modern conditions. The stratigraphic distribution of carbonate fans suggests that specific environmental factors play a role in their development and preservation. In Mesoproterozoic carbonate successions, fans are restricted to intertidal environments (Bartley et al., 2000). Sea floor precipitated carbonates are generally rare; however, they do appear in enigmatic carbonates often superposed with glacial deposits (Kennedy, 1996; Hoffman et al., 1998; James et al., 2001; Hoffman and Schrag, 2002). James et al. (2001) suggested, aragonite fan pseudomorphs deposited in cap carbonates of the Mackenzie Mountains also formed in limestone beds within siliciclastic-dominated settings. Therefore, similar sized carbonate fans in the modern are now restricted to diagenetic environments (James et al., 1988) and are not known to occur in open marine conditions on the seafloor. The stratigraphic distribution of carbonate fans, their overall rarity in post-Proterozoic sections, and their occurrence in otherwise enigmatic carbonates (i.e. Snowball Earth and Lower Triassic carbonates) suggests that rare environmental factors are required to foster their formation. A better understanding of specific fan occurrences in the geologic record might ultimately provide insight into why fans form where they form. Exceptionally, sea floor-precipitated carbonate fans of cm-sized preserved and recorded in the Neoproterozoic, Rainstorm Member of the Ediacaran Johnnie Formation, Death Valley region, eastern California (Pruss et al., 2008).

4.5.2 Conditions fostering fan formation

It was considered, laminated or radial-fibrous microbiolites with fine, extremely even and uniformly thick lamination, regardless of depositional orientation, as “precipitates”. These precipitates formed almost exclusively by inorganic deposition of calcium carbonate, with little evidence of involvement of cyanobacteria. Unambiguous remnants of cyanobacterial communities, that could

be responsible for accretion of precipitates by deposition, trapping or binding of sediments, have not been observed within these textures. The cyanobacteria or heterotrophic bacteria, as a result of their metabolic activity, probably changed the environments and indirectly facilitated the carbonate precipitation (Chafetz and Buczynski, 1992; Grotzinger and Knoll, 1995; Seong-Joo and Golubic, 1999, 2000; Bartley et al., 2000). The radial fibrous precipitated structures are well preserved on surface of thick and compact Kajrahat Limestone of the Lower Vindhyan. These radial-fibrous textures are composed of radiating to subparallel blades of fibrous crystals. Bartley et al. (2000) suggested that morphologically identical radial-fibrous fans were located near the intertidal and supratidal facies of an arid tidal flat, where evaporation of seawater resulted in significant carbonate oversaturation. The growth of radial-fibrous structures was quenched by a change in water chemistry, resulting from flooding, reduced concentration of inorganic carbon or overgrowth of cyanobacterial mats. The decomposed mats probably were the centers for initial carbonate precipitation because organic molecules that inhibited this process were consumed heterotrophically making the microenvironments favorable for carbonate precipitation. In some cases, nucleation occurred directly at the sediment–water interface and the fans grew rapidly, penetrating the mats and entombing allochthonous microorganisms. The growth of radial-fibrous textures was intermittent, with periods of low precipitation punctuated by rapid growth of the radial-fibrous fabric. When the nucleation occurred slightly below the sediment–water interface, the radial fan-like structures were formed (Bartley et al. 2000). The size and shape of fibrous crystals resembles the fibers that constitute botryoidal aragonite (Ginsburg and James, 1976; Folk and Assereto, 1976; Grotzinger and Read, 1983; Hofmann and Jackson, 1987), although this growth habit may also occur in calcite (Bartley et al., 2000). Also during the Archean and palaeoproterozoic, precipitate carbonate textures formed in a variety of environments including unrestricted open marine settings (Sumner and Grotzinger, 1996). Although the relative abundance of precipited carbonate textures varies widely from basin to basin. Most Mesoproterozoic carbonate succession, in turn, contain accretionary precipitates only in restricted coastal marine environments (Cao, 1992), at least some of which are associated with development of evaporites (Kah and Knoll, 1996). By the later Neoproterozoic Era, macroscopic precipitated textures formed only under

anomalous condition conditions such as those associated with post glacial cap carbonates (Grotzinger and Knoll, 1995). These structures are common features in early Precambrian succession and Mesoproterozoic-Neoproterozoic sedimentary record.

4.6 Precambrian Palaeobiology and Problems of Contamination

To a great extent, Precambrian Biostratigraphy is based on studies of macro, microfossils, cyanobacteria and eukaryotic algae. Studies of acritarchs are important in this context. Evitt, (1963), and Downie et al. (1963) given definition of acritarchs, as organic microstructures of uncertain taxonomic affinities records containing in sedimentary rocks. However, during previous study, a number of morphotypes originally described as microfossils by Walcott (1914) and more recently by other investigators, have been reexamined by among others, (Hofman, 1971; Cloud and Morrison, 1979). The biological origin of many of these forms could not be confirmed. The presence of microorganism in the siliciclastic rocks both Phanerozoic and Precambrian require Hydrofluoric acid, digestion to remove organic walled microfossils from the mineral matrix. Complete removal of minerals material is in practical terms, impossible. Furthermore some workers study the same insoluble matter in the Scanning Electron Microscope (SEM) to look for microfossils. During such investigation, Fuxing and Quling (1982) discovered some structures with a morphology which could have been misinterpreted as fossils. The rocks matrix of shales and carbonates in powder forms, have been macerated to separate the microfossils associated in the constituent formation of the Lower Vindhyan sediments. Details about the macerations techniques, adopted here, are described in chapter 3. In the case of microfossils, recovered through palynological maceration of shales, (acid resistant organic residue recovered by digestion of rocks in HF, HCL, and other mineralic acids) the rock matrix, the very evidence necessary to prove the syngenesity of the microfossils is lost. This has resulted in inadvertently describing extant microflora as Precambrian microfossils. These contaminations are introduced in the samples in the field, during macerations processes through water or at the time of preparation of slides (aeroflora). Several Precambrian workers have discussed these problems and have suggested methods to overcome them (Maithy and Pflug

1978, Manoharachari et al., 1990; Shukla et al., 1992). In the present study it is also found out the effect of mineralic acids on some known forms of extant cyanobacteria. These are discussed in this chapter with figures. The present observations bring out that many of the changes occurring after acid treatment in extant cynobacteria are similar to those in fossils. Morphological featurs are in increasing order are affected by acid, comonaly used for maceration. Earlier, Fuxing and Quiling (1982) described during their study that acritarch like artifacts, 'pseudomicrofossils' may be easily produced during acid maceration of samples. Also, they observed, the most common pseudomicrofossils' are microstructures which have specific gravities less than unity.

Earlier, most of the workers have described the contamination problems in macerated microfossils as 'pseudomicrofossils' (Karkhanis, 1977; Fuxing and Qiling, 1982; Manoharachari et al., 1990; Shukla et al., 1992). According to them the morphological similarity is significant because it was found that the light microfossils can be produced in the laboratory from bubbles (Djenzhuraev, 1977) and aggregates of fine grained organic particles. According to previous study on contamination problems, it was suggested, when maceration methods are used to prepare slides of actritarchs for microscopic examination, usually numerous bubbles evolve in the solutions at the various steps during samples preparation. Small particles of the kerogen liberated from the samples rocks may be attached to the surface of the bubbles. When air escapes from bubbles, the flocculated kerogen particles usually retain a basically spherical shape and they do not disperse. These spherical aggregates may eventually flatten and convert them into disc like shapes. The entire process is producing these artifacts, from the easily recognizable bubbles to the pseudomicrofossils. On the basis of above practically results, same problems have been noted and photographed of generated pseudomicrofossils (Plate 4.26, 4.27, 4.28). It is noted that all of the pseudomicrofossils, which are prepared and are differentiated from the real Precambrian acritarchs recorded under transmitted light microscope. The size of these pseudomicrofossils, are varied between 20 and 88 µm, in diameter. More than 36 contaminated specimens are noted, photographed and measured in size and morphology. All are spherical in shape (Plate 4.26, 4.27, 4.28).

PLATE-4.1

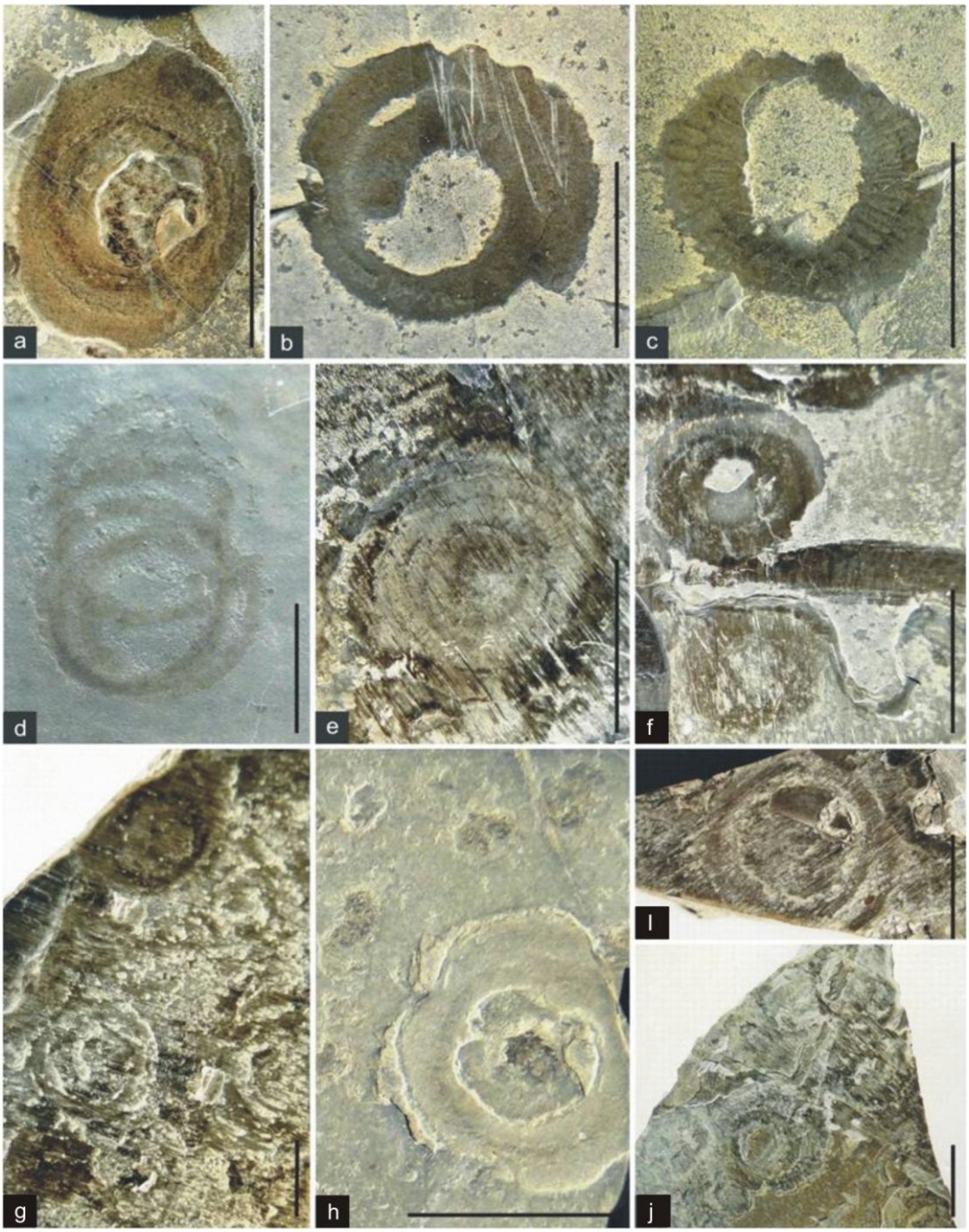

Helically **c**oiled megascopic fossils on the parting surfaces of carbonate rock from the Rohtasgarh Limestone, Amehta mine, exposed in Maihar area, M.P. Specimens photographed in reflected light. (a, d and f-k) *Grypania spiralis* Walcott 1976, showing smooth coiled specimens; d- shows carbonaceous remains on the specimens and tightly coiled spiral; (b, c and e) *Katnia singhii* Tandon and Kumar 1977, is showing segmented coiled specimens; e- Tightly coiled specimen with segmentations at irregular intervals; (b, c) loosely coiled specimen with segmentation at regular intervals. Scale bar = 1.2 cm for all the photographs.

PLATE-4.2

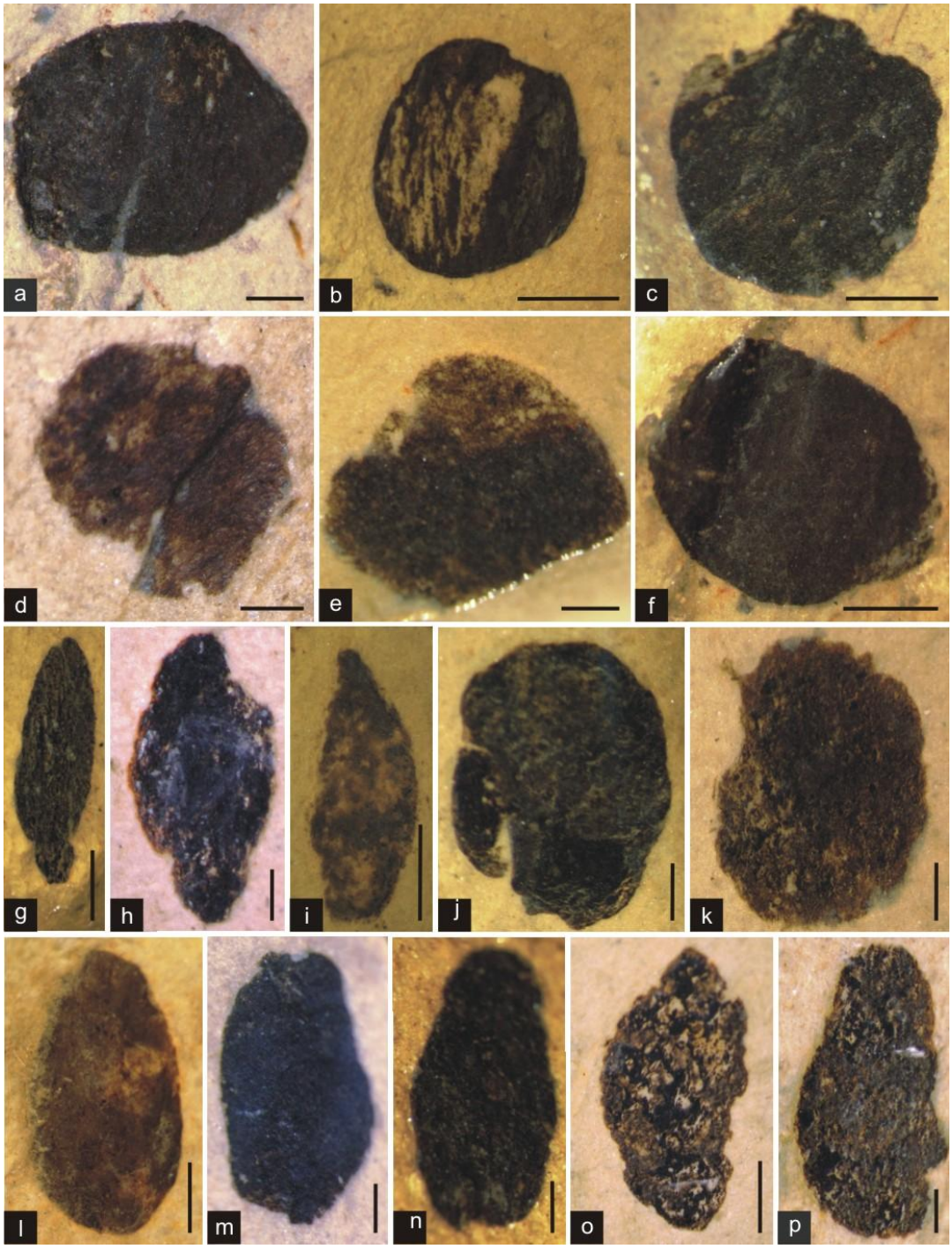

Carbonaceous megafossil recovered from the parting surfaces of gray shale from the Rampur Shale, Rampur village, exposed in Maihar area, M.P. (a-f, j, k) *Chuaria circularis*, Walcott 1899, showing *c*ircular to elliptical shape, preserved as carbonaceous film; (g, h, i) *Tuanshanzia platyphylla* Yan 1995, preserved with carbonaceous impression film; (h) Showing platyphyllous blades like morphology and (h, i) showing leaf like thallus morphology, and sharp apex at the upper end; (l- p) *Tuanshanzia lanceolata* Yan 1995, showing broad sheet-like and lanceolate morphology. All are widest in the middle; (m, n) preserved as compression and (l, o, p) as impression. All are preserved as carbonaceous film. Scale bar = 1 mm for c, f, g, l, o and for others 0.5 mm).

PLATE-4.3

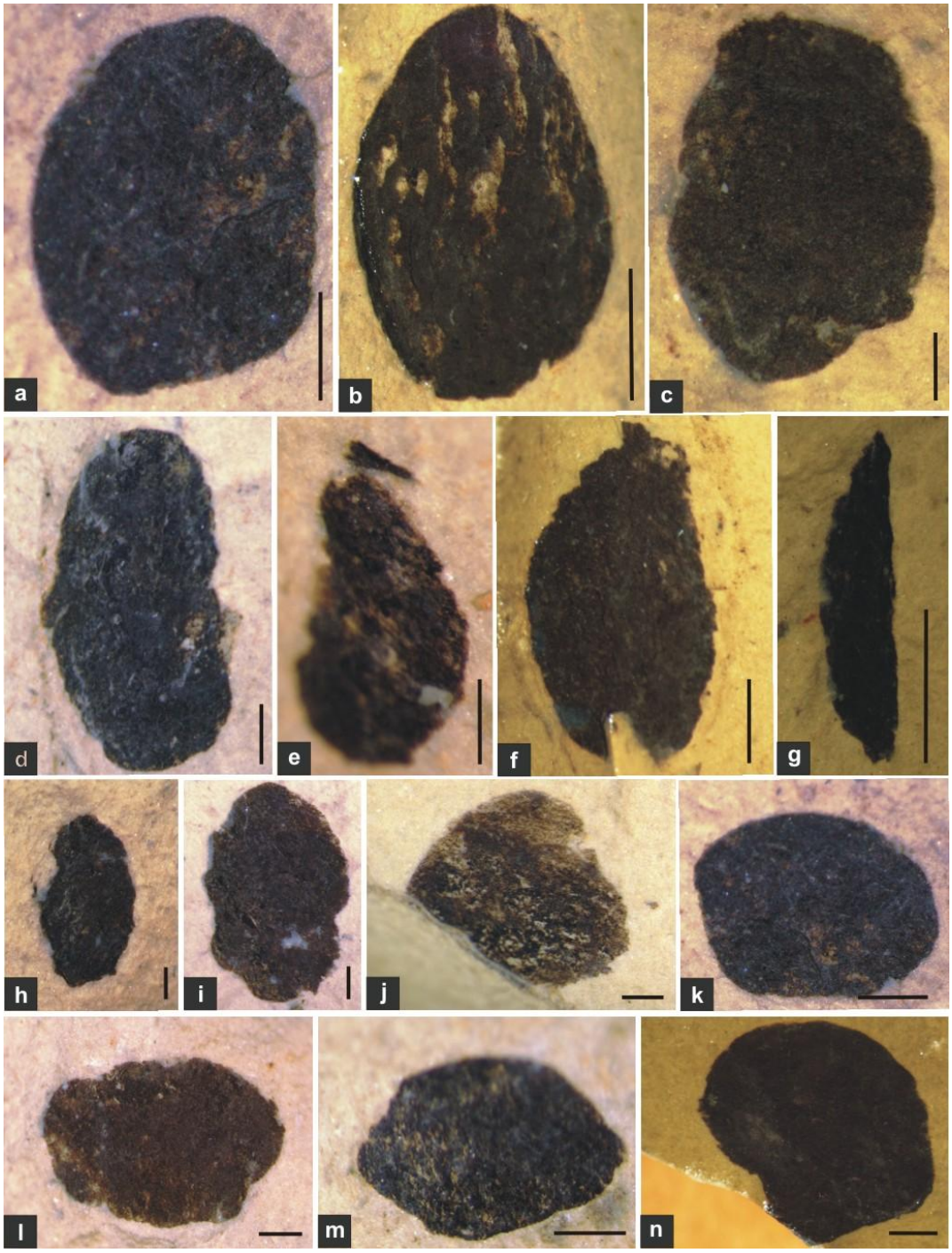

Carbonaceous megafossil recovered from the gray shale from the Rampur Shale, exposed in Rampur village, Maihar area, M.P. (a, b, c, j-n) *Chuaria circularis*, Walcott 1899, showing circular to elliptical shape, preserved as carbonaceous film; (a, c, n) preserved as impression; (d) *Tawuia dalensis* Hofmann 1979, showing carbonaceous film and compression preservation. It is slightly curved and thick rod like structure; (e- i) *Tuanshanzia platyphylla* Yan 1995, preserved with carbonaceous film with compression; (g) Showing leaf like morphology, and sharper at both end. All are widest in the middle. Scale bar = 1 mm for a, b, c, d, f, i and for others 0.5 mm).

PLATE-4.4

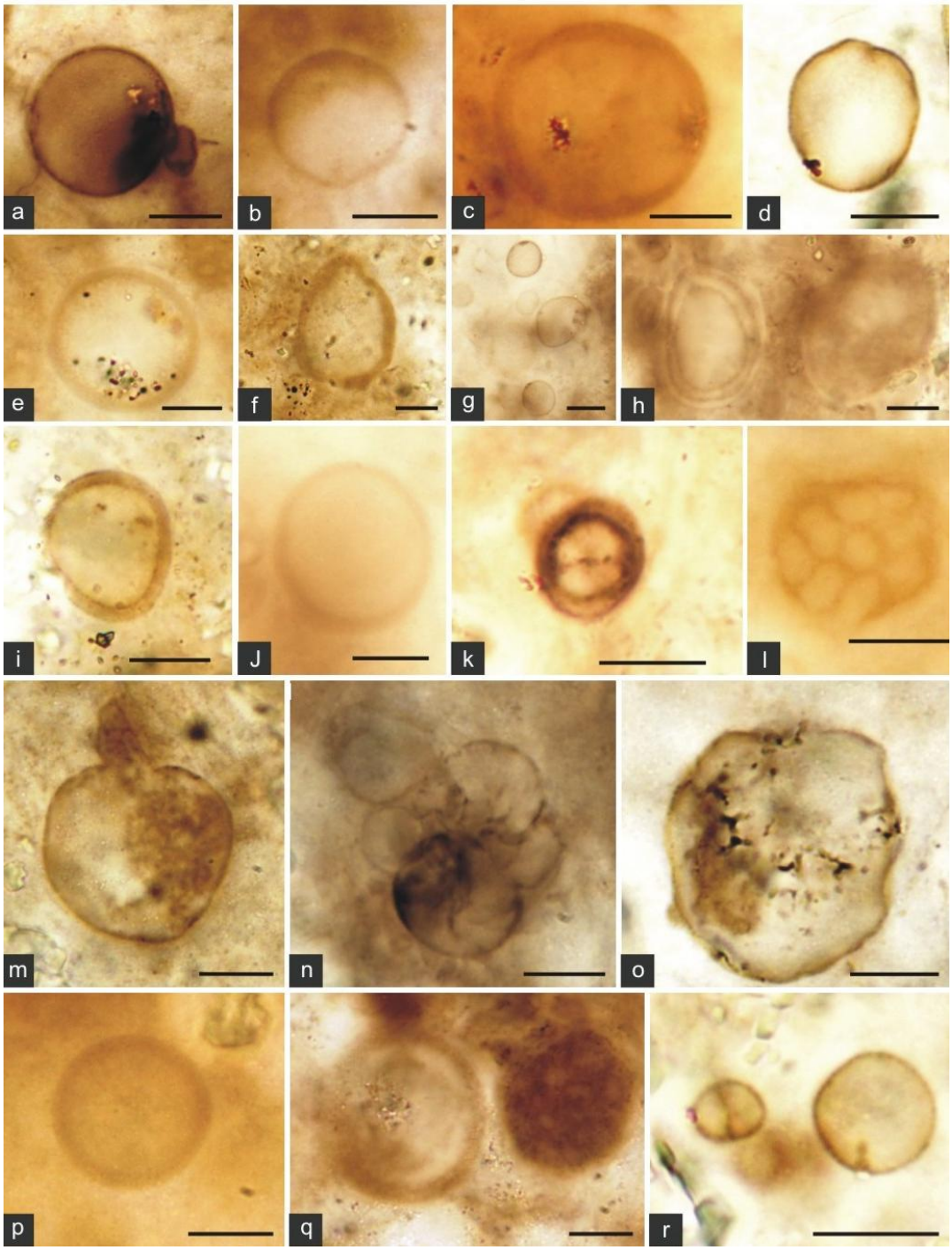

Microbial assemblage recorded from bedded chert of the Salkhan Limestone, exposed near Bansagar Lake, Maihar area, Satna District, M.P. (a, b, c, e, f, h-k, p, q) *Huroniospora* Barghoorn, 1965, are preserved as single cells, spherical to oval shape; (a, b, c, e, j, k, p q) showing spherical single cells; (f, h, i) showing oval shape, with thick wall, a minute aperture at the more constricted at upper end; (d, g, m, n, o, r) *Glenobotrydion majorinum* Schopf and Blacic 1971, Nyberg & Schopf, 1984, single layered sphereoidal to ellipsoidal cells, globular with smooth surface with sharp margin in outer wall; (l) *Eoentophysalis dismallakesensis* Horodyski and Donaldson 1980, spheroidal, ellipsoidal or polyhedral cells enclosed by multilamellated envelopes and occurring octets in a colon. Scale bar = 10 µm for all specimens. Specimens details- (a)-9/29-15 (b, p)- 9/21 B- 17, 31 (c)- 9/19 E- 7 (d, i, m, n ,o)-9/26 A-11, 7, 1, 10, 21 (e-h, q, r)-70, 52, 64, 42, 49, 54 (j)- 9/17 D- 27 (k)- 9/26 B-15 (l)- 9/20 A-1.

PLATE-4.5

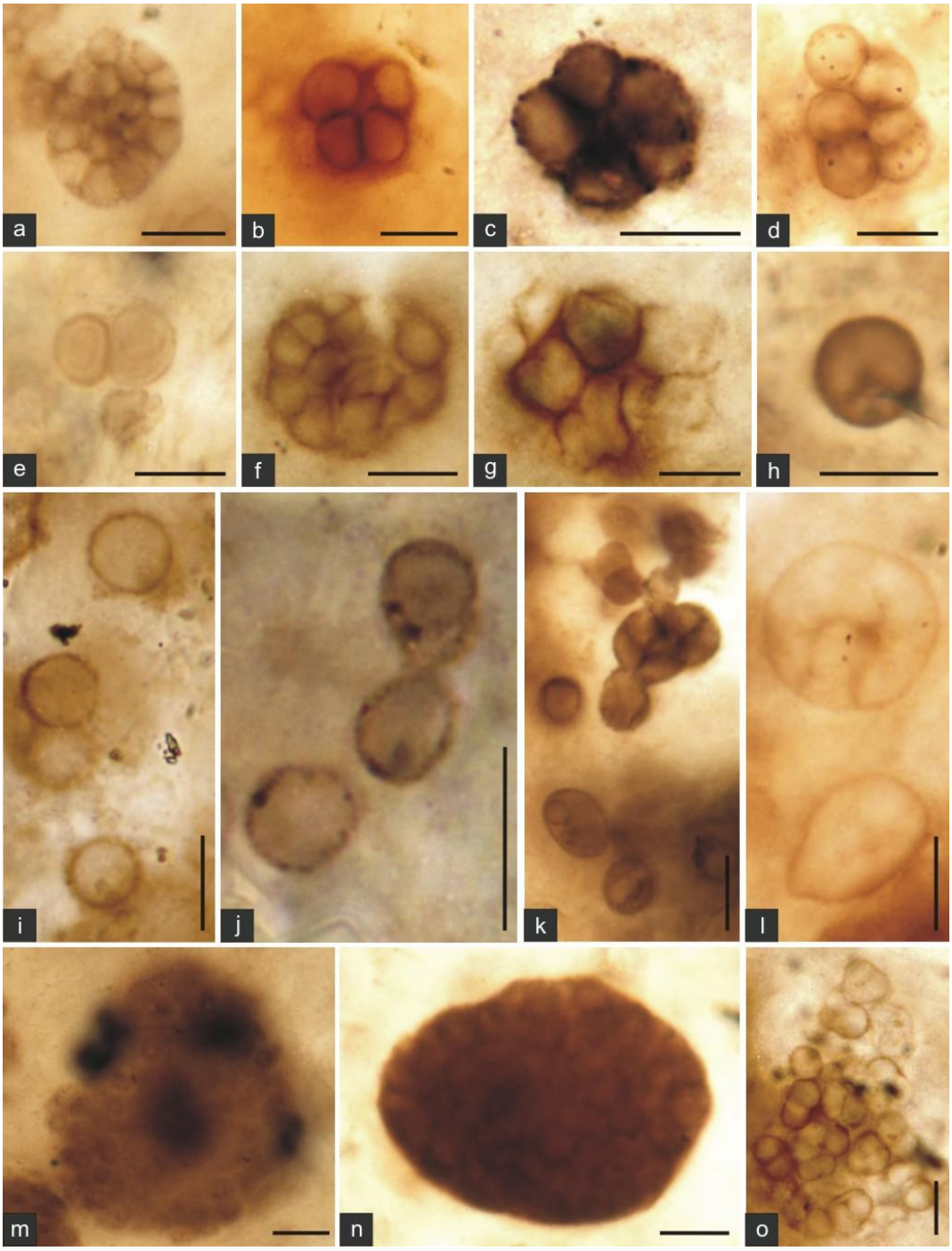

Microbial assemblage recorded from bedded chert of the Salkhan Limestone, exposed near Bansagar Lake, Maihar area, Satna District, M.P. (a- o) *Eoentophysalis dismallakesensis* Horodyski and Donaldson 1980, spheroidal, ellipsoidal or polyhedral cells enclosed by multilamellated envelopes and occurring as single cell, tetrad and multiple cells in colonial form. Scale bar = 10 µm for all specimens. Specimens details- (a, l)- 9/21 A- 37, 17 (b)- 9/17 D- 29 (c, j, k)- 9/29- 35, 1 (d)- 9/26 B- 19 (e, n, o)-9/17 A-5, 33, 45 (f)- 9/17 B- 7 (g)- 9/20 B- 17 (h, i)- 9/9-17, 31 (k)-9/29- 63 (m)- 9/28 A-72.

PLATE 4.6

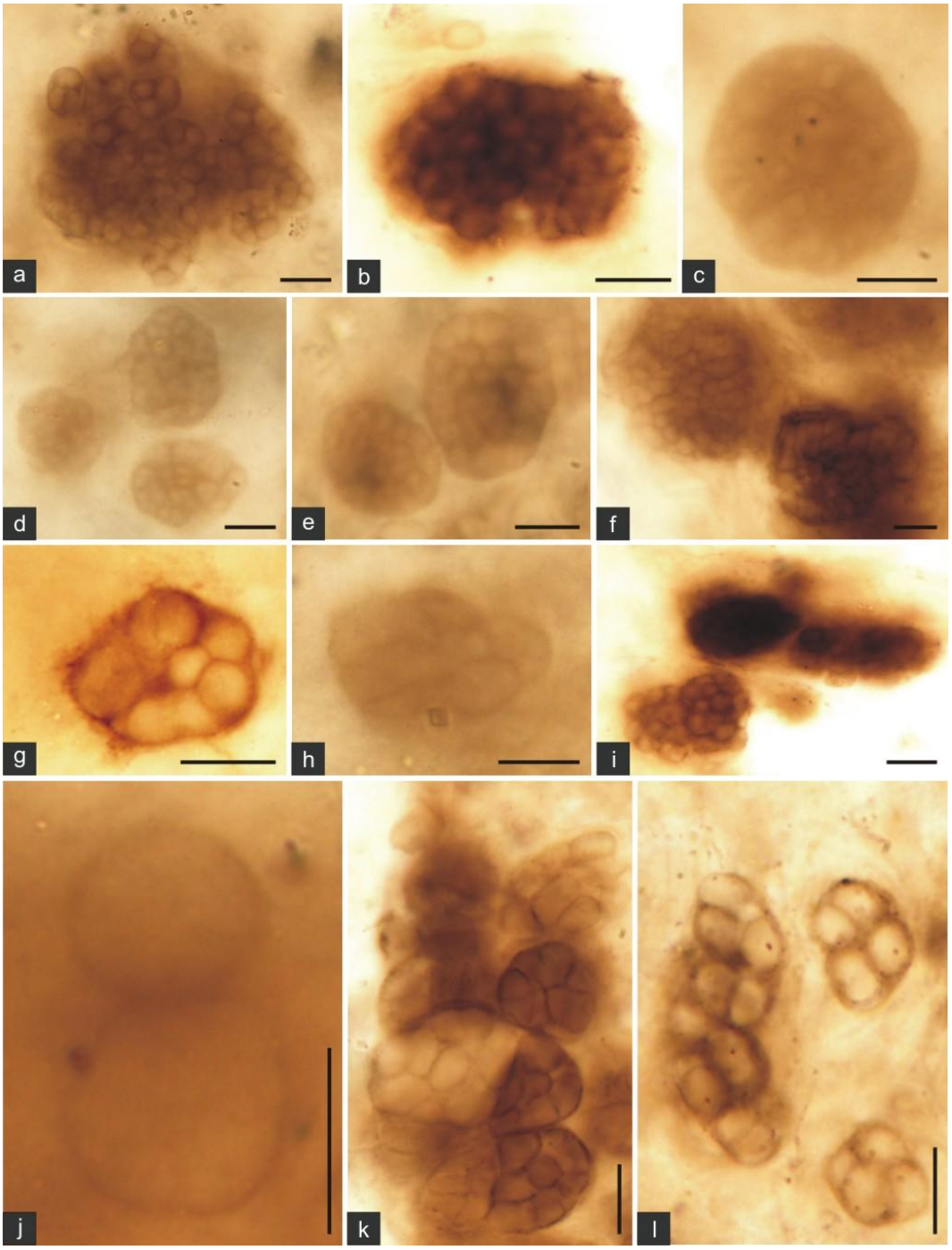

Microbial assemblage recorded from bedded chert of the Salkhan Limestone, exposed near Bansagar Lake, Maihar area, Satna District, M.P. (a, b, c, e, g, h, j, k) *Eoentophysalis belcherensis* Hofmann 1976, Cells polygonal, sphaeroidal, ellipsoidal, occur in solitary and in pairs, planar tetrads, irregular clusters and colonies; (d, f, i, l) *Eoaphanocapsa oparinii* Nyberg and Schopf 1984, preserved as single walled and multilamellated spheroidal and ellipsoidal vesicles. Scale bar = 10 µm for all specimens. Specimens details- (a, f)- 9/17 E- 19, 11 (b, i)- 9/20 B – 37, 35 (c, d)- 9/21 B- 33, 25 (e)- 9/21 A- 15 (g)-9/17 D-25 (h)- 9/21 C- 1 (k) 9/28 A- 76 (l)-9/26 B- 17.

PLATE 4.7

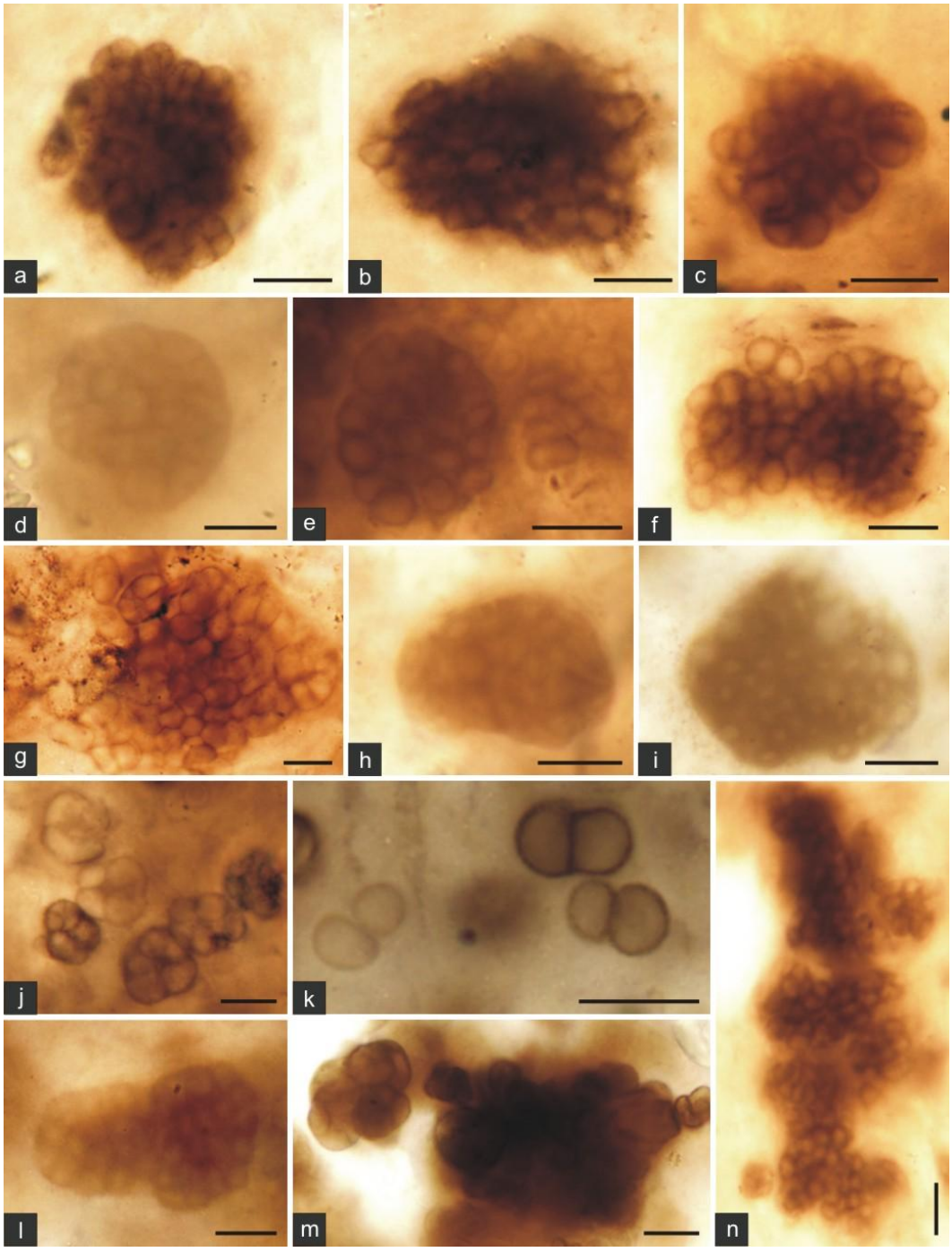

Microbial assemblage recorded from bedded chert of the Salkhan Limestone, exposed near Bansagar Lake, Maihar area, Satna District, M.P. (a, b, c, e, f, g, n) *Sphaerophycus parvum* Schopf, 1968, have polygonal, sphereoidal, ellipsoidal cells occurring in irregular clusters and colonies; (d, h, i, l) *Coniuntiophycus conglobatum* Zang 1980, preserved as clusters of single walled sphereoidal to ellipsoidal cells; (j, k, m) *Sphaerophycus medium* Horodyski and Donaldson 1980, preserved with sphaeroidal cells; (j) Has tetrad cells. (k) Has two joined cells; (m) Tetrad cells joined as clusters. Scale bar = 10 µm for all specimens. Specimens details- (a, b, f, n)- 9/20 B- 7, 1, 21, 23 (c, m)- 9/29- 49, 67 (d)- 9/17 E- 21 (e, j)- 9/9 – 27, 41 (g)-9/28 A-87 (h, i)- 9/19 E- 9, 13 (l)- 9/21 B-27.

PLATE-4.8

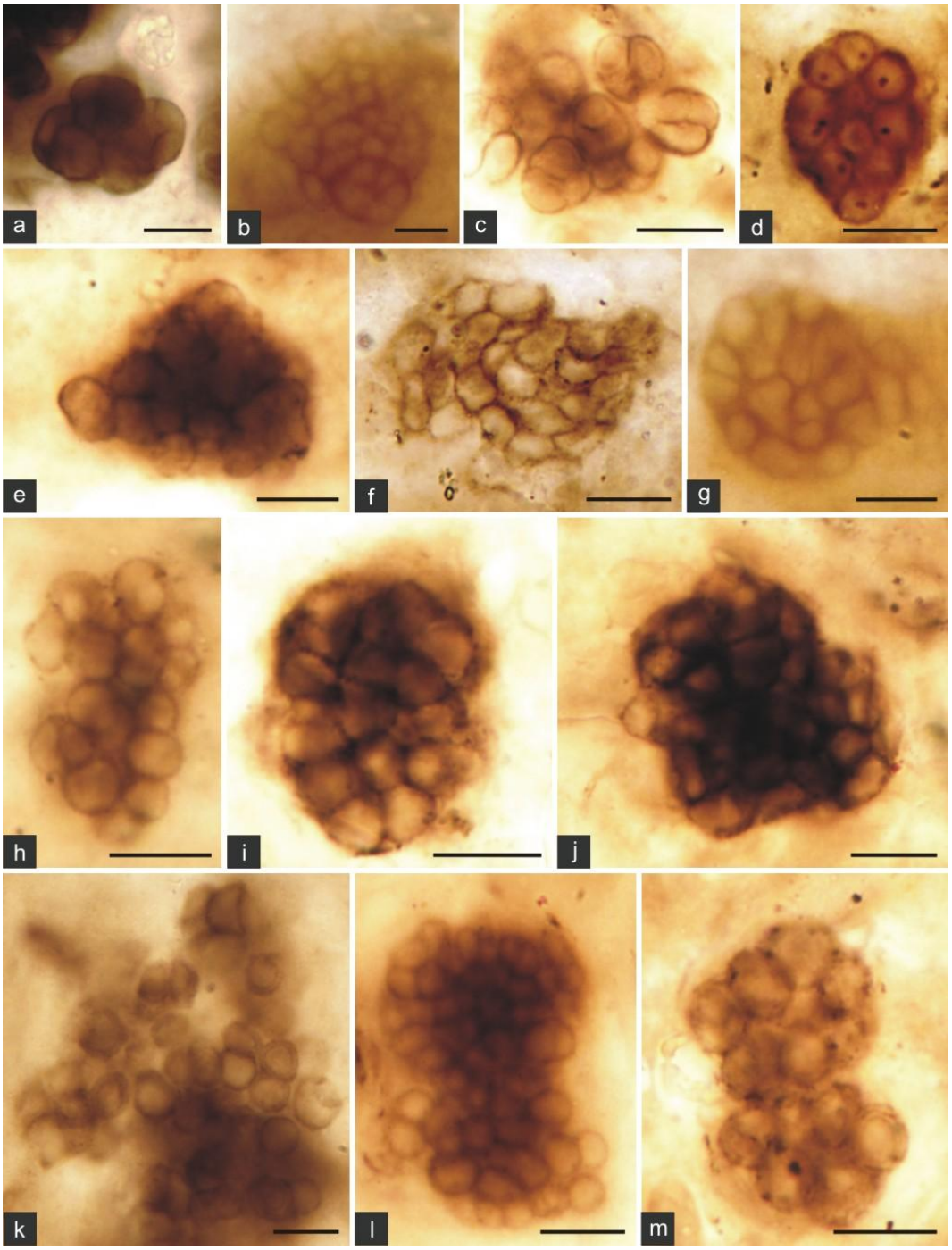

Microbial assemblage recorded from bedded chert of the Salkhan Limestone, exposed near Bansagar Lake, Maihar area, Satna District, M.P. (a) *Sphaerophycus parvum* Schopf, 1968, have polygonal tetrad cells occurring as clusters; (b, d, k, l, m) *Eoaphanocapsa oparinii* Nyberg and Schopf 1984, preserved as clusters of single and multiple cells; (d) Have spherical cells joined in a clusteres with vesicles; (e, f, g, h, i, j) *Scissilisphaera obtusa* Green, Knoll and Swett 1989, preserved as clusters of spheroidal and polygonal cells. Scale bar = 10 µm for all specimens. Specimens details- (a,)- 9/29- 13 (b, g)- 9/17 E- 1, 23 (c, d, h, i, j, m)- 9/26B-29, 23, 37, 31, 25 (f, k)- 9/17 E- 9, 11 (h)-9/17 B-11 (l)- 9/20 B- 21.

PLATE-4.9

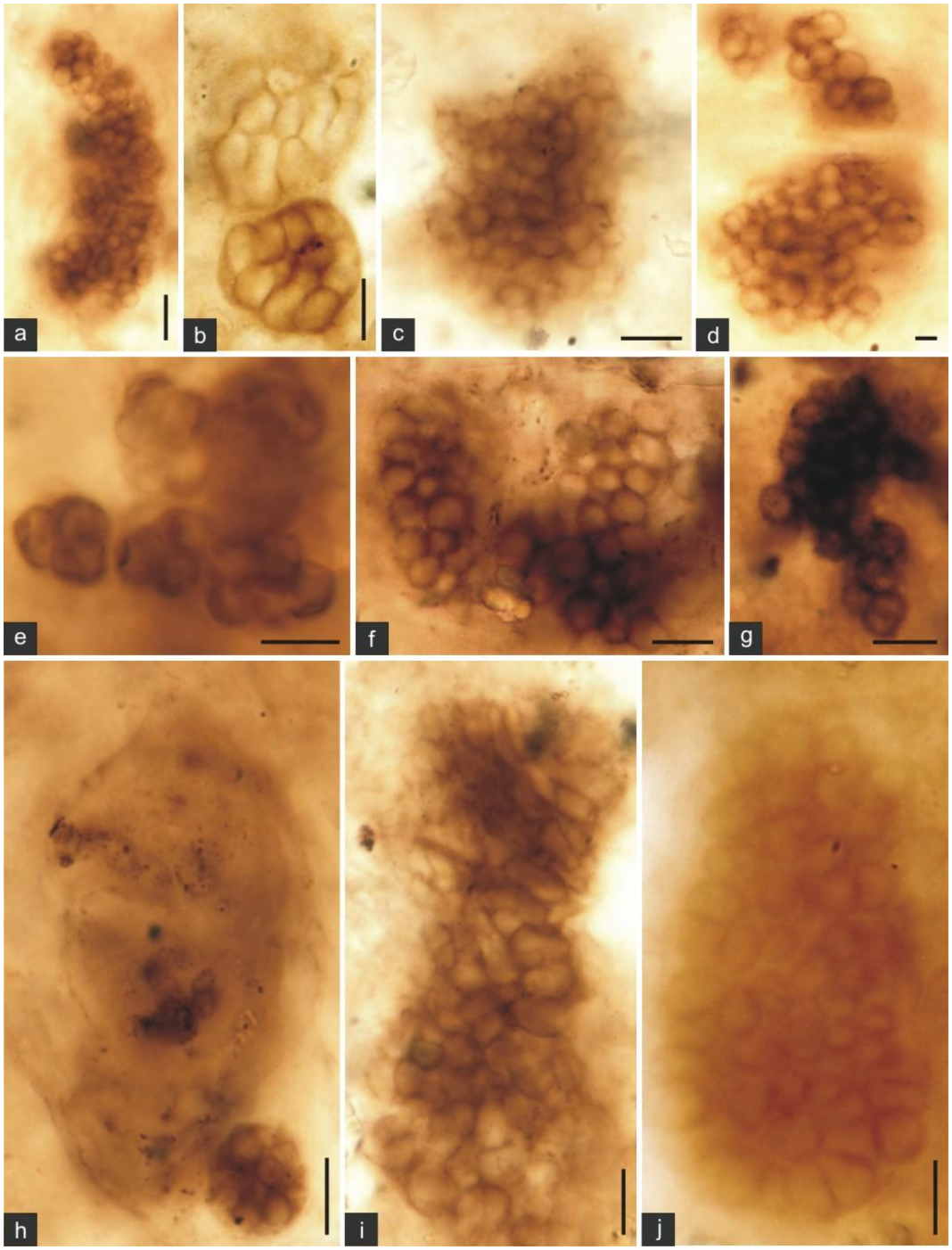

Microbial assemblage recorded from bedded chert of the Salkhan Limestone, exposed near Bansagar Lake, Maihar area, Satna District, M.P. (a, c, d, f, g) *Sphaerophycus medium* Horodyski and Donaldson 1980, have spheroidal cells occurring as clusters;(b, e, i, j) *Eoentophysalis belcherensis* Hofmann 1976, preserved as clusters of single and multiple cells; (h) Sheath preserved only. Scale bar = 10 µm for all specimens. Specimens details- (a, d, h, i)- 9/20 B- 13, 41, 25, 9 (b)- 9/26 A- 5 (c, j)- 9/17 D- 17, 31 (e)- 9/19 E- 5 (f)-9/17 E- 15 (g)- 9/9- 23.

PLATE-4.10

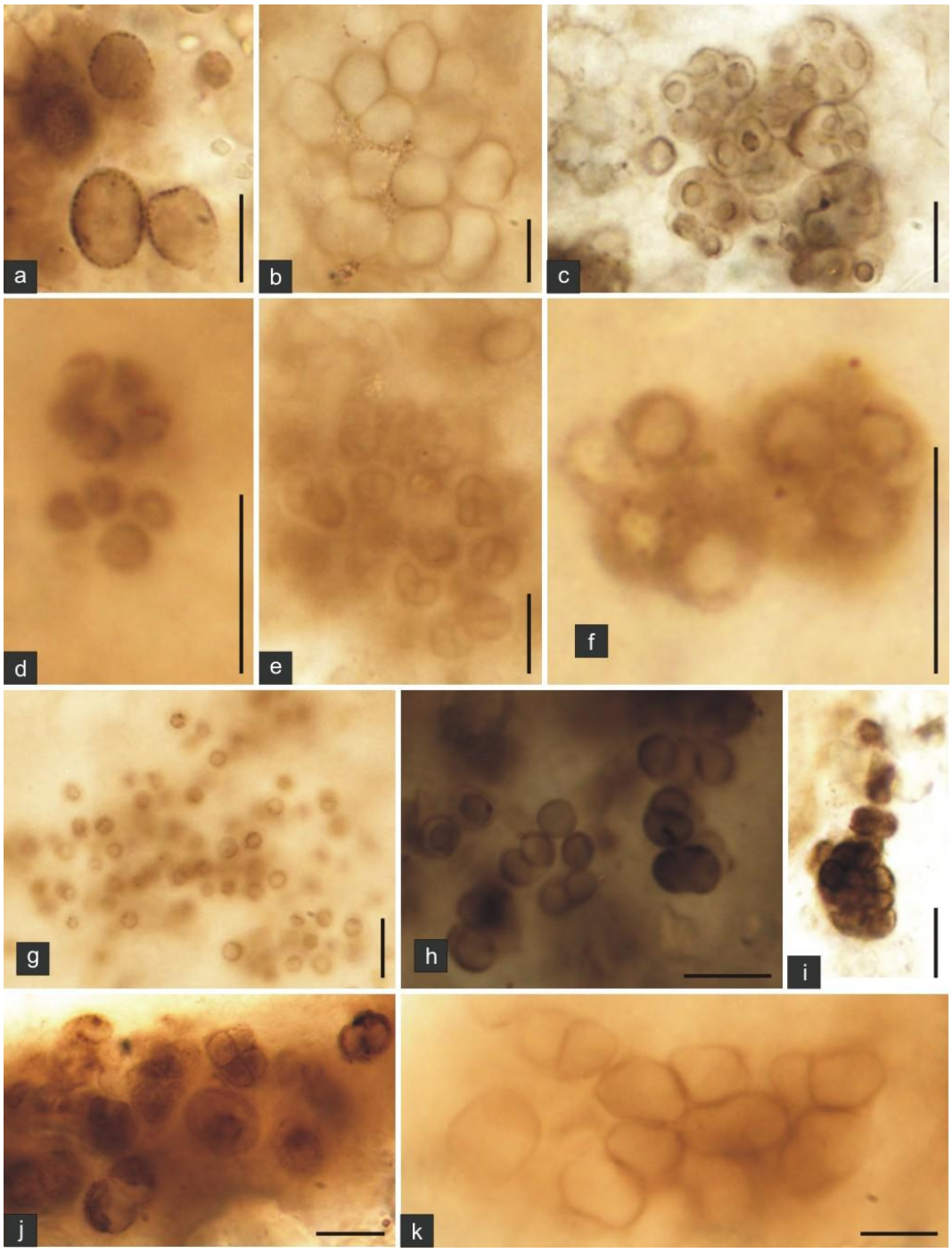

Microbial assemblage recorded from bedded chert of the Salkhan Limestone, exposed near Bansagar Lake, Maihar area, Satna District, M.P. (a) *Huroniospora* Barghoorn, 1965, are preserved as single spherical cells occurring; (b, k) *Myxococcoides inornata* Schopf 1968, preserved as clusters of elliptical cells; (c, d, e, j) *Eoentophysalis belcherensis* Hofmann 1976; (c) cells are preserved with sheath as clusters form; (e) Cells joined as triad form; (j) cells are in tetrad form; (f) *Eoaphanocapsa oparinii* Nyberg and Schopf 1984, cells are joined as clusters trough muscles; (g, h, i) *Sphaerophycus medium* Horodyski and Donaldson 1980, sphearoidal cells preserved in separate;(g) and as clusters form;(i). Scale bar = 10 µm for all specimens. Specimens details- (a, i) - 9/28 A- 78, 29 (b)- 9/17 E- 17 (c)- 9/26 A- 15 (d, g)- 9/21 B- 37, 1 (e)-9/17 A-17 (h, j)- 9/29 – 27, 39 (k)- 9/17 D- 39.

PLATE -4.11

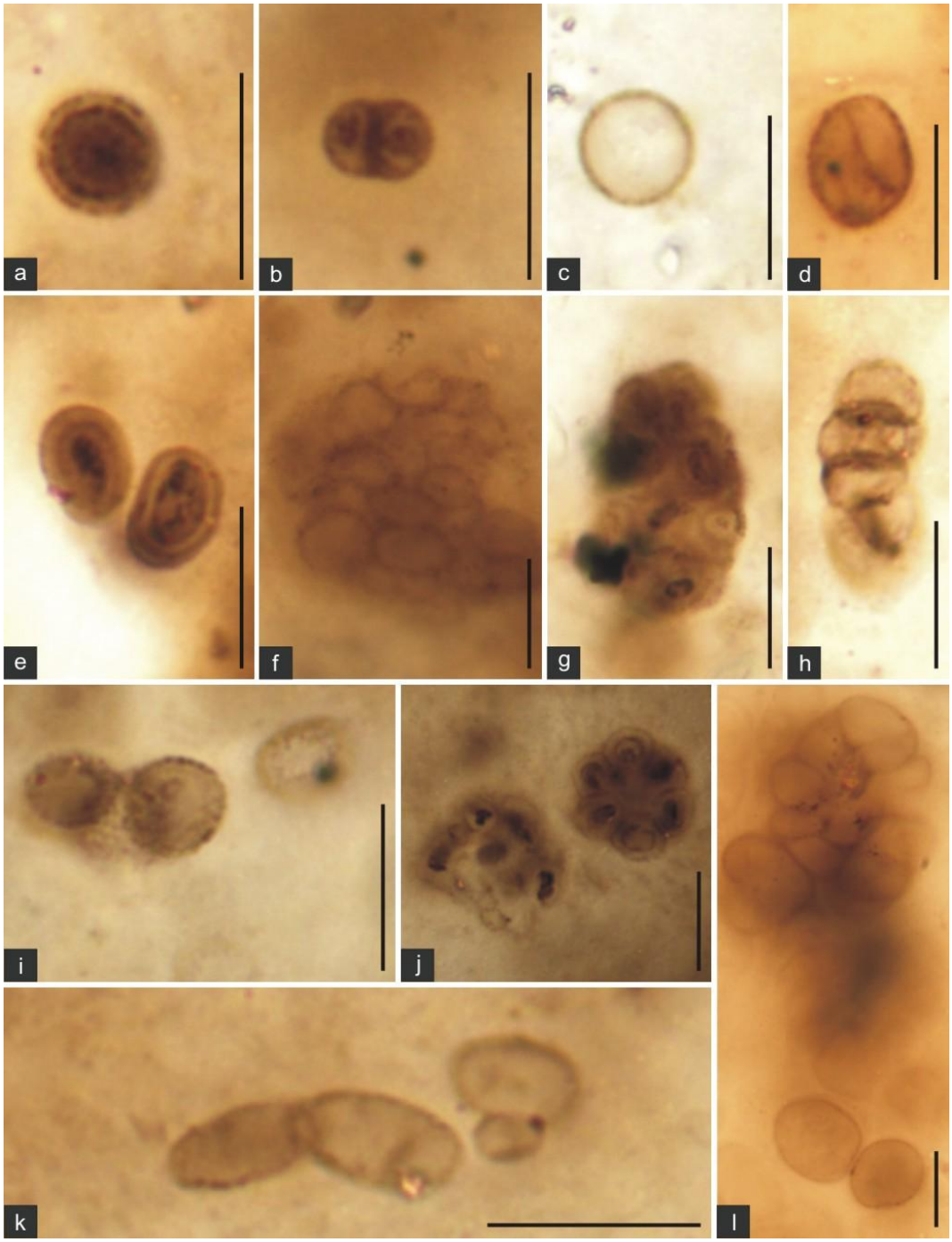

Microbial assemblage recorded from bedded chert of the Salkhan Limestone, exposed near Bansagar Lake, Maihar area, Satna District, M.P. (a, e) *Gloeodiniopsis obtusa* Schopf 1968, spherical cells;(a) with prominent inner and outer wall are preserved; (e) elliptical cells with thick outer wall is preserved; (b) *Sphaerophycus medium* Horodyski and Donaldson 1980, two cells are joined as sheath; (c, d) *Huroniospora* Barghoorn, 1965; (f, h, l) *Myxococcoides inornata* Schopf 1968; (g, j) *Eoentophysalis belcherensis* Hofmann 1976, sheath and muscles are prominent; (i) *Myxococcoides* sp; (k) *Eosynechococcus moorie* Hofmann 1976, two single ellipsoidal cells are joined. Scale bar = 10 µm for all specimens. Specimens details- (a)- 9/9- 29 (b, f)- 9/17B D- 9, 17 (c, e, h, k)- 9/28 A- 50, 60, 34, 66 (d)- 9/17 E- 3 (g, i)-9/19 A-7, 1 (j)- 9/29-33 (l)- 9/17 D- 37.

PLATE-4.12

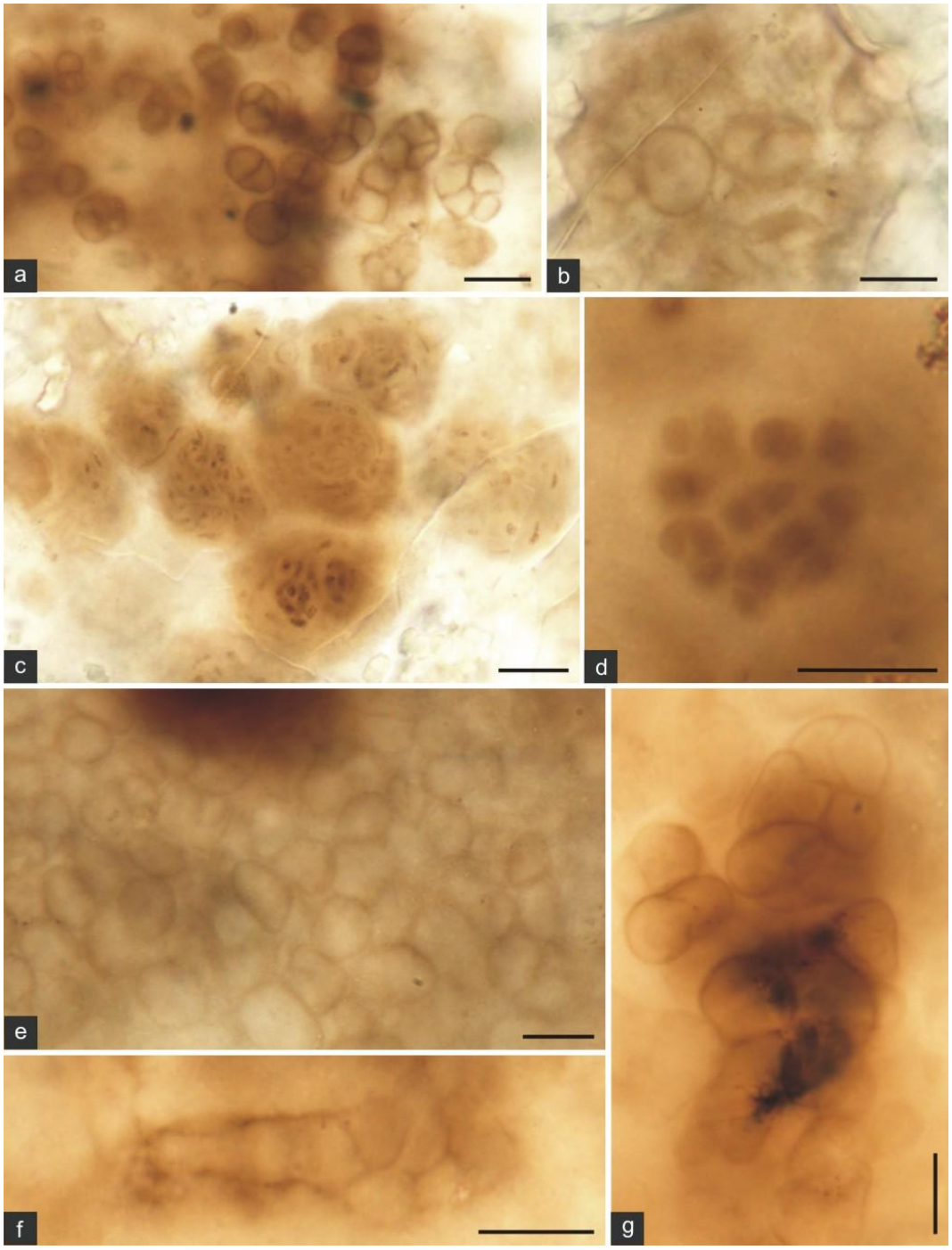

Microbial assemblage recorded from bedded chert of the Salkhan Limestone, exposed near Bansagar Lake, Maihar area, Satna District, M.P. (a) *Sphaerophycus parvum* Schopf, 1968, have polygonal diad, triad, tetrad cells occurring as clusters; (b, g) *Myxococcoides inornata* Schopf 1968; (c, d) *Eoentophysalis belcherensis* Hofmann 1976; (e, f) *Myxococcoides minor* Schopf 1968. Scale bar = 10 µm for all specimens. Specimens details- (a)- 9/9- 15 (b)- 9/17 A- 21 (c)- 9/19 A- 3 (d)- 9/17 B- 15 (e)-9/21 A- 41 (f)- 9/17 C- 15 (g)- 9/17 D- 35.

PLATE-4.13

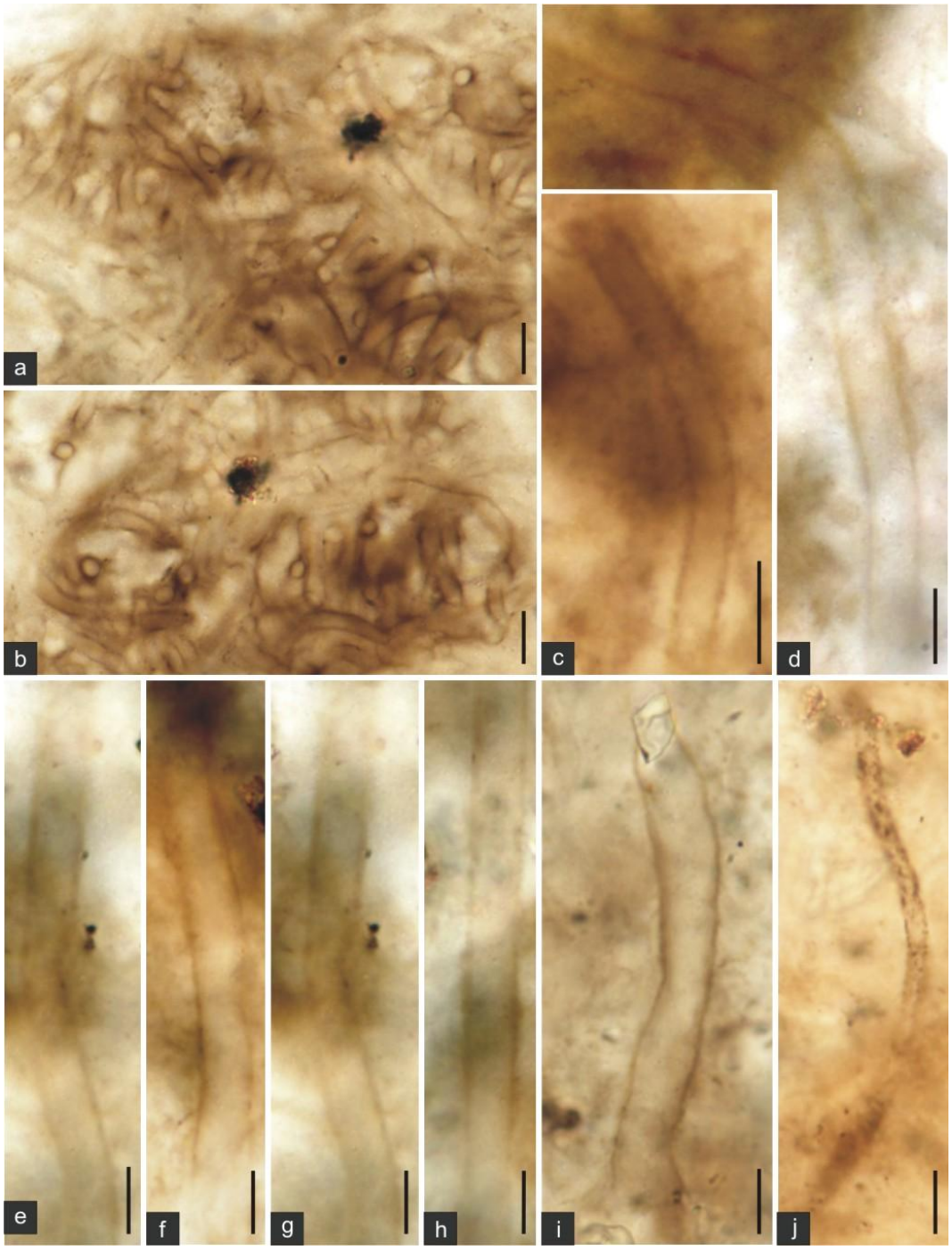

Microbial assemblage recorded from bedded chert of the Salkhan Limestone, exposed near Bansagar Lake, Maihar area, Satna District, M.P. (a, b, j) *Siphonophycus robustum* Schopf 1968 emend Knoll and Golubic 1979 emend Knoll Swett and Mork 1991, showing mat like structures; (c-i) *Siphonophycus solidum* Gloub 1979 emend Butterfield 1994, preserved in filamentous form. Scale bar = 10 µm for all specimens. Specimens details- (a, b, i)- 9/26 A- 23, 27, 3 (c, d, e, g, h)- 9/9- 38, 37 (j) 9/26 B- 3.

PLATE-4.14

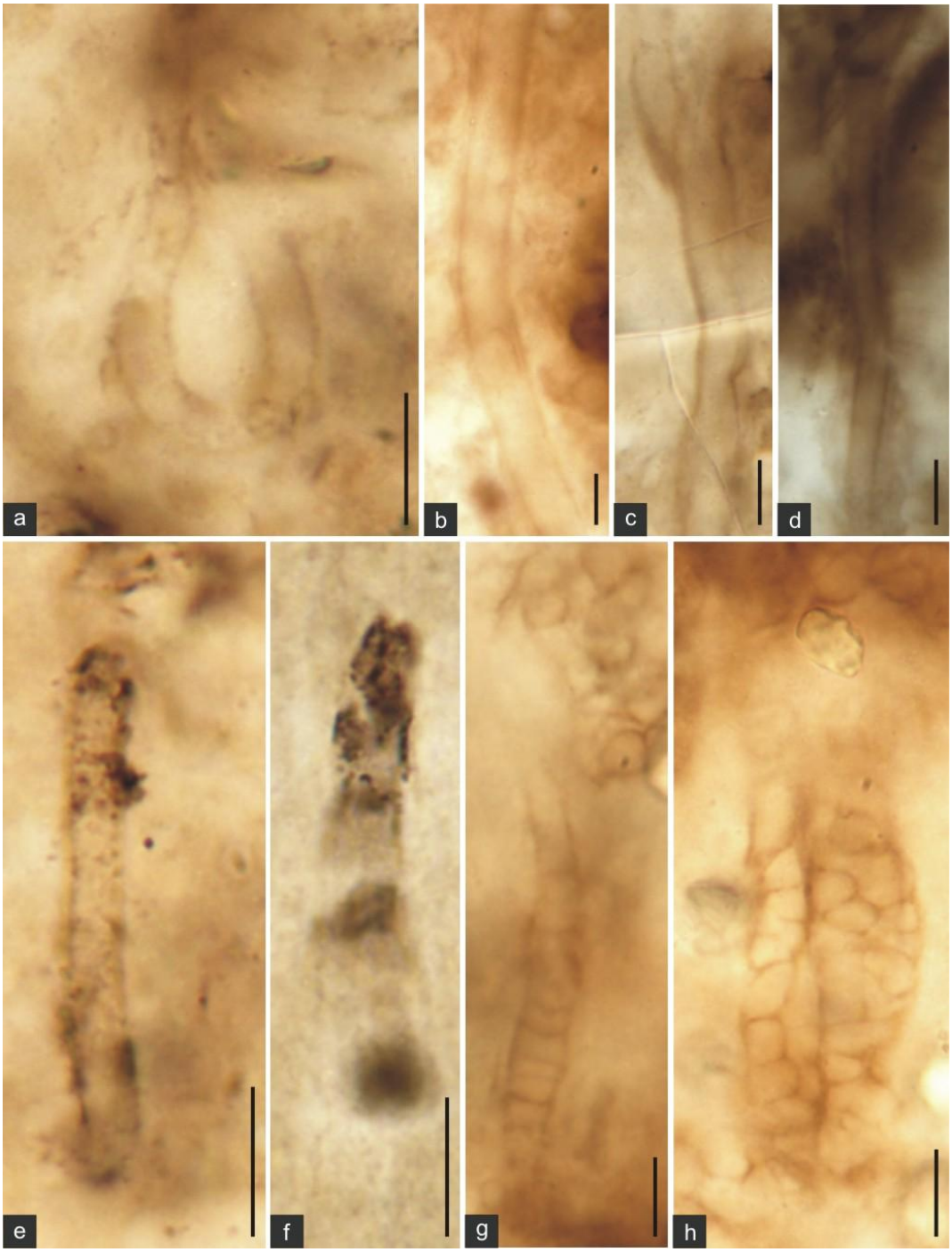

Microbial assemblage recorded from bedded chert of the Salkhan Limestone, exposed near Bansagar Lake, Maihar area, Satna District, M.P. (a, b, c) *Siphonophycus solidum* Gloub 1979 emend. Butterfield 1994; (d) *Siphonophycus robustum* Schopf 1968 emend. Knoll and Golubic 1979 emend Knoll Swett and Mark 1991, showing filamentous form; (e, f, g), *Siphonophycus kestron* Schopf 1968 preserved as filamentous form; (h) *Palaeopleurocapsa fusiforum* Knoll Bharghoorm and Golubic, 1975, Scale bar = 10 µm for all specimens. Specimens details- (a, c, d)- 9/9- 1, 6, 39 (b)- 9/17 D- 24 (c)- 9/26 B- 21 (f)- 9/26 A- 20 (g, h) 9/17 C- 9, 7.

PLATE-4.15

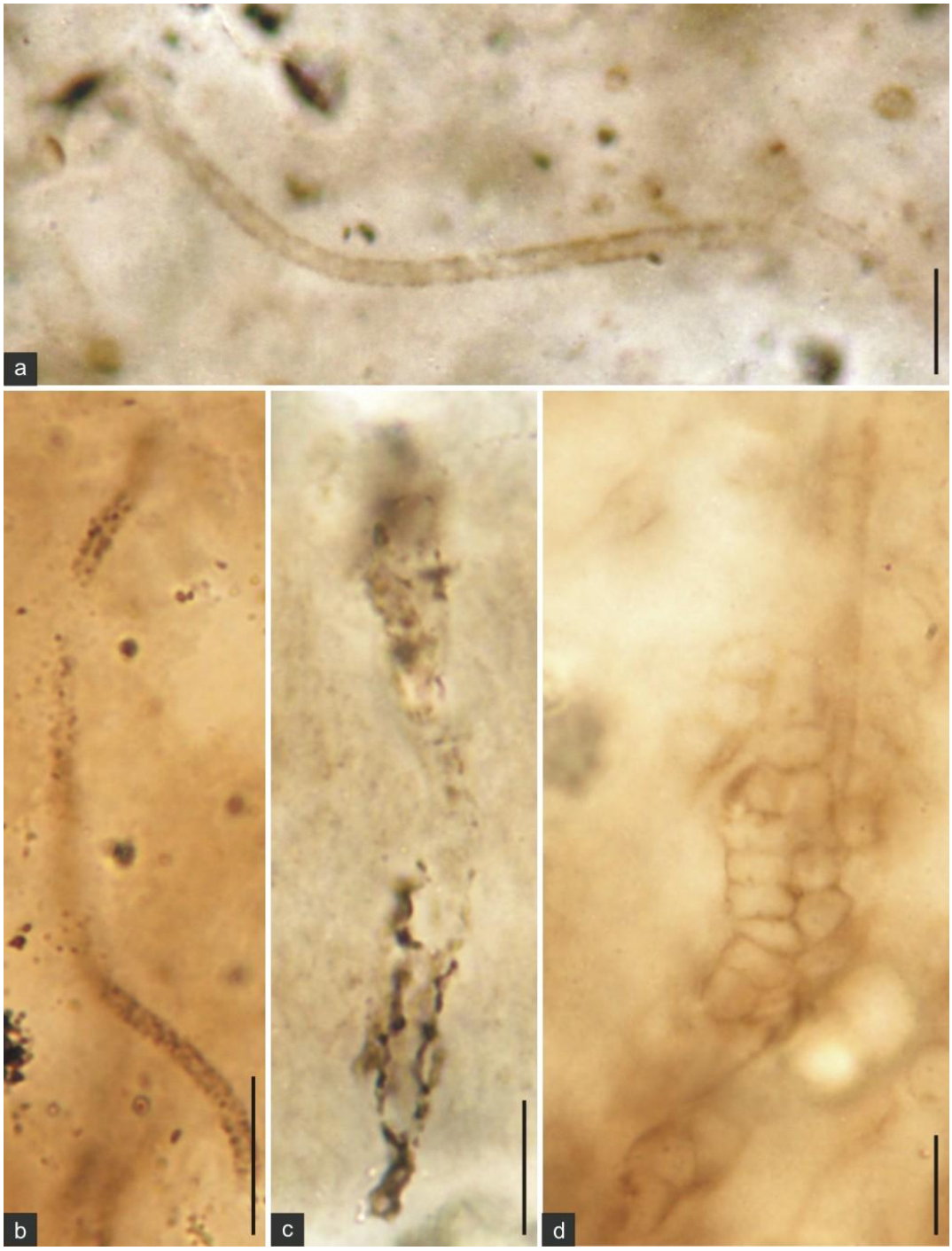

Microbial assemblage recorded from bedded chert of the Salkhan Limestone, exposed near Bansagar Lake, Maihar area, Satna District, M.P. (a, b,) *Siphonophycus robustum* Schopf 1968 emend Knoll and Golubic 1979 emend. Knoll Swett and Mork 1991, showing empty sheath of hormogonian (Oscillatariacean) Cyanobacteria; (c, d) *Palaeopleurocapsa fusiforum* Knoll Bharghoorm and Golubic, 1975, Pleurocapsalean stalked Cyanobacterium. Scale bar = 10 µm for all specimens. Specimens details- (a)- 9/9- 19 (b)- 9/26 B- 11 (c)- 9/26 A- 20 (d)- 9/17 C – 11.

PLATE-4.16

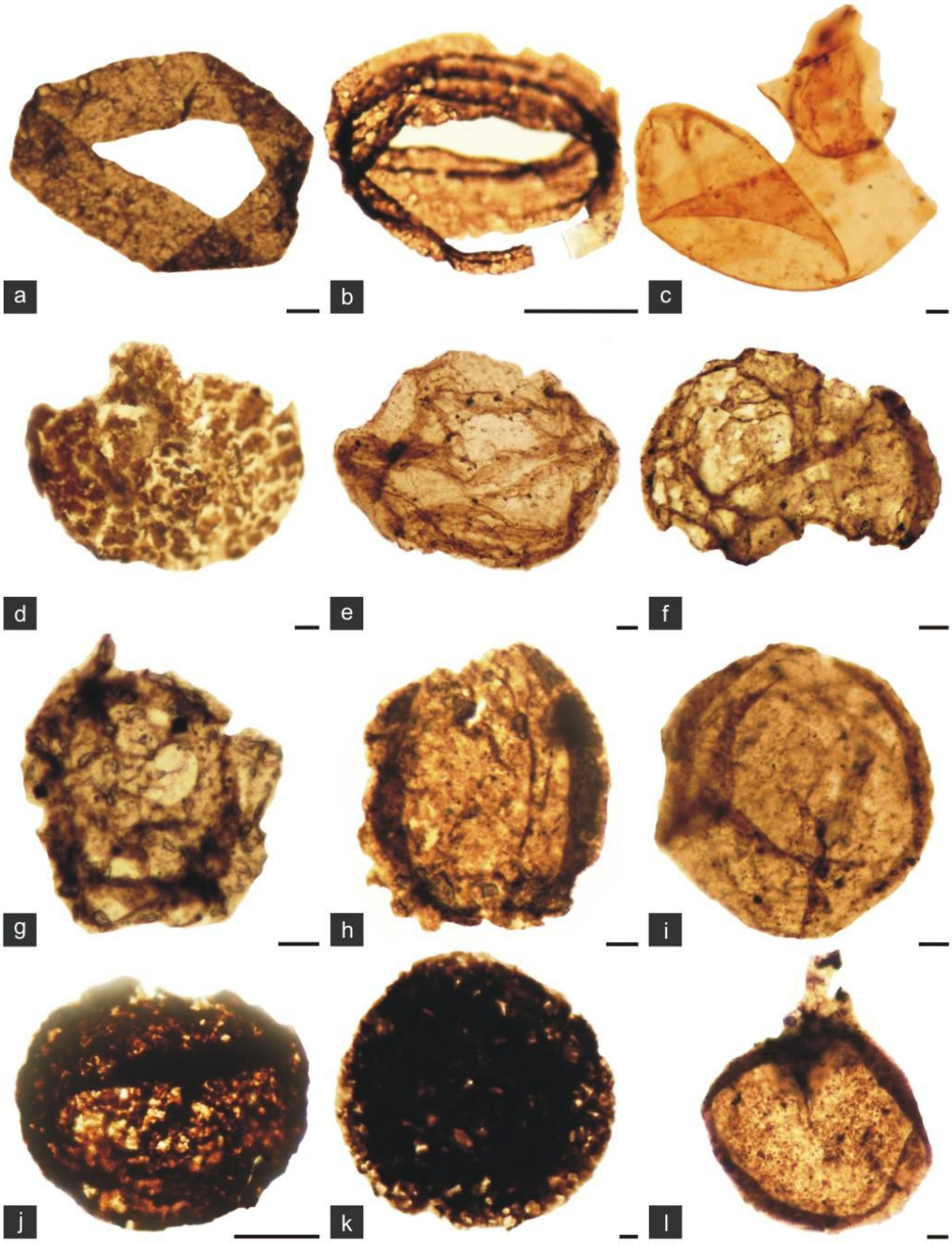

Carbonaceous microfossils and sphaeromorphic acritarchs recovered from the black shale unit of the Rohtasgarh Limestone, Badanpur Mine, Maihar area, Satna District, M.P. a- Flat carbonaceous film of *Siphonophycus* sp.; b-Spirally coiled carbonaceous filament possibly belonging to *Siphanophycus costatus* Jankaustas, 1979; c-Brocken piece of sphaeromorphic acritarchs; d-*Satka favosa* Jankaustas, 1979; e-*Trachyhystricosphaera parva* Jankaustas, 1979; (f-i) *Leiosphaeridia exscupta* Timofeev, 1969; (j, k) *Dictyosphaera delicata* Hu and Fu, 1982; l-*leiosphaeridia* sp. Scale bar= 50 µm for b, j; for others = 10 µm.a-A25- A(22-23m) -2; b- A25- C(18-19)-2; c- A25-A (18-19)-2; d- E15-(43-44)-1; e- A25- A (15-16) -2; f- A25-C(21-22)-18; g-S6-D-2; h-E15-A(24-25)-2; i- A25-C (21-22)-8; j- A25-B(17-18) -2; k- E15-C(37-38)-2; l-S11-C-2.

PLATE-4.17

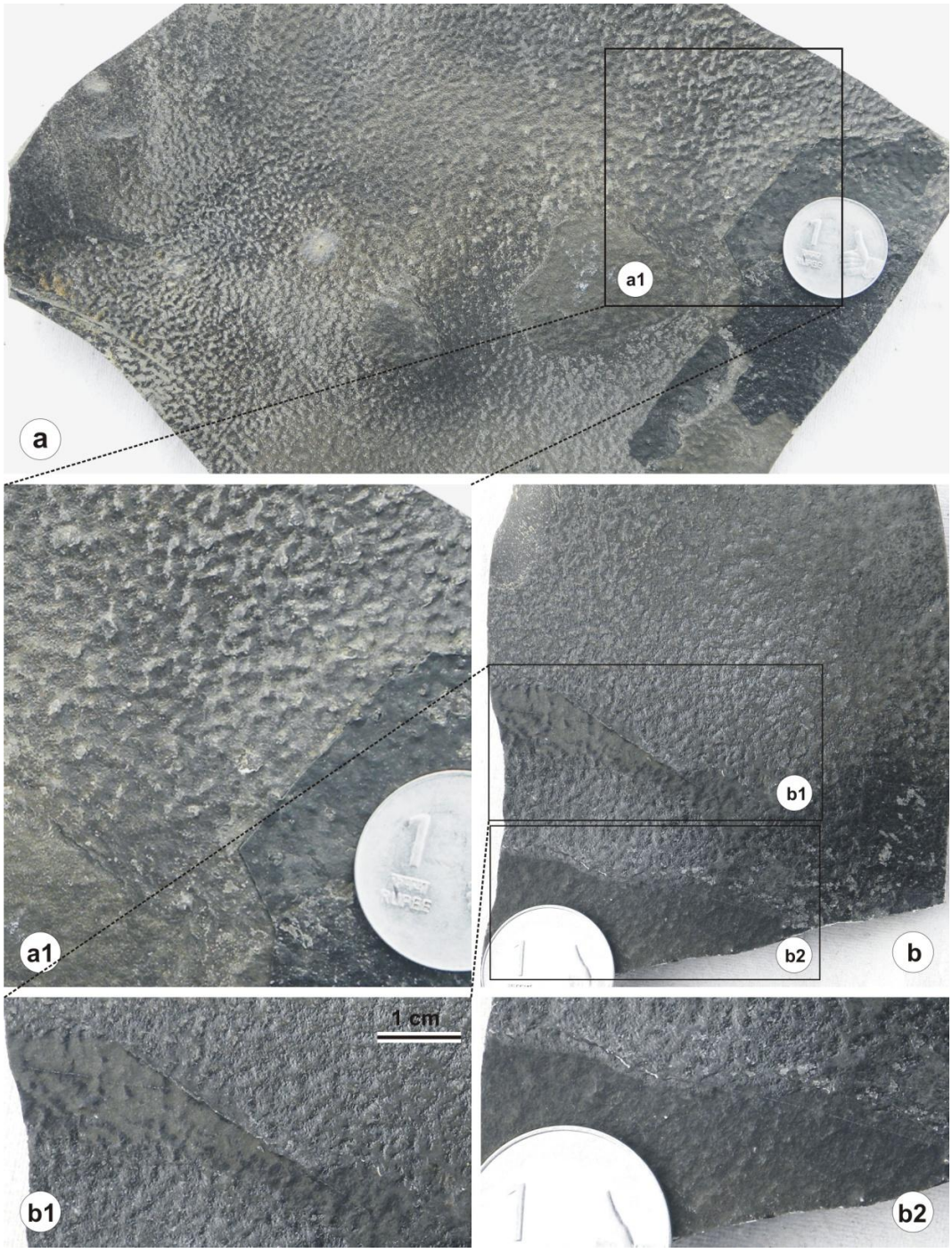

Photographs showing some microbial buildups from the Rohtasgarh Limestone exposed in Bistara mine, Katni District, M.P. (a, b), showing wrinkle structures preserved as Elephant skin' texture on bedding surface of fine-grained limestone bed on macroscopic view.(a1, b1, b2) showing zoom view of photographs (a, b). Scale bar, coin diameter = 2.4 cm for a, b, a1 b2 and for b1 = 1 cm.

PLATE-4.18

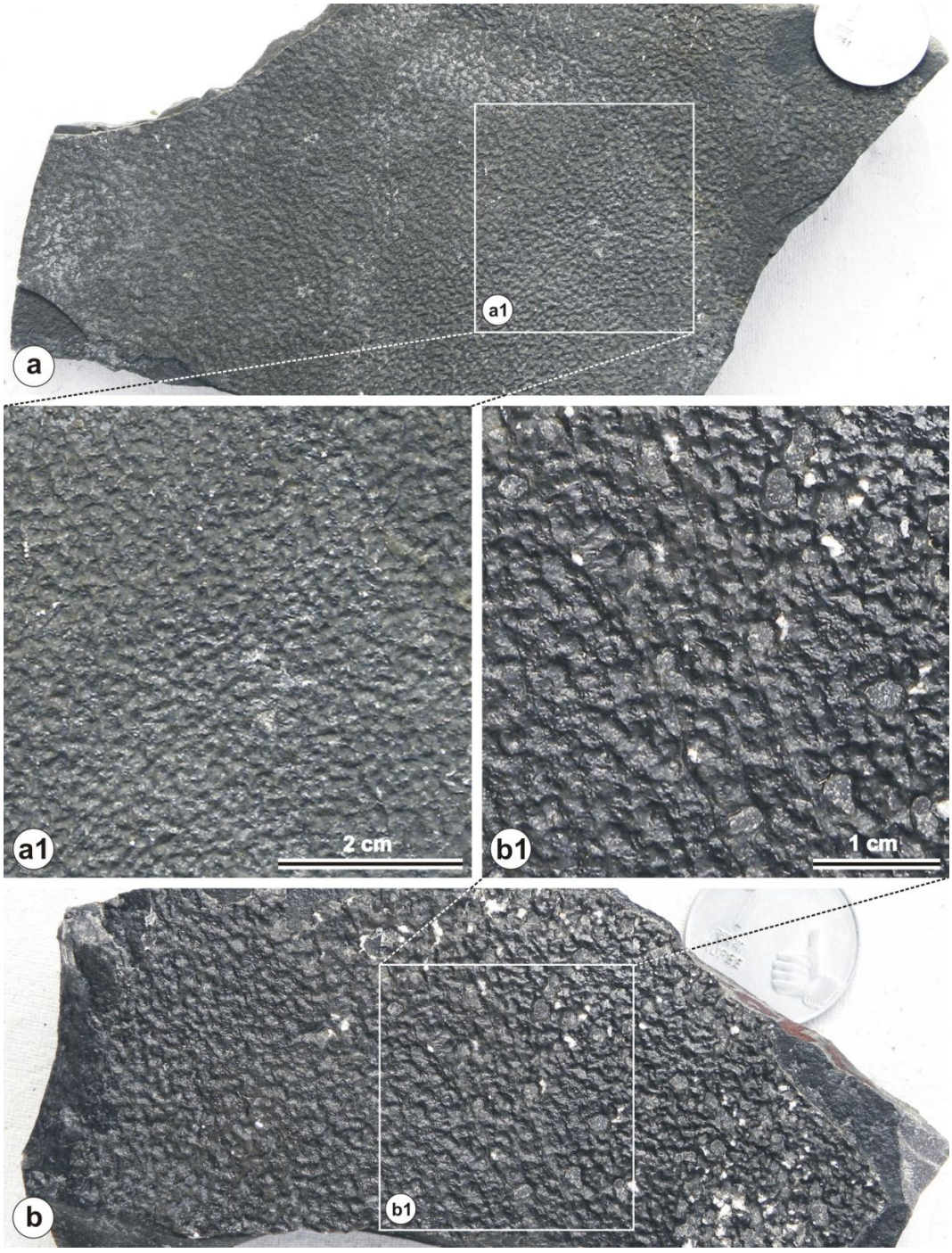

Photographs showing some microbial buildups from the Rohtasgarh Limestone exposed in Bistara mine, Katni District, M.P. (a, b), showing wrinkle structures preserved as Elephant skin' texture on bedding surface of fine-grained limestone bed on macroscopic view, these structures are showing a irregular network pattern in (a1, b1, b2) showing zoom view of photographs (a, b). Scale bar, coin diameter = 2.4 cm for a, b for b1 = 1 cm, a1= 2 cm.

PLATE-4.19

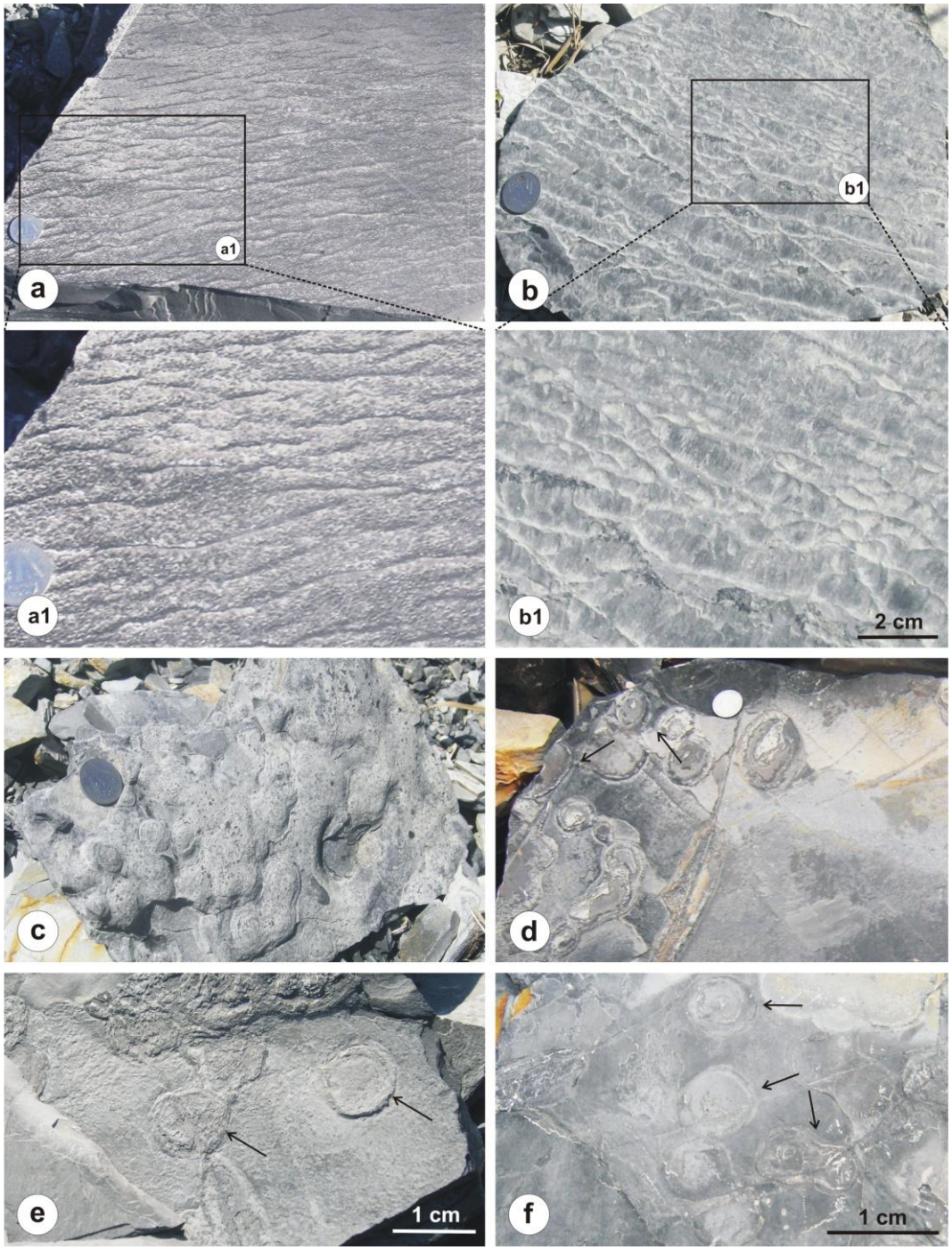

Photographs showing some microbial buildups from the Rohtasgarh Limestone exposed in Muralipahar, Rohtas District, Bihar. (a, b) Mat-protected ripples are common in mat structures of the Rohtasgarh Limestone. Due to the protection of mat layers, previously formed ripple marks are protected from wave erosion and are superimposed with subsequent ripple marks, forming irregular network patterns; (a1, b1) showing zoom view of photographs (a, b). (c, e) showing thick layer of oncolite- like concretion on bedding plane, the concretion have clear shells but no nuclei; (d, f) Showing, plain view of gas domes (or blisters). Radiating ruptures and central depression are present in some of dome is shown by arrow. Scale bar, coin diameter = 2.4 cm for a, b, a1, c, d for b1 = 2 cm, e, f= 1 cm.

PLATE-4.20

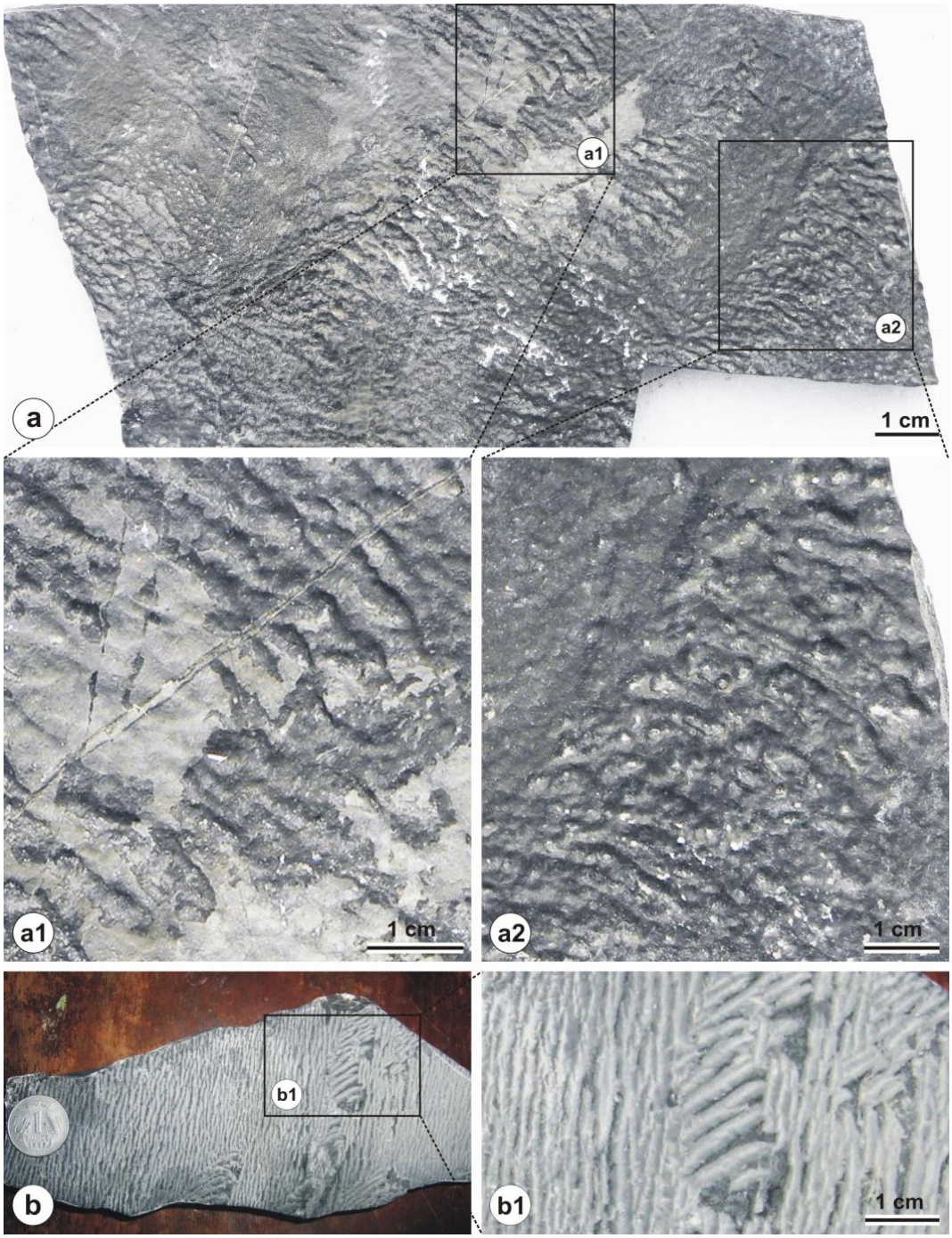

Photographs showing some microbial buildups from the Rohtasgarh Limestone exposed in Bistara mine, Katni District, M.P. (a, b) Mat-protected ripples are common in mat structures of the Rohtasgarh Limestone. Due to the protection of mat layers, previously formed ripple marks are protected from wave erosion and are superimposed with subsequent ripple marks, forming irregular network patterns. The microbial mats are preserved on the surface with macroreticulate features; (b), the ripples associated with binding of microorganism and sediments are parallel to each other. These structures are commonly considered as a type of mat growth structures (Eriksson et al., 2007). (a1, a2) showing zoom view of photographs (a). (b1) is showing, impression of microbial growth against the wave action on bedding plane. Scale bar, coin diameter = 2.4 cm for b and for others = 1 cm.

PLATE-4.21

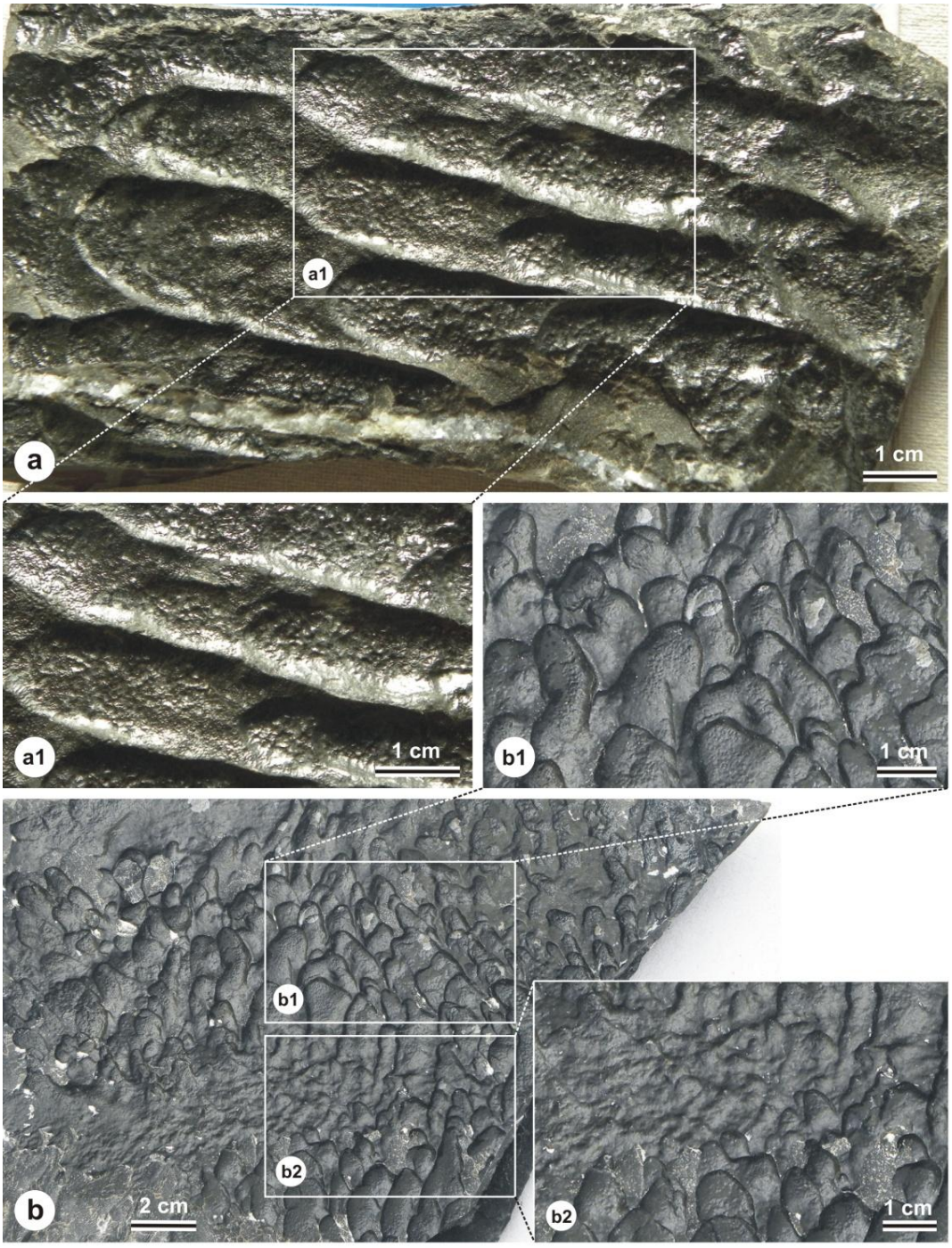

Photographs showing some microbial buildups from the Rohtasgarh Limestone exposed in Bistara mine, Katni District, M.P. (a, b), A *Manchuriophycus*-style structures preserved resulting from thicker mats developed within the troughs, between ripples. This kind of structure is characterized by straight ridges waving in ripple valleys, but rarely on ripple ridges; (a1) zoom view of (a) is showing the growth ridges, tiny pinnacles or pustules within ripples; (b) Microbial mat protected convolute bedding aligned in straightway parallel to each other. (b1, b2) zoom view of (b) showing clear view. Scale bar = 2 cm for b, for others = 1 cm.

PLATE-4.22

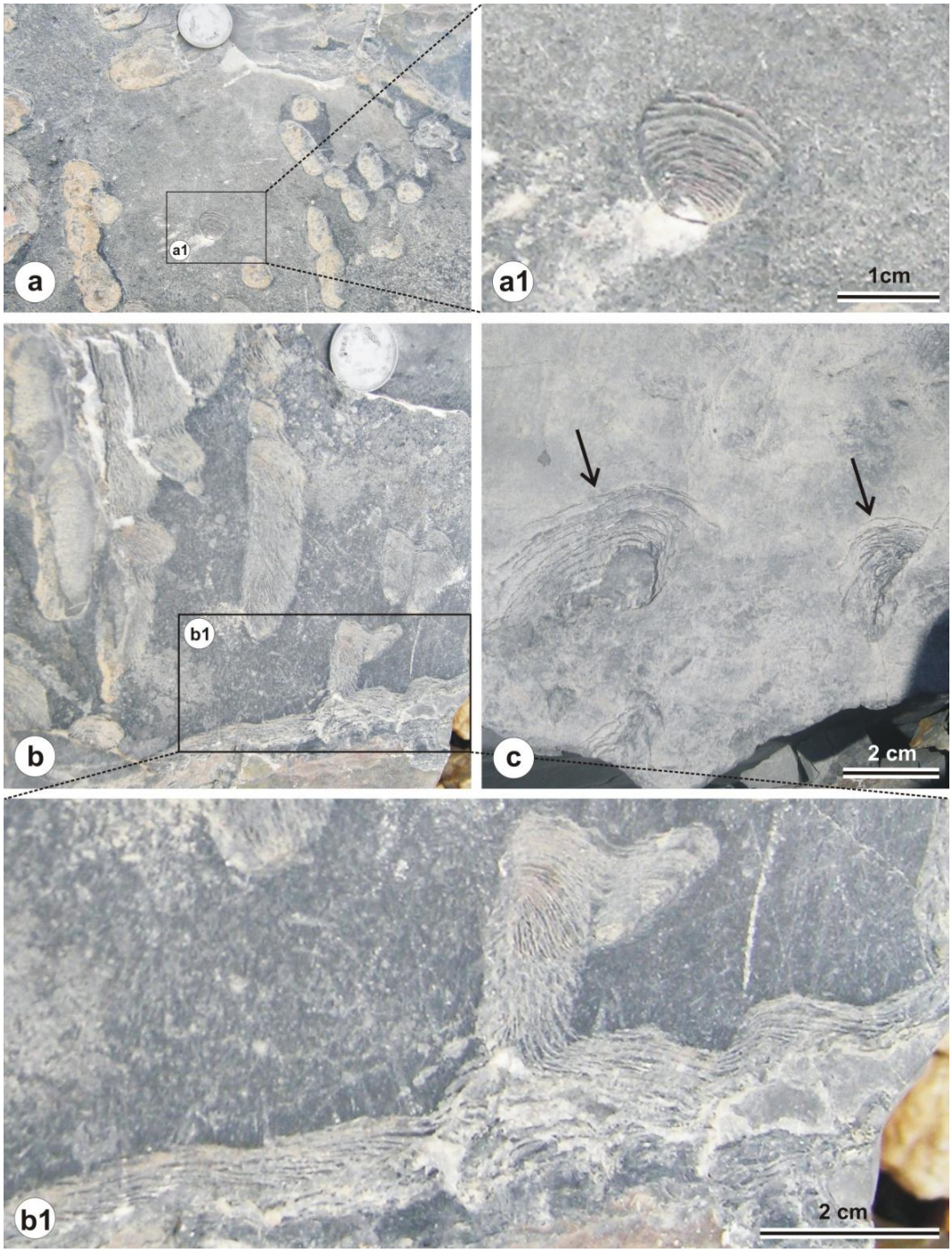

Photographs showing some microbial buildups from the Rohtasgarh Limestone exposed in Muralipahar, Rohtas District, Bihar. (a, b, c), showing pear shape, microbial mat formation pattern against the microbial activity and binding of sediments; (a1) zoom view of (a) is showing the layering structures developed due to sediments binding with microbial algae; (b1) is zoom view of (b) showing microbial mat growing in vertical and laterally. Scale bar, coin diameter = 2.4 cm for a, b for a1 = 1 cm and for c, b1 = 2 cm.

PLATE 4.23

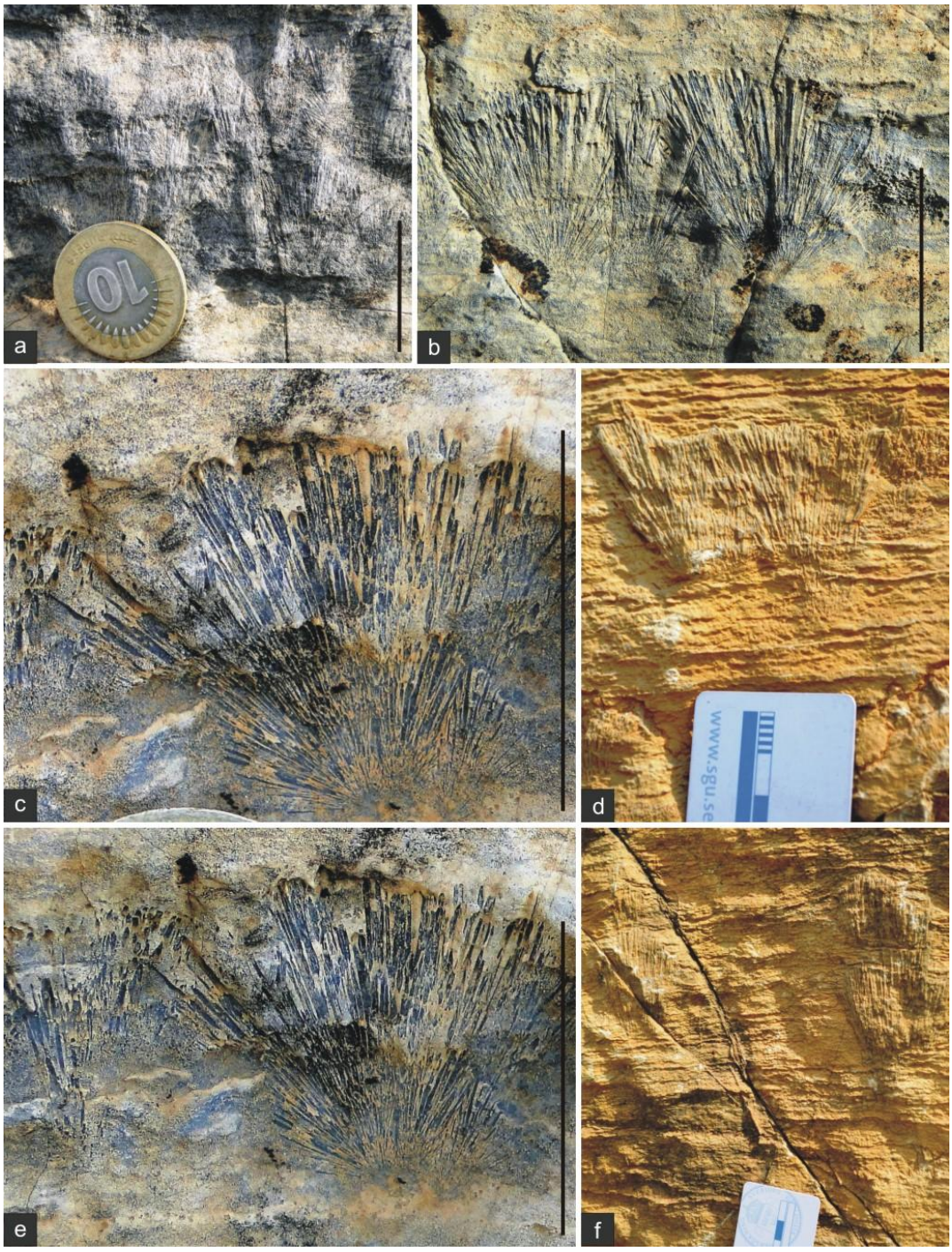

Field photograph showing fan- fabric structures on precipitated carbonate of the Kajrahat Limestone, exposed in the Kuteshwar area, Satna District, M.P. (a) fan- fabric structures on surface outcrop; (b, c, e) showing zoom part of photograph of (a); (d, f) crystal of fan – fabric on partially weathered outcrop surface. Scale bar = 2.7 cm for all photograph.

PLATE-4.24

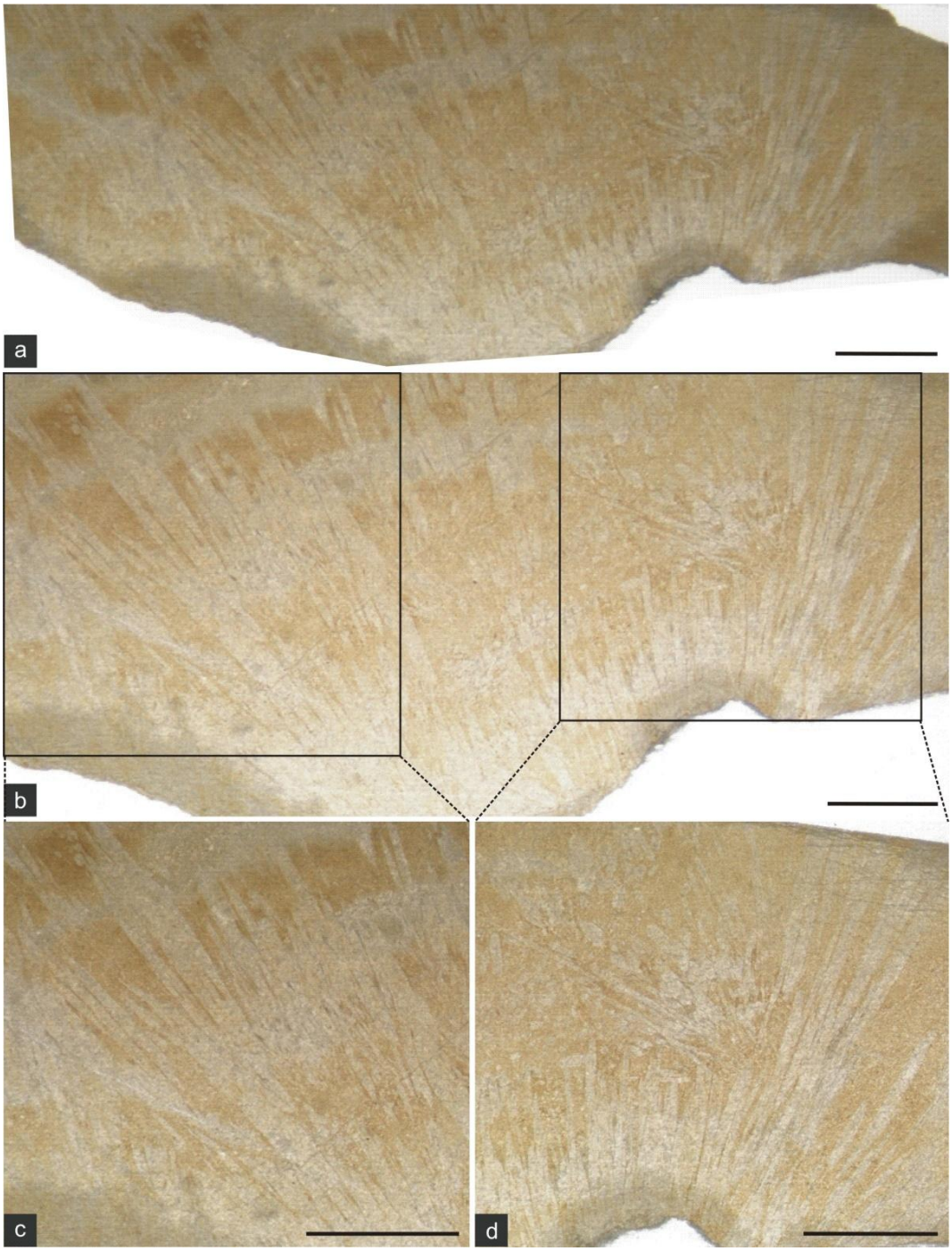

Thin section photographs showing fan- fabric structures of precipitated carbonate in the Kajrahat Limestone, exposed in the Kuteshwar area, Satna District, M.P. (a, b) fan- fabric structures on thin section, crystals are radiating in upward direction; (c, d) showing clear crystals of fan – fabric of photograph (b). Scale bar = 1 mm for all photographs.

PLATE-4.25

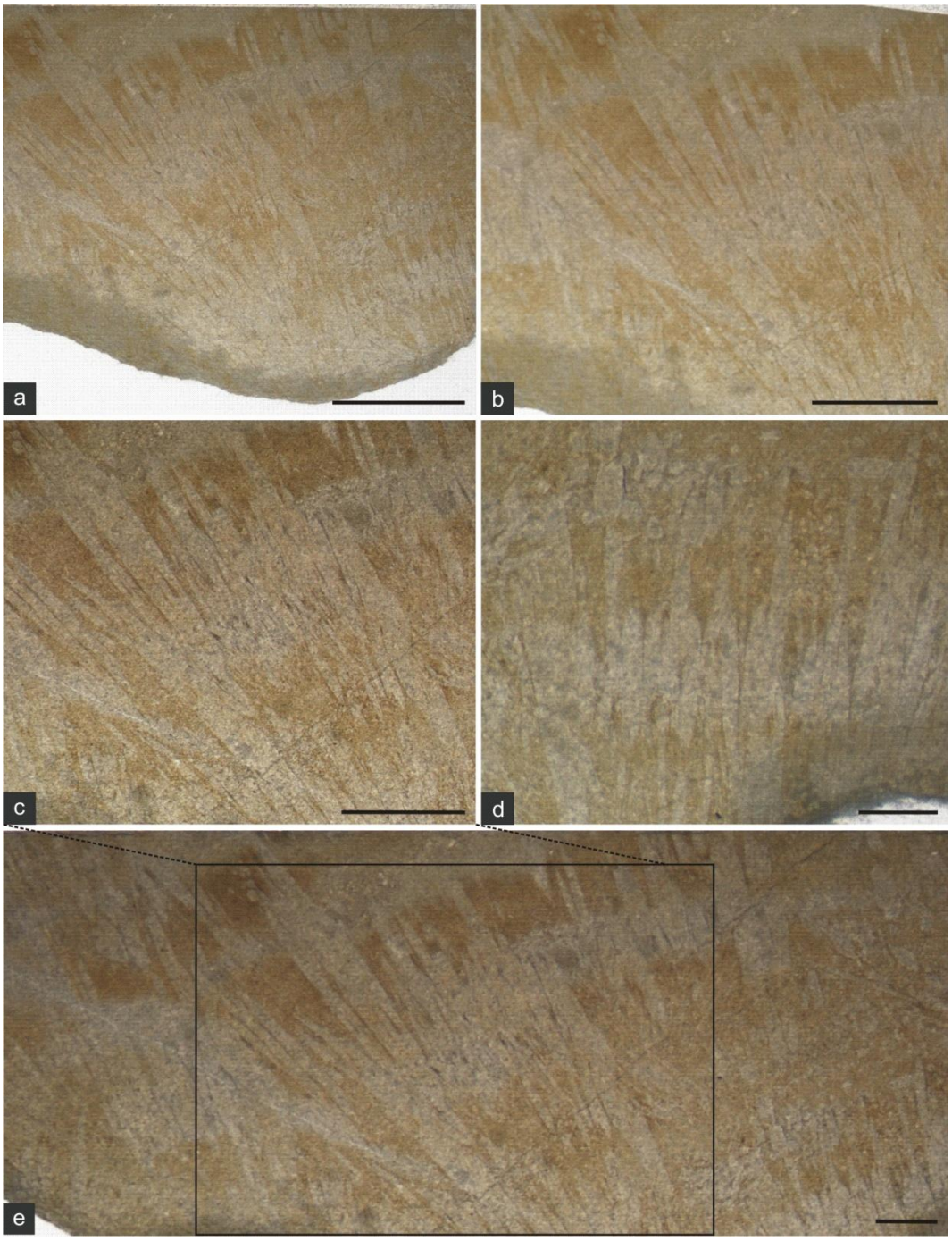

Thin section photographs showing fan- fabric structures of precipitated carbonate in the Kajrahat Limestone, exposed in the Kuteshwar area, Satna District, M.P. (a, b, c, d) showing fan- fabric structures in thin section, enlarged part; (e) crystals are radiating in upward direction. Scale bar = 1 mm for all photographs.

PLATE-4.26

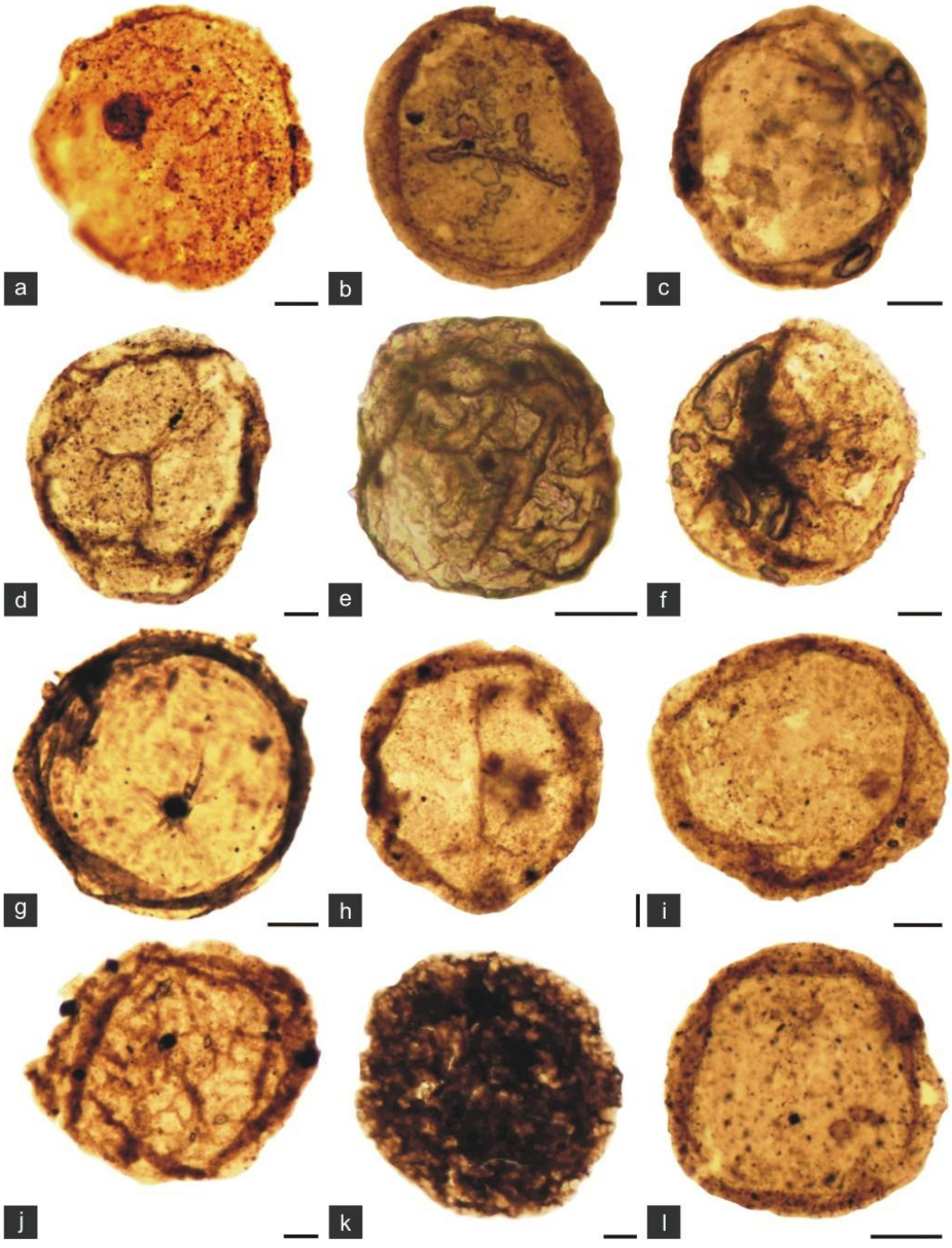

Contaminations in macerated microbial assemblage recorded from black shale unit of the Rohtasgarh Limestone, exposed in Maihar area, Satna District, M.P. (a- l) showing large scale contaminations similar to microfossils. Scale bar = 10 µm for all photographs.

PLATE 4.27

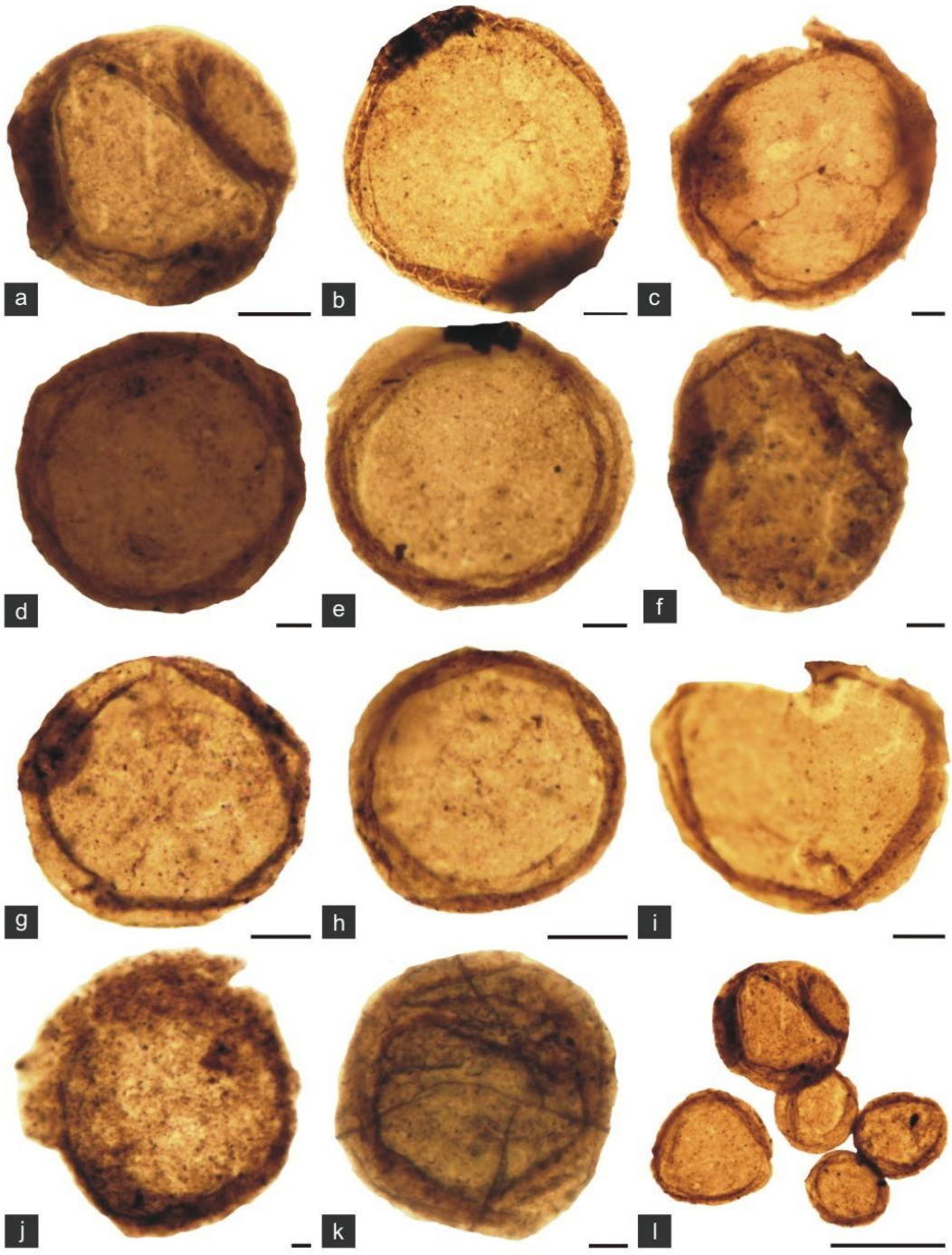

Contaminations in macerated microbial assemblage recorded from black shale unit of the Rohtasgarh Limestone, exposed in Maihar area, Satna District, M.P. (a- l) showing large scale contaminations similar to microfossils. Scale bar = 10 µm for all photographs.

PLATE-4.28

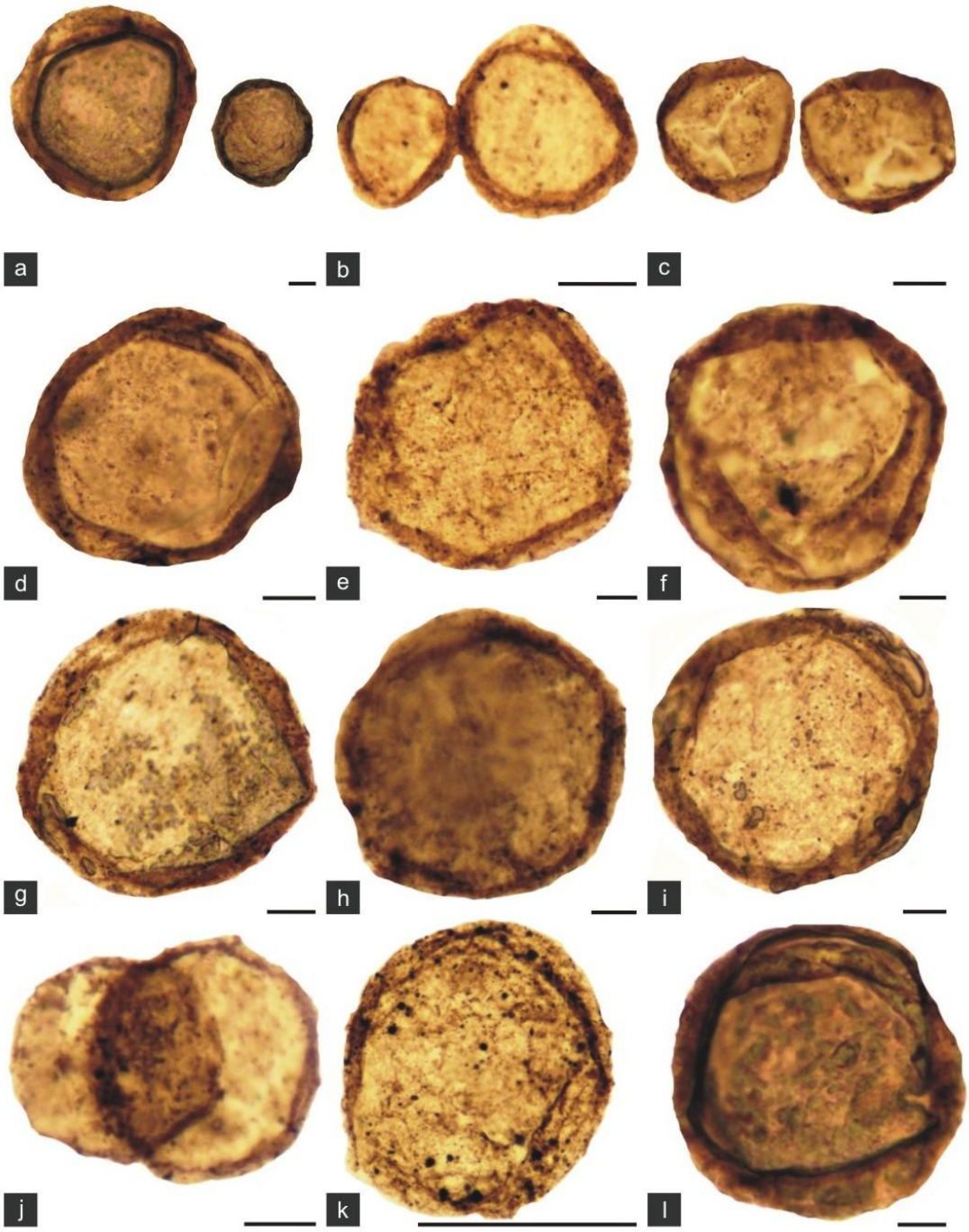

Contaminations in macerated microbial assemblage recorded from black shale unit of the Rohtasgarh Limestone, exposed in Maihar area, Satna District, M.P. (a- l) showing large scale contaminations similar to microfossils. Scale bar = 10 µm for all photographs.

Chapter 5

ORGANIC GEOCHEMISTRY

The Proterozoic basins from different parts of the world viz. Lena Tunguska, Siberia; Amadeus and McArthur basins, Australia; Sichuan and Tarim basins, China and Huqf basin, Oman etc. have reported commercial production of oil and gas (Mayerhoff, 1980; Granthan et al., 1988; Jackson et al., 1988; Crick et al., 1988; Korsch et al., 1991). Stromatolitic algae and bacteria are potential sources capable of generating petroleum and consequently stromatolitic bearing Precambrian/ Proterozoic carbonate rocks are considered as future targets for new hydrocarbon accumulations /resources (Murray et al., 1980). India has six Proterozoic basins viz., Vindhyan, Cuddapah, Chhattisgarh, Bastar, Bhima and Kaladgi (Kalpana et al., 2010). These basins, also known as Purana Basins, are poorly explored for hydrocarbon prospects. Proterozoic shales and carbonate rocks are generally organic-poor and are considered insignificant as hydrocarbon source rocks (Hunt 1995). However, organic-rich shales are reported from many Proterozoic basins (Condie et al., 2001) and some of them probably sourced ancient petroleum accumulations. At places, these organic-rich shales are considered as possible hydrocarbon source rocks, viz., in the Rice Formation (Newell et al., 1993) and Nonesuch Formation, U.S.A (Imbus et al., 1988). Organic-rich (TOC up to 7%), mature kerogens of the Mesoproterozoic Velkerri Formation and Barney Creek Formation of Australia are comparable to potential Phanerozoic hydrocarbon source rocks and have been targeted for oil exploration (Crick 1992; Warren et al., 1998). A low degree of thermal alteration characterizes both these shales. Organic-rich shales of Neoproterozoic have sourced a number of oil and gas fields in the Sichuan basin of China (Korsch et al., 1991). Biomarker analysis of these organic-rich shales provides insights into the early evolution of microbial life (Buick et al., 1998; Dutkiewicz et al., 2002; Greenwood et al., 2004). Study of such shales may also provide valuable clues related to the burial history of Proterozoic sedimentary basins (Korsch et al., 1991; Crick 1992; Newell et al., 1993) and estimates for paleo-geothermal gradient (Price et al., 1996). Shukla and Chakraborty (1994) suggested that organic richness which has bearing upon the Proterozoic Vindhyan basin shales, in terms of being prospective

hydrocarbon source rocks has yet to be evaluated. Also petrographic and geochemical investigations of the black shales are in the nascent stage (Banerjee and Schieber, 2003). Quality and maturation of organic matter of these black shales are yet to be estimated. Maturation data are essential in order to ascertain the hydrocarbon generating potential of the shales and thermal history of the Vindhyan basin. This chapter presents results and a brief discussion on the Organic Matter (O.M.) of the black shales of the Proterozoic Vindhyan basin noted in the Maihar area, and provides bulk characteristics of their organic matter content. Quantity, quality and maturation of organic matter of individual black shale formations are estimated and assessed separately. Specific attention is given to the temperature of the maximum pyrolytic degradation of organic matter and light hydrocarbon in order to estimate its catagenetic stage.

This study also reviews the basics of accumulation and preservation of organic matter in Lower Vindhyan sedimentary rocks, the generation of hydrocarbons, and the application of the Rock-Eval/TOC pyrolysis technique to the characterization of sedimentary organic matter. The main objective of this study is to obtain basic information about the type and amount of organic matter contained in rocks of the Lower Vindhyan. The black shales and carbonates of the Rohtasgarh limestone were sampled for TOC analyses and Rock-Eval Pyrolysis. The information obtained from these analyses will reinforce previous palaeo-biological studies based on micro and macro fossils remains in the basin. Palaeo-biological investigations permit the establishment of the age of the basin. The samples are taken for geochemical studies from different sections of the Rohtasgarh limestone, well exposed in the Maihar area, M.P. To evaluate the maturity and source rocks potential, Rock-Eval pyrolysis and GC-C-IRMS were carried out on 42 black shales and carbonates samples. These samples were collected from limestone mine quarrying up to 40 m depth and outcrop sections. The geochemical parameters discussed here are based on analyzed samples, in the Petroleum Geochemistry Laboratory of NGRI, Hyderabad. Procedural details about materials and methods adopted are described in chapter 3. The following studies, results, their significance and discussion about hydrocarbon prospects of the area are summarized in this chapter.

- Total Organic Carbon (TOC), in carbonates and black shales of the Rohtasgarh Limestone.
- Rock-Eval Pyrolysis of carbonates and black shales which have ≥0.5 % TOC.
- Absorbed light gaseous hydrocarbons (C1-C5) compositions and their origin of occurrence.

5.1 Total Organic Carbon (TOC)

Total organic carbon (TOC) analysis was performed with Elementar Liqui TOC Analyzer with the solid sample module. Selected samples from different black shale and carbonate units were chosen for TOC analysis for the amount, quality and maturity of organic matter (Table 5.1, 5.2, 5.3, and 5.4). For this carbonates and black shales samples have been collected from two stratigraphic horizons, the Kajrahat limestone and the Rohtasgarh limestone. Characterization of the finely disseminated organic material was performed using a Rock-Eval. TOC data are provided below:

Total organic carbon contents vary with stratigraphic units in Lower Vindhyan. The carbonates of the Rohtasgarh limestone have 0.1 to 0.3% TOC (Table 5.1 & 5.2). In Kajrahat limestone of Kuteshwar mine section, the TOC is observed to be in the range of 0.1% to as high as 4.1% (Table 5.3). The black shales, separated from the Rohtasgarh limestone are showing high content of TOC, i.e. 0.1 to 3 % (Table 5.4). These results indicate, yields of extractable TOC are low in carbonates and average in black shales for source rock and generation of Hydrocarbon.

Table 5.1- Total Organic Carbon (TOC) distribution in Rohtasgarh Limestone, Bistara mine section, Katni District, M.P. Sampling interval is 50 cm.

Sample No.	Stratigraphic Unit	Lithology	TOC (ppm)/%
1 **(Bottom)**	Rohtasgarh Limestone	Ferroan Calcite	1030
2	Rohtasgarh Limestone	Ferroan Calcite	1225
3	Rohtasgarh Limestone	Ferroan Calcite	1114
4	Rohtasgarh Limestone	Ferroan Calcite	1348
5	Rohtasgarh Limestone	Ferroan Calcite	1889
6	Rohtasgarh Limestone	Ferroan Calcite	1148
7	Rohtasgarh Limestone	Ferroan Calcite	1673
8	Rohtasgarh Limestone	Ferroan Calcite	1835
9	Rohtasgarh Limestone	Ferroan Calcite	1883
10	Rohtasgarh Limestone	Ferroan Calcite	1330
11	Rohtasgarh Limestone	Calcite	1933
12	Rohtasgarh Limestone	Ferroan Calcite	1080
13	Rohtasgarh Limestone	Ferroan Calcite	3015
14	Rohtasgarh Limestone	Ferroan Calcite	1194
15	Rohtasgarh Limestone	Calcite	890
16	Rohtasgarh Limestone	Ferroan Calcite	1784
17	Rohtasgarh Limestone	Ferroan Calcite	1272
18	Rohtasgarh Limestone	Ferroan Calcite	1152
19	Rohtasgarh Limestone	Ferroan Calcite	1553
20	Rohtasgarh Limestone	Ferroan Calcite	1483
21	Rohtasgarh Limestone	Calcite	1461
22	Rohtasgarh Limestone	Ferroan Calcite	1283
23	Rohtasgarh Limestone	Ferroan Calcite	1784
24	Rohtasgarh Limestone	Ferroan Calcite	2341
25	Rohtasgarh Limestone	Ferroan Calcite	2189
26	Rohtasgarh Limestone	Ferroan Calcite	1300
27	Rohtasgarh Limestone	Ferroan Calcite	1323
28	Rohtasgarh Limestone	Ferroan Calcite	1252
29	Rohtasgarh Limestone	Ferroan Calcite	2025
30	Rohtasgarh Limestone	Ferroan Calcite	1810
31	Rohtasgarh Limestone	Ferroan Calcite	1482
32	Rohtasgarh Limestone	Calcite	1570
33	Rohtasgarh Limestone	Ferroan Calcite	1482
34	Rohtasgarh Limestone	Ferroan Calcite	1532
35	Rohtasgarh Limestone	Ferroan Calcite	1979
36	Rohtasgarh Limestone	Ferroan Calcite	1942
37	Rohtasgarh Limestone	Ferroan Calcite	1509
38	Rohtasgarh Limestone	Calcite	1158
39	Rohtasgarh Limestone	Ferroan Calcite	1570
40 **(Top)**	Rohtasgarh Limestone	Ferroan Calcite	1482

Table 5.2-Total Organic Carbon (TOC) distribution in Rohtasgarh Limestone, Badanpur Mine Section, Maihar area, M.P. sampling interval is 50 cm.

Sample No.	**Stratigraphic Unit**	**Lithology**	**TOC (ppm)/%**
1 **(Bottom)**	Rohtasgarh Limestone	Ferroan Calcite	1267
2	Rohtasgarh Limestone	Ferroan Calcite	1162
3	Rohtasgarh Limestone	Ferroan Calcite	2036
4	Rohtasgarh Limestone	Ferroan Calcite	2356
5	Rohtasgarh Limestone	Ferroan Calcite	1661
6	Rohtasgarh Limestone	Ferroan Calcite	2294
7	Rohtasgarh Limestone	Ferroan Calcite	1634
8	Rohtasgarh Limestone	Ferroan Calcite	1999
9	Rohtasgarh Limestone	Ferroan Calcite	2519
10	Rohtasgarh Limestone	Ferroan Calcite	3461
11	Rohtasgarh Limestone	Ferroan Calcite	2017
12	Rohtasgarh Limestone	Ferroan Calcite	1980
13	Rohtasgarh Limestone	Calcite	1741
14	Rohtasgarh Limestone	Ferroan Calcite	3522
15	Rohtasgarh Limestone	Ferroan Calcite	1707
16	Rohtasgarh Limestone	Ferroan Calcite	1622
17	Rohtasgarh Limestone	Ferroan Calcite	2023
18	Rohtasgarh Limestone	Ferroan Calcite	2126
19	Rohtasgarh Limestone	Ferroan Calcite	2121
20	Rohtasgarh Limestone	Calcite	3205
21	Rohtasgarh Limestone	Ferroan Calcite	1535
22	Rohtasgarh Limestone	Ferroan Calcite	1875
23 **(Top)**	Rohtasgarh Limestone	Ferroan Calcite	1617

Table 5.3- Total Organic Carbon (TOC) distribution in the Kajrahat Limestone, Kuteshwar mine section, Maihar area, M.P. Sampling interval is 50 cm.

Sample No.	Stratigraphic Unit	Lithology	TOC(ppm)/%
1 (Bottom)	Kajrahat Limestone	Ferroan Calcite	6963
2	Kajrahat Limestone	Calcite	1425
3	Kajrahat Limestone	Calcite	2407
4	Kajrahat Limestone	Calcite	2236
5	Kajrahat Limestone	Calcite	4715
6	Kajrahat Limestone	Calcite	1079
7	Kajrahat Limestone	Calcite	1223
8	Kajrahat Limestone	Calcite	1321
9	Kajrahat Limestone	Calcite	4.02%
10	Kajrahat Limestone	Calcite	5824
11	Kajrahat Limestone	Calcite	1526
12	Kajrahat Limestone	Ferroan Calcite	2725
13	Kajrahat Limestone	Calcite	1406
14	Kajrahat Limestone	Calcite	2.54%
15	Kajrahat Limestone	Calcite	4.198%
16	Kajrahat Limestone	Calcite	1741
17	Kajrahat Limestone	Calcite	1.303%
18	Kajrahat Limestone	Calcite	1282
19	Kajrahat Limestone	Calcite	2.653%
20	Kajrahat Limestone	Calcite	8537
21	Kajrahat Limestone	Calcite	3.625%
22	Kajrahat Limestone	Calcite	1.131%
23 (Top)	Kajrahat Limestone	Calcite	9796

Table 5.4- Total Organic Carbon (TOC) distribution in black shale unit of the Rohtasgarh Limestone from Badanpur mine (core samples), Maihar area, and other sections in Katani area, M.P. Sampling interval is 1m in core samples.

Sample No. and depth	Stratigraphic unit	Lithology	TOC(ppm)
A1-25, 10-11	Rohtashgarh Limestone	Black Shale	1088
A1-25, 11-12	Rohtashgarh Limestone	Black Shale	4594
A1-25, 12-13	Rohtashgarh Limestone	Black Shale	1556
A1-25, 14-15	Rohtashgarh Limestone	Black Shale	1171
A1-25, 15-16	Rohtashgarh Limestone	Black Shale	7602
A1-25, 16-17	Rohtashgarh Limestone	Black Shale	3392
A1-25, 17-18	Rohtashgarh Limestone	Black Shale	6421
A1-25, 18-19	Rohtashgarh Limestone	Black Shale	5982
A1-25, 19-20	Rohtashgarh Limestone	Black Shale	8230
A1-25, 20-21	Rohtashgarh Limestone	Black Shale	3713
A1-25, 21-22	Rohtashgarh Limestone	Black Shale	4280
A1-25, 22-23	Rohtashgarh Limestone	Black Shale	4900
A1-25, 23-24	Rohtasgarh Limestone	Black Shale	2081
A1-25, 24-25	Rohtashgarh Limestone	Black Shale	6576
E1-15, 23-24	Rohtashgarh Limestone	Black Shale	1274
E1-15, 24-25	Rohtashgarh Limestone	Black Shale	1228
E1-15, 25-26	Rohtashgarh Limestone	Black Shale	1263
E1-15, 26-27	Rohtashgarh Limestone	Black Shale	2043
E1-15, 27-28	Rohtashgarh Limestone	Black Shale	1795
E1-15, 28-29	Rohtashgarh Limestone	Black Shale	3356
E1-15, 29-30	Rohtashgarh Limestone	Black Shale	1183
E1-15, 30-31	Rohtashgarh Limestone	Black Shale	1292
E1-15, 31-32	Rohtashgarh Limestone	Black Shale	1846
E1-15, 32-33	Rohtashgarh Limestone	Black Shale	1516
E1-15, 33-34	Rohtashgarh Limestone	Black Shale	3039
E1-15, 34-35	Rohtashgarh Limestone	Black Shale	2576
E1-15, 35-36	Rohtashgarh Limestone	Black Shale	1999
E1-15, 36-37	Rohtashgarh Limestone	Black Shale	2254
E1-15, 37-38	Rohtashgarh Limestone	Black Shale	1185
E1-15, 38-39	Rohtashgarh Limestone	Black Shale	1994
E1-15, 39-40	Rohtashgarh Limestone	Black Shale	1581
E1-15, 40-41	Rohtashgarh Limestone	Black Shale	1404
E1-15, 41-42	Rohtashgarh Limestone	Black Shale	1563
E1-15, 42-43	Rohtashgarh Limestone	Black Shale	1930
E1-15, 43-44	Rohtashgarh Limestone	Black Shale	3764
S-1 (Badanpur Mine)	Rohtashgarh Limestone	Limestone	3403
S-3 (Bistara Mine)	Rohtashgarh Limestone	Black Shale	5649
S-4 (Bistara Mine)	Rohtashgarh Limestone	Black Shale	4552
S-6 (Amehta Mine)	Rohtashgarh Limestone	Black Shale	7498
S-11 (Badwar Well-1)	Rohtashgarh Limestone	Black Shale	1.241
S-13 (Badwar Well-2)	Rohtashgarh Limestone	Pyrite	3.326%
S-14 (Badwar Well-2)	Rohtashgarh Limestone	Black Shale	2923

5.2 Rock-Eval Pyrolysis and Kerogen Type

Petroleum generation results from the transformation of organic matter in the subsurface under the influence of both temperature and geologic time. This transformation can be ascribed to the thermal cracking of the kerogen which releases micropetroleum into the pore system of the source rock (Tissot and Welte, 1984; Huc, 1990). Rock-Eval Pyrolysis permits rapid evaluation of the organic matter type, quantity and maturity and thus, yields information on the petroleum-generative potential. This technique is based on the production of hydrocarbons from a rock sample by steadily heating it. In this study, the rock samples with high TOC (>0.5%) were selected for the Rock Eval Pyrolysis study, for hydrocarbon maturation level. Through Rock Eval Pyrolysis, the hydrocarbon generative potential of the organic matter, S1, S2, S3, T_{max}, derivatives hydrogen index (HI), oxygen index (OI) and total organic carbon (TOC) are determined. The parameters obtained during the Rock Eval Pyrolysis are briefly described below:

- S1- corresponds to hydrocarbons formed in the subsurface and already present in the rock. The S1 peak is measured during the first stage of pyrolysis at the fixed temperature of 300º C.
- S2- represents hydrocarbons generated during the pyrolysis process from the cracking of kerogen.
- T_{max} represents the temperature at which the largest amount of hydrocarbons is produced in the laboratory when a whole rock sample undergoes a pyrolysis treatment.
- TOC values represent the total amount of organic carbon present in the rock.
- S3 expresses the milligrams of carbon dioxide generated from a gram of rock during temperature programming up to 390º C.
- Pyrolysed Carbon (PC) is as the ratio (S1+S2)/100, another organic type indicator.
- Production index (PI) which is defined as the ratio S1/(S1+S2).

Total 15 samples were selected for the Rock Eval Pyrolysis, based on organic matter more than 0.5% of TOC. The results are summarized in the Table 5.5.

Table 5.5: Rock-Eval Pyrolysis of black shale unit of Rohtasgarh Limestone, Maihar and Katni area, M.P.

Sample No.	Qty (mg)	S1	S2	S3	PI	Tmax	TpkS 2	S3CO	S3' CO	S3'	PC%	RC%	TOC%	HI	OI CO	OI	Pyro MIN C%	Oxi MIN C%	MIN C%
S-1 Badanpur Mine	52.81	0.08	0	0.05	1	439	0	0.01	0	9.2	0.01	0.19	0.2	0	5	25	0.25	5.11	3.69
S-3 Bistara Mine (Katni)	61.64	0.03	0	0.17	1	439	0	0.01	0.1	6.5	0.01	0.23	0.24	0	4	71	0.18	3.51	1.14
S-11 Badwar Well-1	56.39	0.07	0.25	0.05	0.21	523	562	0	0	4	0.03	0.76	0.79	32	0	6	0.11	1.04	0.09
S-14 Badwar Well-2	54.14	0.04	0	0.22	0.91	358	397	0	0	1.7	0.01	0.07	0.08	0	0	275	0.05	0.04	1.91
S-6 Amehta Mine (Katni)	56.82	0.13	0.21	0.03	0.38	503	542	0.01	0	8.3	0.03	0.38	0.41	51	2	7	0.23	1.68	4.43
U-4 Bistara Mine	53.11	0.14	0.07	0.12	0.41	513	552	0.05	0.1	8.1	0.02	0.23	0.25	28	20	48	0.22	4.21	5.73
U-13 Badwar Well-2	49.21	0.03	0.02	0.49	0.69	404	443	0.04	0	14.7	0.02	0.19	0.21	10	19	233	0.4	5.33	3.1
A1-25, 11-12 (Top)	51.78	0.08	0.08	0.04	0.49	512	551	0.01	0	11.4	0.01	0.26	0.27	30	4	15	0.31	2.79	3.1
A1-25, 15-16	53.33	0.05	0.15	0.04	0.25	516	555	0.04	0	10	0.02	0.53	0.55	27	7	7	0.27	2.83	2.34
A1-25,18-19	58.4	0.05	0.11	0.04	0.39	490	529	0.02	0	9.9	0.02	0.41	0.43	26	5	9	0.27	2.07	3.2
A1-25,19-20	58.9	0.04	0.06	0.05	0.36	401	540	0.02	0	10.7	0.01	0.21	0.22	27	9	23	0.29	2.91	2.59
A1-25,22-23	65.92	0.07	0.09	0.04	0.44	511	550	0.02	0	10	0.02	0.31	0.33	27	6	12	0.27	2.32	0.13
A1-25,21-22	53.25	0.02	0.03	0.05	0.5	510	549	0.05	0	12.8	0.01	0.27	0.28	11	18	18	0.35	3.86	4.21
A1-25,24-25 (Bottom	57.78	0.03	0.05	0.08	0.4	492	531	0.02	0	15	0.01	0.29	0.3	17	7	27	0.41	2.29	2.7
E1-15,43-44	58.41	0.01	0	0.03	0.42	439	0	0.01	0	8.6	0	0.03	0.03	0	33	100	0.23	0.08	0.31

Two types of diagrams are widely used to interpret the maturation level, type of organic matter and hydrocarbon generation potential. Of these two diagrams, one is Hydrogen Index (HI) versus Total Organic Carbon (TOC) diagram (Fig. 5.1) and the other is the Hydrogen Index (HI) versus T_{max} diagram (Fig. 5.2).

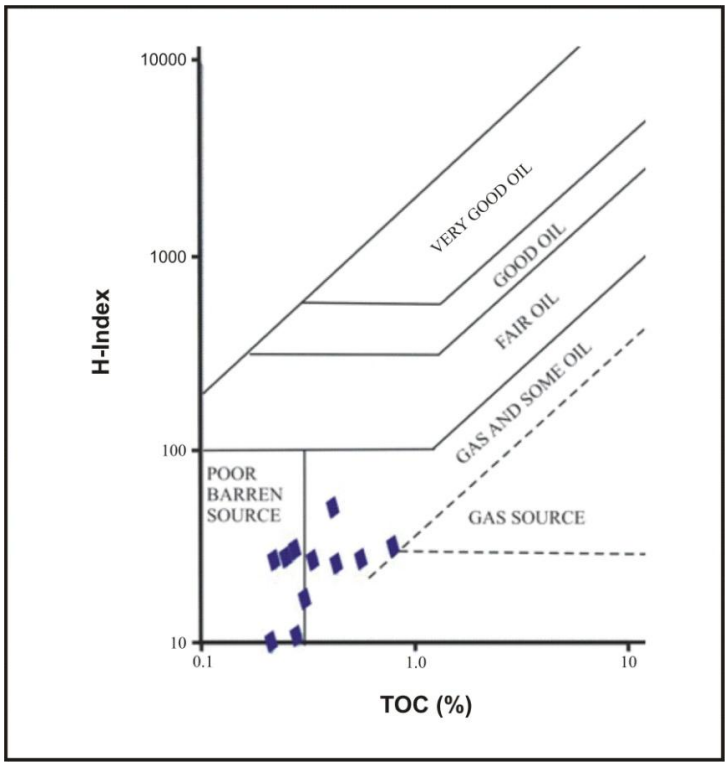

Fig. 5.1- Showing source richness of black shale samples from the Rohtasgah Limestone.

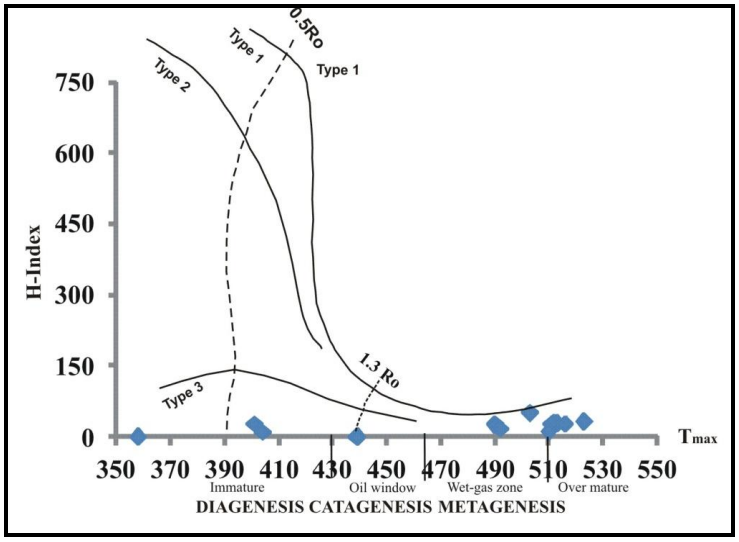

Fig. 5.2- Composite HI-Tmax diagram for the interpretation of kerogen type and maturity of organic carbon content of black shales from the Rohtasgarh Limestone.

The Hydrogen Index (HI) versus T_{max} diagram (Gorin and Feist-Bukhardt, 1990) is based on the amount of hydrogen that the kerogen contains and the amount of energy necessary to produce hydrocarbons from that type of kerogen in the laboratory over a short period of time. Espitalié et al., (1977) defined the Hydrogen Index (HI) versus Oxygen Index (OI) program where HI and OI are (S2/TOC) x 100 and (S3/TOC) x 100 respectively. This diagram provides rough information on the type of organic matter which represents the proportion of hydrogen bound in the organic structure. The HI represents the hydrogen richness and the OI depicts the organic oxygen content of the sample, both relative to the total organic carbon content (Snowdon, 1989). The type of organic hydrogen is controlled by the nature of the organic matter. Aquatic organic matter has high hydrogen content whereas terrestrially derived organic matter has low hydrogen content and variable high oxygen content.

All samples of this study are very similar in organic matter content and type. These samples show very erratic T_{max} and Production Index (PI) values, and low pyrolysis values varies such as S1 (0.0 and 0.14, average 0.08 mg HC/g rock), S2 (0-0.25 mg HC/g rock), S3 (0.05-0.5 mg HC/g rock), TOC (0.2-0.6 wt. %), HI ~30 mg HC/g rock, and highly variable OI.

The Production Index (PI) and T_{max} are indicators of the degree of thermal maturity (Peters, 1986). It is also an indication of the amount of hydrocarbon which has been produced geologically relative to the total amount of hydrocarbon which the sample can produce. In general, PI values below 0.4 indicate immature organic matter; PI values between 0.4 and 1.0 indicate mature organic matter; and PI values above 1.0 are indicative of over mature organic matter. The T_{max} values lower than 435º C indicate immature organic matter (organic matter). T_{max} values between 435º C and 455º C indicate "oil window" conditions (mature organic matter), between 455º C and 470º are considered transitional. A T_{max} higher than 470º C represents the wet-gas zone and over mature organic matter (Peters, 1986). Here PI values are more than 0.4 and mostly ~1. T_{max} is ~ 500º C in all samples. The lower S2 values at a higher TOC in the study samples imply the presence of hydrogen index in low concentration and over-mature organic matter (Sikander et al., 2000).

In our studies the sample shows the depletion in S1 and S2 and high S3 values primarily due to weathering. PI is defined as the ratio S1/(S1+S2), and,

hence, depletion of S1 and S2 may induce changes on actual PI values. Immature sediments commonly yield poorly separated S1 and S2 values which can lead to anomalous results. Oxidation is the most common form of degradation of organic matter. Oxidation removes hydrogen and adds oxygen to the kerogen, and therefore, HI values are usually lower and OI values higher for outcrop samples than for fresh-core samples in Table 5.5. The S1 vs. S2 plot (Fig. 5.3) showing weak linear correlation which indicates least capacity of the TOC for hydrocarbon generation.

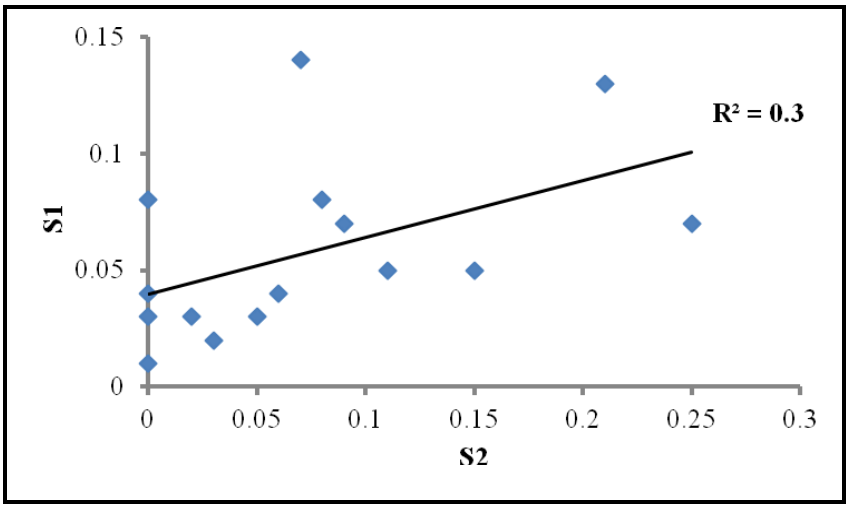

Fig. 5.3- A plot of S1 vs. S2 showing a weak positive correlation, between S1 & S2 implies that the organic matter of the black shales in Rohtasgarh Limestone was derived from a mixed origin.

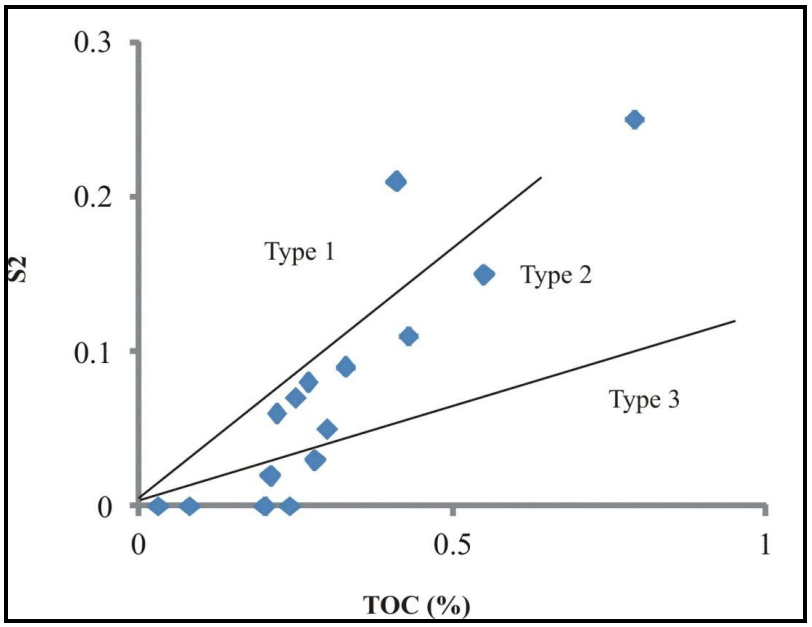

Fig. 5.4- A plot of S2 vs. TOC defines a predominance of Type II organic matter in the black shales unit of the Rohtasgarh Limestone.

The hydrogen index values are generally low ranging from 0 to 51 mg HC/g TOC (Table 5.5). The plots of HI vs TOC (Jackson et al., 1985) indicate a poor barren source to gas-prone source rock for the black shales unit of Rohtasgarh Limestone in Figure 5.1. It means the poor source beds were probably deposited in oxic conditions (Demaison and Moore, 1980; Olugbemiro et al., 1997).

In the plot of HI vs T_{max} (Espitalie et al., 1984), where maximum samples plot on the Type I and Type II (gas prone) kerogen field in Figure 5.2. In this diagram maximum samples lie in T_{max} ranges, between 490 and 520^0C, which indicate over maturation of organic matter. Exceptionally, only one sample lies in oil window zone i.e in catagenesis and three samples lie in immature zone i.e. in diagenesis with negligible, HI in Figure 5.2. It may be due to weathering and oxidation of organic matter. Ramanampisoa and Radke, (1992) suggested, the values of S1+S2 is lower than 1mg HC/g rock and S1 of less than 0.4 mg HC/g rock indicates barely free hydrocarbons in the potential source rocks. In this study this type of indication shows, with the values of S1+S2 $\leq$ 1 and also the values of S $\leq$ 10.4.

Burgan and Ali (2009), plotted a diagram, S2 vs TOC in order to know the characterization of the Black Shales of the Temburong Formation in West Sabah, East Malaysia, and suggested the types of organic matter content in it. On the basis of this, in the present study most of the samples lie in Type II organic matter (Fig. 5.4). This is also supports the results obtained in Figure 5.2. Most of the samples in the oxygen index (OI) vs. hydrogen index (HI) diagram (Fig.5.5) are indicating type II kerogen. Which is supporting, the results obtained by the S2 vs TOC (Fig. 5.4) and HI vs. T_{max} (Fig.5.2) diagram.

5.3 Light Hydrocarbon Gases (C1-C5)

In this study, the magnitude of each of the five light hydrocarbon gases that are absorbed on to the clay matrix of black shales constituents (C1, C2, C3, *i*C4 *n*C4, *i*C5 and *n*C5), measured and expressed in ppb. The compositional characteristics of these hydrocarbon gases in black shales indicate the presence of methane (C1) 800 to 2300 ppb, ethane (C2) 50 to 1100 ppb, propane (C3) 4 to 300 ppb, *i*-butane (*i*C4) 7 to 150 ppb, *n*-butane (*n*C4) 5 to 50 ppb, *i*-pentane (*i*C5) 8 to 147 ppb and *n*-pentane (*n*C5) 8 to 100 ppb. Values for each analyzed shales gas

constituents are summarized in Table 5.6. The distribution of C1, C2 and C3 gases in the shales showed high concentration.

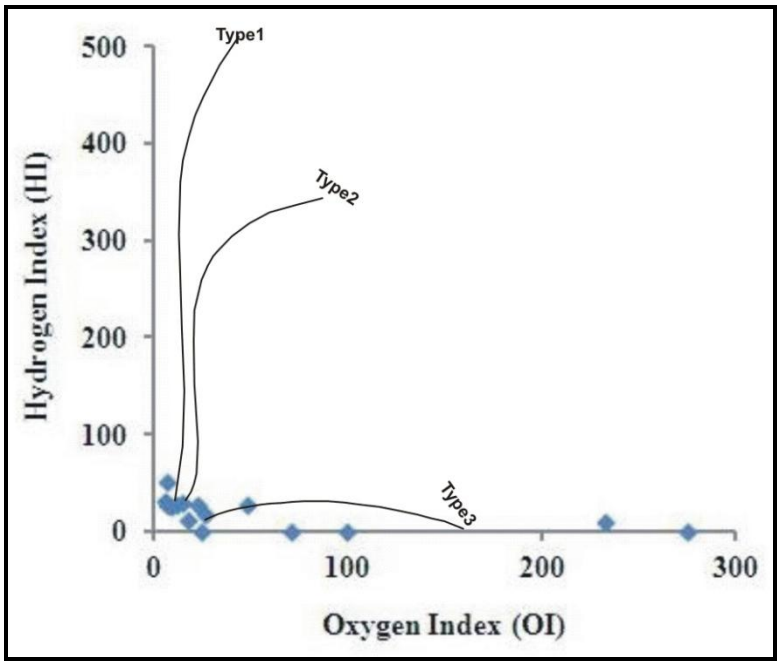

Fig. 5.5- A plot of HI vs. OI from Rock–Eval Pyrolysis of black shales unit from the Rohtasgarh Limestone, showing that the organic matter lies within the Kerogen Type I and Type II.

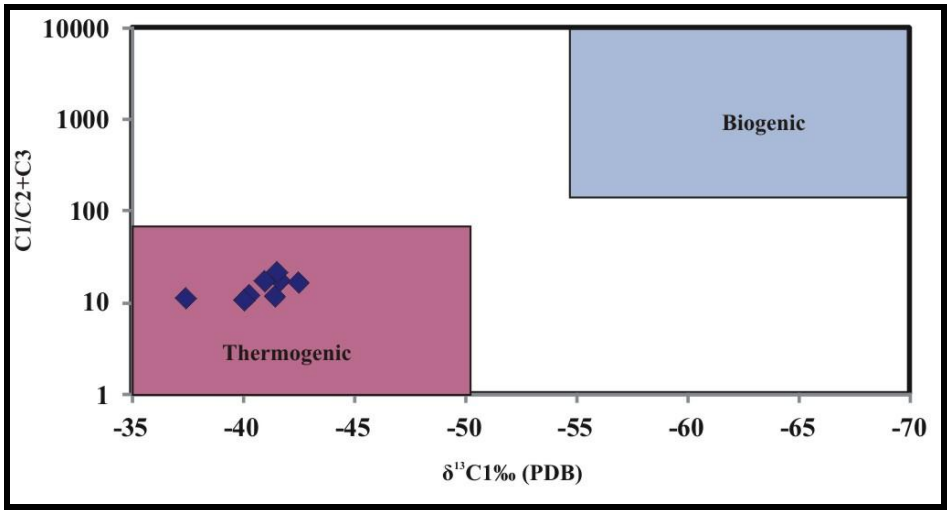

Fig. 5.6- δ13C1 versus C1/(C2 + C3) ratio plot to indicate source of light hydrocarbons.

Bernard plots

Stable carbon isotopes yield information on the origin of hydrocarbons from varied locations or sources (Fuex, 1977; Faber and Stahl, 1983; 1984; Schoell, 1983; Stahl, 1977; Stahl et al. 1981; Whiticar, 1996; 1999). A Bernard plot can be

used to differentiate light hydrocarbon gases derived from thermogenic or bacterial sources (Bernard, 1978). C1/C2+C3 ratios <100 and δ^{13}C1 heavier than -60 ‰ are characteristic of thermogenic hydrocarbons; whereas C1/C2+C3 ratios > 1000 and δ^{13}C1 lighter than -60 ‰ indicate an origin from biogenic sources (Bernard 1978). A Bernard plot showing the relationship between methane δ^{13}C1 and C1/C2+C3 from the black shales samples of the Lower Vindhyan is shown in Figure 5.6. The carbon isotopic compositions of δ^{13}C1 are in ranges between –37.45‰ and –42.2‰ (PDB). Which indicate that these gases are of thermogenic origin and in all likelihood of a thermogenic source for the light hydrocarbons.

Also gases of thermogenic origin generally show a trend of decrease in concentration from methane to pentane i.e. C1>C2>C3>C4>C5 (Klusman, 1993; Tedesco, 1995; Sanez, 1984). This type of trend is summarized in Table 5.6.

Table 5.6- Light Hydrocarbon (C1-C5 ppb) distribution in black shale unit of Rohtasgarh Limestone Vindhyan Supergroup, Satna and Katni Districts, M.P. Sampling interval is 1m.

Sample No. , Depth (m)	**Stratigraphic Unit**	**C1**	**C2**	**C3**	**iC4**	**nC4**	**iC5**	**nC5**
A1-25, 10-11 (Top)	Rohtasgarh Limestone	16565	686	119	15	16	0	0
A1-25, 11-12	Rohtasgarh Limestone	22332	1735	293	19	29	20	9
A1-25, 12-13	Rohtasgarh Limestone	8636	384	69	0	0	0	0
A1-25, 14-15	Rohtasgarh Limestone	30223	1315	198	20	26	27	16
A1-25, 15-16	Rohtasgarh Limestone	10164	722	112	0	0	0	0
A1-25, 16-17	Rohtasgarh Limestone	16610	931	152	12	16	17	7
A1-25, 17-18	Rohtasgarh Limestone	22464	1586	277	26	24	8	18
A1-25, 18-19	Rohtasgarh Limestone	6023	67	4	0	0	0	0
A1-25, 19-20	Rohtasgarh Limestone	856	49	11	0	0	0	0
A1-25, 20-21	Rohtasgarh Limestone	18261	1394	251	21	32	11	4
A1-25, 21-22	Rohtasgarh Limestone	3094	140	27	0	0	0	0
A1-25, 22-23	Rohtasgarh Limestone	13232	996	143	7	0	0	0
A1-25, 23-24	Rohtasgarh Limestone	12301	621	101	15	5	0	0
A1-25, 24-25 (Bottom)	Rohtasgarh Limestone	5253	266	49	0	0	0	0
E1-15, 23-24 (Top)	Rohtasgarh Limestone	6645	260	75	11	12	0	10
E1-15, 24-25	Rohtasgarh Limestone	23696	971	370	170	100	147	99
E1-15, 25-26	Rohtasgarh Limestone	7785	302	52	4	6	0	1
E1-15, 26-27	Rohtasgarh Limestone	13614	646	171	29	25	35	17
E1-15, 27-28	Rohtasgarh Limestone	9469	302	60	9	0	0	0
E1-15, 28-29	Rohtasgarh Limestone	4978	238	65	10	11	0	6
E1-15, 29-30	Rohtasgarh Limestone	10285	448	120	21	30	59	59
E1-15, 30-31	Rohtasgarh Limestone	2753	173	75	33	28	79	35
E1-15, 31-32	Rohtasgarh Limestone	9295	653	229	49	51	88	114
E1-15, 32-33	Rohtasgarh Limestone	19803	889	273	72	55	97	100
E1-15, 33-34	Rohtasgarh Limestone	5826	433	155	28	27	38	20

E1-15, 34-35	Rohtasgarh Limestone	3202	199	73	12	18	61	9
E1-15, 35-36	Rohtasgarh Limestone	4202	200	46	0	0	0	0
E1-15, 36-37	Rohtasgarh Limestone	3172	194	64	11	13	33	24
E1-15, 37-38	Rohtasgarh Limestone	8101	379	76	8	8	0	0
E1-15, 38-39	Rohtasgarh Limestone	12728	702	146	15	20	0	4
E1-15, 39-40	Rohtasgarh Limestone	4691	239	57	1	0	0	3
E1-15,40-41	Rohtasgarh Limestone	965	56	15	0	0	0	0
E1-15, 41-42	Rohtasgarh Limestone	5225	245	45	0	0	0	0
E1-15, 42-43	Rohtasgarh Limestone	1313	73	22	0	0	0	0
E1-15, 43-44 (Bottom)	Rohtasgarh Limestone	4276	209	46	0	0	0	0
S-1(Badanpur Mine)	Rohtasgarh Limestone	5916	308	90	19	23	75	128
S-3 (Bistara Mine)	Rohtasgarh Limestone	9585	1198	353	45	69	53	69
S-4 (Bistara mine)	Rohtasgarh Limestone	3703	329	100	17	18	27	17
S-6 (Amehta Mine)	Rohtasgarh Limestone	381	31	6	0	0	0	0
S-11 (Badwar well-1)	Rohtasgarh Limestone	3314	401	73	0	0	26	27
S-13 (Badwar)	Rohtasgarh Limestone	9779	329	39	0	0	0	0
S-14 (Badwar well-2)	Rohtasgarh Limestone	360	42	7	0	0	0	0

The isotopic signatures of a few samples also show a progressive depletion in $\delta^{13}C$ from propane to ethane to methane (Table 5.7). However, an enrichment of $\delta^{13}C2$ compared to $\delta^{13}C3$ is observed in a few samples which may be due to mixing between thermal gases of different maturities (Berner and Faber, 1988; Chung et al., 1988; James, 1990; Mani et al., 2011b).

Table 5.7 - GC- IRMS Isotope data of Black Shale unit of the Rohtasgarh Limestone, Badanpur Mine, Maihar area, M.P. Sampling interval is 1 m.

Sample No. and depth	**Lithostratigraphy Unit**	**Lithology**	**$^{13}\delta C1$ ‰**	**$^{13}\delta C2$ ‰**	**$^{13}\delta C3$ ‰**
A1-25, 11-12 (Top)	Rohtasgarh Limestone	Black Shale	-40-24	-38.4	-
A1-25, 14-15	Rohtasgarh Limestone	Black Shale	-41.5	-35.9	-
A1-25, 17-18	Rohtasgarh Limestone	Black Shale	-40.29	-40.0	-
A1-25, 20-21	Rohtasgarh Limestone	Black Shale	-37.45	-8.29	-
A1-25, 22-23 (Bottom)	Rohtasgarh Limestone	Black Shale	-41.39	-0.03	-
E1-15-24-25 (Top)	Rohtasgarh Limestone	Black Shale	-42.47	-5.21	-31.09
E1-15 29-30	Rohtasgarh Limestone	Black Shale	-41.39	-35.8	-
E1-15 32-33 (Bottom)	Rohtasgarh Limestone	Black Shale	-40.96	-36.8	-39.29

Prasanna et al., (2010), worked on soil samples of Vindhyan basin and find out that the adsorbed soil gas results indicate the presence of methane, ethane,

propane and butane in Sagar District M.P. They observed the anomalies of C1 and ΣC2+ concentrations in the northern and southern parts of Sagar, and northeast of Deori. According to them the adsorbed soil gas and carbon isotope studies suggested that these seeped hydrocarbons are of thermogenic origin and sediments are petroliferous in nature. Adsorbed soil gas and carbon isotope studies show good regional evaluation of hydrocarbon potential and indicate that the area is warm for hydrocarbon exploration. The light hydrocarbon ratios are used to predict the oil/gas potential of the basin. The classification of compositional ratio of C3/C1×1000 given by Jones and Drozd (1983) predicts that the C3/C1×1000 ratio between 60–500 fall in the oil zone, 20–60 in gas-condensate zone and 2–20 in the dry gas zone. Here out of 42 samples only 6 samples are showing, C3/C1×1000 ratio between 20 and 60 that is in gas-condensate zone. Rest 36 samples are showing, C3/C1×1000 ratio between 2 and 20 which in the dry gas zone. Out of 42 samples 23 samples have all the gases composition (C1 to C5), and very high concentration of methane comparatively in Table 5.6.

Cross-plots

A cross-plot illustrates the correlation between two compositional variables and provides information on a hydrocarbon's source and the effects of secondary alteration. Cross-plots between light gaseous hydrocarbons (C1-C5) are plotted (Fig. 5.7, 5.8 and 5.9). The plots of C1 vs C2 (Fig. 5.7), C2 vs C3 (Fig. 5.8) and C1 vs ΣC2+ i.e. sum of ethane, propane, *i*-butane, *n*-butane, *i*-pentane and *n*-pentane (Fig. 5.9), are showing linear correlations, suggesting a thermogenic origin for the hydrocarbons (Belt and Rice, 2002; Jones and Drozd, 1983). Gases of thermogenic origin generally show a trend of decrease in concentration from methane to pentane i.e. C1>C2>C3>C4>C5 (Klusman, 1993; Tedesco, 1995; Sanez, 1984). The light hydrocarbon gases from the Rohtasgarh Limestone's black shale samples are highly correlatable and follow a similar pattern as shown by the cross-plots (Fig. 5.7, 5.8, 5.9).

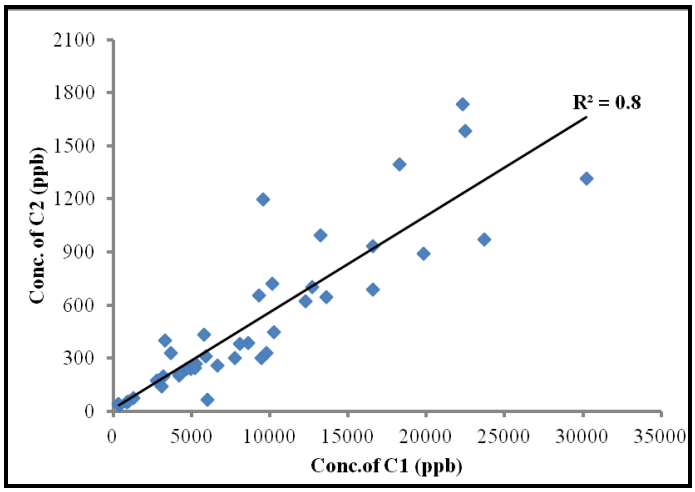

Fig. 5.7- Black shale gas hydrocarbons cross-plot of ethane (C2), versus methane (C1) showing linear correlation.

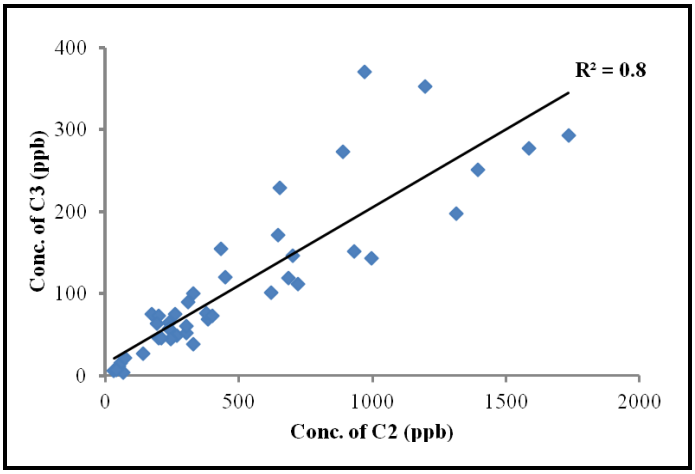

Fig. 5.8- Black shale gas hydrocarbons cross-plot of propane (C3) versus ethane (C2), is showing linear correlation.

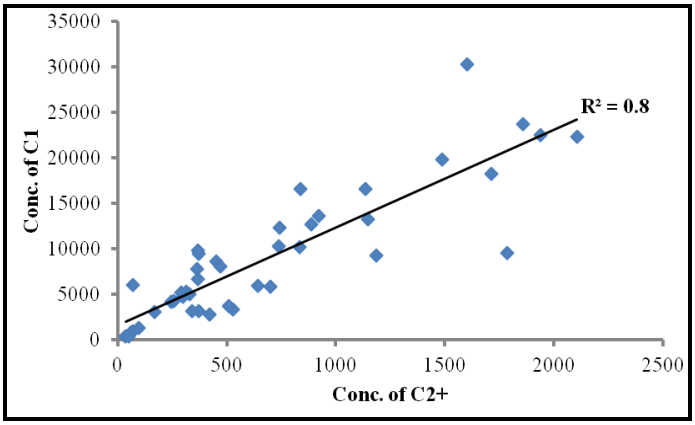

Fig. 5.9- Black shale gas hydrocarbons cross-plot of methane versus ethane plus higher hydrocarbons (ΣC2+), showing linear correlation.

Haworth, Sellens, and Whitaker (1985), had given the interpretation of light hydrocarbon gases (C1-C5), using mud log data. They used some parameters and given the mathematical formula to calculate these ratios. The ratios were calculated as provided below:

Wetness (Wh) = ((C2 + C3 + iC4 + nC4 + iC5 + nC5)/ (C1 + C2 + C3 + iC4 + nC4 + iC5 + nC5)) × 100

Balance (Bh) = (C1 + C2) / (C3 + iC4 + nC4 + iC5 + nC5)

Character (Ch) = (iC4 + nC4 + iC5 + nC5) / C3

Set points used for the Wh ratio were as follows:

< 0.5 = very dry gas.

0.5 - 17.5 = gas, density increases as Wh increases.

17.5 - 40 = oil, density increases as Wh increases.

> 40 = residual oil.

When plotted together, Wh and Bh give an interpretation of fluid character as follows:

- If Bh is greater than 100, the zone has very dry gas.
- If Wh indicates a gas phase and Bh is greater than Wh, gas is indicated,
- If Wh indicates a gas phase and Bh is less that Wh, gas/oil or gas/condensate is

indicated.

- If Wh is in the oil phase and Bh is less than Wh, oil is indicated.

When Wh is greater than 40, Bh will be much less than Wh, indicating residual oil.

The Ch ratio was chosen to interpret shows where, in certain circumstances, high

methane readings indicated a lighter hydrocarbon fluid character, using only Wh and

Bh,

Ch is used only to clarify the interpretation of Wh and Bh when they indicate gas. The resultant Ch is interpreted as follows:

- If Ch is less than 0.5, the Wh and Bh interpretation of gas is correct.
- If Ch is greater than 0.5, the gas character by the Wh and Bh ratios in associated with oil.

Table 5.8- Wetness (Wh), Balance (Bh) and Character (Ch) ratios distribution in black shale unit of the Rohtasgarh Limestone, Lower Vindhyan .Satna & Katni Districts, M.P., sampling interval is 1m.

Sample No.	Stratigraphic Unit	C1+C2	C1+	C3+	iC4+	Wh	Bh	Ch
A1-25, 10-11 (Top)	Rohtasgarh Limestone	17251	17401	150	31	4.8	115	0.26
A1-25, 11-12	Rohtasgarh Limestone	24067	24437	370	77	8.61	65.05	0.26
A1-25, 12-13	Rohtasgarh Limestone	9020	9089	69	0	4.98	130.7	0
A1-25, 14-15	Rohtasgarh Limestone	31538	31825	287	89	5.03	109.9	0.45
A1-25, 15-16	Rohtasgarh Limestone	10886	10998	112	0	7.58	97.2	0
A1-25, 16-17	Rohtasgarh Limestone	17541	17745	204	52	6.4	85.99	0.34
A1-25, 17-18	Rohtasgarh Limestone	24050	24403	353	76	7.95	68.13	0.27
A1-25, 18-19	Rohtasgarh Limestone	6090	6094	4	0	1.17	1523	0
A1-25, 19-20	Rohtasgarh Limestone	905	916	11	0	6.55	82.27	0
A1-25, 20-21	Rohtasgarh Limestone	19655	19974	319	68	8.58	61.61	0.27
A1-25, 21-22	Rohtasgarh Limestone	3234	3261	27	0	5.12	119.8	0
A1-25, 22-23	Rohtasgarh Limestone	14228	14378	150	7	7.97	94.85	0.05
A1-25, 23-24	Rohtasgarh Limestone	12922	13043	121	20	5.69	106.8	0.2
A1-25, 24-25 (Bottom)	Rohtasgarh Limestone	5519	5568	49	0	5.66	112.6	0
E1-15, 23-24 (Top)	Rohtasgarh Limestone	6905	7013	108	33	5.25	63.94	0.44
E1-15, 24-25	Rohtasgarh Limestone	24667	25553	886	516	7.27	27.84	1.39
E1-15, 25-26	Rohtasgarh Limestone	8087	8150	63	11	4.48	128.4	0.21
E1-15, 26-27	Rohtasgarh Limestone	14260	14537	277	106	6.35	51.48	0.62
E1-15, 27-28	Rohtasgarh Limestone	9771	9840	69	9	3.77	141.6	0.15
E1-15, 28-29	Rohtasgarh Limestone	5216	5308	92	27	6.22	56.7	0.42
E1-15, 29-30	Rohtasgarh Limestone	10733	11022	289	169	6.69	37.14	1.41
E1-15, 30-31	Rohtasgarh Limestone	2926	3176	250	175	13.3	11.7	2.33
E1-15, 31-32	Rohtasgarh Limestone	9948	10479	531	302	11.3	18.73	1.32
E1-15, 32-33	Rohtasgarh Limestone	20692	21289	597	324	6.98	34.66	1.19
E1-15, 33-34	Rohtasgarh Limestone	6259	6527	268	113	10.7	23.35	0.73
E1-15, 34-35	Rohtasgarh Limestone	3401	3574	173	100	10.4	19.66	1.37
E1-15, 35-36	Rohtasgarh Limestone	4402	4448	46	0	5.53	95.7	0
E1-15, 36-37	Rohtasgarh Limestone	3366	3511	145	81	9.66	23.21	1.27
E1-15, 37-38	Rohtasgarh Limestone	8480	8572	92	16	5.49	92.17	0.21
E1-15, 38-39	Rohtasgarh Limestone	13430	13615	185	39	6.51	72.59	0.27
E1-15, 39-40	Rohtasgarh Limestone	4930	4991	61	4	6.01	80.82	0.07
E1-15,40-41	Rohtasgarh Limestone	1021	1036	15	0	6.85	68.07	0
E1-15, 41-42	Rohtasgarh Limestone	5470	5515	45	0	5.26	121.6	0
E1-15, 42-43	Rohtasgarh Limestone	1386	1408	22	0	6.75	63	0
E1-15, 43-44 (Bottom)	Rohtasgarh Limestone	4485	4531	46	0	5.63	97.5	0
S-3 (Bistara Mine)	Rohtasgarh Limestone	10783	11372	589	236	15.7	18.31	0.67
6 (Amehta Mine)	Rohtasgarh Limestone	412	418	6	0	8.85	68.67	0
S-1(Badanpur Mine)	Rohtasgarh Limestone	6224	6559	335	245	9.8	18.58	2.72
S-11 (Badwar well-1)	Rohtasgarh Limestone	3715	3841	126	53	13.7	29.48	0.73
S-14 (Badwar well-2)	Rohtasgarh Limestone	402	409	7	0	12	57.43	0
S-4 (Bistara mine)	Rohtasgarh Limestone	4032	4211	179	79	12.1	22.53	0.79
S-13 (Badwar)	Rohtasgarh Limestone	10108	10147	39	0	3.63	259.2	0

The maximum Wetness (Wh) ratios, values of present study, ranges between 0.5 and 17.5 which indicate gas bearing. These values are very near to dry gas with high density. All the samples are showing Wetness (Wh) ratios < Balance (Bh) ratios, which indicates gas phase. Balance (Bh) ratios values are greater than 100 in 13 samples out of 42, which indicate very dry gas and rests samples are in high density gas. The 80 % samples are showing Character (Ch) ratios, values are less than 0.5 which are supporting the Wh and Bh interpretation of gas is correct. Rest values of Character (Ch) ratios, which are greater than 0.5, showing the gas character by the Wh and Bh ratios, in associated with oil ratios, are supporting. These values are summarized in Table 5.8.

Chapter 6

DISCUSSION AND CONCLUSIONS

6.1 Discussion

The present thesis addresses five aspects of the Lower Vindhyans exposed in the Maihar area. The palaeobiological remains, Microbially Induced Sedimentary Structures and problems of contamination constitute the biotic elements of the study. Whereas the Radial Fan Fabric recorded in the Kajrahat Limestone denotes an event phenomenon. Microbial fossils present Precambrian biodiversity in the Salkhan Limestone. All these evidence are discussed in developing biostratigraphic framework. Results of the Geochemical studies on the black shales and carbonates of the Semri Group are discussed to know the hydrocarbon potentiality of these rocks. The Rohtasgarh Limestone of the Lower Vindhyan Basin yielded abundant carbonaceous megafossils, microfossils and microbial mat structures, described in the Chapter 4. These fossil assemblages are recorded from Rampur Shale and the Rohtasgarh Limestone, of the Semri Group. The palaeoenvironmental interpretation of the assemblages and significance of the macro and microfossils are also discussed in this part.

6.2 Carbonaceous megafossils

Charles Doolittle Walcott described certain circular carbonaceous discs from Chuar Group, USA which were later named as *Chuaria circularis* (Walcott, 1899, pp. 234–235; pl. 27, Figs. 12 and 13; Ford and Breed, 1973). Even after a century of its discovery it is a matter of discussion, about the origin, affinity and morphology of this taxon. It has been variously assigned to hyolithids, gastropods, brachiopods, chitinous foraminifera, medusoides and trilobite eggs, or even considered as inorganic (Spamer, 1988). Most of the workers place it in the Plant Kingdom (Ford and Breed, 1973; Duan, 1982; Sun, 1987; Hofmann, 1992; Vidal et al., 1993). Several attempts have been made to decipher and elucidate its life cycle (Sun, 1987; Kumar, 2001; Kumar and Srivastava, 2003; Maithy, 2003; Maithy and Babu, 2004, Sharma et al., 2009). Another constituent of the *Chuaria* assemblage is the tomaculate, slender carbonaceous macrofossils. Hofmann and

Aitken (1979) described it, as *Tawuia dalensis* Hofmann. This form is often found in association with *Chuaria.* Therefore, it has been considered to constitute the *Chuaria–Tawuia* complex. Their close association was further supported by allometric growth curves for *Tawuia* (Knoll, 1982; Hofmann, 1985). Earlier, White (1928) suggested, affinity of *Chuaria* an alga. Ford and Breed (1973) suggested that *Chuaria* was algal in origin. Duan (1982) believed that it was a multicellular alga with possible relationship to the brown algae. Suresh and Sundara Raju (1983) thought that *Chuaria* was most likely a colonial alga similar to *Volvox,* whereas Sun (1987) apparently demonstrated that *Chuaria* was a colonial form constituted of filamentous cyanobacteria comparable to the modern species *Nostoc microscopicum*. Steiner (1997), though agreed with Sun, yet proposed that *Chuaria* may have had various biological affinities ranging between prokaryotic colonies to eukaryotic algae, a view similar to Hofmann (1977) who earlier suggested that *Chuaria*, as a fossil remnant, represents different biological groups. Kumar (2001), suggested that there was a certain relationship among *C. circularis*, *Tawuia* and *Tilsoia*, three taxa of carbonaceous megafossils recorded from the Suket Shale of the Vindhyan Basin, and these forms represent three different parts of a multicellular Chlorophycean/Xanthophycean plant; *C. circularis* representing a compressed cyst-like spherical body attached to *Tawuia* a filamentous thallus, of which *Tilsoia* acted as a holdfast. Kumar further argued that another species of *C. vindhyanensis* represented spores of *C. circularis*. Kumar and Srivastava (2003) proposed a relationship between *C. circularis*, *C. dulniensis* and *Bhanderia*, the last one being a ring-like body believed to have been produced by *Chuaria*. Maithy (2003) believed that he could decipher an alternation of generations in the *Chuaria–Tawuia* complex. Maithy and Babu (2004) added few more discoidal forms in the proposed gametophytic generation of *Chuaria* and *Tawuia* association. They suggested that a variety of carbonaceous remains assigned to *Chuaria*, *Rohtasea*, *Amjohrea*, *Ramapuraea*, *Nostoc*, *Tawuia*, *Sinosabellidites*, *Protoarenicola*, etc. constitute different stages in the life cycle of a single taxon, of which *Chuaria* most probably represents the vegetative stages of the life cycle.

Recently, first time structural analysis was used by Sharma et al. (2009) and proposed a "Hybrid model" based on 'Thin Pressure Vessel Theory'. It was used to test the closeness and possible life cycle relationship within *Chuaria-Tawuia*

complex and their preservation variants. They have used the biometric and structural engineering tool to find out a relationship within Chuaria-Tawuia complex and micro-FTIR (Fourier Transform Infrared Spectroscopy) analysis to understand the biological affinity of *Chuaria circularis*. This model was applied on collected carbonaceous megafossils from different biostratigraphic and geographic localities i.e. Suket Shale of Mesoproterozoic and Halkal Shales of Bhima Group Neoproterozoic, of peninsular India. On these collections the structural engineering tool (thin walled pressure vessel theory) was applied to investigate the implications of possible geometrical shapes (sphere and cylinder), membrane (cell wall) stresses and ambient pressure environment on morphologically similar *C. circularis* and *Tawuia*. The results suggest that membrane stresses developed on the structures similar to *Chuaria– Tawuia* complex were directly proportional to radius and inversely proportional to the thickness in both cases. In case of hollow cylindrical structure, the membrane stresses in circumferential direction (hoop stress) are twice of the longitudinal direction indicating that rupture or fragmentation in the body of *Tawuia* would have occurred due to hoop stress. It appears that notches and discontinuities seen in some of the specimens of *Chuaria* may be related to rupture suggesting their possible location in 3D *Chuaria*. On the basis of proposed "Hybrid model", it was suggested that *Chuaria circularis* most likely was a part of *Tawuia* like cylindrical body of algal origin.

Chuaria has a wide geographical distribution and is recorded from United States, Canada, Russia, Australia, China, Kajakhstan, Spain, Namibia, Benin, Iran, Argentina, India, Antarctica, Sweden, and Moldova/Ukraine. Ford and Breed (1973) considered C*huaria* as potential index fossils for the time range of 1000 Ma to 750 Ma. But, Hofmann and Chen (1981) and Du and Tian (1985) reported C*huaria* from sedimentary sequences of Palaeoproterozoic age. Recently, a *Chuaria-Tawuia* assemblage has also been found from the Palaeoproterozoic Changzhougou Formation in the Yanshan Range, north China (Zhu et al., 2000). Vidal et al. (1993) discussed the significance of time range of *Chuaria- Tawuia* assemblage with emphasis on the 700-840 Ma interval, which generally predates the Varanger glacial event. A similar conclusion was also reached by Sun (1987) mentioning that *Chuaria* occurrences fall in time range of the 700-1000 Ma. However, Steiner (1994) reported *Chuaria* from early Cambrian (520-545 Ma)

Yanjiahe Formation at Heziao and Jijapo, Hubei province, south China. Based on the fossils discoveries in an underlying unit, Amard (1997) suggested an early Cambrian age for *Chuaria* from the Pendjari Formation of West Africa. Therefore, on the basis of presence of *Chuaria*, recorded stratigraphic range of *Chuaria circularis* seems to range from the Palaeoproterozoic to early Cambrian. Accordingly, *Chuaria circularis* cannot be used as a biostratigraphic tool for global correlation of Proterozoic sedimentary sequences. Hofmann (1985) indicated an age of 600-1000 Ma as Chuarian period but *Tawuia dalensis* is not known below 840 Ma. *Tuanshanzia lanceolata* recorded from the Rampur Shale is morphologically similar with known form from the 1,700 Ma old sediments (Yan, 1995) and the Changcheng system ranging 1700-1400 Ma sediments (Yan, 1995; Yan and Liu, 1997, 1998) belonging to Tuanshanzi Formation and Yanshan basin in Jinxian, Hubei of China. Also, the present form of *Tuanshanzia platyphylla* recorded from the Rampur Shale is morphologically similar form from the 1700 Ma sediments belonging to Tuanshanzi Formation in Jixian, Hebei (Yan, 1995). Sharma (2006c), was also recorded a variety of millimetric (macroscopic) carbonaceous films of *Tuanshanzia lanceolata* and *Tuanshanzia platyphylla*, from the Olive Shale (Koldaha Shale) of the Semri Group, exposed in the Newari area of the Sonbhadra District, Uttar Pradesh. In his study, it is also suggested, recoded megafossils represented the oldest megascopic carbonaceous remains from India and may belong to the select band of oldest carbonaceous macroscopic fossil assemblage found in Knob Lake Group, Canada; Michigamme Shales and Negaunee Formation, Michigan, USA and Changcheng Group (Changzhougou, Chauanlinggou and Tuanshanzi Formation) of Jixian, north China.

Recently, Rasmussen et al. (2002) have dated the silicified tuffs bounding the Rampur Formation by SHRIMP U-Pb Zircon method and provided the depositional age of this formation should be 1628 ± 8 Ma or 1599 ± 8 Ma. Based on a review of the age and geographical distribution of *C. circularis*, it is concluded that *C. circularis* cannot be considered as an index fossil for the biostratigraphic subdivision of the Proterozoic. Only, *Tuanshanzia lanceolata* and *Tuanshanzia platyphylla* recorded from the Rampur Formation can be provided some help in its biostratigraphic division.

Helically coiled megafossils

Helically coiled megascopic carbonaceous fossils such as *Grypania spiralis* and *Katniia Singhii* are recorded from the Rohtasgarh Limestone. The coiled megascopic fossil, *Grypania spiralis*, is one of the most important members of the carbonaceous remains reported from Late Palaeoproterozoic to Mesoproterozoic successions of America, China and India.

Coiled fossils were first described by Walcott more than a century ago and subsequently reported by different workers. In India, *Grypania* is known only from the Vindhyan basin. In 1919, a solitary fossil spiral impression on a single slab from Saraidanr near Rohtas was reported by Beer from the Rohtas Limestone exposed in Bihar. After Walcott's record, it was only the second report of coiled fossils from any other part of the world. Later, from the central part of the Vindhyan basin in Madhya Pradesh (MP), well-preserved, rich assemblages of helically coiled fossils were recorded and Tandon and Kumar (1978) originally designated these fossils as *Katnia singhii* and described them as the fossil remnants of an annelid. Detailed account was presented by Kumar (1995). All these helically coiled fossil assemblages were invariably recorded from the Rohtas Formation of the Semri Group of the Vindhyan Supergroup. After nearly 90 years, Sharma and Shukla (2009a, b) recorded another specimen of the fossil *Grypania,* from the same area where from Beer (1919) reported a similar fossil. Earlier, taxonomic investigation of *Grypania* fossils has concentrated mainly on morphologic details observable by reflected light microscopy. Through these observations Palaeoproterozoic *Grypania* (~1.9 Ga) has been interpreted as algae (Han and Runnegar, 1992) and as composites of prokaryotic filaments (Samuelsson and Butterfield, 2001). Investigations of Mesoproterozoic *Grypania* (~1.4-1.6 Ga) have led to interpretations as trace fossils, (Walcott, 1899), algae (Du et al., 1986; Walter et al., 1976; Walter et al., 1990), composites of prokaryotic filaments (Vidal, 1989), a transitional form from microscopic to megascopic life (Srivastava and Bali, 2006), and as cyanobacteria (Sharma and Shukla, 2009a, b).

Age implication of *Grypania*

Earlier, *Grypania spiralis* has been identified from Palaeoproterozoic and Mesoproterozoic rocks from the United States, China, and India. Although *Grypania* is restricted to a single locality in the Palaeoproterozoic (Negaunee Iron Formation, Marquette Range Supergroup, USA; Han and Runnegar, 1992), it has a much more geographically widespread occurrence in the Mesoproterozoic. Mesoproterozoic *Grypania* occurs in three localities, including the Greyson Shale Belt Supergroup, USA (Walcott, 1899; Horodyski, 1993), the Gaoyuzhuang Formation, Changcheng System, China (Du et al., 1986; Walter et al., 1990), and the Rohtas Formation Semri Group, Vindhyan Basin, India (Kumar, 1995; Sharma and Shukla, 2009a, b). The maximum age of the Greyson Shale is constrained by the plutonic basement rocks in southwestern Montana 1880-1860 Ma (Mueller et al., 2002) and mafic intrusions which intrude Lower Belt strata and are dated at 1468 ± 2 Ma, 1469 ± 2.5 Ma, and 1457 ± 2 (Anderson and Davis, 1995; Sears et al., 1998). Younger mafic rocks within the Middle Belt Carbonate constrain the minimum age of the Greyson Shale at 1454 ± 9 (Sears et al., 1998). Together, these dates suggest *Grypania* encompassing Belt Supergroup to be early Mesoproterozoic in age.

It is suggested that the age of the Gaoyuzhuang Formation is 1625 ± 6Ma (Lu and Li, 1991). Additionally Pb-Pb dating of carbonate in the overlying Yangzhuang Formation provides an age of 1496 ± 82 Ma (Jahn and Cuvellier, 1994). Jahn and Cuvellier (1994) suggested that the Gaoyuzhuang Formation was deposited in the early Mesoproterozoic, between ~1600-1500 Ma. An early Mesoproterozoic age for *Grypania*-bearing strata is also consistent with stromatolite assemblages (Walter et al. 1990), C-isotopes stratigraphy of the overlying Jixian System (which suggests an age >1.3 Ga; Xiao et al., 2000) and preserved microfossil assemblages (Chen, 1985; Walter et al., 1990; Zhang, 2006). *Grypania* assemblages were found in the upper part of the Rohtasgarh Limestone, exposed around Katni District (Kumar, 1995; Sharma and Shukla, 2009a, b). Sharma and Shukla (2009a, b) suggested that the Rohtas Formation in the eastern sector of the Vindhyan basin is a shallowing upward, increasingly calcareous shale–carbonate interbedded succession developed on an epeiric shelf, whereas the lower part of the Rohtas Formation represents an oxygen-depleted outer shelf.

U/Pb SHRIMP age dating of the zircon crystals recovered from the ash beds at the top of the Rampur Shale has yielded an age of 1599 ± 8 Ma or 1628 ± 8 Ma (Rasmussen et al., 2006). The Rohtasgarh Limestone of Semri Group exposed in Tikaria locality, Katni District of M.P. was dated as 1599 ± 48 Ma by Sarangi et al. (2004) through Pb-Pb, isochron method. Recently, Bengtson et al. (2009) dated the Tirohan Limestone (= Rohtasgarh Limestone) of the Semri Group exposed near Jankikund, Chitrakut area, M.P. as 1650 ± 89 Ma by Pb-Pb, isochron method. On the basis of above observations, and the correlation of strata of the Rohtas Formation exposed in different sectors of the Vindhyan Basin, are considered, *Grypania spirallis* bearing beds of the Rohtasgarh Limestone have deposited in Mesoproterozoic age (~1600 Ma).

6.3 Microfossils

Salkhan Limestone facies is exposed over a vast tract in the Son Valley in Central India. The first record of the microfossils from the black bedded chert of the Salkhan Limestone exposed in the Salkhan area of Uttar Pradesh was reported by Kumar (1978), which was later described in detail by McMenamin et al. (1983). Kumar and Srivastava (1995) reported a new assemblage of microfossils from Salkhan Limestone exposed in Newari area (Newari is 30 km west of Salkhan) also in Uttar Pradesh. Recently, Sharma (2006) has described the microfossils reported from stromatolitic chert, from the Salkhan Limestone from Bihar state. It reported both coccoid and filamentous forms. Also, the black-bedded chert and other varieties of chert have yielded the well-preserved microbial assemblages from the Salkhan Formation exposed in Bihar State (Sharma, 2006). In present study, microfossils are recorded from the black bedded chert of the Salkhan Limestone, exposed near Maihar area, M.P. These microfossils are recorded and put in 12 Genera of 18 specimens. These are morphologically simple, filamentous and coccoidal fossils, very well preserved in black bedded chert. Varied well-preserved, randomly distributed sphaeroidal and filamentous microfossils are preserved in a matrix of primary chalcedonic chert with kerogen (microfossils are separately described in chapter 4).

The microbiota of the Salkhan Limestone is quite similar to that described from other Mesoproterozoic localities of the world, viz., Balbirini Dolomite,

McArthur Group of Australia (~1500Ma) by Oehler (1977); the Dismal Lakes Group (1250 Ma) of Arctic Canada by Horodyski and Donaldson (1980); Cliffs Formation and Victor Bay Formation of Uluksan Group (~1250Ma), Bylot Supergroup, Canada by Hofmann and Jackson (1991).

Palaeoenvironmental interpretation of microfossils

The microfossils of Salkhan Limestone are three dimensionally preserved in a structurally little altered condition as organic residue within the bedded chert. In different types of cherts, solitary, planktic and randomly occurring microfossils are considered mat dwellers as inferred by the orientation and density of microfossils; those occurring in groups in organized fashion and benthic in nature are termed as mat builders. It is likely that the microbial assemblage of the Salkhan Limestone grew in shallow, relatively saline water (Sharma, 2006). This is suggested by analogy with modern entophysalidacean mats that occur in arid, shallow-water environments often in intertidal to supratidal flats (Logan et al., 1974; Horodyski and Vonder Haar 1975; Golubic 1973, 1976; Kinsman and Park 1976; Playford and Cockbain 1976; Walter 1976; Horodyski et al. 1977; Margulis et al., 1980; Sergeev et al., 1995, 1997; Sharma, 2006c). An analogous condition of colouring in modern *Entophysalis* is apparently a response to highlight intensity and is characteristic of cyanobacteria, which live in areas of high salt content (Fritsch 1945; Drouet 1968; Fogg et al., 1973; Walsby 1974). The noticeable difference in the composition and level of preservation of the biota in bedded chert suggests that each one of them represents a different zone of carbonate tidal flat of intertidal to supratidal region. Similar assemblages are reported in various Proterozoic basins from different parts of the world (Knoll et al., 1989, 1991; Sergeev et al., 1997). It is presumed that the biological communities preserved in different cherts may be analogous to those described from several extant environmental niches such as in the Hamelin Pool, Shark Bay (Logan et al., 1974), Coastal Lagoon, Laguan Mormona, Baja California, Mexico (Horodyski et al., 1977; Margulis et al., 1980; Green et al., 1987). The well-preserved mats of *Eoentophysalis* recorded in the bedded cherts seem to be analogous with the ‘pustular mats’ built by *Entophysalis major* in the middle to upper intertidal zones of the Hamelin Pool. The compressed mats of *Eoentophysalis* in the same chert forming organic laminae may be

compared with the ‘film mats’ desiccated ecomorphs of pustular mat (Logan et al., 1974). He reported in his discussion about film mat, from the upper intertidal to supratidal zones of the Hamelin Pool. The most common mat forming benthic form is *Eoentophysalis* and to some extent *Eosynechococcus* a coccoid cyanobacterium and *Siphonophycus* is the individual filamentous form. The *Eoentophysalis* dominated assemblage of the Salkhan Limestone provides probably the best biological point of comparison between the modern and ancient environment in totality Salkhan Limestone. Which are strikingly similar to the modern environment for the consideration of microbial morphologies, taxonomy, morphology of the associated stromatolites and position within the carbonate intertidal zone (Sharma, 2006).

The microbial assemblage consisting of *Sphaerophycus* resembles the population reported from ‘gelatinous mat’ in the lower to middle intertidal zones of Hamelin Pool. Coccoid unicells of the genus *Myxococcoides* are common in the assemblage and probably represent fossilized chroococacean cyanobacteria. Different species of *Myxococcoides* either occur along with the *Eoentophysalis* mats or are dispersed freely in organic mass/kerogen. This spatial relationship suggests that *Myxococcoides* were mat dwellers rather than actually having contributed to the building of the organic laminae. The other important constituents of bedded chert include *Eosynechococcus, E. moorei*, and some species of *Sphaerophycus.* Of these the species of *Eosynechococcus* and along with a large amount of mucilaginous sheath suggest their growth in arid and harsh conditions. Their isolated and patchy distribution above the *Eoentophysalis* mat/layers in darker laminae, sometimes even transgressing into the lighter laminae, suggests that these forms were free floating. Also, the same results have been encountered by Sharma, (2006) from the Salkhan Chert. In all cases, *Entophysalis* populations dominate in warm, shallow, hypersaline bodies of quiet water in the intertidal zone or in coastal ponds that have only limited access to the open ocean (Knoll and Golubic, 1979). On the other hand, modern *Entophysalis* species live along the air/water interface (Golubic, 1983); thus, their extension to subtidal waters could be explained by seasonal changes in sea level (Kinsmann and Park, 1976). Also present day coastlines, *Entophysalis* species form mats where rates of sediment influx are relatively low, but are excluded from peritidal environments characterized by high rates of sediment influx. *Eoentophysalis* may

have colonized such habitats throughout the Proterozoic age. However, these populations were preserved as fossils only when penecontemporaneous precipitation enhanced their otherwise low preservation potential. This explanation is consistent with the observation by Kah and Knoll (1996) that the stratigraphic and environmental distribution of *Eoentophysalis*-dominated mat assemblages coincides with that of seafloor carbonate precipitates. *Siphonophycus* filaments can be preserved in lower intertidal to shallow subtidal environments. *E. oparinii* are locally abundant as mat dwellers, thin-sheathed *Siphonophycus* mats in lower intertidal environments host diverse mat dwellers, including species of *Coniunctiophycus, Gloeodiniopsis, Myxococcoides* and *Eosynechococcus* (Green et al., 1989; Knoll et al., 1991).

Age significance of microfossils and achritarchs

The Salkhan microbiotas exhibit considerable taxonomic diversity. Entophysalid-dominated mat association is a characteristic of a number of Proterozoic Formations, the oldest being the 2000 Ma old cherts of the Kasegalik and McLeary Formations, Belcher Islands Canada (Hofmann 1976) and the youngest being the 570 Ma old Yudoma Suit, Eastern Siberia (Lo, 1980). The other younger and older *Eoentophysalis* dominated assemblages have been reported from 1500 Ma Amelia Dolomite, Australia (Muir, 1976), the slightly younger Balbirini Dolomite, also of Australia (Oehler, 1977), 1400–1500 Ma old Gaoyuzhuang Formation, China (Zhang, 1981), the 1200 Ma old Dismal Lakes Group, Canada (Horodyski and Donaldson, 1980) and the 750–790 Ma old Bitter Springs Formation, Australia (Knoll and Golubic, 1979), 1500 Ma old Debengda Formation, Siberia (Sergeev et al., 1994), 1500–1250 Ma old Billyakh Group (Sergeev et al., 1995). Most of the taxa of the Salkhan Limestone assemblage are long ranging prokaryotes; the overall character of the assemblage is characteristically Mesoproterozoic with its major features comparable to the coeval floras of Australia, Canada, China and Russia. The biostratigraphic significance of Salkhan microbiota is very limited. Most of the taxa including the rarely occurring nonseptate filaments and small coccoids are long ranging in age. They are abundant in the Proterozoic and even continue into the Phanerozoic. In comparison with known palaeobiological records, silicified biota of Salkhan

assemblage can be dated ~1600 Ma, consistent with the age for the Semri Group based on radiometric and stromatolite biostratigraphic data. The Salkhan microfossils of Maihar area add significant data on the habit of cyanobacteria during Precambrian Eon. The colonial habit of cyanobacteria as represented by two genera of colonial coccoid microfossils in the Salkhan assemblage is a testimony of regular colonial morphologies and polarity of organisation as exhibited by *Eoentophysalis,* and *Myxococcoides.* The *Eoentophysalis*, is an endopsore forming cyanobacteria, is wide spread in the Salkhan assemblage. The occurrences of this cyanobacterium from 2000 Ma to 540 Ma old sediments from Belcher Island Formation to Narssarssuk Formation provides circumstantial evidences for the earlier development of the process of endospore formation. The other apparent examples of Precambrian sporangia or sexual mode of reproduction include 700 Ma old endosporangia of *Sphaerocongregus variabilis* Moorman (Moorman 1974; Cloud et al., 1975). Recently well-preserved akinetes of heterocystous cyanobacteria have been recorded from several Mesoproterozoic localities (Golubic et al., 1995; Sergeev et al., 1995; Knoll and Sergeev 1995; Srivastava 2005, Sharma 2006). Sharma and Sergeev (2004), summarized the reported chert bearing microfossils from different formation of the world including India, and their age, provided in the Table 6.1.

Table 6.1- Comparative study of silicified microfossils from the various Mesoproterozoic formations.

Unit name	Age	Location	Dominant and Conspicuous microfossil taxa
Jaradag Fawn Limestone Formation	Early Mesoproterozoic	Bihar, India	*Eoentophysalis belcherensis*, *Archaeoellipsoides* spp., Short trichomes
Kotuikan and Yusmastakh Formations	Early Mesoproterozoic	Anabar Uplift, Siberia	*Eoentophysalis belcherensis*, *Archaeoellipsoides* spp., *Myxococcoides grandis*
Kyutingda Formation	Early Mesoproterozoic	Olenek Uplift, Siberia	*Eoentophysalis belcherensis*, *E. dismallakesensis*, Short trichomes
Debengda Formation *typicum*	Mesoproterozoic	Olenek Uplift, Siberia	*Eoentophysalis belcherensis*, *E. dismallakesensis*, *Siphonophycus*
Svetlyi Formation	Mesoproterozoic	Uchur-Maya Region, Siberia	*Siphonophycus robustum*, *S. typicum*, *S. solidum*
Dismal Lakes Group	Mesoproterozoic	Northern Canada	*Eoentophysalis dismallakesensis*, *Archaeoellipsoides* spp.
Gaoyuzhuang and Wumishan Formations	Mesoproterozoic	Northern China	*Eoentophysalis belcherensis*, *Coccostratum dispergens*, *Archaeoellipsoides* spp., *Siphonophycus* spp.
Sukhaya Tunguska Formation	Late Mesoproterozoic	Turukhansk Uplift, Siberia	*Eoentophysalis dismallakesensis*, *Polybessurus bipartitus*, *Siphonophycus* spp
Society Cliff Formation	Late Mesoproterozoic	Northern Canada	*Eoentophysalis belcherensis*, *Polybessurus bipartitus*, *Siphonophycus* spp.,

The present records of microfossils from the bedded chert of the Salkhan Limestone, on comparison also supports the age of Salkhan Formation ~ Mesoproterozoic (~1600 Ma).

The Rohtasgarh Limestone has well preserved achritachs in black shales. These achritachs are separated from black shales through acid maceration technique and described in Chapter 4. The recorded acritarchs are widely distributed and long ranging of Palaeoproterozoic to Neoproterozic age. Only *Dictyosphaera delicata* can be used in this study consisted of a single acritarch species. It is comprisable with recorded from the Ruyang Group in Shanxi Province (Kaufman and Xiao, 2003). The Ruyang are consistent with marine sediments deposited between about 1,250 and 1,900 Myr ago, the equivalence of microfossil assemblages in the Ruyang and the radiometrically constrained Roper Group of Australia suggests an age closer to 1,400 Ma. Also, acritarchs of this antiquity are interpreted as resting cysts of photosynthetic eukaryotes, although

their organic encasements were synthesized during active growth and should thus reflect primary photosynthetic processes.

6.4 Microbial Mat

The mat structures from the Rohtasgarh Limestone have associated features of mat growth; mat destruction and wrinkles structures. Most of the reported MISS are from siliciclastics, especially sandstones, whereas, those in the carbonates have rarely been dealt with, except for microbial buildups and biolaminite. In this thesis I have reported MISS from the Rohtasgarh Limestone similar in morphology with those found in the Mesoproterozoic carbonates of the North China platform and described them following the genetic classification scheme proposed by Schieber (2004, 2007) and Eriksson et al. (2007). Many workers are described mat structures from siliciclastic rocks in Mesoproterozoic age of the world. These structures are identified as different morphological features but rarely identified mat structures in carbonates. Banerjee and Jeevankumar (2005) described the microbial mat structures in siliciclastic rocks from the Chorhat Sandstone. Shi et al. (2008) has been described the microbial mats in the Mesoproterozoic carbonates of the Upper Gaoyuzhuang Formation and the Lower Wumishan Formation of the north China platform. Christophe Dupraz et al. (2009) suggested warm climate and anoxic/euxinic conditions in the Mesoproterozoic Ocean facilitated, high microbial productivity and organic burial in sediments. Microbial mats are typically formed by filamentous, entangled organisms that produce a macroscopic "mat like" structure. Stal (2000) recorded the reasons why cyanobacteria were the most successful organisms in mat building and resulted in documentation of a combination of characteristics unique to this group. Cyanobacteria are the only known oxygenic phototropic prokaryotes. They display a great resilience to changes and fluctuations of environmental conditions. Microbial mats are organic-rich layers formed by microbes and their extracellular polymeric substances (EPS) through binding, trapping, and baffling sediments at the water/sediment interface (Noffke et al., 2003, 2001; Gerdes et al., 2000). In normal marine environments, the majority of mats will be consumed by metazoan grazing or destroyed by aerobic degradation prior to burial, and can rarely be preserved as direct sedimentary records. In contrast, in anoxic/dysoxic, sulfidic,

and super-salinity waters, where metazoans are largely depressed, microbial mats are often well developed and have a great potential to be preserved. In the Precambrian, microbial mats must be widespread on the seafloor, but their identification is still a challenge. MISS, as a significant supplement to microbial buildups, has been taken as one of the important biosignatures for ancient microbial communities and mats (Noffke, 2009; Noffke et al., 2003, 2001; Gerdes et al., 2000) and has drawn extensive attention in recent years.

6.5 Fan- fabric structures

Calcium carbonate seafloor fans are unusual features of the geologic record, and the conditions that fostered their formation are still poorly understood. Carbonate fans are common features of Archaean and Palaeoproterozoic carbonate platforms (Kah and Knoll, 1996; Sumner and Grotzinger, 1996b; Sumner and Grotzinger, 2000), occur mostly in intertidal settings of the Mesoproterozoic (Bartley et al. 2000), and are conspicuous features of carbonates that cap low latitude glacial deposits of the Neoproterozoic (Kennedy, 1996; Hoffman et al. 1998; Hoffman and Schrag, 2002). Seafloor-precipitated carbonate fans are preserved in the Kajrahat Limestone of Lower Vindhyan exposed around Maihar area, M.P. central India. In case of geological distribution of fan- fabric structures, Bartley et al. (2000) suggested that in Mesoproterozoic carbonate successions, fans are restricted to intertidal environments. These structures are common features in early Precambrian succession and Meso-Neoproterozoic sedimentary record in worldwide. Recently, Ray et al. (2002) proposed the age of the Kajrahat Limestone 1631 Ma by U-Pb Zircon method. Therefore, the recorded fan-fabric structures are supporting the age of deposition of Kajrahat Limestone in Late Palaeoproterozoic and Early Mesoproterozoic. On the basis of globally exposed fan-fabric structures, it is suggested that the environment of deposition is Intertidal-Subtidal. The present recorded fan- fabric suggested the Kajrahat Limestone is deposited in this type of environment. Bose et al. (2001) also suggested, depositional environment of this formation was the Subtidal to Peritidal.

6.6 Organic Geochemistry

The Proterozoic basins from different parts of the world viz. Lena Tunguska, Siberia; Amadeus and McArthur basins, Australia; Sichuan and Tarim basins, China and Huqf basin, Oman etc. have reported commercial production of oil and gas (Mayerhoff, 1980; Granthan et al., 1988; Jackson et al., 1988; Crick et al., 1988; Korch et al., 1991). In India there are six Proterozoic basins viz., Vindhyan, Cuddapah, Chhattisgarh, Bastar, Bhima and Kaladgi (Kalpana et al., 2010) known as Purana Basins, and are poorly explored for hydrocarbon prospects. The reason is that Proterozoic shales and carbonate rocks are generally organic-poor and are considered insignificant hydrocarbon source rocks (Hunt 1995). However, organic-rich shales are reported from many Proterozoic basins and some of them probably sourced ancient petroleum accumulations (Condie et al., 2001). Organic-rich (TOC up to 7%), mature kerogens of the Mesoproterozoic Velkerri Formation and Barney Creek Formation of Australia are comparable to potential Phanerozoic hydrocarbon source rocks and have been targeted for oil exploration (Crick 1992; Warren et al., 1998). Shukla and Chakraborty (1994) suggested that organic richness which has bearing upon the Proterozoic Vindhyan Basin shales, in terms of being prospective hydrocarbon source rocks has yet to be evaluated. Maturation data are essential in order to ascertain the hydrocarbon generating potential of the shales and thermal history of the Vindhyan basin. In the present study, the black shale and carbonates were analyzed to ascertain the Organic Matter (O.M.) of the black shales of the Proterozoic Vindhyan basin noted in the Maihar area, and provide bulk characteristics of their organic matter content. Quantity, quality and maturation of organic matter of individual black shale formations are estimated and assessed separately. Here the samples of carbonate and black shale are analyzed for source rock evaluation. Total organic carbon contents vary with stratigraphic units in Lower Vindhyan. The carbonates of the Rohtashgarh Limestone have 0.1 to 0.3% TOC. In the Kajrahat Limestone the TOC is in the range of 0.1% to as high as 4.1%. The black shales of the Rohtasgarh Limestone are showing high content of TOC, i.e. 0.1 to 3 %. These results indicate, a yield of extractable TOC is low in carbonates and average in black shales for source rock and generation of Hydrocarbon. Through Rock Eval Pyrolysis, the hydrocarbon generative potential of the organic matter, S1, S2, S3, Tmax, derivatives hydrogen

index (HI), oxygen index (OI) and total organic carbon (TOC) are determined. These samples show very erratic Tmax and Production Index (PI) values, and low pyrolysis values varies such as S1 (0.0 and 0.14, average 0.08 mg HC/g rock), S2 (0-0.25 mg HC/g rock), S3 (0.05-0.5 mg HC/g rock), TOC (0.2-0.6 wt. %), HI ~30 mg HC/g rock, and highly variable OI. PI values are >0.4 and Tmax is ~ 500º C in all samples. Mostly samples are showing depletion in S1 and S2 and high S3 values. It may be due to weathering. The S1 vs. S2 plot showing weak linear correlation which indicates least capacity of the TOC for hydrocarbon generation. The hydrogen index values are low ranging between 0 to 51 mg HC/g TOC. The plots of HI vs. TOC (Jackson et al., 1985) indicate a poor barren source to gas-prone source rock for the black shales unit of Rohtasgarh Limestone. The plot of HI vs. Tmax is showing Type I and Type II (gas prone) kerogen field. Tmax values between 490 and 520, indicating over maturation of organic matter. Exceptionally, only one sample lies in oil window zone and three samples lie in immature zone i.e. in diagenesis zone. It may be due to weathering and oxidation of organic matter. S2 vs. TOC diagram is showing Type II organic matter. Also, the oxygen index (OI) vs. hydrogen index (HI) diagram is indicating type II kerogen. Which is supporting, the results obtained by the S2 vs TOC and HI vs. Tmax diagram.

In light gaseous hydrocarbon analysis, the magnitude of each of the seven light hydrocarbon gases of black shales constituents (C1, C2, C3, *i*C4 *n*C4, *i*C5 and *n*C5), measured in ppb. The distribution of C1, C2 and C3 gases in the shales showed high concentration. Stable carbon isotopes yield information on the origin of hydrocarbons from varied locations or sources (Fuex, 1977; Faber and Stahl, 1983; 1984; Schoell, 1983; Stahl, 1977; Stahl et al. 1981; Whiticar, 1996; 1999). Bernard suggested C1/C2+C3 ratios <100 and δ^{13}C1 heavier than -60 ‰ are characteristic of thermogenic hydrocarbons; whereas C1/C2+C3 ratios > 1000 and δ^{13}C1 lighter than -60 ‰ indicate an origin from biogenic sources. In our study the carbon isotopic composition of $\delta^{13}C_1$ ranges are between –37.45‰ and –42.2‰ (PDB) indicating, these gases are of thermogenic origin. A trend of methane to pentane, C1>C2>C3>C4>C5 is also suggesting the thermogenic origin. The 94 percent samples are showing C3/C1×1000 ratio between 2 and 20 which in the dry gas zone. Out of 42 samples 23 samples have the gases composition (C1 to C5), and very high concentration of methane comparatively. Cross-plots between light

gaseous hydrocarbons (C1-C5) are showing linear correlations, and are also suggesting a thermogenic origin for the hydrocarbons. The maximum Wetness (Wh) ratios, values of present study, ranges between 0.5 and 17.5 which indicate gas bearing. These values are very near to dry gas with high density. All the samples are showing Wetness (Wh) ratios< Balance (Bh) ratios, which indicates gas phase. Balance (Bh) ratios values are greater than 100 in 13 samples out of 42, which indicate very dry gas and rests samples are in high density gas. The 80 % samples are showing Character (Ch) ratios, values are less than 0.5 which are supporting the Wh and Bh interpretation of gas is correct. Rest values of Character (Ch) ratios, which are greater than 0.5, showing the gas character by the Wh and Bh ratios, in associated with oil ratios, are supporting.

Conclusions

Present records of fossils assemblages, Microbial mat structures, and precipitated fan fabric structures from the constituent formations of the Lower Vindhyan, favour the age of the Lower Vindhyan as Palaeoproterozoic to Mesoproterozoic. This is mainly based on the correlation of palaeobiological remains in the Semri Group and the fossils assemblages of the other part of the world. The geochemical study records to the total organic carbon content, their type, maturation level and light gaseous hydrocarbon content compositions within the black shales unit of Rohtasgarh Limestone. This is also correlated with the other basins of the world of the same age. The present study lead to the following salient conclusions:

- The palaeobiological assemblages from constituent formation in the Lower Vindhyan Basin is represented by diversified remains viz. helically coiled macrofossils, carbonaceous megafossils, microbially induced sedimentary mat structures, acritarchs, microfossils and precipitated carbonate fan fabric structures.
- The Rohtasgarh Limestone has yielded helically coiled megafossils and acritarch. These coiled megascopic remains include smooth, filamentous sheaths possibly of cyanobacterial origin, identified as *G. spiralis*. The other filamentous form with segmentation, also possibly of cyanobacterial origin, is identified as *K. singhii*. This formation has also abundant microbially induced

sedimentary structures in carbonate rocks, preserved on bedding surface. Since, *Grypania spiralis* has been identified from Palaeoproterozoic age only in the United States and mostly recorded from Mesoproterozoic rocks from, China, and India. Also recorded acritarch *Dictyosphaera delicata* suggest the age of the Rohtasgarh Limestone should be very near to ~ 1600 Ma. Therefore, these fossils form suggest the age of Rohtasgarh Limestone is Mesoproterozoic i.e. ≤ 1600 Ma. The microbial mat structures suggest the environment of deposition of this formation is shelf, shallow marine.

- The Rampur Formation has yielded abundant carbonaceous megafossil films. The preserved carbonaceous forms are attributed to *Chuaria circularis, Tuanshanzia platyphylla, Tuanshanzia lanceolata,* and *Tawuia dalensis*. These are preserved as compression and impressions. The present forms of *Tuanshanzia platyphylla* and *Tuanshanzia lanceolata* suggest the age of deposition of the Rampur Shale is ~1600-1400 Ma old.
- The Salkhan Limestone has yielded abundant preservation of microfossils in bedded chert. The microfossils are recorded as coccoids and filamentous forms. Their preservation is recorded as single cell, diad, triad, tetrad, also clustures in and colonical form. They can be considered prokaryotic benthic and planktic forms (cyanobacteria). The most abundant form in this formation is mat forming benthic form of *Eoentophysalis* and to some extent *Eosynechococcus* a coccoid cyanobacteria and *Siphonophycus* as the individual filamentous form. In comparison with known palaeobiological records, silicified biota of the Salkhan assemblage can be dated ~1600 Ma, consistent with the age of the Semri Group based on previous records of radiometric and stromatolite biostratigraphic data by Sharma (2006). The microfossils assemblages of the Salkhan Limestone suggest its depositional environment was intertidal to superatidal.
- The Kajrahat Limestone has well precipitated carbonate fan fabric structures. These are measured up to 10 cm long radiating crystals. Globally recorded carbonate fan- fabrics are suggestive of it as a common feature of Archaean and Palaeoproterozoic carbonate platforms which occur mostly in intertidal settings. The present records of fan- fabric structures suggest the age of the Kajrahat Limestone is Palaeoproterozoic-Mesoproterozoic and deposited in intertidal to subtidal environment.

- The total organic carbon content in the Kajrahat Limestone is high, up to 4%, in comparision to the Rohtasgarh Limestone that is less than 0.3% maximum.
- The black shales unit of the Rohtasgarh Limestone has higher TOC is comparision to carbonate rocks. The hydrogen index values are generally low ranging, 0 to 51 mg HC/g TOC. The plots of HI vs. TOC indicate a poor barren source to gas-prone source rock for the black shales unit of Rohtasgarh Limestone. A Tmax higher than 470º C represents the wet-gas zone to over maturation of organic matter. The HI vs. Tmax values are showing Type I and Type II (gas prone) kerogen field. Also, Oxygen Index (OI) vs. Hydrogen Index (HI) diagram indicate type II kerogen.
- The light gaseous hydrocarbon compositions are showing higher concentration of C1, C2 and C3 gases in the shales and present in all the black shales samples.
- The associated light gaseous hydrocarbon in black shale have C1/C2+C3 ratios <100, $\delta^{13}C1$ heavier than -60 ‰, and decreasing trend in concentration from methane to pentane i.e. C1>C2>C3>C4>C5 showing characteristic of thermogenic origin of hydrocarbons.
- 95 % of samples show C3/C1×1000 ratio between 2 and 20, which are lying in the dry gas zone. The combination of Wetness (Wh) ratio, Balance ratio (Bh) and Character ratio (Ch) are suggesting the gaseous hydrocarbons are light density (dry gas) hydrocarbons, associated with oil.

SUMMARY

The present thesis incorporates the results of a detailed study which has been carried out regarding the palaeobiology and organic geochemistry of the Semri Group sediments exposed around Maihar area, M.P. Carbonaceous megafossils, microfossils, microbially induced sedimentary structures (MISS) and carbonate precipitated fan fabric structures are used as tools to find out the age of the Semri Group. The Organic Matter maturation and hydrocarbon potentiality of the constituent formation of the Semri Group is identified. The important conclusions of the present work is summarized chapter wise.

Chapter 1

The first chapter deals with objectives and the reasons for taking up research into the Lower Vindhyan. This chapter provides a brief introduction about the problem, study area and the significance of the work in global perspective. With the present state of knowledge, the Vindhyan Basin occurs as a sickle-shaped basin on the Bundelkhand-Aravalli Province, which stabilized prior to 2.5 Ga. The Vindhyan Supegroup overlies a variety of Precambrian basement rocks including Bundelkhand Granite, Mahakoshal Group, Bijawar Group, Gwalior Group, Banded Gneissic Complex (BGC) and Chhotanagpur Gneissic Complex (CGC). The occurrence of macroscopic carbonaceous compressions in the Palaeo-Mesoproterozic sediments holds important clue for understanding the atmospheric oxygen concentration, evolution of obligatory photosynthetic eukaryotes (such as red and green algae) and ability for nitrogen fixation. The indirect evidence for the presence of eukaryotes in Archaean and Palaeoproterozoic comes from steranes in 2700 Ma shales just south of North Pole in NW Australia and 1700 Ma bitumen of the McArthur Group, Northern Australia. The Vindhyan Supergroup has revealed the presence of carbonaceous megafossils from different horizons. So far the oldest horizon which has yielded the carbonaceous megafossils in sediments of the Semri Group in the Koldaha Shale and exposed in the Central India. The Vindhyan sediments have consistently been searched for evidence of life, since the beginning of twentieth century. The fossil reports of the Vindhyan Supegroup include microfossils, organo-sedimentary structures, carbonaceous fossils,

Ediacaran fossils, trace and body fossils of metazoans. Different types of microfossils were reported from both the argillaceous rocks and carbonates of the Vindhyan Supergroup. In general, the microfossil record suggested Mesoproterozoic age for the Semri Group. Even though lot of discoveris have been made in Vindhyan Basin. However, many controversies are remaining still there regarding age of the basin. The present studies are confined mainly two aspects. One of them is to investigate the Palaeobiology and other is to understand the Organic Geochemistry of the Lower Vindhyan stratigraphic sections, exposed around Maihar area, Satna District, M.P. This area is chosen due to well exposed stratigraphic horizons of the Lower Vindhyan in the Son Valley i.e. Eastern part of the Vindhyan Basin.

The main objectives of present study are-

- Palaeobiological study of the constituent formations of the Semri Group.
- Documentation of biomat features within carbonate rocks of the Semri Group and microbial mat influence on carbonate depositional system.
- Total Organic Carbon analysis and Hydrocarbon maturation level of black shale in the Semri Group.
- Organic geochemistry and geochemical analysis of carbonate and black shales to search for hydrocarbon potential of the basin.

Chapter 2

This chapter deals with the general geology, lithostratigraphy and basin evolution history of the Vindhyan Supergroup. Last 150 years of studies the brought forward the various geological aspects and plethora of information on Vindhyan Basin. The Vindhyan Basin is one of the largest Proterozoic intracratonic sedimentary basin of the world and comprises a ~5000 m thick sequence of mostly sandstone, shale and limestone sequences. Also, some part has, dolomite with minor conglomerate and volcaniclastic rocks without any metamorphic and tectonic effects in central Indian states of Bihar, Uttar Pradesh, and Madhya Pradesh i.e. the Son Valley and in Rajasthan known as Chambal Valley. These sedimentary successions are known as the Vindhyan Supergroup

(VSG). Sedimentary units in the Vindhyan Basin are primarily represented by shallow marine facies along with distal shelf to deep-water sediments in the Lower Vindhyan. The Semri Group in the Son Valley overlies the Bijawar Series of sediments and lavas, which contains volcanic rocks, that correlates to the 1815 Ma of Gwalior Volcanic. The entire Vindhyan Supergroup is divisible in the following stratigraphic orders:

Upper Vindhyan

Bhander Group

Rewa Group

Kaimur Group

Lower Vindhyan

Semri Group

Each group is again subdivided into several formations.

The Semri Group is constituted by carbonates and siliciclastics in equal proportions and also contains significant volcaniclastics. The sedimentation has taken place in tectonically active setting in contrary to tectonic quiescence during the upper Vindhyan in the Son Valley area. The Semri Group comprises of five formations, viz. Deoland, Kajrahat, Porcellanite, Kheinjua and Rohtas Formations in the order of superposition. The Deoland Formation is dominated by conglomerate and sandstone. The immediately overlying the Kajrahat Formation is divisible in two parts, viz. the Arangi Shale at the base and the Kajrahat Limestone at the top. The Kajrahat Limestone consists of limestone and dolomite with widespread development of stromatolites. The sedimentary successions are consisting of silicified shales, pyroclastics and volcanic tuffs, named as Porcellanite Formation, overlies the Kajrahat Formation. The Kheinjua Formation consists of shale, sandstone and local dolomite. The Kheinjua Formation has two tiers- the lower shaly member is known as the Koldaha Shale and the upper sandy Member is known as Chorhat Sandstone. A thin and patchy dolomite occasionally interrupts the predominantly siliciclastic Kheinjua Formation and is described as Fawn Dolostone or Salkhan Limestone. Rohtas Formation is two-tiered, Rampur Shale occurs at the base and Rohtas Limestone occurs at the top.

There have been several attempts to interpret depositional setting and paleogeography of the Vindhyan basin. Most of the workers interpreted the Vindhyan successions as nearshore marine deposition with intermittent subaerial exposure.

The lithostratigraphy of the Vindhyan Basin differs considerably in the different sections due to facies variation. In present study it has been tried to research of palaeobiological remains in associated geological formation of the Semeri Group. The present study area included mainly the Kajrahat Limestone, the Fawn Limestone, the Rampur Shale and the Rohtasgarh Limestone sections, exposed near Maihar area, Satna and Katni Disctrics, M. P.

Chapter 3

This chapter of the thesis deals with the materials and methods used in the present study. Here two methods are used, one is the field work and other is the laboratory work. The field work is necessary part of geological observation which has been done in following sections-

- Chhoti Mahanadi –Kuteshwar Mine section (Kajrahat Limestone)
- Amarpatan-Bansagar Lake section (Rohtasgarh Limestone and Salkhan Limestone)
- Badanpur, Bistara and Amehta Mines section (Rohtasgarh Limestone)

During field work, samples were collected for palaeobiological and geochemical studies. For these studies, the following methods are adopted:

- Thin sections preparation and their microscopic study.
- Acid maceration technique.
- Staining.
- Measurement of Total Organic Carbon (TOC) of black shale and carbonate rock for identification of Hydrocarbon prospect.
- Rock- Eval Pyrolysis.
- Gas Chromatograph-Combustion-Isotope Ratio Mass Spectrometer (GC-C-IRMS) to find out the composition, quantity and their origin of occurrence of light gaseous hydrocarbon (C1-C5) of black shale (source rosck).

Details of the analytical procedure and principle and instrumentation of the instruments is also described.

Chapter 4

This chapter deals with the discussion on the previous palaeobiological studies and also taxonomically described forms of the carbonaceous mega fossils remains, microfossils and microbial mats. One of the main objectives of the present work is discussed in this chapter. The results recorded in the present thesis are outcome of the systematic palaeobiological investigation of the sediments of the Semri Group. A full taxonomic treatment with special reference to documented diversity of unicellular and multicellular forms has been attempted. The carbonaceous megafossils are recorded as film. Following forms have been identified:

Helically coiled fossils

Under this *Grypania spiralis* and *Katnia singhii* are reported from the Rohtashgarh Limestone.

Mega fossils

Chuaria circularis,Tauwia dalensis, Tuanshanzia platyphylla, Tuanshanzia lanceolata are carbonaceous megafossils reported from the Rampur Shale.

Microfossils

Coniunctiophycus conglobatam, Glenobotrydion majorinum, Eoentophysalis dismallakesensis, Eoentophysalis, belcherensis, Eoaphanocepra oparinii, Huroniospora microreticulata, Scissilisphaera regularis, Siphonophycus robustum, Siphonophycus solidum, Sphaerophycus kestron, Sphacerophycus parrum, Sphacerophycus medium, Myxococcoides inornata, Myxococcoides sp., *Palaeopleurocepra fusiforum.*

These microfossils are reported from the bedded chert of the Salkhan Limestone. The preserved microfossils are measured in their size, shape and

preservation nature. The cells of microfossils are identified in solitary single cells and also in multiple cells as clusters form. Mainly coccoids, filamentous and sheath forms are noted. The cells are sphereoidal, ellipsoidal and in polygonal shapes are observed. In addition to well documented microbially induced sedimentary structures (MISS) and mat related structures are recorded from the Rohtasgarh Limestone during fieldwork. The wrinkle structures and other structures are identified, related to mat growth and mat destruction. The carbonate precipitated fan-fabric structures are identified from the Kajrahat Limestone, which are extensively preserved on surface outcrop. The problems of contaminations in Precambrian palaeobiology are also discussed in acid maceration technique. The formation of pseudomicrofossils during acid maceration of rock samples are described.

Chapter 5

This chapter concern with the geochemical analysis results of black shale and carbonate rocks of different formation of Semri Group. The geochemical analysis was carried out in the Department of Petroleum Geochemistry of National Geophysical Research Laboratory (NGRI), Hyderabad. Also, the analyzed data are interpreted regarding to their significance in Hydrocarbon prospect and organic matter maturation. The total organic carbon (TOC) content of carbonate of the Kajrahat Limestone represents more amount in comparision to the Rohtasgarh Limestone. The associated black shale unit of the Rohtasgarh Limestone is indicating good amount of TOC (>1 %). The black shales which have TOC >0.5% analyzed for Rock-Eval Pyrolysis. The Rock-Eval Pyrolysis results interpreted the type of organic matter, type of kerogen, potentiality of source rock, and level of organic matter maturation. The Hydrogen Index, TOC, and Tmax results are suggesting the wet gas-dry gas bearing and over maturation of organic matter. Total 42 samples of black shales are also analyzed in GC-C-IRMS in terms of light gaseous hydrocarbon compositional variation and their origin. There are very good amount of light gaseous hydrocarbon composition (C1-C5) recorded in black shales. The cross plots of (C1-C5), are showing increasing trends of (C1-C5) and Bernard plot is suggesting the thermogenic origin of these gases. There is also calculated Wetness ratio (Wh), Balance ratio (Bh) and Character ratio (Ch)

through the composition of the light gaseous hydrocarbon (C1-C5) composition. These ratios help interpret the type of hydrocarbon in terms of density.

Chapter 6

This chapter deals with exhaustive discussion on the palaeobiological evidences hydrocarbon potentiality in Lower Vindhyan sediments. It has been also discussed about the hydrocarbon prospect through geochemical analysis of black shales and carbonates. The conclusions of the studies are that the Lower Vindhyan sediments range from Late Palaeoprotezoic to Early Mesoproterozoic. There is scope of extensive studies of MISS and hydrocarbon potential of the rocks.

Therefore the main contribution of the thesis is the documentation of palaeobiological remains and some aspects of hydrocarbon potentiality of the Semri Group. On the basis of these remains and their study it is concluded that the stratigraphic units of the Semri Group exposed in Maihar area belongs to the Palaeoproterozoic to Mesoproterozoic age i.e (~1600-1100 Ma).

References

Ahmad, F., 1955. Glaciation in the Vindhyan System. Curr. Sci., 24: 231.

Ahmad, F., 1958. Paleogeography of Central India in the Vindhyan Period. Rec. Geol. Surv. India, 87: 513-548.

Ahmad, F., 1971. Geology of the Vindhyan System in the eastern part of the Son Valley in Mirzapur District, U.P. Rec. Geol. Surv. India, 96: 1-41.

Ahmad, F., 1981. Some problems in the paleogeography of the Vindhyan times in central India. Misc. Publ. Geol. Surv. India, 56: 69-74.

Aizenshtat, Z.G., Lipiner, G., Cohen, Y., 1984. Biogeochemistry of Carbon and Sulfur in the microbial mats of the Solar Lake (Sinai). In: Cohen, Y., Castenholz, R.W., Halvorson, A.R., (Eds.) "Microbial mats: Stromatolites", Liss, New York.

Akhtar, K., 1996. Facies, sedimentation processes and environments in the Proterozoic Vindhyan basin. In: Bhattacharyya, A. (Ed.), Recent Advances in Vindhyan Geology. Mem. Geol. Soc. India, 36: 127-136.

Amard, B., 1992. Ultrastructure of *Chuaria* (Walcott) Vidal and Ford (Acritarcha) from the Late Proterozoic Pendjari Formation, Benin and Burkina-Faso, West Africa. Precab. Res., 57:121-133.

Amard, B., 1997. *Chuaria pendjariensis* n. sp. Acritarche du bassin des Volta, Benin et Burkina-Faso, Africa de l'Ouest: un taxon nouveau du Cambrien inf˝erieur; Comptes Rendus de l Academie des Sciences Paris (s´erie Iia), 324: 477-483.

Anbarasu, K., 2001. Facies variation and depositional environment of Mesoproterozoic Vindhyan sediments of Chitrakut area, Central India. Jour. Geol. Soc. India, 58: 341-350.

Anderson, H.E., Davis, D.W., 1995. U-Pb geochronology of the Moyie sills, Purcell Supergroup, Southeastern British Columbia: Implications for Mesoproterozoic geological history of the Purcell (Belt) basin. Canadian Jour. Earth Sci., 32: 1180-1193.

Arouri, K.R., Greenwood, P.F., Walter, M.R., 1999. A possible chlorophycean affinity of some Neoproterozoic acritarchs. Org. Geochem., 30: 1323-1337.

Auden, J.B., 1933. Vindhyan sedimentation in Son Valley, Mirzapur district. Mem. Geol. Surv. India, 62: 141–250.

Awasthi, N., 1964. Studies on Vindhyan sedimentology. (Unpublished Ph.D.Thesis) University of Lucknow, Lucknow.

Azmi, R.J., 1998. Discovery of Lower Cambrian small shelly fossils and brachiopods from the Lower Vindhyan of Son Valley, central India. Jour. Geol. Soc. India, 52: 381–389.

Azmi, R.J., Joshi, D., Tiwari, B.N., Joshi, M.N., Srivastava, S.S., 2008. A synoptic view on the current discordant geo-and biochronological ages of the Vindhyan Supergroup. Himl. Geol., 29(2): 177-191.

Babu, R, Singh, V.K., 2011. Record of aquatic carbonaceous metaphytic remains from the Proterozoic Singhora Group of Chhattisgarh Supergroup, India and their significance. Jour. Evol. Bio. Res., 3(5): 47-66.

Bandyopadhyay, B., Roy, A., Huin, A.K., 1995. Structure and tectonics of a part of central Indian Shield. In: Sinha Roy, S., Gupta, K.R. (Eds.), Continental Crust of the Northwestern and Central India. Mem. Geol. Soc. India, 3: 433-467.

Banerjee, D.M., Frank, W., 1999. Workshop on Vindhyan Stratigraphy and Palaeobiology, Lucknow, 44: 151-153.

Banerjee, I., 1964. On some broader aspects of Vindhyan sedimentation. Report 22nd Intl. Geol. Cong., Delhi, 15: 189-204.

Banerjee, I., 1974. Barrier coastline sedimentation model and the Vindhyan example. Quart. Jour. Geol. Min. Met. Soc. India, 46: 101-127.

Banerjee, S., 1997. Facets of Mesoproterozoic Semri sedimentation, Son valley, M.P. Unpublished Ph.D. Thesis, Jadavpur University, Kolkata, India.

Banerjee, S., 2000. Climate versus tectonic control on the storm cyclicity in Mesoproterozoic Koldaha Shale, Vindhyan Supergroup, Central India. Gond. Res., 3: 521-528.

Banerjee, S., Bhattacharyya, S.K., Sarkar, S., 2007. Carbon and oxygen isotopic variations in peritidal stromatolite cycles, Paleoproterozoic Kajrahat Limestone, Vindhyan basin of central India. Jour. of Asian Earth Sci., 29: 823-831.

Banerjee, S., Jeevankumar, S., 2003. Facies motif and paleogeography of Kheinjua Formation, Vindhyan Supergroup, eastern Son valley. Gond. Geol. Mag. Spec. pub., 7: 363-370.

Banerjee, S., Jeevankumar, S., 2005. Microbially originated wrinkle structures on sandstone and their stratigraphic context: Paleoproterozoic Koldaha Shale, central India. Sed. Geol., 176: 211-224.

Banerjee, S., Jeevankumar, S., 2007. Facies and depositional sequence of the Mesoproterozoic Rohtas Limestone; eastern Son valley, Vindhyan Basin. Jour. Asian Earth Sci., 30(1): 82-92.

Banerjee, S., Sarkar, S., Bhattacharyya, S.K., 2005. Facies, dissolution seams and stable isotope characteristics of the Rohtas Limestone (Vindhyan Supergroup) in the Son valley area, central India. Jour. Earth Sys. Sci., 114(1): 87-96.

Banerjee, S., Schieber, J., 2003. Paleoproterozoic condensed zone sediments in the Kajarahat Formation, Vindhyan Supergroup, central India. Abstracts with Programs Geol. Soc. America, 35(6): 173.
Barghoorn, E.S., Tyler, S.A., 1965. Microorganism from the Gunflint chert. Science, 147: 563–577.
Bartley, J.K., Knoll, A.H., Grotzinger, J.P., Sergeev, V.N., 2000. Lithification and fabric genesis in precipitated stromatolites and associated peritidal carbonates, Mesoproterozoic Billyakh Group, Siberia. SEPM Spec. Publ., 67: 59–73.
Basu A, Patranabis-Deb S, Schieber J, Dhang, P.C., (2008). Stratigraphic position of the ~1000 ma Sukhda Tuff (Chhattisgarh Supergroup, India) and the 500 Ma question. Precamb. Res., 167: 383-388.
Basumallick, S., Sarkar, B.C., Banerjee, S., 1996. Tidal cyclicity in Lower Bhander Sandstone, Maihar, Madhya Pradesh. Jour. Geol. Soc. India, 47: 189-194.
Beer, E.J., 1919. Note on spiral impression on Lower Vindhyan limestone. Rec. Geol. Surv. India, 50: 109.
Belt, J.Q., Rice, G.K., 2002. Application of statistical quality control measures for near-surface geochemical petroleum exploration. Original Research Article Comp. Geosci., 28(2): 243-260.
Bengtson, S., Belivanova, V., Rasmussen, B., Whitehouse, M., 2009. The controversial 'Cabrian' fossils of the Vindhyan are real but more than a billion years old. Proc. Nat. Acad. Sci., 106: 7729-7734.
Bernard, B. B., 1978. Light hydrocarbons in sediments. Unpublished Ph D dissertation, Texas A&M University, USA, 144p.
Berner, U., Faber, E., 1988. Maturity related mixing model for methane, ethane and propane, based on carbon isotopes. In: Advances in Organic Geochemistry 1987, 67-72.
Bhattacharyya, A., 1996. Proterozoic Kaimur Group, Son Valley: fluvio-marine or fluvio-lacustrine? Jour. Geol. Soc. India, 47: 313-324.
Bhattacharyya, A., Morad, S., 1993. Proterozoic braided ephemeral fluvial deposits: an example from the Dhandraul Sandstone Formation of the Kaimur Group, Son valley, Central India. Sed. Geol., 84: 101-114.
Bose, P.K., Banerjee, S, Sarkar, S., 1997a. Slope-controlled seismic deformation and tectonic framework of deposition of Koldaha Shale, India. Tectonophysics, 269: 151-169.
Bose, P.K., Chakraborty, P.P., 1994. Marine to fluvial transition: Proterozoic Upper Rewa Sandstone, Maihar, India. Sed. Geol., 89: 285-302.
Bose, P.K., Chakraborty, S., Sarkar, S., 1999. Recognition of ancient eolian longitudinal dune: a case study in Upper Bhander Sandstone, Son valley India. Jour. Sed. Res., 69: 86-95.
Bose, P.K., Chaudhuri, A.K., 1990. Tide versus storm in epeiric coastal deposition: two Proterozoic sequences, India. Geol. Jour., 25(2): 81-101.
Bose, P.K., Chaudhuri, A.K., Seth, A., 1988. Facies, flow and bedform patterns across a storm-dominated inner continental shelf: Proterozoic Kaimur Formation, Rajasthan, India. Sed. Geol., 59: 275-293.
Bose, P.K., Sarkar, S., Chakraborty, S., Banerjee, S., 2001. Overview of the Meso- to Neoproterozoic evolution of the Vindhyan basin, Central India. Sed. Geol., 141-142: 395-419.
Brotzen, F., 1941. Några bidrag till Visingso formationens stratigrafi och tektonik. G.F.F., 63: 245–261.
Buick R, Rasmussen B., Krapez , B., 1998. Archean oil: evidence for extensive hydrocarbon generation and migration 2.5–3.5 Ga. AAPG Bull., 82: 50–69.
Burgan A.M., Ali C. A., 2009. Characterization of the Black Shales of the Temburong Formation in West Sabah, East Malaysia. Euro. Jour. Sci. Res., 79-98.
Burzin, M.B., 1990. Modifikatsiya metodiki vydeleniya iz porod organikostennykh mikrofossiliy primentel'no k resheniyu paleobiologicheskikh zadach (A modification of the method of extracting organic-walled microfossils from rocks as applied to the solution of paleobiological problems): Paleontologichekii Zhurnal, 4: 109–113 (in Russian). Published English translation in Paleontological Journal, Scripta Technica Inc., 1990, 104–107).
Butterfield, N. J. 2000. *Bangiomorpha pubescens* n. gen., n. sp.: implications for the evolution of sex, multicellularity and the Mesoproterozoic/Neoproterozoic radiation of eukaryotes. Paleobiology, 26: 386-404.
Butterfield, N.J., Knoll, A.H., Swett, K., 1994. Paleobiology of the Neoproterozoic Svanbergfjelet Formation, Spitsbergen. Fossils and Strata, 34: 1-84.
Cao, F., 1992. Algal microfossils of the Middle Proterozoic Gaoyuzhuang Formation in Pinggu County, Beijing. Geol. Rev., 38: 382–387 (in Chinese).
Casshyap, B., Bhardwaj B.D., Raza, M., Singh, A., Khan, A., 2001. Barrier inlet and associated facies of shore zone: An example from Khardeola Formation of Lower Vindhyan Sequence in Chittaurgarh, Rajasthan. Jour. Geol. Soc. India, 58: 97-111.
Chafetz, H.S., Buczynski, C., 1992. Bacterially induced lithification of microbial mats. Palaios, 7: 277–293.
Chakraborty, C., 1993. Morphology, internal structure and mechanics of small longitudinal (seif) dunes in an aeolian horizon of Proterozoic Dhandraul Quartzite, India. Sedimentology, 40: 79-85.
Chakraborty, C., 1995. Gutter casts from the Proterozoic Bijaigarh Shale Formation, India: their implications for storm-induced circulation in shelf settings. Geol. Jour., 30: 69-78.
Chakraborty, C., 1996. Sedimentary records of erg development over a braid plain; Proterozoic Dhandraul Sandstone, Vindhyan Supergroup, Son Valley. Mem. Geol. Soc. India, 36: 77-99.
Chakraborty, C., 2001. Lagoon-tidal flat sedimentation in an epeiric sea: Proterozoic Bhander Group, Son Valley, India. Geol. Jour., 36: 125-141.
Chakraborty, C., Bhattacharyya, A., 1996. Fan-delta sedimentation in a foreland moat: Deoland formation, Vindhyan Supergroup, Son valley. Mem. Geol. Soc. India, 36: 27-48.

Chakraborty, C., Bose, P.K., 1990. Internal structures of sand waves in a tide-storm interactive system: Proterozoic Lower Quartzite Formation, India. Sed. Geol., 67: 133-142.
Chakraborty, C., Bose, P.K., 1992. Rhythmic shelf storm beds: Proterozoic Kaimur Formation, India. Sed. Geol., 77: 259-268.
Chakraborty, P.P., 2004. Facies architecture and sequence development in a Neoproterozoic carbonate ramp: Lakheri Limestone Member, Vindhyan Supergroup, Central India. Precamb. Res., 132: 29-53.
Chakraborty, P.P., Banerjee, S., Das, N.G., Sarkar, S., Bose, P.K., 1996. Volcaniclastic and their sedimentological bearing in Proterozoic Kaimur and Rewa Groups in Central India. In: Bhattacharyya, A. (Ed.) Recent Advances in Vindhyan Geology. Mem. Geol. Soc. India 36, 59-76.
Chakraborty, P.P., Sarkar, S., Bose, P.K., 1998. A viewpoint on intracratonic chenier evolution: Clue from a reappraisal of the Proterozoic Ganurgarh Shale, Central India. In: Paliwal, B.S. (Ed.), the Indian Precambrian. Scientific Publishers, Jodhpur, 61-72.
Chanda, S.K., Bhattacharyya, A., 1982. Vindhyan sedimentation and palaeogeography: post-Auden developments. In: Valdiya, K.S., Bhatia, S.B., Gaur, V.K., (Eds.), Geology of Vindhyanchal. Hind. Publ. Corp., (India), Delhi, 88-101.
Chapman, F., 1935. Primitive fossils, possibly atrematous and neotrematous Brachiopoda, from the Vindhyans of India. Rec. Geol. Surv. India, 69: 109-120.
Chatterjee, B.K., Sen, P.K., 1988. Spectral analysis of a Precambrian limestone-shale sequence, lower Vindhyan, India. Precamb. Res., 39: 139-149.
Chaudhari, M.S., 1953. Late Precambrian glaciation and its relationship with the Bijawar Series in the type area of Bundelkhand. Proc. 40th India Sci. Cong., 3: 20.
Chaudhuri, A., Bose, P.K., 1982. Exotic features in Rewa tidal sequence around Bhainsrorgarh, Rajasthan, a possible eolian signature. Indian Jour. Earth Sci., 9: 108-115.
Chaudhuri, A.K., Chanda, S. 1991. The Proterozoic basins of Pranhita-Godavari Valley: An overview S.K. Tandon, C.C. Pant, S.M. Casshyap (Eds.) Sedimentary basins of India, 13–29.
Choubey, V.D., 1971. Narmada–Son Lineament, India. Nature 232: 38–40.
Chung, H.M., Gormly, J.R., Squires, R.M., 1988. Origin of gaseous hydrocarbons in subsurface environments: theoretical considerations of carbon isotope distribution. Chem. Geol., 71, 97–103.
Cloud, P., Moorman, M., Pierce, D., 1975 Sporulation and ultrastructure in a Late Proterozoic Cyanophyte: Some implication for taxonomy and plant phylogeny. Quart. Rev. Biol., 50: 131–150.
Cloud, P., Morrison, K., 1979. On microbial contaminants, micropseudofossils and the oldest records of life. Precamb. Res., 9: 81-89.
Condie, K. C., 1989. Plate tectonics and crustal evolution. Book (third edition) Pergamon Press, Oxford, 476p.
Condie, K.C., Marais, D.J.D., Abbott, D., 2001. Precambrian superplumes and supercontinents: a record in black shales, carbon isotopes and paleoclimates? Precamb. Res., 106: 239–260.
Coulson, A.L., 1927. The geology of the Bundi State. Rec. Geol. Surv. India, 60: 164– 204.
Crawford, A.R., 1978. Narmada-Son lineament of India traced into Madagascar. Jour. Geol. Soc. India, 19: 143-153.
Crawford, A.R., Compston, W., 1970. The age of Vindhyan system of peninsular India. Jour. Geol. Soc. Londan., 125: 351-371.
Crick, I.H., 1992. Petrological and maturation characteristics of organic matter from the Middle Proterozoic McArthur Basin, Australia. Australian Jour. Earth Sci., 39: 501–519.
Crick, I.H., Boreham, C.J., Cook, A.C., Powell, T.G., 1988. Petroleum geology and geochemistry of middle Proterozoic McArthur basin, northern Australia II: Assessment of source rock potential. AAPG Bull., 72: 1495–1514.
Das Gupta, S., 1997. Lithostratigraphy and geochemical studies of limestone formations of Rohtas Subgroup in Bhiar; Indian Min., 51: 77–90.
Das, L.K., Misra, D.C., Ghosh, D., Banerjee, B., 1990. Geomorphotectonics of the basement in a part of Upper Son Valley of the Vindhyan basin. Jour. Geol. Soc. India, 35: 445-458.
Deb, M., Thorpe, R., Krstic, D., 2002. Hindoli Group of rocks in the Eastern Fringe of the Aravalli-Delhi Orogenic belt-Archean secondary greenstone belt or Proterozoic supracrustals? Gond. Res., 5: 879–883.
Deb, S.P., Bickford, M.E., Hill, B., Chaudhuri, A.K., Basu, A., 2007. SHRIMP ages of Zircon in the uppermost tuff in Chhattisgarh Basin in central India require 500-Ma adjustment in Indian Proterozoic stratigraphy. Jour. Geol., 115: 407-415.
Demaison, G. F. and Moore, G. T. 1980. Anoxic environments and source bed genesis. AAPG Bull., 64: 1179-1209.
Dickson, J.A.D., 1965. Carbonate identification and genesis as revealed by staining. Jour. Sed. Pet., 36: 491-505.
Djenzhuraev, D.D., 1977. K vaprosu ijutenia 'legki microfossili' dakembria. Izv. ANSSSR, Sed. Geol., 2: 150-154.
Dornbos, S.Q., Noffke, N., Hagadorn, J.W., 2007. Mat-Decay Features. In: Schiber, J. et al., (Eds.), Atlas of Microbial Mat Features Preserved within the Siliciclastic rock record. Elsevier, Amsterdam, 106–110.
Downie, C., Sarjeant, W.A.S., 1963. On the interpretation and status of some hystrichosphere genera. Palaeontology, 6: 83-96.

Drouet, F., 1968. Revision of classification of the Oscillatoriaceae; Acad. Nat. Sci. Philad Monograph, 15: 370 p.
Du, Rulin, Tian Lifu, Li, Hanbang, 1986. Discovery of Megafossils in the Gaoyuzhuang Formation of the Chancheng System, Jixian. Acta Geol. Sin., 60: 115-119.
Du, Rulin, Tian, Lifu, 1985. Algal macrofossils from the Qingbaikou system in the Yanshan range of north China. Precamb. Res., 29: 5–14.
Duan, C.H., 1982. Late Precambrian algal megafossils *Chuaria* and *Tawuia* in some areas of eastern China. Alcheringa, 6(1-2): 57-68.
Dubey, B.S., Chaudhuri, M.S., 1952. Late Precambrian glaciation in Central India. Curr. Sci., 21: 331-332.
Dupraz, C., Reid, R.P., Braissant, O., Decho, A.W., Norman, R.S., Visscher P.T., 2009. Processes of carbonate precipitation in modern microbial mats. Earth-Sci. Rev., 96: 141–162.
Dutkiewicz, A., Volk, H., Ridley, J., George, S., 2002. Biomarkers, brines, and oil in the Mesoproterozoic, Roper Superbasin, Australia. Geology, 31: 981–984
Dutta, S., Steiner, M., Banerjee, S., Erdtmann, B.D., Jeevankumar, S., Mann, U., 2006. *Chuaria circularis* from the early Mesoproterozoic Suket Shale, Vindhyan Supergroup, India: Insights from light and electron microscopy and pyrolysis-gas chromatography. Jour. Earth Syst. Sci., 115: 99-112.
Eisenack, A. 1958. Tasmanites Newton 1875 und Leiosphaeridia n.g.als Gattungen der Hystrichosphaeridea. Palaeontographica, Abt. A, 110(1-3):1-19.
Eriksson, P.G., Mazumder, R., Sarkar, S., Bose, P.K., Alterman, W., Vander-Merwee, R., 1999. The 2.7-2 Ga volcano-sedimentary record of Africa, India and Australia: Evidence for global and local changes in sea-level and continental freeboard. Precamb. Res., 97: 269-302.
Eriksson, P.G., Schieber, J., Bouougri, E., Gerdes, G., Porada, H., Banerjee, S., Bose, P.K., Sarkar, S., 2007. Classification of Structures left by Microbial Mats in their host sediments. In: Schiber, J. et al., (Ed.), Atlas of Microbial Mat Features Preserved within the Siliciclastic rock record. Elsevier, Amsterdam, 39–52.
Eriksson, P.G., Simpson, E.L., Eriksson, K.A., Bumby, A.J., Steyn, G.L., Sarkar, S., 2000. Muddy roll-up structures in siliciclastic interdune beds of the ca. 1.8 Ga Waterberg group, South Africa. Palaios, 15: 177-183.
Espitalie, J., Madec, M., Tissot, B., Mennig, J.J., Leplat, P., 1977. Source rock characterization methods for petroleum exploration, 9th Annual Offshore Technology Conference, Houston, 439-444.
Espitalie, J., Marquis, F., Barsony, I., 1984. Geochemical logging. In: Voorhees, K.J., (Ed.), Analytical Pyrolysis-Techniques and Applications, Butterworth, Guildford, 276-304.
Evitt, W.R., 1963. A discussion and proposals concerning fossil dinoflagellates, hystrichosphaers, and achritarchs, I. Proc. Nat. Acad. Sci., 49: 158-164.
Faber, E., Stahl, W.J., 1983. Analytical procedure and results of an isotope geochemical surface survey in an area of the British North Sea. In: Brooks, J., (Ed.), Petroleum Geochemistry and Exploration of Europe: Jour. Geol. Soc. London, Spec. Publ., 12: 51–63.
Faber, E., Stahl, W.J., 1984. Geochemical surface exploration for hydrocarbon in North Sea. AAPG. Bull., 68: 363–386.
Fogg, G.E., Stewart, W.D.P., Fay, P., Walsby, A.E., 1973. The blue green algae: (London: Academic Press), 459p.
Folk, R.L., Assereto, R., 1976. Comparative fabrics of length-slow and length-fast calcite and calcitized aragonite in a Holocene speleothem, Carlsbad Caverns, New Mexico. Jour. Sediment. Petrol., 46: 486–496.
Ford, T.D., Breed, W.J., 1973. The problematic Precambrian fossil *Chuaria*. Palaeontology, 16: 535-550.
Ford, T.D., Breed, W.J., 1977. *Chuaria circularis* Walcott and other Precambrian fossils from the Grand Canyon. Jour. Pal. Soc. India, 20: 170–177.
Fritch, F.E., 1945. Structure and Reproduction of the Algae; 2 (London: Cambridge University Press), 939p.
Fuex, A. N., 1977. The use of stable carbon isotopes in hydrocarbon exploration. Jour. Geochem. Explor., 7: 155–188.
Fuxing, W., Qiling, L., 1982. Precambrian acritarchs, a cautionary note. Precamb. Res., 16: 291-302.
Garrett, P., 1970. Phanerozoic stromatolites: noncompetitive ecologic restriction by grazing and burrowing animals. Science, 169: 171–173.
Gavin, L., Sacks, Ying Zhang, J. Thomas Brenna, 2007. Fast Gas Chromatography Combustion Isotope Ratio Mass Spectrometry, Anal. Chem., 79(16): 6348–6358.
Geitler, L., 1925. Synoptische Darstellung du cyanophycean in morphologisches and systematiches Hinsicht. Beih. Bot. Zbl., 41: 63.
Geitler, L., 1932. *Cyanophyceae Rabenhorst's Kryptogamen- Flora*; Akademie Verlagsgesellschaft, Leipzig, Band., 14: 1196p.
Gerdes, G., Klenke, T., Noffke, N., 2000. Microbial signatures in peritidal siliciclastic sediments. Sedimentology, 47: 279-308.
Gerdes, S., 2007. Structures Left by Modern Microbial Mats in Their Host Sediments. In: Schiber, J. et al., (Eds.); Atlas of Microbial Mat Features Preserved within the Siliciclastic rock record. Elsevier, Amsterdam, 5–38.
Ghosh, S.K., 1971a. A note on basal Vindhyan conglomerate in Sidhi district, M.P. Quart. Jour. Geol. Min. Met. Soc. India, 43: 95-98.

Ghosh, S.K., 1971b. Petrology of Porcellanite rocks of the Samaria area, Sidhi District, Madhya Pradesh. Quart. Jour. Geol. Min. Met. Soc. India, 43: 153-164.
Ginsburg, R.N., James, N.P., 1976. Submarine botryoidal aragonite in Holocene reef limestones, Belize. Geology, 4: 431–436.
Glaessner, M.F., 1984. The Dawn of Animal Life. A Biohistorical Study. Cambridge University Press, Cambridge, 244p.
Golovenok, V.K., Belova, M.Y., 1984. Stomatolity I microfitolity v stratigraphii dokembria: nadezhdy i realnost (Stromatolites and micrphytolites in Precambrian stratigraphy: hopes and reality); Sovetskaya Geologiya, 8: 43–54.
Golubic, S. & Hofmann, H.J. 1976. Comparison of modern and mid-Precambrian Entophysalidaceae (Cyanophyta) in stromatolitic algal mats: cell division and degradation. J. Paleont., 50: 1074- 1082.
Golubic, S. 1983. Cyanophyta or cyanobacteria - recommendations for taxonomic treatment of greater prokaryotes. Schweiz. Z. Hydrol.,45: 272-273.
Golubic, S., 1973. Stromatolites, fossils and recent: a case history; In: Westbroek, P., de Jong Reidel, E.W., (Ed.). Biomineralization and Biological Metals Accumulation, Dordrecht, 313–326.
Golubic, S., 1976. Organisms that build stromatolites. In: Walter, M.R., (Ed.), Stromatolites: Elsevier Amsterdam, 113–126.
Golubic, S., Sergeev, V.N. Knoll, A.H., 1995. Mesoproterozoic *Archaeoellipsoides*: akinetes of heterocystous cyanobacteria. Lethaia, 28: 285–298.
Granthan, P.J., Lijnbach, G.W.M., Posthuma, J., Hughes C., M.W., Willink, R.J., 1988. Origin of crude oil in Oman. Jour. Petrol. Geol., 11: 61–80.
Green, J. W., Knoll, A. H., Golubic, S. Swett, K. 1987. Paleobiology of Distinctive Benthic Microfossils from the Upper Proterozoic Limestone Dolomite “Series” Central East Greenland. Ammeri. Jour. Bot., 74 (6): 928-940.
Green, J. W., Knoll, A. H., Swett, K.,1989. Microfossils from silicified stromatolitic carbonates of the Upper Proterozoic Limestone-Dolomite 'Series', central East Greenland. Geol. Mag. 126 (5): 567-585.
Greenwood, P.F., Aoruri, K.R., Logan, C.A., Summons, R.E., 2004. Abundance and geochemical significance of C-2n dialkylanes and highly branched C-3n alkanes in diverse Meso-Neoproterozoic sediments. Org. Geochem., 35: 331–346.
Gregory, L.C., Meert, J.G., Pradhan, V., Pandit, M.K., Tamrat, E., Malone, S.J., 2006. A palaeomagnetic and geochronologic study of the Majhgawan Kimberlite, India; implication for the age of upper Vindhyan Supergroup. Precamb. Res., 149(1-2): 65-75.
Gregory, M.R., Johnston, K.A., 1987, A nontoxic substitute for hazardous heavy Liquids – aqueous sodium polytungstate ($3Na_2WO_49WO_4H_2O$) solution (Note): New Zealand Jour. Geol. and Geophy., 30: 317–320.
Grey, K., 1999. A modified palynological preparation technique for the extraction of large Neoproterozoic acanthomorph acritarchs and other acid-insoluble microfossils. Geol. Surv. Western Australia, 23p.
Grotzinger, J.P., Knoll, A.H., 1995. Anomalous carbonate precipitates: is the Precambrian the Key to the Permian? Palaios, 10: 578–596.
Grotzinger, J.P., Read, J.F., 1983. Evidence for primary aragonite precipitation, lower Proterozoic (1.9 Ga) Rocknest Dolomite, Wopmay Orogen, northwest Canada. Geology, 11: 710–713.
Gupta, S., Jain, K.C., Srivastava V.C., Mehrotra R. D., 2003. Depositional environment and tectonism during the sedimentation of the Semri and Kaimur Groups of Rocks, Vindhyan basin. Jour. Pal. Soc. India, 48: 181-190.
Hagadorn, J.W., Bottjer, D.J., 1999. Restriction of a late Neoproterozoic biotope: suspect-microbial structures and trace fossils at the Vendian– Cambrian transition. In: agadorn, J.W., Pflu¨ger, F., Bottjer, D.J. (Eds.), Unexplored Microbial Worlds. Palaios, 14: 93p.
Haines, P.W., 1998. *Chuaria* Walcott, 1899 in the lower Wessel Group, Arafura Basin, northern Australia. Alcheringa, 22: 1-8.
Han, T., Runnegar, B., 1992. Megascopic eukaryotic algae from 2.1 billion year old Negaunee Iron Formation, Michigan. Science, 257: 232-235.
Haworth, J., Sellens, J., Whittaker, A., 1985. Interpretation of hydrocarbon shows using light (C1-C5) hydrocarbon gases from mud-log data: AAPG Bulletin, 69: 1305-1310.
Haworth, J.,. Sellens, M., Whittaker, A., 1985. Interpretation of hydrocarbon shows using light (C1-C5) hydrocarbon gases from mud-log data. AAPG Bull., 69:1305-1310.
Herman, T., 1974. Nakhodi massevikh skoplyennii trikhomov V. Rifeyi ii microphytofossilii Proterozya i Rannoyogo Palaeozoa SSSR: 6–10 (The discovery of massive accumulations of trichomes in Riphean; microphytofossils of Proterozoic and Lower Paleozoic SSSR): 6–10.
Heron, A.M., (1936). Geology of Southeastern Rajputana. Mem. Geol. Sur. India, 68: 120 p.
Heron, A.M., 1922. The Gwalior and the Vindhyan System in southeastern Rajasthan. Mem. Geol. Surv. India, 45: 129–184.
Heron, A.M., 1953. The geology of central Rajputana. Mem. Geol. Surv. India, 79: 389p.
Hoffman, P. F., Kaufman, A. J., Halverson, G. P., Schrag, D. P., 1998. A Neoproterozoic snowball Earth, Sci. 281:1342–1346.
Hoffman, P.F., Kaufman, A.J., Halverson, G.P., 1998. Comings and goings of global glaciations on a Neoproterozoic tropical platform in Namibia. GSA Today, 8(5): 1–9.

Hoffman, P.F., Schrag, D.P., 2002. The snowball Earth hypothesis; testing the limits of global change. Terra Nova, 14(3): 129–155.
Hofmann, H.J, Jinbiao, C., 1981. Carbonaceous megafossils from the Precambrian (1800 Ma) near Jixian Northern China. Canad. Jour. Earth Sci., 18: 443-447.
Hofmann, H.J., 1971. Precambrian fossils, pseudofossils and problematic in Canada. Geol. Surv. Can. Bull., 189: 146p.
Hofmann, H.J., 1976. Precambrian microflora, Belcher Island, Canada: significance and systematics. Jour. Paleontol., 50:1040–1073.
Hofmann, H.J., 1977. The problematic fossil *Chuaria* from the Late Precambrian Uinta Mountain Group, Utah. Precamb. Res., 4: 1-11.
Hofmann, H.J., 1985a. Precambrian Carbonaceous Megafossils. Palaeogeology: Contemporary Research and Applications. In: Toomey, D.F., Nitecki, M.H., (Eds.). Springer-Verlag Berlin Heiddelber, 19-33.
Hofmann, H.J., 1985b. The Mid-Proterozoic Little Dal microbiota, Mackenzie Mountains, North West Canada, Palaeontology, 28: 331-354.
Hofmann, H.J., 1992a. Proterozoic Carbonaceous films. In: Schopf, J.W., Klein, C., (Eds.). The Proterozoic Biosphere, A Multidisciplinary Study, Cambridge University Press, 349-357.
Hofmann, H.J., 1992b. Proterozoic and selected Cambrian megascopic dubiofossils and pseudofossils. In: Schopf, J.W., Klein, C., (Eds.). The Proterozoic Biosphere, A Multidisciplinary Study, Cambridge University Press, 1035-1053.
Hofmann, H.J., 1992c. Summary: Current status of Proterozoic Biostratigraphy. In: Schopf, J.W., Klein, C., (Eds.). The Proterozoic Biosphere, A Multidisciplinary Study, Cambridge University Press, 513-514.
Hofmann, H.J., Aitken, J.D., 1979. Precambrian biota from the Little Dal Group, Mackenzie Mountains, northwestern Canada. Canad. Jour. Earth Sci., 16: 150-166.
Hofmann, H.J., Chen, J., 1981. Carbonaceous megafossils from the Precambrian (1800 Ma) near Jixian, northern China. Canada. Canad. Jour. Earth Sci., 18: 443-447.
Hofmann, H.J., Jackson, C.D., 1987. Proterozoic ministromatolites with radial-fibrous fabric. Sedimentology, 34: 963–971.
Hofmann, H.J., Rainbird, R.H., 1994. Carbonaceous megafossils from the Neoproterozoic Shaler Supergroup of Arctic Canada. Palaeontology, 37: 721-731.
Hofmann, H.J., Schopf, J.W., 1983. Early Proterozoic microfossils. In: Schopf, J.W., (Ed.). "Earth's Earliest Biosphere: It's origin and Evolution" (Princeton, New Jersey: Princeton University Press), 321–360.
Horodyski, R. J., Blesser, B., Vonder Haror, S., 1977. Laminated algae mats from a coastal lagoon Laguna Marmond, Boja California, Mexico.Jour. Sed. Petro. 47: 680-696.
Horodyski, R.J., 1993. Paleontology of Proterozoic shales and mudstones: examples from the Belt Supergroup, Chuar Group and Pahrump Group, western USA. Precamb. Res., 61: 241-278.
Horodyski, R.J., Donaldson, J.A., 1980. Microfossils from the Middle Proterozoic Dismal Lakes Group, Arctic Canada. Precamb. Res., 11: 125–159.
Horodyski, R.J., Donaldson, J.A., 1983. Distribution and significance of microfossils in cherts of the Middle Proterozoic Dismal Lakes Group, District of Mackenzie, Northwest Territories; Canad. Jour. Earth Sci., 17: 1166–1173.
Horodyski, R.J., Von der Haar S., 1975. Recent calcareous stromatolites from Laguna Mormona, Mexico. Jour. Sediment. Petrol., 45: 894–906.
Hu, Y., Fu, J., 1982. Micropalaeoflora from the Gaoshanhe Formation of Late Precambrian of Luonan, Shaanxi and its stratigraphic significance. Bulletin of the Xi'an Institute of Geology and Mineral Resources, Chin. Acad.Geol. Sci., 4: 102-111.
Huc A.Y., 1990: Understanding organic facies: a key to improved quantitative petroleum evaluation of sedimentary basins, in Deposition of Organic facies. (Ed) Huc A.Y. A.A.P.G. Studies in Geology, 3o: 1-11.
Hunt, J.M., 1995. Petroleum Geochemistry and Geology. (New York: W.H. Freemen and company) 2nd edition, 743p.
Imbus, S.W., Engel, M.H., Elmore, R.D., Zumberge, J.E., 1988. The origin, distribution and hydrocarbon generation potential of organic-rich facies in the Nonesuch Formation, central North American Rift System: A regional study. Org. Geochem., 13: 207–219.
Jackson, I., Sweet, P., Powell, T.G., 1988. Studies on petroleum geology and geochemistry of the middle Proterozoic McArthur Basin, northern Australia petroleum potential. Aust. Petrol. Assoc. Jour., 28: 283–302.
Jackson, K.S., Hawkins, P.J., Bennett, A.J.R., 1985. Regional facies and geochemial evolution of the southern Denison Trough. APEA Journal, 20: 143-158.
Jahn, B., Cuvellier, H., 1994. Pb-Pb and U-Pb geochronology of carbonate rocks: an assessment. Chem. Geol., 115: 125-151.
James, A.T., 1990. Correlation of reservoired gases using the carbon isotopic compositions of wet gas components. AAPG Bull., 74:1441-1458.
James, N.P., Narbonne, G.M., Kyser, T.K., 2001. Late Neoproterozoic cap carbonates; Mackenzie Mountains, northwestern Canada; precipitation and global glacial meltdown. Canadian Jour. Earth Sci., 38(8): 1229–1262.

James, N.P., Wray, J.L., Ginsburg, R.N., 1988. Calcification of encrusting aragonitic algae (Peyssonneliaceae); implications for the origin of late Paleozoic reefs and cements. Jour. Sediment. Petrol., 58(2): 291–303

Javaux, F.J., Knoll, A.H., Walter, M.R., 2001. Recognizing and interpreting the fossils of early eukaryotes. Origin Life Evol. B., 33: 75-94.

Jokhan R., Shukla, S.N., Parmanik, A.G., Varma, B.K., Gyanesh, C., Murty, M.S.N., 1996. Recent investigations in the Vindhyan basin: Implications for the basin tectonics. Mem. Geol. Soc. India, 36: 267–286.

Jones, H.C., 1909. General Report. Rec. Geol. Surv. India, 38(1): 66.

Jones, V.T. and Drozd, R.J. (1983) Predictions of Oil or Gas Potential by Near Surface Geochemistry. AAPG Bull., 67(6):932-952.

Jones, V.T., Drozd, R.J., 1983. Predictions of Oil or Gas Potential by Near Surface Geochemistry. AAPG Bull., 67(6): 932-952.

Kah, L.C., Knoll, A.H., 1996. Microbenthic distribution of Proterozoic tidal flats: environmental and taphonomic considerations. Geology, 24: 79–82

Kaila, K.L., Murthy, P.R.K., Mall, D.M., 1989. The evolution of the Vindhyan basin visà- vis the Narmada-Son lineament, Central India, from deep seismic soundings. Tectonophysics, 162: 277-289.

Kalpana, G., Madhavi, T., Patil, D.J., Dayal, A.M., Raju, S.V., 2010. Light gaseous hydrocarbon anomalies in the near surface soils of Proterozoic Cuddapah Basin: Implications for hydrocarbon prospects. Jour. Petro. Sci. Engg., 73: 161–170.

Karkhanis, S.N., 1977. Artifacts produced by chemical processing of samples for micropalaeontology and organic geochemistry. A note of caution. Precamb. Res. 4, 229-236. Lo S C 1980 Microbial fossils from the Lower Yudoma Suite, Earliest Phanerozoic eastern Siberia; Precamb. Res., 13: 109–166.

Kathal, P.K., Patel, D.R., Alexander, P.O., 2000. An Ediacaran fossil Spriggina (?) from the Semri group and its implication on the age of the Proterozoic Vindhyan Basin, Central India. N. Jb. Geol. Palaont. Mon., 6: 321-332.

Kennedy, M.J., 1996. Stratigraphy, sedimentology, and isotopic geochemistry of Australian Neoproterozoic postglacial cap dolostones; deglaciation, delta (sub 13) C excursions, and carbonate precipitation. Jour. Sediment. Res., 66(6): 1050–1064.

Kinsman, D.J., Park, R.K., 1976. Algal belt and coastal sabkha evolution, Trucial Coast, Persian Gulf, In: Walter, M.R., (Ed.), Stromatolites: Developments in Sedimentology. Elsevier Amsterdam, 20: 421–433.

Klusman, R.W., 1993. Soil Gas and Related Methods for Natural Resource Exploration. John Wiley & Sons, Ltd., Chichester, United. Kingdom, 483.

Knoll, A., Barghoorn, E.S. & Golubic, S. 1975. *Palaeopleurocapsa wopfnerii* gen. et sp. nov., a late-Precambrian blue-green alga and its modern counterpart. Proc. Nat. Acad. Sci. USA 72: 2488-2492.

Knoll, A.H., 1982. Microfossil-based biostratigraphy of the Precambrian Hecla Høek sequence, Nordaustlandet, Svalbard. Geol. Mag., 119: 269-279.

Knoll, A.H., 1982b. Microfossils from the late Precambrian Draken Conglomerate, NY Friesland, Svalbard; Jour. Paleontology., 56: 755–790.

Knoll, A.H., 1992. The early evolution of eukaryotes a geological perspective. Science, 256: 622-627.

Knoll, A.H., Calder, S., 1983. Microbiotas of the Late Precambrian Rysso Formation, Nordaustlandet, Svalbard. Palaeontology, 26(3): 467-496.

Knoll, A.H., Golubic, S., 1979. Anatomy and Taphonomy of a Precambrian algal stromatolites. Precamb. Res., 10: 115– 151.

Knoll, A.H., Grotzinger, J.P., Sergeev, V.N., 1993. Carbonate precipitation in stratiform and domal structures from the Mesoproterozoic Kotuikan Formation, northern Siberia. Geol. Soc. Am. 5(6): 357.

Knoll, A.H., Javaux, E.J., Hewitt, D., Cohen, P., 2006. Eukaryotic organisms in Proterozoic oceans. Phil. Trans. Roy. Soc. B, 361: 1023–1038.

Knoll, A.H., Sergeev, V.N., 1995. Taphonomic and Evolutionary changes across the Mesoproterozoic–Neoproterozoic Transition. N. Jb. Geol. Palaeont. Mh., 195: 289–302.

Knoll, A.H., Sweet, K., Burkhandt, E., 1989 Palaeoenvironment distribution of microfossils and stromatolites in Upper Proterozoic, Backlundtoppen Formation, Spitsbergen. Jour. Palaeont., 62: 129–145.

Knoll, A.H., Swett, K., Mark, J., 1991. Paleobiology of a Neoproterozoic tidal flat/lagoonal complex: the Draken Conglomerate Formation, Spitsbergen. Jour. Palaeont., 65: 531–570.

Korsch, R.J., Mai, H., Sun, Z., Gorter, J.D., 1991. The Sichuan Basin, southwest China – a Late Proterozoic (Sinian) petroleum province. Precamb. Res., 54: 45–63.

Kreuzer, H., Harre, W., Kursteu, M., Schnitzer, W.A., Murty, K.S., Srivastava, N.K.,1977. K-Ar dates of two glauconites from the Chandarpur Series Chhatisgarh/India). Geol. Jahrb. B, 28: 23-26.

Krishnamurthy, R.V., Bhattacharyya, S.K., Mathur, S.M., 1986. Carbon isotope ratio of the coaly matter from the basal part of the Proterozoic Vindhyan Supergroup. Jour. Geol. Soc. India, 27: 119-120.

Krishnan, M.S., 1968. Geology of India and Burma. Higginbothems (P) Ltd. Madras, 211p.

Kumar, A., Gopalan, K., Rajagopalan, G., 2001. Age of the Lower Vindhyan sediments, Central India. Curr. Sci., 81: 806-898.

Kumar, B., Das Sharma, S., Sreenivas, B., Dayal, A.M., Rao, M.N., Dubey, N., Chawla, B.R., 2002. Carbon, oxygen and strontium isotope geochemistry of Precambrian carbonate rocks of the Vindhyan Basin, central India. Precam. Res., 113: 43-63.

Kumar, S., 1982. Vindhyan stromatolites and their stratigraphic testimony. In: Valdiya, K.S., Bhatia, S.B., Gaur, V.K. (Eds.), Geology of Vindhyanchal. Hind. Publ. Corp., New Delhi, 102-112.
Kumar, S., 1995. Megafossils from the Mesoproterozoic Rohtas Formation (the Vindhyan Supergroup), Katni area, central India. Precamb. Res., 72: 171-184.
Kumar, S., 1999a. Discovery of siliceous sponge spicules from the Neoproterozoic Bhander Limestone, Maihar area, Madhya Pradesh. Jour. Pal. Soc. India, 44: 141- 148.
Kumar, S., 2001. Mesoproterozoic megafossil *Chuaria-Tawuia* association may represent parts of a multicellular plant, Vindhyan Supergroup, Central India. Precamb. Res., 106: 187-211.
Kumar, S., Pandey, S. K., 2008. Discovery of organic walled microbiota from the black- bedded chert, Balwan Limestone, the Bhander Group, Lakheri area, Rajasthan. Curr. Sci., 94(6): 797-800.
Kumar, S., Pandey, S. K., 2008. Discovery of organic walled microbiota from the black- bedded chert, Balwan Limestone, the Bhander Group, Lakheri area, Rajasthan. Curr. Sci., 94(6): 797-800.
Kumar, S., Schidlowski, M., Joachmaski, M.M., 2005. Carbon isotope stratigraphy of the Palaeo-Neoproterozoic Vindhyan Supergroup, Central India: Implications for basin evolutions and intrabasinal correlation. Jour. Pal. Soc. India, 50 (1): 65-81.
Kumar, S., Schidlowski, M., Joachmaski, M.M., 2005. Carbon isotope stratigraphy of the Palaeo-Neoproterozoic Vindhyan Supergroup, Central India: Implications for basin evolutions and intrabasinal correlation. Jour. Pal. Soc. India, 50 (1): 65-81.
Kumar, S., Singh, A.K., 1978. Palaeoenvironment analysis of the Vindhyan sequence, Chitrakut area districts Banda (U.P.) and Satna, (M.P.). Bull. Ind. Geol. Assoc., 11(1): 56-62.
Kumar, S., Srivastava, P., 1992a. Discovery of microfossils from the nonstromatolitic middle Proterozoic Vindhyan Chert, Chitrakut area, U.P. Jour. Geol. Soc. India, 38: 511–515.
Kumar, S., Srivastava, P., 1992b. Middle to Late Proterozoic microbiota from the Deoban Limestone, Garwal Himalaya, India. Precamb. Res., 56: 291–318.
Kumar, S., Srivastava, P., 1995. Microfossils from the Kheinjua Formation, Mesoprotesozone semiri Group, Newari area, central India. Precamb. Res., 74: 91-117.
Kumar, S., Srivastava, P., 1997. A note on the carbonaceous megafossils from the Neoproterozoic Bhander Group, Maihar area, Madhya Pradesh. Jour. Pal. Soc. India, 42: 141-146.
Kumar, S., Srivastava, P., 2003. Carbonaceous megafossils from the Neoproterozoic Bhander Group, Central India. Jour. Pal. Soc. India, 48: 139-154.
Lamb, D.M., Awramik, S.M., Zhu, S., 2007. Palaeoproterozoic compression like structures from the Changzhouggou Formation, China: Eukaryotes or clasts?. Precamb. Res., 154: 236-247.
Laxmanan, S., 1968. On the nature of basal conglomerate of the Semri Series on the Son valley. Proc. Natl. Inst. Sci. India A, 34: 50-55.
Lo, S.C., 1980. Microbial fossils from the lower Yudoma suite, earliest Phanerozoic, Eastern Siberia. Precamb. Res., 13: 109–166.
Logan, B.W., Hoffman, P., Gebelin, C.D., 1974. Algal mats, cryptalgal fabrics and structures, Hamelin Pool, Western Australia. Am. Soc. Pteroleum Geologists Mem., 22: 140–194.
Lu, S., Li, H., 1991. A precise U-Pb single zircon age determination for the volcanics of Dahongyu Formation, Chenchang System in Jixian. Bull. Chinese Acad. Sci., 22: 137-146.
Maithy, P.K., 2003. Pre-phanerozoic evidences of life from Central India: Implication to Biostratigraphy and Evolution. Gond. Geol. Mag., 7: 401-412.
Maithy, P.K., Babu, R., 1988. The mid- Proterozoic Vindhyan macrobiota from Chopan, south east Uttar Pradesh. Jour. Geol. Soc. India, 31: 584-590.
Maithy, P.K., Babu, R., 1996. Carbonaceous macrofossils and organic-walled microfossils from the Hulkal Formation, Bhima Group, Karnataka with remark on age. Palaeobotanist, 45: 1-6.
Maithy, P.K., Babu, R., 2004. Some new informations on the carbonaceous macrofossils *Chuaria*, *Tawuia* and related remains from the Indian Mesoproterozoic sequences. In: Bahadur, B. (Ed.), Gleaning in Botanical Research, Current Scenario. Kiran Nangia, Dattsons, J. Nehru, Marg, Nagpur, 175-187.
Maithy, P.K., Pflug, H.D., 1978. Proof for the synsedimentary biota in Precambrian shales. Palaeobotanist, 28-29: 1-7.
Maithy, P.K., Shukla, M., 1977. Microbiota from the Suket Shale, Rampura, Vindhyan System, Madhya Pradesh. Palaeobotanist, 23: 176–188.
Maithy, P.K., Shukla, M., 1984. Biological remains from the Suket Shale Formation, Vindhyan Supergroup. Geophytology, 14: 212-215.
Mallet, F.R., 1869. On the Vindhyan Series in the northeastern and central provinces. Mem. Geol. Surv. India, 7(1): 1 – 129.
Malone, S.J., Meert, J.G., Banerjee, D.M., Pandit, M.K., Tamrat, E., Kamenov, G.D., Pradhan, V.R., Sohl, L.E., 2008. Paleomagnetism and detrital Zircon geochronology of the Upper Vindhyan sequence, Son Valley and Rajasthan, India: A ca. 1000Ma Closure age for the Purana Basins? Precamb. Res., 164: 137 – 159.
Mani, D., 2008. Surface geochemical indicator and their application in hydrocarbon prospecting study for Saurashtra Basin, Gujarat, India (Unpublished Ph.D. thesis, Osmania University, Hyderabad).
Mani, Patil, D J., Kalpana, M. S., Dayal, A. M., 2011. Evaluation of Hydrocarbon Prospects using Surface Geochemical data with Constraints from Geological and Geophysical observations: Saurashtra Basin, India. Jour. Petrol. Geol., 35(1): 67-83.

Manoharachary, C., Shukla, M., Sharma, M., 1990. Problem of fungal contamination in Precambrian palaeobiology. A cautionary note-1. Palaeobotanist, 37(3): 292-298.
Margulis, L., Barghoorn, E.S., Ashendorf, D., Banerjee, S., Chase, D., Francis, S., Giovannoni, S., Stolz, J., 1980. The microbial community in the layered sediments at Laguna Fiueroa, Baja California, Mexico: does it have Precambrian analogues? Precamb. Res., 11: 93–123.
Mars, 2010. Spare Parts / Pieces Detachees Rock-Eval 6. Ed : 1, VINCI Technologies.1-16.
Mathur, S.M., 1954. Late Precambrian glaciation in Central India-rejoinder. Curr. Sci., 23: 7-8.
Mathur, S.M., 1960. A note on the Bijawar Series in the eastern part of the type area. Rec. Geol. Surv. India, 86: 539-544.
Mathur, S.M., 1964. Coaly matter in the Vindhyan system. Indian Miner., 18(2): 158-165.
Mathur, S.M., 1965. *Indophyton* – a new stromatolite form genus. Curr. Sci. 34 (3), 81 – 85.
Mathur, S.M., 1981. Basal Vindhyan diamictite in the Son Valley, Central India. In: Hambrey, M.J., Harland, W.B. (Eds.). Earth's pre-Pleistocene Glacial Records, Cambridge University Press, Cambridge, 424-427.
Mathur, S.M., 1983. A new collection of fossils from the Precambrian Vindhyan Supergroup of Central India. Curr. Sci. 52, 363-365.
Mathur, S.M., 1989. Sedimentary environmental analysis of the Precambrian basins in peninsular India. In: Proc. Fifth India Assoc. Sed., 8: 103-120.
Mayerhoff, A.A., 1980. Geology and petroleum fields in Proterozoic and Lower Cambrian Strata, Lena-Tunguska petroleum province, eastern Siberia. In: Halbouty, M.T. (Ed.). Giant oil and gas fields of the decade: 1968–1978, AAPG Memoir, 30: 225–252.
Mazumder, R., Bose, P.K., Sarkar, S., 2000. A commentary on the tectonic-sedimentary record of the Pre-2.0 Ga evolution of Indian craton vis-à-vis Pre-Gondwana Afro- Indian Supercontinent. Jour. African Earth Sci., 30: 201-217.
McMenamin, D.S., Kumar, S., Awramic, S.M., 1983. Microbial fossils from the Kheinjua Formation, Middle Proterozoic Semri Group (Lower Vindhyan), Son Valley area, Central India. Precamb. Res., 21: 247–271.
Meddlicott, H.B., 1860. Vindhyan rocks and associates in Bundelkhand. Mem. Geol. Surv. India, 2 (1): 96 – 276.
Mehrotra, M.N., Banerjee, R., Dalela, R.K., Lal, P., 1985. The Son Porcellanite Formation: an example of volcaniclastic sedimentation in India. Indian Jour. of Earth Sci., 12: 21-33.
Mendelson, C.V., Schopf, J.W., 1982. Proterozoic microfossils from the Sukhaya Tungusks, Shorikha and Yudoma Formations of Siberian Platform, USSR. Jour. Palaeontol., 56: 42–83.
Mendelson, C.V., Schopf, J.W., 1992. Proterozoic and selected Early Cambrian microfossils and microfossil-like objects. In: Schopf, J.W., Klein, C. (Eds.). Evolution of the Proterozoic biosphere — a multidisciplinary study: New York, Cambridge University Press, 865–951.
Mikhaylova, N.S., German, T.N. [Hermann, T.N.], 1989. Mikrofossilii dokembriya SSSR. [Precambrian microfossils of the USSR.] Nauka, Leningrad, 190 p.
Mishra, P.S., Chibber, I.B., Shenoi, R.S., 1990. Some salient aspects of Precambrian Geology, Bansagar Project in Son- Tons Sub- Basin, Madhya Pradesh. Geol. Surv. Ind. Sp. Publ., 28: 135-155.
Misra, R.C., 1969. The Vindhyan System. Presidential Address. Proc. Indian Sci. Cong. Assoc., 56th Session, Bombay, 2: 111-142.
Misra, R.C., Bhatnagar, G.S., 1950. On carbonaceous discs and algal dust from the Vindhyan Precambrian. Curr. Sci., 19(3): 88-89.
Moczydłowska, M., Vidal, G., Rudavskaya, V.A., 1993. Neoproterozoic (Vendian) phytoplankton from the Siberian Plateform, Yakutia. Palaeontology, 36: 495-521.
Mondal, M.E.A., Goswami, J.N., Deomurari, M.P., Sharma, K.K., 2002. Ion microprobe $^{207}Pb/^{206}Pb$ ages of zircons from the Bundelkhand massif, Northern India: Implications for crustal evolution of the Bundelkhand-Aravalli protocontinent. Precamb. Res., 117: 85 – 100.
Moorman, M., 1974 Microbiota of the Late Proterozoic Hector Formation, Southwestern Alberta, Canada. Jour. Palaeontol., 48: 524–539.
Mueller, P.A., Heatherington, A.L, Kelly, D.M., Wooden, J.L., Mogk, D.W., 2002. Paleoproterozoic crust within the Great Falls tectonic zone: Implications for assembly of southern Laurentia. Geology, 30: 127-130.
Muir, M.D., 1976. Proterozoic microfossils from the Amelia Dolomite, McArthur Basin, Northern Territory. Alcheringa, 1: 143–158.
Murray, G.E., Kaczor, M.J., McArthur, R.E., 1980. Indigenous Precambrian petroleum revisited. AAPG Bull., 64(10): 1681–1700.
Nageli, C., 1849. Gattungen einzelliger Algen, physiologisch und under systematisch bearbeitet; F. Schulthes, Z¨urich, 139 p.
Naqvi, S.M., Rogers, J.J.W., 1987. Precambrian Geology of India, Clarendron press, Oxford., 223p.
Narbonne, G.M., 2005. The Ediacara biota Neoproterozoic origin of animals and their ecosystems. Annu. Rev. Earth Planet. Sci., 33: 421- 442.
Newell, K.D., Burruss, R.C., Palacas, J.G., 1993. Thermal maturation and organic richness of potential petroleum source rocks in Proterozoic Rice Formation, north American midcontinent rift system, northeastern Kansas. Bull. Am. Assoc. Petrol. Geol., 77: 1922–1941.

Noffke, N., Gerdes, G., Klenke, T., 2003. Benthic cyanobacteria and their influence on the sedimentary dynamics of peritidal depositional systems (siliciclastic, evaporitic salty, and evaporitic carbonic). Earth-Sci. Rev., 62: 163–176.

Noffke, N., Gerdes, G., Klenke, T., Krumbein, W.E., 2001a. Microbially induced sedimentary structures-A new category within the classification of primary sedimentary structures. Jour. Sediment. Res., 71(5): 649-656.

Noffke, N., Gerdes, G., Klenke, Th., and Krumbein, W.E., 2001, Microbially induced sedimentary structures indicating climatological, hydrological and depositional conditions within Recent and Pleistocene coastal facies zones (southern Tunisia): Facies, v. 44, p. 23–30.

Noffke,N., 2009. The criteria for the biogenicity of microbially induced sedimentary structures (MISS) in Archean and younger, sandy deposits. Earth-Sci. Rev., 96: 173–180.

Nyberg, A.V., Schopf, J.W., 1984. Microfossils in stromatolitic cherts from the upper Proterozoic Minyar Formation, Southern Ural Mountains, USSR. Jour. Paleontol., 58: 738-772.

Oehler, D.Z., 1977. Pyrenoid-like structures in late Precambrian algae from the Bitter Springs Formation of Australia. Jour. Paleontol., 51: 885-901.

Ogurtsova, R.N., Sergeev, V.N., 1987. The microbiota of Upper Precambrian Chichkanskaya Formation in the Lesser Karatau Region (southern Kazakhistan) Palentologicheskii Zhurnal, 2: 101–112 (english version).

Oldham, R.D., 1856. Remarks on the classification of the rocks of Central India resulting from the investigation by the geological survey. Jour. Asiatic Soc. Bengal, 25: 224 – 256.

Oldham, R.D., Vredenburg, E., Datta, P.N., 1901. Geology of the Son Valley in Rewah State and of parts of the adjoining districts of Jabalpur and Mirzapur. Mem. Geol. Surv. India, 31(1): 1 – 178.

Olugbemiro, R.O., Liqouis, B., Abaa, S.I., 1997. The Cretaceous series in the NE Nigeria. Source rock potential and maturity. Jour. Petrol. Geol., 20: 51- 68.

Pascoe, E.H., 1975. A manual of geology of India and Burma. Govt. of India Press, Calcutta, part II, 485-1343.

Paul, D.K., Rex, D.C., Harris, P.G., 1975. Chemical characteristics and K-Ar ages of Indian kimberlites. Bull. Geol. Soc. America, 86: 364-366.

Peters, K. E., 1986. Guidelines for evaluating petroleum source rock using programmed pyrolysis. AAPG. Bull., 70: 318-329.

Pettijohn, F.J., Potter, P.E., 1964. Atlas and Glossary of Primary Sedimentary Structures. Berlin, Springer, 370 pp.

Pflüger, F., 1999. Matground Structures and Redox Facies. Palaios, 14(1): 25–39.

Phipps, D., Playford, G., 1984. Laboratory techniques for extraction of palynomorphs from sediments: University of Queensland Papers, Department of Geology, 11: 1–23.

Pjatiletov, V.G., 1988. Mikrofitofossilii pozdnego dokembriya Uchuromajaskogo rajona (Microphytofossils from the late Precambrian of Ucur-Maia region) In: Khomentovsky, V.V., Schenfil, Vy (Eds.). Pozdnij Dokembrij I Rannji Paleozoj Sibiri Rifej i Vend, 47-104.

Playford, P.E., Cockbain, A.E., 1976. Modern Algal Stromatolites at Hamelin Pool, a hypersaline barred basin in Shark Bay, Western Australia; In: Walter, M.R. (Ed.). Stromatolites: Developments in Sedimentology. Elsevier Amsterdam, 20: 389–411.

Porada, H., Ghergut, J., Bouougri, E. H., 2008. *Kinneyia*-Type Wrinkle Structures Critical Review and Model of Formation. Palaios, 23(2): 65–77.

Prakash, R., Dalela, K., 1982. Stratigraphy of the Vindhyan in Uttar Pradesh: a brief review. In: Valdiya, K.S., Bhatia, S.B., Gaur, V.K. (Eds.), Geology of Vindhyanchal. Hind. Publ. Corp., New Delhi, 55-79.

Prasad, B., 1975. Lower Vindhyan formations of Rajasthan. Rec. Geol. Surv. India, 106: 31-53.

Prasad, B., 1984. Geology, sedimentation and paleogeography of the Vindhyan Supergroup, SE Rajasthan. Mem. Geol. Surv. India, 116: 1-107.

Prasad, B., Verma, K.K., 1991. Vindhyan basin- a review. In: Tandon, S.K., Pant, C.C., Casshyap, S.M. (Eds.), Sedimentary basins of India: Tectonic Context. Gyanodaya Prakashan, Nainital, 50-62.

Prasad, B.R., Rao, V.V., 2006. Deep seismic reflection study over the Vindhyan of Rajasthan: Implication for the geophysical study of the basin. Jour. Earth. Syst. Sci, 115(1): 135-147.

Prasanna, M.V., Rasheed, M.A., Madhavi, T., Kalpana, G., Patil, D.J., Dayal, A.M., 2010. Light gaseous hydrocarbon anomalies in the near-surface soils of Sagar District, Vindhyan Basin, India. Curr. Sci., 99(11): 1586-1590.

Price, K.L., Huntoon, J.E., Mcdowell, S.D., 1996. Thermal history of the 1.1 Ga Nonesuch Formation, North American mid-continent rift, White Pine, Michigan. Bull. Am. Assoc. Petrol. Geol., 80: 1–15.

Pruss, S.B., Corsetti, F.A., Fischer, W.W., 2008. Seafloor-precipitated carbonate fans in the Neoproterozoic Rainstorm Member, Johnnie Formation, Death Valley Region, USA. Sediment. Geol., 207: 34-40.

Raha, P.K., Sastry, M.V.A., 1982. Stromatolites and Precambrian Stratigraphy in India. Precamb. Res., 18: 293 – 318.

Rai, V., Gautam, R., 1998. New occurrence of carbonaceous megafossils from the Meso- to Neoproterozoic horizons of the Vindhyan Supergroup Kaimur–Katni areas, Madhya Pradesh, India. Geophytology, 26: 13–25.

Rai, V., Shukla, M., Gautam, R., 1997. Discovery of carbonaceous megafossils (*Chuaria- Tawuia* assemblage) from the Neoproterozoic Vindhyan succession (Rewa Group), Allahabad-Rewa area, India. Curr. Sci., 73: 783-788.

Ram, J., 2005. Hydrocarbon exploration in onland frontier basins of India-prospectives and challenges. Jour. Pal. Soc. India, 50: 1-16.

Ram, J., Shukla, S.N., Pramanik, A.G., Verma, B.K., Chandra, G., Murthy, M.S.N., 1996. Recent investigations in the Vindhyan Basin: Implications for the basin tectonics. In: Bhattacharyya, A. (Ed.), Recent Advances in Vindhyan Geology. Mem. Geol. Soc. India, 36: 267-286.

Ramanampisoa, L., Radke, M., 1992. Thermal maturity and hydrocarbon generation in rocks from the sedimentary basins of Madagascar. Jour. Petrol. Geol., 15: 379-396.

Rao, K.S., Chaman Lal & Ghosh, D.B. (1977). Algal Stromatolites in the Bhander Group, Vindhyan Supergroup, Satna District, Madhya Pradesh. Rec. Geol. Sur. India, 109: 38-47.

Rao, T.K., Soni, M.K., Sisodiya, D.S., 1979. Status of work on the Vindhyan Supergroup of rocks in M.P. Unpublished, Repport, Geol. Surv. India.

Rao. K.S., Neelakantam, S., 1978. Stratigraphy and sedimentation of Vindhyans in parts of Son Valley area, Madhya Pradesh. Rec. Geol. Surv. India, 110: 180-193.

Rasmussen, B., Fletcher, I.R., Bengtson, S., McNaughton, N.J., 2004. SHRIMP U-Pb dating of diagenetic xenotime in the Stirling Range Formation, Western Australia: 1.8 Billion year minimum age for the Stirling biota. Precamb. Res., 133: 329-337.

Rathore, S.S., Vijyan, A.R., Krishna, Prabhu, B.N. Misra, K.N., 1999. Dating of glauconites from Sirbu Shales of Vindhyan Super Group, India, Proceedings of the third International Petroleum Conference & Exploration Petrotech, 99: 191-196.

Ray, J.S., Martin, M.W., Veizer, J., Bowring, S.A., 2002. U-Pb zircon dating and Sr isotope systematics of the Vindhyan Supergroup, India. Geology, 30: 131-134.

Ray, J.S., Veizer, J., Davis, W.J., 2003. C, O, Sr and Pb isotope systematics of carbonate sequences of the Vindhyan Supergroup, India: age, diagenesis, correlations and implications for global events. Precamb. Res., 121: 103-140.

Raza, M., Casshyap, S.M., Khan, A., 2002. Geochemistry of Mesoproterozoic Lower Vindhyan Shales from Chittaurgarh, Southeastern Rajasthan and its bearing on source rock composition, palaeoweathering conditions and tectono-sedimentary environments. Jour. Geol. Soc. India, 60: 505-518.

Rippka, R., Josette, D., Waterbury, J.B., Michael, H., Stanier, R.Y., 1979. Generic assignments, Strain histories and properties of pure cultures of Cyanobacteria. Jour. Gen. Microbiology, 111: 1–61.

Rogers, J.J.W., 1986. The Dharwar craton and assembly of peninsular India. Jour. Geol., 94: 129-144.

Roy, A., Bandyopadhyay, B.K., 1990. Tectonics and structural pattern of the Mahakoshal belt of Central India. Spec. Publ. Geol. Surv. India, 28: 226-240.

Roy, S., Banerjee, S., 2001. Facies and petrography of the Porcellanite Formation around Chopan, Uttar Pradesh. Jour. Indian Assoc. Sedimentol., 20(2): 195 – 205.

Runnegar, B. 1998. Precambrian-Cambrian boundary in the southern Great Basin, California and Nevada and the base of the Sauk sequence. Geol. Soc. American Abst. Prog., 30(3): 63.

Runnegar, B., 1991. Precambrian oxygen levels estimated from the biochemistry and physiology of early eukaryotes. Palaeogeogr. Palaeoclimatol. Palaeoecol., 97: 97–111.

Sahni, M.R., 1936: *Fermoria minima*: a revised classification of organic remains from the Vindhyans of India. Rec. Geol. Surv. India, 69: 458-468.

Samuelsson, J., Butterfield, N.J., 2001. Neoproterozoic fossils from the Franklin Mountains, northwestern Canada: stratigraphic and palaeobiological implications. Precamb. Res., 107: 235-251.

Sanez, G., 1984. Geochemical prospecting in Mexico. Org. Geochem., 6: 715–725.

Sarangi, S., Gopalan, K., Kumar, S., 2004. Pb-Pb age of earliest megascopic eukaryotic alga bearing Rohtas Formation, Vindhyan Supergroup, India: Implications for Precambrian atmospheric oxygen evolution. Precamb. Res., 132: 107-121.

Sarkar, S., 1981. Ripple marks in intertidal lower Bhander sandstone (late Proterozoic), central India: a morphological analysis. Sediment. Geol., 29: 241-282.

Sarkar, S., Banerjee S., Samanta P., Jeevankumar S., 2005b. Microbial mat-induced sedimentary structures and their implications: examples from Chorhat Sandstones, M.P., India. Jour. Earth Sys. Sci. 115: 113-134.

Sarkar, S., Banerjee, S., Bose, P.K., 1996. Trace fossils in the Mesoproterozoic Koldaha Shale, Central India, and their implications. N. Jb. Geol. Paleont. Mh. 7, 425-438.

Sarkar, S., Banerjee, S., Chakraborty, C., Bose, P.K., 2002. Shelf storm flow dynamics: insight from the Mesoproterozoic Rampur Shale, central India. Sediment. Geol., 147: 89- 104.

Sarkar, S., Banerjee, S., Eriksson, P.G., Catuneanu, O., 2005a. Microbial mat control on siliciclastic Precambrian sequence stratigraphic architecture: examples from India. Sediment. Geol., 176: 195-209.

Sarkar, S., Bose, P. K., Samanta, P., 2008. Microbial Mat Mediated Structures in the Ediacaran Sonia Sandstone, Rajasthan, India, and Their Implications for Proterozoic Sedimentation. Precamb. Res., 162(1–2): 248–263.

Sastry, M.V.A., Moitra, A.,K., 1984. Vindhyan Stratigraphy: A Review; Geol. Surv. India Mem., 116(II): 109–148.

Savage, N.M., 1988. The use of sodium polytungstate for conodont separations: Jour. Micropal., 7: 39–40.

Schieber, J., 1999. Microbial Mats in Terrigenous Clastics: The Challenge of Identification in the Rock Record. Palaios, 14(1): 3–12.

Schieber, J., 2004. Microbial mats in the siliciclastic rock record: a summary of the diagnostic features, In: Erikson, P.G., Altermann, W., Nelson, D.R., Mueller, W.U., Catuneanu, O. (Eds.), The Precambrian Earth: Tempos and Events. Development in Precambrian Geology, 12. Elsevier, Amsterdam, 663-673.

Schieber, J., 2007. Microbial mats on muddy substrates- Examples of possible sedimentary features and underlying processes. In: Schieber, J., et al., (Eds.). Atlas of Microbial mat features preserved within the silici-clastic rock record. Elsevier, Amsterdam, 117-133.

Schneider, D.A., Bickford, M.E., Cannon, W.F., Schultz, K.J., Hamilton, M.A., 2002. Age of volcanic rocks and syndepositional iron formations, Marquette Range Supergroup; implications for the tectonic setting of Palaeoproterozoic iron formations of the Lake Superior region. Candian. Jour. Earth. Sci., 39(6): 999-1012.

Schoell, M., 1983b. Isotope technique for tracing migration of gases in sedimentary basins. Jour. Geol. Soc. London, 140: 415–422.

Schopf, J.W., 1968. Microflora of the Bitter Springs Formation, Late Precambrian, Central Australia. Jour. Paleontol., 42: 651–688.

Schopf, J.W., 1992. Historical development of Proterozoic micropaleontology. In: Schopf, J.W. and Klein, C. (Eds.), Evolution of the Proterozoic biosphere — a multidisciplinary study: Cambridge Univ. Press., New York, 179–183.

Schopf, J.W., 1999. Cradle of Life. Princeton University Press, Princeton, NJ, 367 p.

Schopf, J.W., Blacic, B.M., 1971. New microorganisms from the Bitter Springs Formation (Late Precambrian) of the north–central Amadeus Basin, Central Australia. Jour. Paleontol., 45: 925–960.

Schopf, J.W., Haugh, B.N., Molnar, R.E., Salterthwait, D.E., 1973. On the development of metaphytes and metazoans. Jour. Palaeontol., 47: 1-9.

Schopf, J.W., Klein, C., 1992. The Proterozoic Biosphere, Cambridge Univ. Press, 1348 p.

Sears, J.W., Chamberlain, K.R., Buckley, S.N., 1998. Structural and U-Pb geochronological evidence for 1.47 Ga rifting in the Belt Basin, western Montana. Canadian Jour. Earth Sci., 35: 467-475.

Seilacher, A., 1999. Biomat-related lifestyles in the Precambrian. Palaios, 14: 86–93.

Seilacher, A., Bose, P.K., Pflüger, F., 1998. Triploblastic animals more than 1 billion years ago: Trace fossil evidence from India. Science, 282: 80-83.

Seong-Joo, L., Golubic, S., 1999. Microfossil populations in the context of synsedimentary micrite deposition and acicular carbonate precipitation: Mesoproterozoic Gaoyuzhuang Formation, China. Precamb. Res., 96: 183–208.

Seong-Joo, L., Golubic, S., 2000. Biological and mineral components of an ancient stromatolite: Gaoyuzhuang Formation, Mesoproterozoic of China. SEPM Spec. Publ., 67: 91– 102.

Sergeev, V.N, Knoll, A.H., Grotzinger, J.P., 1995. Paleobiology of the Mesoproterozoic Billyakh Group, Anabar uplift, Northern Siberia. Palaeontol. Soc. Mem., 39: 1–37.

Sergeev, V.N., 1994. Microfossils in cherts from the Middle Riphean (Mesoproterozoic)Avzyan Formation, southern Ural Mountains, Russian Federation. Precamb. Res., 65: 231–254.

Sergeev, V.N., 2006. Precambrian microfossils in chert: their paleobiology, classification and biostratigraphic usefulness. GEOS Moscow, 280p.

Sergeev, V.N., Knoll, A.H., Kolosova, S.P., Kolosov, P.N., 1994. Microfossils in cherts from the Mesoproterozoic Debengda Formation, Olenek Uplift, northeastern Siberia. Stratigr. Geol. Correlation, 2: 23–38.

Sergeev, V.N., Knoll, A.H., Petrov, P.Y., 1997. Paleobiology of the Mesoproterozoic– Neoproterozoic Transition: The Sukhaya Tunguska Formation, Turukhansk Uplift, Siberia. Precamb. Res., 85: 201–239.

Sergeev, V.N., Schopf, J.W., 2010. Taxonomy, paleoecology and biostratigraphy of the Late Neoproterozoic Chichkan microbiota of south Kazakhstan: the marine biosphere on the eve of metazoan radiation. Jour. Paleontol., 84(3): 363-401.

Shaowu, N., 1998. Confirmation of the genu Grypania (megascopic alga) in Gaoyuzhuang Formation (1434 Ma) in Jixian (Tianjin) and its significance. Precamb. Res., 21(4): 1–10.

Sharma, A.K., 1980. Petrological study of the lower Vindhyan rocks of western Son valley, District Sidhi, M.P. Quart. Jour. Geol. Min. Met. Soc. India, 52: 57-62.

Sharma, M., 1993 Contributions to the Palaeobiology of Mesoproterozoic Vindhyan Sediments of India; Unpublished Ph.D. Thesis, Lucknow University, 299p.

Sharma, M., 1996. Microbialites (Stromatolites) from the Mesoproterozoic Salkhan Limestone, Semri Group, Rohtas, Bihar: their systematics and significance. Mem. Geol. Soc. India, 36: 167-196.

Sharma, M., 2003. Age of Vindhyans; Palaeobiological evidence; A Paradigm Shift (?). Jour. Pal. Soc. India, 48: 191 – 214.

Sharma, M., 2006. Palaeobiology of Mesoproterozoic Salkhan Limestone, Semri Group, Rohtas, Bihar, India: Systematics and significance. Jour. Earth Sys. Sci., 115(1): 67 – 98.

Sharma, M., 2006a. Small-sized akinetes from the Mesoproterozoic Salkhan Limestone, Semri Group, Bihar, India. Jour. Pal. Soc. India, 51(2): 109-118.

Sharma, M., 2006b. Late Palaeoproterozoic (Statherian) carbonaceous films from the Olive Shale (Koldaha Shale), Semri Group, Vindhyan Supergroup, India. Jour. Pal. Soc. India, 51(2), 27–35.

Sharma, M., Mishra, S., Dutta, S., Banerjee, S. Shukla, Y., 2009. On the affinity of *Chuaria–Tawuia* complex: A multidisciplinary study. Precamb. Res., 173: 123 – 136.

Sharma, M., Sergeev, V.N., 2004. Genesis of carbonate precipitate patterns and associated microfossils in Mesoproterozoic formations of India and Russia- a comparative study. Precamb. Res., 134: 317-347.

Sharma, M., Shukla, M., Venkatachala, B.S., 1992. Metaphyte and metazoan fossils from Precambrian sediments of India: a critique. Palaeobotanist, 40: 8-51.

Sharma, M., Shukla, M., Venkatachala, B.S., 1992. Metaphyte and Metazoan fossils from Precambrian sediments of India: a critique. Palaeobotanist, 40: 8–51.

Sharma, M., Shukla, Y., 2009a. Taxonomy and affinity of Early Mesoproterozoic megascopic helically coiled and related fossils from the Rohtas Formation, the Vindhyan Supergroup, India. Precamb. Res., 173(1-4): 105 – 122.

Sharma, M., Shukla, Y., 2009b. The evolution and distribution of life in the Precambrian eon-Global perspective and the Indian record. Jour. Biosci., 34(5): 1–12.

Shi Xiaoying, Zhang Chuanheng, Jiang Ganqing, Liu Juan, Wang Yi, Liu Dianbo, 2008. Microbial Mats in the Mesoproterozoic Carbonates of the North China Platform and Their Potential for Hydrocarbon Generation. Journal of China University of Geosciences, 19(5): 549–566.

Shukla, M., Misra, P.K., Sharma, M. 1992. Artificial chemical degradation of some extant Cyanobacteria with special refernce to Precambrian contaminants- ACautionary Note-II. Palaeobotanist, 39(3): 327 – 332.

Shukla, S.N., Chakraborty, D., 1994. Status of exploration and future programme of hydrocarbon exploration in Vindhyan and Gondwana basins; In: Biswas, S.K., Dave, A., Garg, P., Pandey, J., Maithani, A., Thomas, N.J., (Eds.). Proceeding of the Second Seminar on Petroliferous basins of India, 3: 63–100.

Sikander, A. H., Basu, S., Rasul, S.M., 2000. "Geochemical Source- Maturation and Volumetric Evaluation of Lower Paleozoic Source Rocks in the west Libya Basins". In: Salem, M.J., Oun, K.M., Seddiq, H.M., (Eds.). The Geology of Northwest Libya (Ghadamis, Jifarah,Tarabulus and Sbratah Basins), V(III): 3-53.

Singh, I.B., 1973. Depositional environment of the Vindhyan sediments in the Son valley area. In: Recent Researches in Geology. Hind. Publ. Corp., New Delhi, 1: 140-152.

Singh, I.B., 1980. Precambrian sedimentary sequences of India: their peculiarities and comparison with modern sediments. Precamb. Res., 12: 411-436.

Singh, I.B., 1985. Paleogeography of the Vindhyan basin and its relationship with Late Proterozoic basins of India. Jour. Pal. Soc. India, 30: 35-41.

Singh, S.P., Sinha, P.K., 2001. Vindhyan Supergroup of Bihar- an overview. In: Singh, S.P. (Ed.), Precambrian Crustal Evolution and Metallogeny of India. South Asian Association of Economic Geologists, Patna, 107-126.

Singh, S.P., Thakur, L.K., Sinha, A.K., 2001. Stratigraphy of the Semri Group in the Bhaunathpur area, Garwah District, Jharkhand. In: Singh, S.P. (Ed.), Precambrian Crustal Evolution and Metallogeny of India. South Asian Association of Economic Geologists, Patna, 95-106.

Snowdon, L. R. 1989. Organic matter properties and thermal evolution. In: Short course in burial diagenesis. Edited by: Hutcheon, I. E. Mineralogical Association of Canada, Short Course Handbook, 15:39-40.

Soni, M.K., Chakrabarty, S., Jain, V.K., 1987. Vindhyan Supergroup-A review. Mem. Geol. Surv. India, 6: 87–138.

Spamer, E.E., 1988. Geology of the Grand Canyon, v.3. Part III. An annotated bibliography of the world literature on the Grand Canyon typefossil *Chuaria circularis* Walcott, 1899, an index fossil for the Late Proterozoic. Geol. Soc. America, Microfilm Publication 17:4 cards.

Srivastava, A.P., Rajagopalan, G., 1988. F-T ages of Vindhyan Glauconitic sandstone beds exposed around Rewatbhata area, Rajasthan. Jour. Geol. Soc. India, 32: 527- 529.

Srivastava, D.C., Sahay, A., 2003. Brittle tectonics and pore-fluid conditions in the evolution of the Great Boundary Fault around Chittaurgarh, Northwestern India. Jour. Struc. Geol., 25: 1713-1733.

Srivastava, P., 2004. Carbonaceous fossils from the Panna Shale, Rewa Group (Upper Vindhyans), central India: a possible link between evolution of micro-megascopic life. Curr. Sci., 86: 644-646.

Srivastava, P., 2005. Vindhyan akinetes: an indicator of Mesoproterozoic biospheric evolution; Origins of life and Evolution of Biosphere, 35: 175–185.

Srivastava, P., Bali, R., 2006. Proterozoic carbonaceous remains from the Chorhat Sandstone: oldest fossils of the Vindhyan Supergroup, Central India. Geobios, 39(6): 873-878.

Srivastava, R. N., Srivastava K.N., Singh, K.N., Redcliffe, R.P., 2003. Sedimentation and depositional environment of the Chopan Porcellanite Formation, Semri Group, Vindhyan Supergroup in parts of Sonbhadra district, Uttar Pradesh. Jour. Pal. Soc. India, 48: 167-179.

Srivastava, R.N., 1977. Environmental significance of some depositional structures in banded porcellanites (Lower Vindhyan) of Mirzapur District, U.P. Jour. Indian Ass. Sediment., 1: 45-51.

Srivastava, R.N., 1978. On the provenance and mode of deposition of the Glauconite Sandstone, Semri Series, Mirzapur District, U.P. Rec. Geol. Surv. India, 110: 203-210.

Stahl, L.J., 2000. Microbial mats and stromatolites. In: Whitton, B.A., Potts, M. (Eds.).The Ecology of Cyanobacteria. Their Diversitty in Time and Space. Kluwer, Dordrecht.

Stahl, W., 1977. Carbon isotopes in petroleum geochemistry. In: Jager, E., Hunziger, J.C., (Eds.). Lectures in Isotope Geology, Springer-Verlag, Berlin, 1979, 274–282.

Stahl, W., Faber, E., Carey, B.D., Kirksey, D.L., 1981. Near-surface evidence of migration of natural gas from deep reservoirs and source rocks. American Assoc. Petrol. Geol. Bull., 65: 1543–1550.

Stainer, R.Y., Sistrom, W.R., Hansen, T.A., Whitton, B.A., Castenholz, R.W., Pfenning, N., Gorlenko, V.N., Kondratieva, E.N., Eimhjellen, K.E., Whittenbury, R., Gherna, R.L., Truper, H. G., 1978. Proposal to place nomenclature of the cyanobacteria (blue green algae) under the rules of International Code of Nomenclature of bacteria. Int. Jour. Syst. Bacteriology, 28: 335–336.

Steiner, M., 1997. *Chuaria circularis* Walcott 1899- "Megasphaeromorph Acritarch" or Prokaryotic Colony? In: Fatka, O., Servais, T. (Eds.), C.I.M.P. Acritarch in Praha. Acta Universitatis Carolinae, Geologica, 40: 645-665.

Steiner,M.,1994.Dieneoproterozoischen Megaalgen Sudchinas Berlinerg geowissenschafftiliche Abhandlungen E, 15: 1-46.

Stinchcomb, B. L., Levis, H. L., Echols, D. J., 1965. Precambrian graphitic compressions of possible biologic origin from Canada. Science, 148: 75-76.

Sumner, D.Y., Grotzinger, J.P., 1996. Were kinetics of Archean calcium carbonates precipitation related to oxygen concentration? Geology, 24: 119–122.

Sun, W., 1987. Palaeontology and biostratigraphy of Late Precambrian macroscopic colonial algae: *Chuaria* Walcott and *Tawuia* Hofmann. Paläontographica Abh. B, 203: 109-134.

Suresh, R., Sundara Raju, T.P., 1983. Problematic *Chuaria* from the Bhima Basin, south India. Precamb. Res., 23: 79-85.

Talyzina, E., 2000. Ultrastructure and morphology of *Chuaria circularis* (Walcott, 1899) Vidal and Ford (1985) from the Neoproterozoic Visingsö Group, Sweden, Precamb. Res., 102: 123-134.

Tandon, K.K., Kumar, S., 1977a. New fossil finds from the lower Vindhyan rocks (Precambrian of Central India). Curr. Sci., 46(6): 563.

Tandon, K.K., Kumar, S., 1977b. Discovery of annelid and arthropod remains from Lower Vindhyan Rocks (Precambrian) of central India. Geophytology, 7(1): 126–129.

Tedesco, S.A., 1995. Surface Geochemistry in Hydrocarbon Exploration. Chapman & Hall, New York, 206p.

Thuret, G., 1875. Essai de classification des nostocines. Annales des Sciences Naturelles, Paris (Botanique), 6: 372-382.

Timofeev, B.V., 1969. Spheromorphides of the Proterozoic (Sferomorfidy roterozoya). 145 p. Nauka, Moskva.

Timofeev, B.V., 1970. Sphaeromorphida ge´ants dans le Pre´-cambrien avance´. Rev. Palaeobot. Palynol., 10: 157–160.

Timofeev, B.V., Herman, T. N., Mikhalova, N.S., 1976. Microphytofossils from the Precambrian, Cambrian and Ordovician. Nauka, Leningrad, p. 106. (In Russian).

Timofeev, B.V., Hermann, T.N., Mikhailova, M.S., 1976. Microfossils of the Precambrian, Cambrian and Ordovisian; Institute of Geology and Geochronology, Academy of Sciences, USSR, 106 p. (in Russian).

Tissot, B.P., Welte, D.H., 1984. Petroleum Formation and Occurrence, 2nd edition, Springer Verlag, Berlin, 699p.

Traverse, A., 1988, Paleopalynology: Boston, Unwin Hyman, 600p.

Tyler, S.A., Barghoorn, E.S., Barret, L.P., 1957. Authentic coal from Precambrian Upper Huronian black shale of the Iron River District, Northern Michigan. Geol. Soc. America Bull., 68: 1293-1304.

Valdiya, K.S., 1982. Tectonic prospective of the Vindhyanchal region. In: Valdiya, K.S., Bhatia, S.B. and Gaur, V.K. (Eds.), Geology of Vindhyachal, Hindustan Publishing Corporation (India): 23 – 29.

Venkatachala, B.S., Sharma, M., Shukla, M., 1996. Age and life of Vindhyans: facts and conjectures. In: Bhattacharyya, A. (Ed.), Recent Advances in Vindhyan Geology, Mem. Geol. Soc. India, 36: 137-166.

Venkatachala, B.S., Yadav, V.K., Shukla, M., 1990. Middle Proterozoic microfossils from the Nauhata Limestone (Lower Vindhyan), Rohtasgarh, India. In: Naqvi, S.M., (Ed.), Precambrian Continental Crust and its economic resources. Development in Precambrian Geology, 8: 471-485.

Verma, P.K., Banerjee, P., 1992. Nature of continental crust along the Narmada-Son Lineament inferred from gravity and deep seismic sounding data. Tectonophysics, 202: 375-397.

Vidal, G., 1989. Are late Proterozoic carbonaceous megafossils metaphytic algae or bacteria?: Lethaia, 22: 375 – 379.

Vidal, G., Ford, T.D., 1985. Microbiotas from the Late Proterozoic Chuar Group (Northern Arizona) and Unita Mountain Group (Utah) and their chronostratigraphic implications. Precamb. Res., 28: 349-389.

Vidal, G., Moczydłowska, M., Rudavskaya, V., 1993. Biostratigraphical implications of a *Chuaria-Tawuia* assemblage and associated acritarchs from the Neoproterozoic of Yakutia. Palaeontology, 36: 387-402.

Vinogradov, A.P., Tugarinov, A.I., Zhikov, C.I., Stanikova, N.I., Bibikova, E.V., Khorre, K., 1964. Geochronology of the Indian Precambrian. Report 22nd Int. Geol. Cong. 10, New Delhi: 553-567.

Vredenburg, E., 1906. Suggestions for the classification of Vindhyan System. Rec. Geol. Surv. India, 33(4): 262 – 314.

Walcott, C.D., 1899. Precambrian fossiliferous formations. Geol. Soc. America Bull., 10: 199-244.

Walcott, C.D., 1914. Cambrian geology and paleontology III. No.2, Precambrian Algonkian algal flora. Smithsonian Misc. Coll., 64: 77-156.

Walsby, A.E., 1974. The isolation of gas vesicles from bluegreen algae. Methods Enzymol., 31A: 678–686.

Walter, M. R., Rulin Du, Horodyski, R. J., 1990. Coiled carbonaceous megafossils from the Middle Proterozoic of Jixian (Tianjin) and Montana. American Jour. Sci., 290-A: 133- 148.

Walter, M.R., 1976. *Stromatolites*; Developments in Sedimentology. Elsevier Amsterdam, 790 p.

Walter, M.R., Heys, G.R., 1985. Links between the rise of Metazoa and the decline of stromatolites. Precamb. Res. 29, 149–174.

Walter, M.R., Oehler, J.H., Oehler, D. Z., 1976. Megascopic algae 1300 Million Years old from the Belt Supergroup, Montana: A reinterpretation of Walcott's *Helminthoidichnites*. Jour. Paleontol., 50: 872-881.

Warren, J.K., George, S.C., Hamilton, P.J., Tingate, P., 1998. Proterozoic source rocks: Sedimentology and organic characteristics of the Velkerri Formation, Northern Territory, Australia. Bull. Am. Assoc. Petrol. Geol., 82: 442–463.

Waterbury, J.B., Stainer, R.Y., 1978. Patterns of growth and development in pleurocapasalean cyanobacteria. Microbiol. Rev., 42: 2–44.

Wettestein, F.V., 1924. Handbuch der Systematischer Botanik; 3rd edn, Franz Deutike Leipzig, Band, 1: 1017.

White, D., 1928. Study of the fossil floras in the Grand Canyon. Carnegie Instn. Washington, Year book, 27: 389-390.

Whiticar, M.J., 1996. Stable isotope geochemistry of coals, humic kerogen and related natural gases. Internat. Jour. Coal Geol. 32, 191–215.

Whiticar, M.J., 1999. Carbon and hydrogen isotope systematics of bacterial formation and oxidation of methane. Chem. Geol., 161(1–3): 291–314.

Williams, G.E., Schmidt, P.W., 1996. Origin and paleomagnetism of the Mesoproterozoic Gangau tilloid (basal Vindhyan Supergroup), central India. Precamb. Res., 79: 307-325.

Windley, B.F., 1977. Recent advances in Vindhyan geology; book review. Sediment. Geol., 112 (3-4): 305.

Woese, C., Fox, G., 1977. Phylogenetic structure of prokaryotic domain. Proc. Nat. Acad. Sci. USA, 74: 5088–5090.

Woese, C.R., Kandler, O., Wheelis, M.L., 1990. Towards a natural system of organisms Proposal for the domains Archaea Bacteria and Eucarya. Proc. Nat. Acad. Sci. USA, 87: 4576-4579.

Xiao, S., Knoll, A.H., 2000. Phosphatized animal embryos in the Neoproterozoic Doushantuo Formation at Weng'An, Guizhou, south China. Jour. Paleontol., 74: 767-788.

Yakschin, M.S., 1990. K voprosu o prirode microstruktur rannerifeiskih plastovyh stromatolitov (Origin of microstructures in the Early Riphean flat-laminated stromatolites). In "Iskopaemye problematiki SSSR" (The bizarre fossils of the U.S.S.R.) Moscow, Nauka, 5–13.

Yakschin, M.S., 1991. Vodoroslevaya mikrobiota nizhnego rifeya anabarskogo podnyatia (Algal microbiota from the Lower Riphean deposits of Anabar Uplift). Novosibirsk,Nauka, Sibirskoe Otdelenie, 61p.

Yan Yu, Liu- Zhi- Li, 1997. Tuanshanzian macroscopic algae of 1700 Ma B. P. From the Changcheng System of Jinxian China. Acta Palaeontol. Sin., 36(1): 18-41.

Yan Yu, Liu- Zhi- Li, 1998. On the relationship between biocommunities and palaeoenvironments in Changcheng Period of Yanshan Basin, North China Does *Sangshuania* represent eukaryotic algae or trace fossils. Acta Micropal. Sin., 58: 1249-266.

Yan, Y.Z., 1995. Discovery and preliminary study of megascopic algae (1,700 Ma) from the Tuanshanzi Formation in Jixian, Hebei. Acta Micropal. Sin., 12(2): 107-126.

Yankauskas, T.V. [Jankauskas, T.V.]. 1979. Srednerifeyskie microbiota Yuzhnogo Urala i Bashkirskogo Priural'ya. [Lower Riphean microbiotas of the Southern Urals.] Akademiya Nauk SSSR, Doklady, 248(1): 190-193. [English translation p. 51-54.]

Yin Leiming, Weiguo, S., 1994. Microbiota from the Neoproterozoic Liulaobei Formation in the Huainan region, northern Anhui China. Precamb. Res., 65: 95-114.

Zang, W., Walter, M.R., 1992. Late Proterozoic and Cambrian microfossils and biostratigraphy, Amadeus Basin, central Australia. Assoc. Australia Palaeontol. Mem., 12: 132.

Zhang, X. L., Hua, H., Reitner, J., 2006. A new type of Precambrian megascopic fossils: the Jixian biota from northeastern China. Facies, 52: 169-181.

Zhang, Y., 1981. Proterozoic Stromatolite microflora of the Gaoyuzhuang Formation (Early Sinian: Riphean), Hebei, China. Jour. Paleontol., 55: 485–506.

Zhang, Y., Leiming, Y., Xiao, S., Knoll, A.H., 1998. Permineralised fossils from the Terminal Proterozoic Doushantuo Formation, South China. Jour. Palaeontol. 72: 1–52.

Zhang, Z., 1997. A new Palaeoproterozoic clastics facies microbiota from the Chuanlinggou Formation (1800 Ma) near Jixian, North China. Jour. Micropal., 5(2): 9-16.

Zhu, S., Sun, S., Huang, X., He, Y., Zhu, G., Sun, L., Zhang, K., 2000. Discovery of carbonaceous compressions and their multicellular tissues from the Changzhougou Formation (1800 Ma) in the Yanshan range, North China. Chinese Sci. Bull., 45: 841-847.